NASA TECHNICAL NOTE

NASA TN D-5016

NASA TN D-5016

AERODYNAMIC DATA ON LARGE SEMISPAN TILTING WING WITH 0.4-DIAMETER CHORD, SINGLE-SLOTTED FLAP, AND SINGLE PROPELLER 0.22 CHORD BELOW WING

by Marvin P. Fink

Langley Research Center
Langley Station, Hampton, Va.

NATIONAL AERONAUTICS AND SPACE ADMINISTRATION • WASHINGTON, D. C. • JANUARY 1969

NASA TN D-5016

AERODYNAMIC DATA ON LARGE SEMISPAN TILTING WING WITH 0.4-DIAMETER CHORD, SINGLE-SLOTTED FLAP, AND SINGLE PROPELLER 0.22 CHORD BELOW WING

By Marvin P. Fink

Langley Research Center
Langley Station, Hampton, Va.

NATIONAL AERONAUTICS AND SPACE ADMINISTRATION

For sale by the Clearinghouse for Federal Scientific and Technical Information
Springfield, Virginia 22151 – CFSTI price $3.00

AERODYNAMIC DATA ON LARGE SEMISPAN TILTING WING WITH 0.4-DIAMETER CHORD, SINGLE-SLOTTED FLAP, AND SINGLE PROPELLER 0.22 CHORD BELOW WING

By Marvin P. Fink
Langley Research Center

SUMMARY

An investigation has been made in the Langley full-scale tunnel to determine the longitudinal aerodynamic characteristics of a large-scale semispan V/STOL tilt-wing configuration with a single propeller which was tested for both up-at-the-tip and down-at-the-tip modes of rotation. The wing had a ratio of chord to propeller diameter of 0.4, a 40-percent-chord single-slotted flap, an aspect ratio of 6.14 (3.07 for the semispan), a taper ratio of 1.0, and an NACA 4420 airfoil section.

The data have not been analyzed in detail but have been examined to observe the predominant trends. The direction of propeller rotation was found to have a very significant effect on the lift and descent capability (as determined from drag-lift ratios attainable without stalling of any part of the wing within the propeller slipstream) and that up-at-the-tip rotation gave the more favorable results. The use of a trailing-edge flap was also very effective in increasing the descent capability. The use of flow-control devices (slats and fences) was very effective in increasing the descent capability and lift for down-at-the-tip propeller rotation where the characteristics without such devices were poor but was much less effective for up-at-the-tip propeller rotation where reasonably favorable results were achieved without these devices. For the most favorable combination of the configuration variables, descent angles of nearly 27° were achieved over the entire test range of power conditions.

INTRODUCTION

Most of the aerodynamic research that has been done on tilt-wing propeller-driven V/STOL configurations in the past has been of an exploratory character and has been done with small-scale models. The interest in this type of airplane has now become so substantial, however, that there is need for large-scale systematic aerodynamic design data for this concept. A program has therefore been initiated at the Langley Research Center to provide such information by means of tests of a large-scale semispan tilt-wing propeller-driven model. The results of tests for the wing-alone configuration with a chord-diameter ratio of 0.6 have been presented in references 1 to 3. The results of tests for the configuration with a chord-diameter ratio of 0.5 have been presented in references 4 to 8. These tests covered variations in the model such as height of propeller, presence of fuselage, and use of a single- or double-slotted flap. The present tests were made to obtain aerodynamic data for a model with a single propeller on a semispan wing, a half-fuselage, a chord-diameter ratio of 0.4, a single-slotted flap, a leading-edge slat, and fences. The investigation covered a range of angle of attack from 5° to 80° and a range of thrust coefficient, based on slipstream dynamic pressure, from 0.30 to 0.90. Tests with both directions of propeller rotation were included in the investigation. The results of this investigation are presented herein without analysis in order to expedite their dissemination to industry and the military services.

SYMBOLS

The positive sense of forces, moments, and angles is shown in figure 1. The pitching-moment coefficients are presented with reference to the wing quarter-chord line. The coefficients are based on the dynamic pressure in the propeller slipstream. Conventional lift, drag, and pitching-moment coefficients based on the free-stream dynamic pressure can be obtained by dividing the slipstream coefficients by $1 - C_{T,s}$; for example, $C_L = C_{L,s}/(1 - C_{T,s})$. The thrust coefficient C_T' may be obtained from the equation $C_T' = \left[C_{T,s}(A/S)\right]/(1 - C_{T,s})$.

Measurements for this investigation were made in the U.S. Customary System of Units and equivalent values are indicated herein in the International System of Units (SI). Factors relating the two systems of units used in this paper can be found in the appendix.

The coefficients and symbols used in this paper are defined as follows:

A total propeller disk area, ft^2 ($meters^2$)

b propeller blade chord, ft (meters); also, wing span, excluding tip fairing, ft (meters)

$C_{D,s}$ drag coefficient based on slipstream, $\frac{D}{q_s S}$

C_L lift coefficient based on free airstream, $\frac{L}{qS}$

$C_{L,s}$ lift coefficient based on slipstream, $\frac{L}{q_s S}$

$C_{m,s}$ pitching-moment coefficient based on slipstream, $\frac{M_Y}{q_s Sc}$

$C_{T,s}$	thrust coefficient based on slipstream, $\frac{T}{q_s \frac{\pi D^2}{4}}$
C'_T	thrust coefficient based on free airstream, $\frac{T}{qS}$
c	wing chord, ft (meters)
c_f	flap chord, ft (meters)
D	propeller diameter, ft (meters); also, total model drag, lbf (newtons)
h	thickness of propeller blade, ft (meters)
L	total model lift, lbf (newtons)
M_Y	pitching moment, lbf-ft (newton-meters)
q	free-stream dynamic pressure, $\frac{\rho V^2}{2}$, $\frac{\text{lbf}}{\text{ft}^2}$ $\left(\frac{\text{newtons}}{\text{meter}^2}\right)$
q_s	slipstream dynamic pressure, $q + \frac{T}{\frac{\pi D^2}{4}}$, $\frac{\text{lbf}}{\text{ft}^2}$ $\left(\frac{\text{newtons}}{\text{meter}^2}\right)$
R	radius of propeller blade, 2.83 ft (0.86 meter)
r	radius to element on propeller blade, ft (meters)
S	area of semispan wing, 15.68 ft^2 (1.46 meters^2)
T	propeller thrust, lbf (newtons)
V	free-stream velocity, $\frac{\text{ft}}{\text{sec}}$ $\left(\frac{\text{meters}}{\text{second}}\right)$
x	distance along wing chord line, ft (meters)
y_l	lower-surface ordinate, ft (meters)
y_u	upper-surface ordinate, ft (meters)
z	vertical distance, ft (meters)

α angle of attack, degrees

δ_f flap deflection, degrees

ρ mass density of air, $\frac{\text{slugs}}{\text{ft}^3}$ $\left(\frac{\text{kilograms}}{\text{meter}^3}\right)$

MODEL

The model used in this investigation was a semispan model which would represent the left panel of the full-span wing and the left half of the fuselage. Sketches of the model are presented in figure 2. A three-view drawing of the fuselage-wing combination is shown in figure 2(a), and the principal dimensions of the wing are given in figure 2(b). Details of the wing slat, flap, and fences are given in figures 3(a) and 3(b). The propeller-blade characteristics are shown in figure 4, and a photograph of the model is presented in figure 5.

The wing was constructed to allow numerous modifications to be made in the test configuration, such as a change of wing planform, change of airfoil, the addition of flow-control devices, deflection of the trailing-edge flap, and change of the direction of rotation of the propeller. The basic structure of the wing consisted of a heavy box-beam spar to which a power train was attached to drive the propellers through spanwise shafting and around which various airfoil contours could be fitted. The propeller location was such that the propeller tip extended out to the wing tip. In the present investigation both directions of propeller rotation were tested. The propeller thrust was measured by a strain-gage balance which was a part of the propeller shaft. The output was fed through sliprings to an indicating instrument. The required values of thrust for each value of $C_{T,s}$ were set by the operator by changing the speed of the propeller drive motor. The blade angle at the 0.75R station of the propeller was held constant at 17° throughout the investigation. The propeller was located 0.22c below the wing chord plane and 0.84c ahead of the wing quarter-chord line as shown in figure 2(b). The thrust line was parallel to the wing chord plane.

The airfoil used on the wing was the NACA 4420 section with a 2.26-ft (0.69-m) chord. This chord length gave a ratio of wing chord to propeller diameter of 0.4. The reference area of the wing based on a semispan of 6.92 ft (2.11m) was 15.68 ft^2 $\left(1.46\ \text{m}^2\right)$ and did not include the area of the tip fairing.

The model had a 0.40c single-slotted trailing-edge flap. The flap ordinates and the positions of the nose for the various deflections are given in figure 3(a). The flap is illustrated in figure 3(a) for the 40° deflection.

The leading-edge slat shown in figure 3(a) was investigated in combination with the flap on this model. With down-at-the-tip rotation only, the inboard section of slat was used (0.21b/2 to 0.51b/2); with up-at-the-tip rotation, the inboard and outboard sections (0.69b/2 to 0.95b/2) were used both separately and together.

Fences with a height of 0.20c and extending from 0.14c on the lower surface around the leading edge including the slat to about 0.75c on the upper surface were installed at two spanwise locations on the wing (see fig. 3(b)) in an attempt to confine the center section stall inboard of the propeller slipstream. When tests were made with fences on, both fences were installed.

TESTS AND RESULTS

The tests were made for a range of single-slotted flap deflections with and without the leading-edge slat and fences. The specific configurations tested and a list of tables and figures in which data for each may be found are given in the following table:

Direction of rotation	Configuration	Flap deflection, δ_f, deg	Wing aerodynamic data	
			Table	Figure
Down at tip	Basic leading edge	0	1	6
		20	2	7
		40	3	8
		60	4	9
	Basic leading edge and fences on	0	5	10
		20	6	11
		40	7	12
		60	8	13
	Inboard slat on	20	9	14
		40	10	15
		60	11	16
	Inboard slat on and fences on	20	12	17
		40	13	18
		60	14	19
Up at tip	Basic leading edge	0	15	20
		20	16	21
		40	17	22
		60	18	23
	Basic leading edge and fences on	0	19	24
		20	20	25
		40	21	26
		60	22	27
	Inboard slat on	20	23	28
		40	24	29
		60	25	30
	Inboard slat on and fences on	20	26	31
		40	27	32
		60	28	33
	Full-span slat on and fences on	20	29	34
		40	30	35
		60	31	36

The tests were made over a range of thrust coefficients from 0.30 to 0.90. For any given test the thrust coefficient was held constant over the angle-of-attack range by adjusting the propeller speed to give the required thrust at each angle of attack. The angle-of-attack range was from 5° to that required to stall the wing or to develop a drag-lift ratio of about 0.3, whichever was lower. The test Reynolds number, based on the wing chord length and the velocity of the propeller slipstream, was about 1.9×10^{6}.

No tunnel-wall corrections have been applied to the data since surveys and analysis had indicated that there would be no significant correction, as explained in reference 1.

DISCUSSION

The data presented have not been analyzed in detail but have been examined to observe general trends. One general observation was that the force-test data could not be used as an indication of the occurrence or extent of wing stalling. The tuft-test results show that the onset of stalling over significant areas of that part of the wing within the propeller slipstream frequently occurs considerably below or above the angle of attack for maximum lift coefficient. The data were examined, in particular, to determine the effect of the various test variables on descent capability, the descent capability being determined from the D/L values attainable prior to indication by the tufts of stalling of any part of the wing within the propeller slipstream.

Effect of Direction of Propeller Rotation

The force- and tuft-test data show that the up-at-the-tip direction of rotation consistently gave higher maximum lift and higher descent capability. In general, the tuft pictures show that rough flow and stalling occurred at an angle of attack as much as 25° to 30° lower with down-at-the-tip rotation than with up-at-the-tip rotation for the higher thrust coefficients $\left(C_{T,s} = 0.90 \text{ and } 0.80\right)$. Down-at-the-tip propeller rotation consistently causes stalling (of the part of the wing in the slipstream) to start inboard of the nacelle, that is, behind the up-going blades. When stall occurred on the wing for the up-at-the-tip mode of rotation, it occurred only outboard of the nacelle.

Effect of Leading-Edge Slat

Comparison of figures 6 to 9 with 14 to 16 for down-at-the-tip rotation and figures 20 to 23 with 28 to 30 for up-at-the-tip rotation gives the effect of the inboard leading-edge slat. With down-at-the-tip rotation, the inboard slat was particularly effective for the lower thrust coefficients $\left(C_{T,s} = 0.30 \text{ and } 0.60\right)$ in alleviating the sharp break in the lift curves at stall. The lift-coefficient curves for the configuration with slats were broader at the tops than those for the configuration without slats, and a nearly constant value of $C_{L,s}$ was obtained over a much higher angle-of-attack range. With up-at-the-tip rotation, where there was no problem with inboard stall, the slat had an adverse effect for some conditions on the aerodynamic characteristics of the wing.

The effect of the full-span slat was only determined for up-at-the-tip rotation (figs. 34 to 36). By comparison with the inboard-slat results (figs. 31 to 33), the tuft tests show that the use of a full-span slat caused a notable increase in descent capability for the 20° flap deflection and a general improvement in wing stall for both $\delta_f = 40^{\circ}$ and 60°.

Effect of Fences

The effect of fences can be ascertained for both directions of propeller rotation for the model with the basic leading edge and with the inboard leading-edge slat installed. Compare figures 6 to 19 for down-at-the-tip rotation and figures 20 to 33 for up-at-the-tip rotation. The results show that the fences were most effective for the down-at-the-tip mode of propeller rotation. In this case the wing had a tendency to stall inboard of the nacelle because of the rotation of the propeller slipstream, and the fences were effective in preventing the center-section stall from spreading and prematurely triggering the stalling of the section of the wing in the propeller slipstream inboard of the nacelle. For this mode of propeller rotation, the fences gave significantly more descent capability over the range of flap deflection, particularly for the higher thrust coefficients.

Effect of Flap Deflection

A progressive increase in maximum lift coefficient and descent capability occurred as the flap deflection was increased. The greatest increment occurred with the deflection from 0° to 20° for either mode of propeller rotation; but it must be pointed out that for down-at-the-tip rotation, the model with $\delta_f = 0^{\circ}$ had a negative descent capability (-D/L). (See fig. 6.) With 20° of flap deflection (fig. 7), a change in the positive direction occurred but still not enough to produce any noticeable descent capability. With up-at-the-tip rotation, increasing the flap deflection from 0° to 20° increased the descent angle from about -14° to about 10° for thrust coefficients of 0.30 and 0.60. (See figs. 20 and 21.) With this direction of rotation, full-span slat, and fences, a descent angle of nearly 27° was obtained with 60° of flap deflection (fig. 36).

CONCLUSIONS

An experimental investigation has been made to determine the longitudinal aerodynamic characteristics of a large-scale semispan V/STOL tilt-wing configuration with a single propeller which was tested for both modes of rotation. The following conclusions were drawn from the results of the investigation:

1. The direction of propeller rotation had a significant effect on the lift and descent capability attainable for most of the configurations tested, the up-at-the-tip mode of propeller rotation giving the more favorable results.

2. Leading-edge stall-control devices were very effective in improving the descent capability for the down-at-the-tip mode of propeller rotation. With fences and leading-edge slats, almost as favorable results could be achieved with this mode of propeller rotation as with up-at-the-tip rotation.

3. The use of flaps was very effective in increasing the lift and the descent capability for either mode of rotation. With 40° or 60° flap deflection and with the most favorable combination of flow-control devices tested, descent angles of nearly 27° were achieved for the entire test range of power conditions.

Langley Research Center,
National Aeronautics and Space Administration,
Langley Station, Hampton, Va., September 26, 1968,
721-01-00-11-23.

APPENDIX

CONVERSION FACTORS – U.S. CUSTOMARY UNITS TO SI UNITS

The International System of Units (SI) was adopted by the Eleventh General Conference on Weights and Measures, Paris, October 1960. (See ref. 9.) The following conversion factors are included in this report for convenience:

Physical quantity	U.S. Customary Unit	Conversion factor (*)	SI Unit
Area	ft^2	0.0929	$meters^2$ (m^2)
Density	$slugs/ft^3$	515.38	$kilograms/meter^3$ (kg/m^3)
Force	lbf	4.448	newtons (N)
Length	in.	0.0254	meters (m)
	ft	0.3048	meters (m)
Moment	lbf-ft	1.356	newton-meters (N-m)
Pressure . . .	lbf/ft^2	47.88	$newtons/meter^2$ (N/m^2)
Velocity. . . .	ft/sec	0.3048	meters/second (m/sec)

*Multiply value given in U.S. Customary Unit by conversion factor to obtain equivalent value in SI Unit.

REFERENCES

1. Fink, Marvin P.; Mitchell, Robert G.; and White, Lucy C.: Aerodynamic Data on a Large Semispan Tilting Wing With 0.6-Diameter Chord, Fowler Flap, and Single Propeller Rotating Up at Tip. NASA TN D-2180, 1964.

2. Fink, Marvin P.; Mitchell, Robert G.; and White, Lucy C.: Aerodynamic Data on Large Semispan Tilting Wing With 0.6-Diameter Chord, Single-Slotted Flap, and Single Propeller Rotating Down at Tip. NASA TN D-2412, 1964.

3. Fink, Marvin P.; Mitchell, Robert G.; and White, Lucy C.: Aerodynamic Data on Large Semispan Tilting Wing With 0.6-Diameter Chord, Single Slotted Flap, and Single Propeller Rotating Up at Tip. NASA TN D-1586, 1964.

4. Fink, Marvin P.; Mitchell, Robert G.; and White, Lucy C.: Aerodynamic Data on a Large Semispan Tilting Wing With 0.5-Diameter Chord, Double-Slotted Flap, and Both Left- and Right-Hand Rotation of a Single Propeller. NASA TN D-3375, 1966.

5. Fink, Marvin P.: Aerodynamic Data on a Large Semispan Tilting Wing With a 0.5-Diameter Chord, a Double-Slotted Flap, and Left- and Right-Hand Rotation of a Single Propeller, in Presence of Fuselage. NASA TN D-3674, 1966.

6. Fink, Marvin P.; and Mitchell, Robert G.: Aerodynamic Data on a Large Semispan Tilting Wing With a 0.5-Diameter Chord, a Single-Slotted Flap, and Both Left- and Right-Hand Rotation of a Single Propeller. NASA TN D-3754, 1967.

7. Fink, Marvin P.: Aerodynamic Data on Large Semispan Tilting Wing With 0.5-Diameter Chord, Single-Slotted Flap, and Single Propeller 0.19 Chord Below Wing. NASA TN D-3884, 1967.

8. Fink, Marvin P.: Aerodynamic Data on Large Semispan Tilting Wing With 0.5-Diameter Chord, Single-Slotted Flap, and Single Propeller 0.08 Chord Below Wing. NASA TN D-4030, 1967.

9. Mechtly, E. A.: The International System of Units – Physical Constants and Conversion Factors. NASA SP-7012, 1964.

TABLE 1.- AERODYNAMIC DATA FOR DOWN-AT-TIP ROTATION, BASIC LEADING EDGE, AND $\delta_f = 0^o$

α, deg	$C_{L,s}$	$C_{D,s}$	$C_{m,s}$	$C_{L,s}$	$C_{D,s}$	$C_{m,s}$
	$C_{T,s} = 0.90$			$C_{T,s} = 0.80$		
5	0.307	-1.415	0.419	0.371	-1.234	0.373
10	.498	-1.355	.435	.587	-1.203	.401
15	.659	-1.304	.455	.771	-1.152	.430
20	.831	-1.230	.476	.960	-1.068	.456
25	.986	-1.140	.484	1.114	-.954	.461
30	1.118	-1.036	.497	1.256	-.822	.471
35	1.238	-.915	.505	1.385	-.690	.484
40	1.345	-.774	.512	1.487	-.523	.490
45	1.439	-.630	.522	1.543	-.369	.486
50	1.476	-.483	.512	1.553	-.198	.473
55	1.513	-.339	.513	1.570	-.046	.486
60	1.523	-.196	.513	1.571	.103	.498
65	1.565	-.037	.534	1.544	.217	.506
70	1.557	.092	.530	1.519	.343	.534
75	1.559	.229	.558	1.485	.477	.547
80	1.531	.375	.560			
	$C_{T,s} = 0.60$			$C_{T,s} = 0.30$		
5	0.383	-0.914	0.286	0.470	-0.435	0.135
10	.646	-.870	.315	.735	-.394	.175
15	.865	-.810	.358	.981	-.328	.229
20	1.101	-.717	.376	1.147	-.220	.217
25	1.283	-.588	.386	1.191	-.091	.186
30	1.409	-.424	.362	1.278	.055	.190
35	1.364	-.276	.347			
40	1.462	-.098	.370			

TABLE 2.- AERODYNAMIC DATA FOR DOWN-AT-TIP ROTATION, BASIC LEADING EDGE, AND $\delta_f = 20^\circ$

α, deg	$C_{L,s}$	$C_{D,s}$	$C_{m,s}$	$C_{L,s}$	$C_{D,s}$	$C_{m,s}$
	$C_{T,s} = 0.90$			$C_{T,s} = 0.80$		
5	0.632	-1.325	0.277	0.729	-1.148	0.230
10	.832	-1.263	.304	.970	-1.085	.258
15	1.002	-1.197	.332	1.183	-.991	.268
20	1.174	-1.086	.332	1.396	-.865	.280
25	1.328	-.963	.337	1.569	-.713	.286
30	1.450	-.818	.340	1.666	-.550	.282
35	1.560	-.672	.354	1.759	-.380	.282
40	1.643	-.515	.357	1.831	-.189	.301
45	1.681	-.366	.358	1.822	-.028	.267
50	1.692	-.207	.348	1.710	.088	.273
55	1.685	-.055	.346	1.674	.201	.300
60	1.678	.080	.376	1.615	.310	.325
65	1.655	.203	.385	1.584	.408	.362
70	1.628	.330	.418	1.536	.520	.405
75	1.582	.433	.442			
80	1.545	.553	.465			
	$C_{T,s} = 0.60$			$C_{T,s} = 0.30$		
5	0.901	-0.822	0.119	1.060	-0.343	-0.041
10	1.187	-.744	.159	1.399	-.240	-.021
15	1.474	-.649	.163	1.736	-.134	-.006
20	1.745	-.493	.174	2.055	.028	.003
25	1.938	-.319	.180	1.759	.175	-.057
30	1.987	-.122	.172	1.644	.312	-.043
35	1.945	.043	.155			
40	1.823	.213	.158			
45	1.801	.346	.175			

TABLE 3.- AERODYNAMIC DATA FOR DOWN-AT-TIP ROTATION, BASIC LEADING EDGE, AND $\delta_f = 40^{\circ}$

α, deg	$C_{L,s}$	$C_{D,s}$	$C_{m,s}$	$C_{L,s}$	$C_{D,s}$	$C_{m,s}$
	$C_{T,s} = 0.90$			$C_{T,s} = 0.80$		
5	0.896	-1.225	0.209	1.038	-1.048	0.139
10	1.078	-1.151	.211	1.260	-.950	.160
15	1.244	-1.047	.230	1.504	-.842	.177
20	1.398	-.924	.250	1.700	-.690	.171
25	1.548	-.785	.253	1.883	-.508	.173
30	1.650	-.614	.247	1.913	-.319	.182
35	1.734	-.452	.251	1.974	-.139	.198
40	1.772	-.290	.265	1.968	.049	.201
45	1.756	-.160	.279	1.831	.159	.197
50	1.767	.001	.287	1.713	.225	.230
55	1.743	.138	.290	1.647	.328	.278
60	1.695	.252	.312	1.611	.451	.296
65	1.640	.363	.336	1.551	.525	.348
70	1.598	.446	.380	1.499	.603	.384
75	1.555	.533	.411			
80	1.513	.667	.434			
	$C_{T,s} = 0.60$			$C_{T,s} = 0.30$		
5	1.199	-0.672	0.037	1.509	-0.200	0.050
10	1.495	-.569	.045	1.782	-.078	-.135
15	1.789	-.440	.054	2.110	.064	-.129
20	2.083	-.253	.043	2.456	.249	-.135
25	2.194	-.065	.057	1.952	.376	-.139
30	2.176	.131	.075	1.763	.504	-.121
35	1.783	.202	.055			
40	1.850	.399	.098			
45	1.790	.519	.121			

TABLE 4.- AERODYNAMIC DATA FOR DOWN-AT-TIP ROTATION, BASIC LEADING EDGE, AND $\delta_f = 60^o$

α, deg	$C_{L,s}$	$C_{D,s}$	$C_{m,s}$	$C_{L,s}$	$C_{D,s}$	$C_{m,s}$
	$C_{T,s} = 0.90$			$C_{T,s} = 0.80$		
5	0.997	-1.114	0.165	1.168	-0.939	0.116
10	1.174	-1.024	.176	1.374	-.821	.120
15	1.331	-.915	.190	1.585	-.693	.133
20	1.478	-.780	.192	1.785	-.517	.117
25	1.609	-.631	.198	1.941	-.326	.123
30	1.697	-.468	.204	1.959	-.166	.141
35	1.767	-.281	.202	1.978	.022	.158
40	1.806	-.111	.215	1.952	.195	.180
45	1.798	.031	.238	1.753	.279	.180
50	1.750	.159	.253	1.618	.295	.213
55	1.713	.310	.255	1.568	.403	.258
60	1.657	.421	.270	1.526	.508	.289
65	1.597	.509	.291	1.455	.558	.340
70	1.529	.516	.354			
75	1.478	.656	.367			
80	1.438	.840	.364			
	$C_{T,s} = 0.60$			$C_{T,s} = 0.30$		
5	1.360	-0.587	0.005	1.623	-0.086	-0.175
10	1.633	-.462	.008	1.931	.050	-.163
15	1.969	-.296	-.001	2.261	.193	-.160
20	2.229	-.097	.009	2.546	.389	-.156
25	2.231	.082	.027	1.891	.457	-.129
30	2.193	.269	.040	1.789	.565	-.122
35	1.906	.375	.043			
40	1.830	.488	.088			
45	1.741	.580	.133			

TABLE 5.- AERODYNAMIC DATA FOR DOWN-AT-TIP ROTATION, BASIC LEADING EDGE, FENCES ON, AND $\delta_f = 0^o$

α, deg	$C_{L,s}$	$C_{D,s}$	$C_{m,s}$	$C_{L,s}$	$C_{D,s}$	$C_{m,s}$
	$C_{T,s} = 0.90$			$C_{T,s} = 0.80$		
5	0.318	-1.389	0.422	0.365	-1.233	0.384
10	.510	-1.352	.442	.575	-1.187	.407
15	.690	-1.300	.462	.767	-1.137	.435
20	.858	-1.235	.481	.958	-1.050	.452
25	1.012	-1.137	.486	1.134	-.947	.471
30	1.158	-1.031	.502	1.293	-.815	.477
35	1.277	-.903	.504	1.424	-.675	.483
40	1.393	-.756	.504	1.546	-.513	.492
45	1.488	-.609	.525	1.538	-.353	.473
50	1.575	-.449	.520	1.552	-.203	.471
55	1.627	-.280	.529	1.569	-.050	.474
60	1.645	-.126	.538	1.586	.101	.499
65	1.631	.007	.545	1.588	.254	.523
70	1.622	.147	.562	1.559	.388	.538
75	1.601	.282	.573	1.507	.473	.564
80	1.577	.405	.589			
	$C_{T,s} = 0.60$			$C_{T,s} = 0.30$		
5	0.396	-0.908	0.294	0.466	-0.436	0.125
10	.645	-.865	.310	.734	-.386	.176
15	.869	-.805	.349	.951	-.318	.202
20	1.065	-.695	.336	1.153	-.195	.201
25	1.231	-.564	.351	1.297	-.055	.204
30	1.340	-.421	.353	1.359	.089	.190
35	1.385	-.272	.348	1.415	.229	.198
40	1.457	-.116	.354			

TABLE 6.- AERODYNAMIC DATA FOR DOWN-AT-TIP ROTATION, BASIC LEADING EDGE, FENCES ON, AND $\delta_f = 20^\circ$

α, deg	$C_{L,s}$	$C_{D,s}$	$C_{m,s}$	$C_{L,s}$	$C_{D,s}$	$C_{m,s}$
	$C_{T,s} = 0.90$			$C_{T,s} = 0.80$		
5	0.628	-1.329	0.282	0.763	-1.189	0.251
10	.850	-1.262	.309	1.004	-1.125	.269
15	1.032	-1.203	.336	1.228	-1.005	.274
20	1.217	-1.095	.338	1.460	-.890	.290
25	1.378	-.966	.353	1.617	-.716	.298
30	1.510	-.818	.351	1.745	-.537	.297
35	1.617	-.661	.346	1.865	-.358	.306
40	1.729	-.474	.347	1.954	-.157	.309
45	2.018	-.277	.361	1.988	.033	.304
50	1.879	-.095	.365	1.683	.038	.314
55	1.800	.022	.368	1.674	.152	.335
60	1.700	.087	.380	1.668	.303	.364
65	1.744	.310	.398	1.673	.488	.396
70	1.719	.417	.424	1.619	.598	.443
75	1.682	.573	.462	1.537	.643	.472
80	1.645	.683	.503			
	$C_{T,s} = 0.60$			$C_{T,s} = 0.30$		
5	0.916	-0.833	0.136	1.060	-0.359	-0.024
10	1.217	-.753	.168	1.427	-.261	-.004
15	1.497	-.654	.180	1.754	-.138	.006
20	1.762	-.486	.186	2.084	.029	.006
25	1.968	-.291	.180	1.809	.204	-.069
30	2.081	-.104	.186	1.793	.372	-.059
35	1.774	.036	.147			
40	1.802	.212	.150			
45	1.715	.312	.191			

TABLE 7.- AERODYNAMIC DATA FOR DOWN-AT-TIP ROTATION, BASIC LEADING EDGE, FENCES ON, AND $\delta_f = 40^o$

α, deg	$C_{L,s}$	$C_{D,s}$	$C_{m,s}$	$C_{L,s}$	$C_{D,s}$	$C_{m,s}$
	$C_{T,s} = 0.90$			$C_{T,s} = 0.80$		
5	0.882	-1.250	0.206	1.038	-1.077	0.153
10	1.089	-1.171	.218	1.264	-.969	.163
15	1.262	-1.068	.229	1.476	-.842	.178
20	1.425	-.938	.238	1.678	-.682	.161
25	1.573	-.782	.251	1.834	-.495	.173
30	1.685	-.623	.242	1.928	-.297	.175
35	1.778	-.443	.253	1.975	-.082	.179
40	1.874	-.233	.254	2.095	.118	.181
45	1.931	-.037	.247	2.073	.299	.192
50	2.108	.123	.252	1.682	.189	.226
55	1.893	.287	.283	1.655	.326	.254
60	1.853	.441	.313	1.667	.482	.301
65	1.658	.369	.322	1.643	.623	.331
70	1.622	.480	.360	1.561	.681	.385
75	1.655	.738	.378			
80	1.584	.828	.416			
	$C_{T,s} = 0.60$			$C_{T,s} = 0.30$		
5	1.215	-0.692	0.038	1.440	-0.204	-0.150
10	1.508	-.574	.034	1.778	-.086	-.136
15	1.798	-.446	.040	2.119	.059	-.116
20	2.040	-.252	.033	2.446	.263	-.136
25	2.198	-.037	.031	1.970	.404	-.176
30	2.279	.167	.041	1.913	.556	-.172
35	2.297	.381	.044			
40	1.823	.380	.062			
45	1.657	.431	.112			
50	1.749	.652	.122			

TABLE 8.- AERODYNAMIC DATA FOR DOWN-AT-TIP ROTATION, BASIC LEADING EDGE, FENCES ON, AND $\delta_f = 60^o$

α, deg	$C_{L,s}$	$C_{D,s}$	$C_{m,s}$	$C_{L,s}$	$C_{D,s}$	$C_{m,s}$
	$C_{T,s} = 0.90$			$C_{T,s} = 0.80$		
5	0.998	-1.146	0.180	1.145	-0.947	0.119
10	1.162	-1.029	.183	1.366	-.827	.136
15	1.335	-.921	.199	1.572	-.695	.130
20	1.473	-.776	.204	1.786	-.521	.122
25	1.591	-.626	.204	1.916	-.319	.138
30	1.700	-.445	.196	1.987	-.127	.149
35	1.793	-.266	.201	2.031	.084	.147
40	1.856	-.051	.208	2.071	.286	.156
45	1.891	.127	.214	1.994	.433	.175
50	1.864	.285	.221	1.593	.294	.228
55	1.831	.458	.236	1.550	.403	.262
60	1.768	.560	.258	1.605	.618	.286
65	1.689	.671	.281	1.538	.694	.338
70	1.592	.709	.316	1.438	.692	.376
75	1.536	.817	.340			
80	1.456	.898	.354			
	$C_{T,s} = 0.60$			$C_{T,s} = 0.30$		
5	1.339	-0.587	-0.015	1.601	-0.077	-0.190
10	1.634	-.456	.001	1.936	.044	-.161
15	1.904	-.319	-.003	2.266	.202	-.166
20	2.170	-.089	-.010	2.514	.433	-.153
25	2.265	.129	-.001	1.939	.526	-.220
30	2.318	.337	0	1.843	.664	-.175
35	2.240	.522	.009			
40	1.710	.435	.086			
45	1.576	.490	.130			
50	1.672	.711	.143			

TABLE 9.- AERODYNAMIC DATA FOR DOWN-AT-TIP ROTATION, INBOARD SLAT ON, AND $\delta_f = 20^o$

α, deg	$C_{L,s}$	$C_{D,s}$	$C_{m,s}$	$C_{L,s}$	$C_{D,s}$	$C_{m,s}$
	$C_{T,s} = 0.90$			$C_{T,s} = 0.80$		
5	0.647	-1.363	0.281	0.726	-1.181	0.243
10	.842	-1.285	.317	.974	-1.111	.261
15	1.024	-1.208	.320	1.212	-1.017	.272
20	1.208	-1.095	.322	1.447	-.896	.293
25	1.378	-.972	.348	1.606	-.745	.305
30	1.460	-.835	.354	1.634	-.586	.307
35	1.532	-.707	.342	1.730	-.415	.311
40	1.605	-.558	.365	1.836	-.226	.333
45	1.694	-.399	.367	1.862	-.047	.331
50	1.726	-.219	.368	1.854	.095	.357
55	1.755	-.059	.387	1.839	.242	.378
60	1.782	.120	.410	1.845	.438	.392
65	1.788	.301	.408	1.805	.590	.421
70	1.748	.421	.429	1.734	.704	.447
75	1.684	.505	.461			
80	1.630	.605	.495			
	$C_{T,s} = 0.60$			$C_{T,s} = 0.30$		
5	0.832	-0.845	0.140	0.924	-0.369	-0.013
10	1.163	-.751	.143	1.341	-.272	-.028
15	1.455	-.641	.160	1.705	-.154	-.023
20	1.742	-.498	.183	2.038	.012	.023
25	1.958	-.319	.219	2.070	.194	.019
30	1.911	-.133	.187	2.284	.435	.001
35	2.014	.053	.215	2.280	.619	.012
40	2.053	.245	.213	2.194	.790	.019
45	2.070	.429	.226	2.108	.927	.021
50	2.053	.595	.242			
55	1.987	.727	.273			
60	1.837	.785	.292			

TABLE 10.- AERODYNAMIC DATA FOR DOWN-AT-TIP ROTATION, INBOARD SLAT ON, AND $\delta_f = 40^o$

α, deg	$C_{L,s}$	$C_{D,s}$	$C_{m,s}$	$C_{L,s}$	$C_{D,s}$	$C_{m,s}$
	$C_{T,s} = 0.90$			$C_{T,s} = 0.80$		
5	0.836	-1.237	0.221	0.974	-1.063	0.150
10	1.047	-1.160	.222	1.235	-.968	.162
15	1.215	-1.052	.234	1.445	-.837	.173
20	1.373	-.937	.256	1.673	-.692	.175
25	1.517	-.780	.253	1.839	-.513	.188
30	1.633	-.626	.257	1.813	-.356	.182
35	1.676	-.497	.272	1.878	-.177	.214
40	1.699	-.349	.284	1.939	.046	.207
45	1.734	-.180	.286	1.941	.199	.228
50	1.747	-.014	.298	1.846	.286	.260
55	1.759	.143	.318	1.823	.438	.287
60	1.749	.317	.308	1.807	.601	.318
65	1.726	.481	.337	1.725	.734	.340
70	1.666	.559	.370	1.635	.821	.387
75	1.610	.623	.414			
80	1.550	.726	.432			
	$C_{T,s} = 0.60$			$C_{T,s} = 0.30$		
5	1.131	-0.707	0.036	1.308	-0.227	-0.136
10	1.473	-.601	.043	1.731	-.087	-.143
15	1.786	-.449	.038	2.088	.059	-.113
20	2.074	-.270	.049	2.379	.252	-.116
25	2.118	-.077	.056	2.225	.432	-.125
30	2.070	.102	.068	2.361	.682	-.127
35	2.150	.317	.091	2.311	.844	-.107
40	2.121	.494	.093	2.234	.988	-.066
45	2.080	.640	.126			
50	2.017	.771	.161			
55	1.899	.842	.195			

TABLE 11.- AERODYNAMIC DATA FOR DOWN-AT-TIP ROTATION, INBOARD SLAT ON, AND $\delta_f = 60^\circ$

α, deg	$C_{L,s}$	$C_{D,s}$	$C_{m,s}$	$C_{L,s}$	$C_{D,s}$	$C_{m,s}$
	$C_{T,s} = 0.90$			$C_{T,s} = 0.80$		
5	0.970	-1.148	0.172	1.121	-0.971	0.108
10	1.190	-1.056	.169	1.368	-.869	.123
15	1.339	-.932	.189	1.616	-.711	.114
20	1.491	-.802	.208	1.828	-.540	.134
25	1.628	-.650	.208	1.959	-.346	.136
30	1.712	-.482	.210	1.943	-.193	.158
35	1.753	-.321	.221	1.966	-.005	.178
40	1.726	-.183	.231	1.986	.184	.193
45	1.757	-.025	.243	1.936	.327	.194
50	1.762	.137	.252	1.857	.430	.235
55	1.752	.298	.264	1.738	.501	.272
60	1.715	.426	.294	1.737	.704	.282
65	1.679	.516	.328	1.657	.818	.321
70	1.614	.621	.358	1.565	.889	.370
75	1.560	.715	.380			
80	1.488	.857	.369			
	$C_{T,s} = 0.60$			$C_{T,s} = 0.30$		
5	1.302	-0.599	-0.009	1.534	-0.129	-0.170
10	1.665	-.464	.008	1.952	.019	-.152
15	1.974	-.297	-.014	2.293	.212	-.168
20	2.222	-.116	.008	2.533	.394	-.136
25	2.235	.069	.033	2.409	.640	-.151
30	2.119	.256	.038	2.434	.839	-.130
35	2.152	.453	.058	2.372	1.014	-.124
40	2.101	.633	.082	2.195	1.081	-.074
45	2.046	.775	.101			
50	1.958	.877	.161			
55	1.852	.940	.215			

TABLE 12.- AERODYNAMIC DATA FOR DOWN-AT-TIP ROTATION, INBOARD SLAT ON, FENCES ON, AND $\delta_f = 20^{o}$

α, deg	$C_{L,s}$	$C_{D,s}$	$C_{m,s}$	$C_{L,s}$	$C_{D,s}$	$C_{m,s}$
	$C_{T,s} = 0.90$			$C_{T,s} = 0.80$		
5	0.623	-1.345	0.283	0.731	-1.184	0.232
10	.837	-1.282	.299	.963	-1.111	.249
15	1.058	-1.197	.305	1.209	-1.016	.266
20	1.213	-1.097	.317	1.434	-.876	.274
25	1.377	-.965	.339	1.603	-.724	.284
30	1.497	-.818	.340	1.732	-.546	.284
35	1.612	-.653	.338	1.842	-.369	.292
40	1.724	-.473	.340	1.948	-.141	.302
45	1.795	-.291	.351	2.008	.056	.312
50	1.868	-.089	.367	2.056	.244	.329
55	1.882	.083	.376	1.993	.399	.349
60	1.860	.234	.387	1.943	.542	.378
65	1.837	.406	.408	1.865	.633	.419
70	1.799	.548	.424	1.806	.805	.454
75	1.729	.652	.435	1.739	.881	.484
80	1.668	.745	.477	1.641	.938	.515
	$C_{T,s} = 0.60$			$C_{T,s} = 0.30$		
5	0.823	-0.848	0.149	0.919	-0.363	-0.016
10	1.157	-.749	.152	1.345	-.264	-.001
15	1.466	-.638	.166	1.702	-.142	.007
20	1.743	-.485	.186	2.061	.034	.017
25	1.951	-.296	.196	2.348	.247	.016
30	2.110	-.092	.196	2.526	.496	.017
35	2.174	.103	.201	2.568	.709	.020
40	2.268	.327	.220	2.378	.851	.012
45	2.284	.520	.236	2.166	.911	.023
50	2.175	.670	.240			
55	2.064	.803	.260			
60	1.912	.845	.307			

TABLE 13.- AERODYNAMIC DATA FOR DOWN-AT-TIP ROTATION, INBOARD SLAT ON, FENCES ON, AND $\delta_f = 40^o$

α, deg	$C_{L,s}$	$C_{D,s}$	$C_{m,s}$	$C_{L,s}$	$C_{D,s}$	$C_{m,s}$
	$C_{T,s}$ = 0.90			$C_{T,s}$ = 0.80		
5	0.822	-1.234	0.186	0.974	-1.077	0.138
10	1.027	-1.150	.195	1.225	-.968	.146
15	1.203	-1.048	.206	1.459	-.845	.164
20	1.377	-.914	.215	1.661	-.674	.154
25	1.515	-.768	.227	1.819	-.495	.156
30	1.633	-.603	.226	1.939	-.284	.162
35	1.730	-.427	.219	2.026	-.088	.166
40	1.813	-.216	.228	2.094	.132	.175
45	1.894	-.022	.246	2.113	.324	.197
50	1.924	.150	.248	2.063	.490	.207
55	1.908	.314	.258	2.003	.620	.241
60	1.874	.479	.268	1.887	.715	.285
65	1.813	.613	.296	1.799	.798	.328
70	1.741	.723	.322	1.723	.910	.360
75	1.659	.809	.351			
80	1.600	.878	.397			
	$C_{T,s}$ = 0.60			$C_{T,s}$ = 0.30		
5	1.120	-0.710	-0.025	1.319	-0.241	-0.129
10	1.207	-.587	.011	1.764	-.101	-.128
15	1.799	-.447	.037	2.121	.063	-.132
20	2.065	-.255	.029	2.466	.256	-.108
25	2.212	-.021	.039	2.692	.526	-.130
30	2.286	.192	.041	2.758	.789	-.134
35	2.335	.395	.053	2.703	.987	-.123
40	2.358	.602	.075	2.668	1.156	-.092
45	2.329	.774	.096	2.248	1.093	-.038
50	2.168	.889	.129			
55	2.027	.959	.176			
60	1.818	.933	.249			

TABLE 14.- AERODYNAMIC DATA FOR DOWN-AT-TIP ROTATION, INBOARD SLAT ON, FENCES ON, AND $\delta_f = 60^o$

α, deg	$C_{L,s}$	$C_{D,s}$	$C_{m,s}$	$C_{L,s}$	$C_{D,s}$	$C_{m,s}$
	$C_{T,s} = 0.90$			$C_{T,s} = 0.80$		
5	0.936	-1.160	0.180	1.097	-0.949	0.099
10	1.139	-1.056	.182	1.337	-.839	.119
15	1.312	-.939	.188	1.573	-.698	.118
20	1.466	-.806	.194	1.783	-.516	.114
25	1.608	-.640	.209	1.890	-.322	.138
30	1.715	-.459	.190	1.982	-.127	.137
35	1.797	-.278	.200	2.044	.074	.134
40	1.857	-.074	.208	2.081	.286	.151
45	1.892	.112	.213	2.078	.458	.167
50	1.882	.271	.226	1.986	.584	.198
55	1.838	.434	.238	1.917	.715	.233
60	1.807	.599	.260	1.808	.808	.268
65	1.730	.692	.284	1.703	.894	.320
70	1.667	.802	.302	1.618	.981	.367
75	1.586	.874	.325			
80	1.494	.944	.355			
	$C_{T,s} = 0.60$			$C_{T,s} = 0.30$		
5	1.314	-0.600	-0.009	1.525	-0.122	-0.181
10	1.652	-.478	-.018	1.947	.027	-.171
15	1.978	-.296	-.014	2.304	.218	-.177
20	2.179	-.107	0	2.539	.392	-.125
25	2.315	.125	.013	2.712	.684	-.152
30	2.349	.344	.026	2.734	.934	-.168
35	2.354	.548	.035	2.675	1.129	-.150
40	2.348	.754	.058	2.315	1.078	-.070
45	2.207	.879	.091			
50	2.068	.995	.113			
55	1.953	1.068	.166			
60	1.754	.995	.247			

TABLE 15.- AERODYNAMIC DATA FOR UP-AT-TIP ROTATION, BASIC LEADING EDGE, AND $\delta_f = 0^o$

α, deg	$C_{L,s}$	$C_{D,s}$	$C_{m,s}$	$C_{L,s}$	$C_{D,s}$	$C_{m,s}$
	$C_{T,s} = 0.90$			$C_{T,s} = 0.80$		
5	0.263	-1.431	0.435	0.310	-1.257	0.380
10	.454	-1.395	.470	.529	-1.214	.421
15	.637	-1.333	.488	.741	-1.151	.445
20	.812	-1.259	.504	.945	-1.072	.467
25	.981	-1.164	.512	1.131	-.960	.475
30	1.137	-1.052	.508	1.273	-.820	.487
35	1.256	-.928	.518	1.406	-.684	.497
40	1.364	-.776	.531	1.530	-.510	.508
45	1.466	-.634	.526	1.634	-.345	.519
50	1.540	-.485	.536	1.714	-.163	.515
55	1.609	-.313	.535	1.765	.011	.511
60	1.643	-.152	.534	1.788	.175	.521
65	1.655	.005	.530	1.789	.345	.522
70	1.659	.144	.532	1.741	.468	.535
75	1.649	.284	.543	1.641	.558	.554
80	1.639	.440	.557	1.497	.606	.542
	$C_{T,s} = 0.60$			$C_{T,s} = 0.30$		
5	0.365	-0.921	0.275	0.441	-0.443	0.106
10	.605	-.878	.310	.715	-.406	.174
15	.844	-.819	.357	.971	-.335	.218
20	1.088	-.725	.363	1.204	-.231	.237
25	1.289	-.600	.385	1.297	-.093	.210
30	1.478	-.434	.384	1.398	.080	.195
35	1.499	-.258	.357	1.437	.221	.166
40	1.550	-.090	.345			

TABLE 16.- AERODYNAMIC DATA FOR UP-AT-TIP ROTATION, BASIC LEADING EDGE, AND $\delta_f = 20^o$

α, deg	$C_{L,s}$	$C_{D,s}$	$C_{m,s}$	$C_{L,s}$	$C_{D,s}$	$C_{m,s}$
	$C_{T,s} = 0.90$			$C_{T,s} = 0.80$		
5	0.593	-1.326	0.306	0.697	-1.145	0.233
10	.792	-1.260	.319	.941	-1.063	.248
15	.985	-1.170	.331	1.163	-.960	.250
20	1.149	-1.066	.321	1.367	-.835	.276
25	1.313	-.925	.342	1.553	-.687	.274
30	1.453	-.777	.337	1.699	-.515	.275
35	1.557	-.616	.328	1.789	-.330	.272
40	1.635	-.450	.327	1.852	-.143	.279
45	1.703	-.280	.328	1.894	.042	.279
50	1.736	-.122	.331	1.911	.206	.288
55	1.751	.036	.326	1.902	.366	.308
60	1.740	.174	.347	1.876	.510	.321
65	1.730	.323	.357	1.819	.635	.340
70	1.696	.445	.378	1.761	.705	.390
75	1.655	.550	.399			
80	1.610	.636	.431			
	$C_{T,s} = 0.60$			$C_{T,s} = 0.30$		
5	0.856	-0.813	0.123	1.019	-0.333	-0.062
10	1.147	-.731	.130	1.382	-.247	-.041
15	1.417	-.602	.145	1.735	-.111	-.028
20	1.702	-.451	.156	2.058	.048	-.018
25	1.872	-.263	.141	2.233	.250	-.024
30	2.002	-.074	.138	2.308	.467	-.033
35	2.031	.106	.141	1.843	.537	-.054
40	2.089	.289	.156	1.801	.692	-.060
45	2.023	.484	.149			
50	1.964	.632	.170			
55	1.798	.717	.173			
60	1.646	.753	.196			

TABLE 17.- AERODYNAMIC DATA FOR UP-AT-TIP ROTATION, BASIC LEADING EDGE, AND $\delta_f = 40^o$

α, deg	$C_{L,s}$	$C_{D,s}$	$C_{m,s}$	$C_{L,s}$	$C_{D,s}$	$C_{m,s}$
	$C_{T,s} = 0.90$			$C_{T,s} = 0.80$		
5	0.833	-1.211	0.201	0.993	-1.013	0.136
10	1.018	-1.123	.215	1.223	-.910	.145
15	1.188	-1.020	.225	1.420	-.785	.159
20	1.357	-.880	.226	1.656	-.621	.148
25	1.491	-.718	.228	1.816	-.438	.158
30	1.629	-.557	.222	1.935	-.245	.159
35	1.740	-.386	.220	1.971	-.067	.173
40	1.786	-.202	.217	2.001	.120	.177
45	1.810	-.045	.231	1.991	.280	.190
50	1.825	.133	.244	1.963	.425	.207
55	1.808	.272	.255	1.919	.552	.239
60	1.757	.363	.259	1.874	.675	.256
65	1.724	.474	.294	1.800	.771	.287
70	1.684	.573	.325	1.713	.810	.342
75	1.618	.638	.349	1.554	.800	.384
80	1.572	.720	.403			
	$C_{T,s} = 0.60$			$C_{T,s} = 0.30$		
5	1.203	-0.661	0.011	1.461	-0.156	-0.183
10	1.474	-.538	.006	1.809	-.030	-.189
15	1.775	-.400	.014	2.107	.119	-.160
20	2.065	-.213	.009	2.402	.289	-.148
25	2.165	-.011	.014	2.598	.501	-.155
30	2.248	.179	.030	2.505	.716	-.155
35	2.221	.351	.033	2.401	.871	-.155
40	2.185	.514	.075	1.823	.830	-.096
45	2.150	.654	.088			
50	2.088	.771	.136			
55	2.012	.867	.169			
60	1.595	.810	.173			

TABLE 18.- AERODYNAMIC DATA FOR UP-AT-TIP ROTATION, BASIC LEADING EDGE, AND $\delta_f = 60^o$

α, deg	$C_{L,s}$	$C_{D,s}$	$C_{m,s}$	$C_{L,s}$	$C_{D,s}$	$C_{m,s}$
	$C_{T,s} = 0.90$			$C_{T,s} = 0.80$		
5	0.925	-1.105	0.193	1.085	-0.897	0.100
10	1.088	-1.016	.195	1.294	-.781	.106
15	1.257	-.892	.195	1.505	-.642	.104
20	1.401	-.747	.197	1.730	-.463	.100
25	1.549	-.575	.182	1.865	-.290	.115
30	1.671	-.393	.182	1.966	-.102	.129
35	1.731	-.231	.184	1.966	.078	.132
40	1.786	-.055	.200	1.967	.249	.142
45	1.804	.124	.200	1.954	.400	.161
50	1.802	.270	.213	1.901	.513	.190
55	1.775	.400	.228	1.861	.654	.197
60	1.735	.504	.250	1.800	.759	.225
65	1.672	.549	.281	1.724	.841	.260
70	1.626	.617	.319	1.632	.880	.322
75	1.568	.650	.365	1.360	.738	.369
80	1.498	.703	.397			
	$C_{T,s} = 0.60$			$C_{T,s} = 0.30$		
5	1.308	-0.541	-0.038	1.632	-0.004	-0.255
10	1.610	-.406	-.047	1.908	.105	-.217
15	1.835	-.271	-.022	2.166	.243	-.199
20	2.060	-.078	-.019	2.440	.425	-.170
25	2.212	.125	.008	2.616	.635	-.159
30	2.235	.334	.005	2.446	.828	-.158
35	2.167	.482	.014	2.330	.961	-.155
40	2.130	.628	.049	1.764	.894	-.093
45	2.080	.751	.088			
50	1.996	.847	.109			
55	1.916	.920	.146			
60	1.417	.738	.197			

TABLE 19.- AERODYNAMIC DATA FOR UP-AT-TIP ROTATION, BASIC LEADING EDGE, FENCES ON, AND $\delta_f = 0^o$

α, deg	$C_{L,s}$	$C_{D,s}$	$C_{m,s}$	$C_{L,s}$	$C_{D,s}$	$C_{m,s}$
	$C_{T,s}$ = 0.90			$C_{T,s}$ = 0.80		
5	0.247	-1.416	0.426	0.299	-1.257	0.376
10	.459	-1.382	.459	.526	-1.224	.416
15	.645	-1.325	.481	.722	-1.150	.432
20	.821	-1.255	.490	.929	-1.064	.463
25	.982	-1.153	.501	1.115	-.954	.467
30	1.137	-1.034	.506	1.278	-.810	.474
35	1.262	-.911	.510	1.418	-.680	.491
40	1.378	-.764	.525	1.560	-.500	.504
45	1.470	-.613	.530	1.662	-.331	.507
50	1.549	-.467	.522	1.735	-.148	.494
55	1.615	-.286	.523	1.772	.024	.499
60	1.623	-.129	.516	1.796	.193	.503
65	1.667	.007	.523	1.782	.337	.511
70	1.661	.157	.534	1.741	.464	.530
75	1.664	.327	.551	1.659	.553	.540
80	1.637	.458	.561	1.492	.584	.534
	$C_{T,s}$ = 0.60			$C_{T,s}$ = 0.30		
5	0.361	-0.930	0.276	0.454	-0.458	0.113
10	.606	-.891	.315	.719	-.411	.168
15	.850	-.826	.362	.985	-.339	.219
20	1.090	-.725	.362	1.231	-.222	.220
25	1.321	-.596	.395	1.359	-.095	.220
30	1.524	-.426	.396	1.438	.083	.190
35	1.515	-.248	.340	1.497	.235	.175
40	1.591	-.075	.345			
45	1.658	.102	.352			
50	1.706	.290	.357			

TABLE 20.- AERODYNAMIC DATA FOR UP-AT-TIP ROTATION,

BASIC LEADING EDGE, FENCES ON, AND $\delta_f = 20^o$

α, deg	$C_{L,s}$	$C_{D,s}$	$C_{m,s}$	$C_{L,s}$	$C_{D,s}$	$C_{m,s}$
	$C_{T,s} = 0.90$			$C_{T,s} = 0.80$		
5	0.578	-1.332	0.306	0.696	-1.146	0.238
10	.797	-1.269	.325	.933	-1.068	.256
15	.993	-1.181	.337	1.152	-.965	.276
20	1.177	-1.057	.326	1.359	-.833	.271
25	1.352	-.915	.335	1.537	-.674	.278
30	1.491	-.759	.335	1.696	-.495	.274
35	1.593	-.601	.333	1.785	-.315	.271
40	1.684	-.418	.321	1.872	-.111	.270
45	1.750	-.240	.316	1.927	.073	.273
50	1.791	-.070	.319	1.940	.244	.279
55	1.808	.095	.338	1.924	.390	.304
60	1.791	.229	.344	1.885	.517	.326
65	1.761	.356	.352	1.832	.629	.350
70	1.736	.495	.386	1.745	.711	.378
75	1.688	.590	.420	1.624	.733	.421
80	1.636	.671	.448	1.421	.712	.427
	$C_{T,s} = 0.60$			$C_{T,s} = 0.30$		
5	0.850	-0.815	0.122	1.023	-0.339	-0.065
10	1.134	-.723	.133	1.374	-.230	-.035
15	1.426	-.601	.149	1.712	-.108	-.028
20	1.694	-.444	.161	2.050	.058	-.007
25	1.917	-.245	.154	2.322	.284	-.033
30	2.060	-.038	.143	2.480	.517	-.051
35	2.150	.154	.142	2.509	.714	-.050
40	2.209	.371	.149	1.937	.763	-.063
45	2.216	.553	.155			
50	2.178	.713	.163			
55	2.120	.854	.190			
60	1.691	.844	.190			

TABLE 21.- AERODYNAMIC DATA FOR UP-AT-TIP ROTATION, BASIC LEADING EDGE, FENCES ON, AND $\delta_f = 40^o$

α, deg	$C_{L,s}$	$C_{D,s}$	$C_{m,s}$	$C_{L,s}$	$C_{D,s}$	$C_{m,s}$
	$C_{T,s} = 0.90$			$C_{T,s} = 0.80$		
5	0.834	-1.208	0.225	0.995	-1.018	0.141
10	1.036	-1.117	.232	1.223	-.912	.162
15	1.213	-1.009	.235	1.423	-.789	.166
20	1.369	-.871	.240	1.633	-.615	.153
25	1.532	-.712	.239	1.818	-.426	.153
30	1.661	-.539	.237	1.932	-.224	.159
35	1.755	-.352	.225	1.994	-.035	.162
40	1.829	-.158	.231	2.016	.160	.159
45	1.852	.009	.239	2.018	.320	.182
50	1.855	.163	.246	1.994	.459	.213
55	1.839	.319	.255	1.942	.572	.238
60	1.788	.421	.281	1.884	.682	.261
65	1.746	.516	.310	1.814	.777	.288
70	1.695	.607	.342	1.703	.816	.336
75	1.639	.671	.383	1.568	.817	.381
80	1.586	.733	.414	1.347	.726	.401
	$C_{T,s} = 0.60$			$C_{T,s} = 0.30$		
5	1.186	-0.669	0.014	1.428	-0.166	-0.178
10	1.469	-.556	.014	1.784	-.041	-.168
15	1.761	-.400	.019	2.122	.100	-.164
20	1.995	-.201	.006	2.417	.293	-.147
25	2.190	.009	.011	2.638	.548	-.166
30	2.270	.217	.010	2.724	.785	-.191
35	2.299	.409	.019	2.693	.982	-.170
40	2.304	.607	.044	2.561	1.146	-.153
45	2.251	.752	.065	1.775	.975	-.092
50	2.205	.903	.092			
55	2.117	1.018	.124			
60	1.584	.873	.165			

TABLE 22.- AERODYNAMIC DATA FOR UP-AT-TIP ROTATION, BASIC LEADING EDGE, FENCES ON, AND $\delta_f = 60^o$

α, deg	$C_{L,s}$	$C_{D,s}$	$C_{m,s}$	$C_{L,s}$	$C_{D,s}$	$C_{m,s}$
	$C_{T,s} = 0.90$			$C_{T,s} = 0.80$		
5	0.934	-1.110	0.198	1.082	-0.919	0.115
10	1.109	-1.014	.210	1.308	-.801	.135
15	1.272	-.908	.223	1.523	-.648	.118
20	1.417	-.755	.216	1.728	-.459	.100
25	1.603	-.564	.192	1.859	-.275	.125
30	1.710	-.381	.188	1.965	-.086	.134
35	1.795	-.192	.196	1.982	.096	.140
40	1.835	-.016	.206	1.994	.278	.147
45	1.839	.141	.207	1.990	.437	.156
50	1.837	.315	.213	1.929	.542	.188
55	1.808	.450	.237	1.868	.652	.214
60	1.743	.515	.260	1.810	.760	.235
65	1.699	.587	.287	1.729	.845	.263
70	1.639	.639	.332	1.635	.896	.316
75	1.584	.684	.380	1.420	.801	.365
80	1.531	.720	.417	1.270	.728	.395
	$C_{T,s} = 0.60$			$C_{T,s} = 0.30$		
5	1.288	-0.554	-0.016	1.635	-0.017	-0.241
10	1.608	-.420	-.009	1.907	.104	-.197
15	1.860	-.277	-.005	2.209	.242	-.183
20	2.073	-.078	.004	2.445	.434	-.180
25	2.216	.140	.009	2.626	.677	-.149
30	2.278	.355	.008	2.646	.896	-.140
35	2.269	.534	.018	2.578	1.070	-.105
40	2.234	.695	.058	1.879	.952	-.047
45	2.180	.823	.086			
50	2.107	.954	.098			
55	1.818	.980	.124			
60	1.457	.825	.182			

TABLE 23.- AERODYNAMIC DATA FOR UP-AT-TIP ROTATION, INBOARD SLAT ON, AND $\delta_f = 20^o$

α, deg	$C_{L,s}$	$C_{D,s}$	$C_{m,s}$	$C_{L,s}$	$C_{D,s}$	$C_{m,s}$
	$C_{T,s} = 0.90$			$C_{T,s} = 0.80$		
5	0.496	-1.283	0.335	0.582	-1.139	0.278
10	.712	-1.258	.356	.819	-1.076	.297
15	.905	-1.190	.379	1.070	-.988	.296
20	1.091	-1.094	.371	1.321	-.855	.289
25	1.260	-.957	.367	1.555	-.697	.274
30	1.409	-.808	.360	1.688	-.522	.266
35	1.551	-.650	.355	1.778	-.341	.266
40	1.680	-.447	.337	1.943	-.120	.271
45	1.749	-.281	.327	1.976	.060	.279
50	1.780	-.114	.337	1.988	.230	.288
55	1.786	.040	.346	1.955	.387	.311
60	1.769	.172	.345	1.929	.527	.326
65	1.753	.317	.359	1.880	.642	.369
70	1.709	.425	.386	1.810	.735	.397
75	1.682	.546	.407	1.715	.774	.425
80	1.641	.632	.444	1.479	.740	.441
	$C_{T,s} = 0.60$			$C_{T,s} = 0.30$		
5	0.704	-0.808	0.149	0.839	-0.345	-0.012
10	1.028	-.734	.157	1.272	-.250	-.023
15	1.335	-.619	.158	1.644	-.135	-.010
20	1.680	-.472	.151	2.021	.027	.001
25	1.893	-.267	.152	2.231	.212	-.010
30	1.906	-.125	.152	2.181	.390	-.030
35	1.913	.031	.163	2.082	.570	-.019
40	1.964	.209	.190			
45	2.040	.454	.179			
50	2.010	.641	.178			
55	1.823	.724	.183			

TABLE 24.- AERODYNAMIC DATA FOR UP-AT-TIP ROTATION,

INBOARD SLAT ON, AND $\delta_f = 40^o$

α, deg	$C_{L,s}$	$C_{D,s}$	$C_{m,s}$	$C_{L,s}$	$C_{D,s}$	$C_{m,s}$
	$C_{T,s} = 0.90$			$C_{T,s} = 0.80$		
5	0.689	-1.218	0.285	0.818	-1.052	0.204
10	.885	-1.154	.289	1.067	-.948	.200
15	1.068	-1.060	.297	1.331	-.823	.191
20	1.250	-.926	.286	1.587	-.643	.158
25	1.443	-.763	.269	1.804	-.459	.149
30	1.580	-.585	.235	1.928	-.246	.159
35	1.703	-.400	.228	2.019	-.055	.156
40	1.789	-.198	.222	2.059	.146	.160
45	1.817	-.034	.229	2.042	.302	.174
50	1.820	.108	.241	1.996	.441	.205
55	1.793	.234	.261	1.958	.568	.228
60	1.772	.361	.276	1.901	.675	.254
65	1.725	.462	.301	1.837	.777	.305
70	1.679	.545	.340	1.755	.818	.358
75	1.630	.631	.374	1.628	.832	.381
80	1.568	.699	.401			
	$C_{T,s} = 0.60$			$C_{T,s} = 0.30$		
5	0.968	-0.694	0.047	1.225	-0.196	-0.154
10	1.321	-.591	.049	1.674	-.075	-.201
15	1.693	-.432	.021	2.061	.098	-.167
20	2.042	-.227	-.004	2.423	.286	-.159
25	2.209	-.022	.020	2.564	.497	-.162
30	2.108	.119	.035	2.399	.649	-.146
35	2.057	.241	.075	2.448	.879	-.143
40	2.038	.389	.099	1.946	.875	-.077
45	2.159	.636	.108			
50	2.133	.800	.134			
55	1.752	.815	.126			
60	1.592	.814	.189			

TABLE 25.- AERODYNAMIC DATA FOR UP-AT-TIP ROTATION,
INBOARD SLAT ON, AND $\delta_f = 60^o$

α, deg	$C_{L,s}$	$C_{D,s}$	$C_{m,s}$	$C_{L,s}$	$C_{D,s}$	$C_{m,s}$
	$C_{T,s}$ = 0.90			$C_{T,s}$ = 0.80		
5	0.758	-1.152	0.263	0.879	-0.960	0.174
10	.954	-1.079	.276	1.132	-.856	.163
15	1.135	-.977	.257	1.394	-.703	.151
20	1.309	-.822	.253	1.651	-.495	.116
25	1.475	-.632	.230	1.849	-.300	.114
30	1.645	-.426	.195	1.961	-.112	.121
35	1.722	-.249	.196	2.029	.088	.124
40	1.772	-.069	.203	2.059	.279	.144
45	1.787	.089	.207	2.003	.427	.150
50	1.787	.248	.221	1.944	.548	.182
55	1.752	.362	.232	1.898	.669	.212
60	1.705	.439	.257	1.854	.786	.243
65	1.663	.530	.295	1.757	.852	.265
70	1.607	.584	.336	1.674	.864	.363
75	1.549	.635	.365	1.542	.848	.377
80	1.502	.676	.407			
	$C_{T,s}$ = 0.60			$C_{T,s}$ = 0.30		
5	1.093	-0.605	0.037	1.399	-0.107	-0.169
10	1.453	-.467	.050	1.809	.061	-.182
15	1.788	-.289	.054	2.145	.215	-.196
20	2.090	-.090	.040	2.450	.416	-.163
25	2.258	.136	.043	2.579	.626	-.170
30	2.111	.260	.073	2.324	.739	-.118
35	2.020	.333	.074	2.378	.972	-.116
40	1.989	.465	.112	1.849	.928	-.070
45	2.084	.732	.095			
50	1.776	.769	.121			

TABLE 26.- AERODYNAMIC DATA FOR UP-AT-TIP ROTATION, INBOARD SLAT ON, FENCES ON, AND $\delta_f = 20^o$

α, deg	$C_{L,s}$	$C_{D,s}$	$C_{m,s}$	$C_{L,s}$	$C_{D,s}$	$C_{m,s}$
	$C_{T,s} = 0.90$			$C_{T,s} = 0.80$		
5	0.498	-1.300	0.342	0.566	-1.125	0.277
10	.688	-1.259	.355	.786	-1.072	.303
15	.864	-1.177	.369	1.045	-.987	.306
20	1.060	-1.079	.362	1.282	-.847	.291
25	1.229	-.953	.365	1.482	-.697	.294
30	1.386	-.794	.356	1.650	-.502	.272
35	1.516	-.641	.353	1.750	-.307	.256
40	1.619	-.463	.344	1.853	-.105	.262
45	1.686	-.286	.339	1.897	.079	.267
50	1.746	-.112	.336	1.912	.247	.270
55	1.767	.048	.337	1.909	.398	.292
60	1.738	.181	.342	1.876	.531	.313
65	1.713	.309	.359	1.816	.647	.349
70	1.683	.424	.378	1.725	.714	.364
75	1.653	.560	.423	1.592	.720	.407
80	1.605	.658	.458			
	$C_{T,s} = 0.60$			$C_{T,s} = 0.30$		
5	0.694	-0.798	0.153	0.810	-0.343	-0.019
10	1.005	-.729	.155	1.240	-.251	-.018
15	1.336	-.616	.157	1.642	-.121	-.006
20	1.663	-.453	.136	1.915	.032	-.013
25	1.929	-.251	.145	1.911	.189	-.048
30	2.084	-.039	.136	1.691	.400	-.044
35	2.139	.159	.137			
40	2.173	.365	.129			
45	2.158	.562	.145			

TABLE 27.- AERODYNAMIC DATA FOR UP-AT-TIP ROTATION, INBOARD SLAT ON, FENCES ON, AND $\delta_f = 40^o$

α, deg	$C_{L,s}$	$C_{D,s}$	$C_{m,s}$	$C_{L,s}$	$C_{D,s}$	$C_{m,s}$
	$C_{T,s} = 0.90$			$C_{T,s} = 0.80$		
5	0.663	-1.189	0.268	0.703	-1.037	0.238
10	.850	-1.147	.295	.952	-.973	.262
15	1.036	-1.056	.292	1.215	-.845	.236
20	1.219	-.926	.285	1.482	-.677	.229
25	1.389	-.772	.289	1.706	-.475	.189
30	1.559	-.578	.249	1.881	-.238	.181
35	1.662	-.405	.231	1.948	-.051	.174
40	1.746	-.211	.232	1.982	.137	.181
45	1.808	-.032	.239	1.995	.303	.201
50	1.818	.130	.250	1.957	.430	.229
55	1.807	.252	.266	1.895	.540	.246
60	1.777	.363	.291	1.843	.645	.283
65	1.736	.466	.311	1.778	.747	.307
70	1.675	.548	.343	1.681	.802	.354
75	1.633	.644	.389	1.601	.826	.413
80	1.580	.719	.425			
	$C_{T,s} = 0.60$			$C_{T,s} = 0.30$		
5	0.985	-0.687	-0.062	1.222	-0.212	-0.132
10	1.314	-.585	.064	1.650	-.071	-.151
15	1.687	-.414	.028	2.021	.099	-.158
20	1.996	-.203	.004	2.380	.280	-.135
25	2.194	.019	.015	2.312	.461	-.135
30	2.293	.245	.005	2.333	.673	-.164
35	2.312	.435	.023	2.223	.852	-.147
40	2.313	.621	.056			
45	2.239	.755	.076			
50	1.983	.845	.084			
55	1.818	.886	.126			

TABLE 28.- AERODYNAMIC DATA FOR UP-AT-TIP ROTATION, INBOARD SLAT ON, FENCES ON, AND $\delta_f = 60^o$

α, deg	$C_{L,s}$	$C_{D,s}$	$C_{m,s}$	$C_{L,s}$	$C_{D,s}$	$C_{m,s}$
	$C_{T,s} = 0.90$			$C_{T,s} = 0.80$		
5	0.705	-1.138	0.257	0.870	-0.948	0.178
10	.905	-1.076	.267	1.127	-.860	.177
15	1.083	-.968	.259	1.384	-.700	.151
20	1.257	-.833	.261	1.671	-.506	.118
25	1.416	-.632	.234	1.835	-.299	.118
30	1.585	-.445	.203	1.930	-.107	.132
35	1.665	-.258	.191	1.968	.088	.129
40	1.723	-.082	.192	1.990	.278	.133
45	1.785	.105	.206	1.955	.417	.156
50	1.801	.263	.213	1.915	.524	.185
55	1.773	.408	.223	1.838	.644	.202
60	1.745	.521	.250	1.802	.752	.239
65	1.678	.553	.292	1.735	.849	.265
70	1.625	.607	.337	1.639	.888	.312
75	1.580	.680	.374	1.526	.851	.369
80	1.508	.719	.421			
	$C_{T,s} = 0.60$			$C_{T,s} = 0.30$		
5	1.097	-0.593	0.044	1.432	-0.071	-0.183
10	1.448	-.456	.019	1.815	.077	-.183
15	1.773	-.286	-.003	2.151	.212	-.164
20	2.044	-.082	-.014	2.471	.430	-.158
25	2.225	.145	-.004	2.388	.611	-.181
30	2.312	.374	-.001	2.370	.827	-.182
35	2.317	.554	.008	2.269	.986	-.162
40	2.291	.715	.046			
45	2.220	.827	.092			
50	2.157	.956	.111			
55	2.050	1.045	.145			
60	1.532	.890	.183			

TABLE 29.- AERODYNAMIC DATA FOR UP-AT-TIP ROTATION, FULL-SPAN SLAT ON, FENCES ON, AND $\delta_f = 20^o$

α, deg	$C_{L,s}$	$C_{D,s}$	$C_{m,s}$	$C_{L,s}$	$C_{D,s}$	$C_{m,s}$
	$C_{T,s} = 0.90$			$C_{T,s} = 0.80$		
5	0.476	-1.292	0.351	0.543	-1.121	0.279
10	.670	-1.239	.349	.781	-1.065	.293
15	.847	-1.168	.362	1.028	-.968	.299
20	1.039	-1.073	.362	1.280	-.841	.293
25	1.216	-.948	.353	1.492	-.681	.288
30	1.363	-.801	.364	1.672	-.500	.272
35	1.499	-.637	.347	1.792	-.300	.267
40	1.600	-.467	.341	1.872	-.104	.268
45	1.678	-.285	.331	1.915	.075	.283
50	1.719	-.111	.328	1.925	.240	.290
55	1.747	.047	.341	1.926	.396	.310
60	1.727	.179	.342	1.895	.536	.340
65	1.702	.304	.367	1.841	.654	.373
70	1.677	.440	.380	1.766	.751	.391
75	1.654	.559	.424	1.672	.781	.445
80	1.612	.676	.458	1.580	.820	.475
	$C_{T,s} = 0.60$			$C_{T,s} = 0.30$		
5	0.650	-0.810	0.149	0.704	-0.340	0.001
10	.980	-.734	.150	1.190	-.251	-.035
15	1.319	-.620	.156	1.619	-.119	-.021
20	1.660	-.439	.150	2.019	.045	-.015
25	1.937	-.270	.162	2.356	.282	-.025
30	2.077	-.036	.146	2.546	.542	-.018
35	2.157	.159	.152	2.562	.761	-.025
40	2.229	.372	.169	2.597	.952	.006
45	2.247	.558	.183	2.565	1.115	.021
50	2.214	.709	.205	2.505	1.241	.069
55	2.179	.870	.230	1.997	1.118	.085
60	2.131	.989	.272			
65	2.027	1.068	.303			

TABLE 30.- AERODYNAMIC DATA FOR UP-AT-TIP ROTATION, FULL-SPAN SLAT ON, FENCES ON, AND $\delta_f = 40^o$

α, deg	$C_{L,s}$	$C_{D,s}$	$C_{m,s}$	$C_{L,s}$	$C_{D,s}$	$C_{m,s}$
	$C_{T,s} = 0.90$			$C_{T,s} = 0.80$		
5	0.628	-1.213	0.279	0.714	-1.040	0.197
10	.819	-1.145	.288	.971	-.950	.212
15	1.005	-1.062	.290	1.247	-.821	.189
20	1.197	-.935	.278	1.515	-.653	.171
25	1.371	-.775	.277	1.744	-.443	.148
30	1.534	-.587	.252	1.896	-.223	.154
35	1.641	-.410	.225	1.961	-.033	.144
40	1.746	-.195	.227	1.997	.153	.163
45	1.792	-.016	.228	2.009	.329	.179
50	1.813	.143	.241	1.968	.461	.213
55	1.794	.279	.256	1.933	.581	.245
60	1.742	.384	.269	1.855	.693	.247
65	1.706	.486	.304	1.807	.795	.287
70	1.657	.580	.327	1.721	.861	.338
75	1.611	.662	.384	1.626	.867	.403
80	1.555	.738	.418			
	$C_{T,s} = 0.60$			$C_{T,s} = 0.30$		
5	0.878	-0.703	0.075	1.041	-0.238	-0.098
10	1.257	-.601	.062	1.585	-.081	-.147
15	1.648	-.435	.032	2.035	.080	-.152
20	1.987	-.211	.012	2.419	.293	-.139
25	2.194	.013	.014	2.679	.541	-.140
30	2.304	.246	.013	2.745	.815	-.157
35	2.355	.447	.027	2.731	1.014	-.118
40	2.341	.628	.058	2.701	1.187	-.091
45	2.299	.766	.098	2.620	1.312	-.029
50	2.230	.906	.127			
55	2.177	1.036	.179			
60	2.086	1.118	.223			
65	1.894	1.117	.263			
70	1.520	1.000	.273			

TABLE 31.- AERODYNAMIC DATA FOR UP-AT-TIP ROTATION, FULL-SPAN SLAT ON, FENCES ON, AND $\delta_f = 60^o$

α, deg	$C_{L,s}$	$C_{D,s}$	$C_{m,s}$	$C_{L,s}$	$C_{D,s}$	$C_{m,s}$
	$C_{T,s} = 0.90$			$C_{T,s} = 0.80$		
5	0.686	-1.154	0.263	0.799	-0.966	0.198
10	.874	-1.065	.272	1.085	-.867	.187
15	1.075	-.973	.272	1.353	-.696	.151
20	1.266	-.814	.258	1.635	-.499	.129
25	1.441	-.637	.243	1.829	-.286	.126
30	1.597	-.428	.206	1.920	-.098	.137
35	1.706	-.241	.214	1.941	.088	.138
40	1.766	-.048	.210	1.989	.288	.149
45	1.793	.107	.231	1.951	.425	.175
50	1.783	.259	.240	1.903	.535	.201
55	1.771	.405	.254	1.843	.658	.214
60	1.717	.493	.269	1.796	.771	.248
65	1.660	.535	.311	1.732	.870	.276
70	1.609	.610	.344	1.627	.913	.328
75	1.551	.664	.384	1.542	.891	.389
80	1.500	.722	.431			
	$C_{T,s} = 0.60$			$C_{T,s} = 0.30$		
5	0.990	-0.630	0.048	1.278	-0.122	-0.135
10	1.402	-.491	.031	1.736	.027	-.178
15	1.772	-.294	-.006	2.140	.207	-.165
20	2.033	-.095	.006	2.493	.412	-.143
25	2.214	.144	.015	2.678	.669	-.144
30	2.310	.370	.023	2.683	.923	-.149
35	2.314	.564	.039	2.655	1.111	-.129
40	2.279	.719	.074	2.657	1.284	-.083
45	2.208	.837	.115	2.523	1.372	-.028
50	2.153	.966	.153			
55	2.073	1.062	.180			

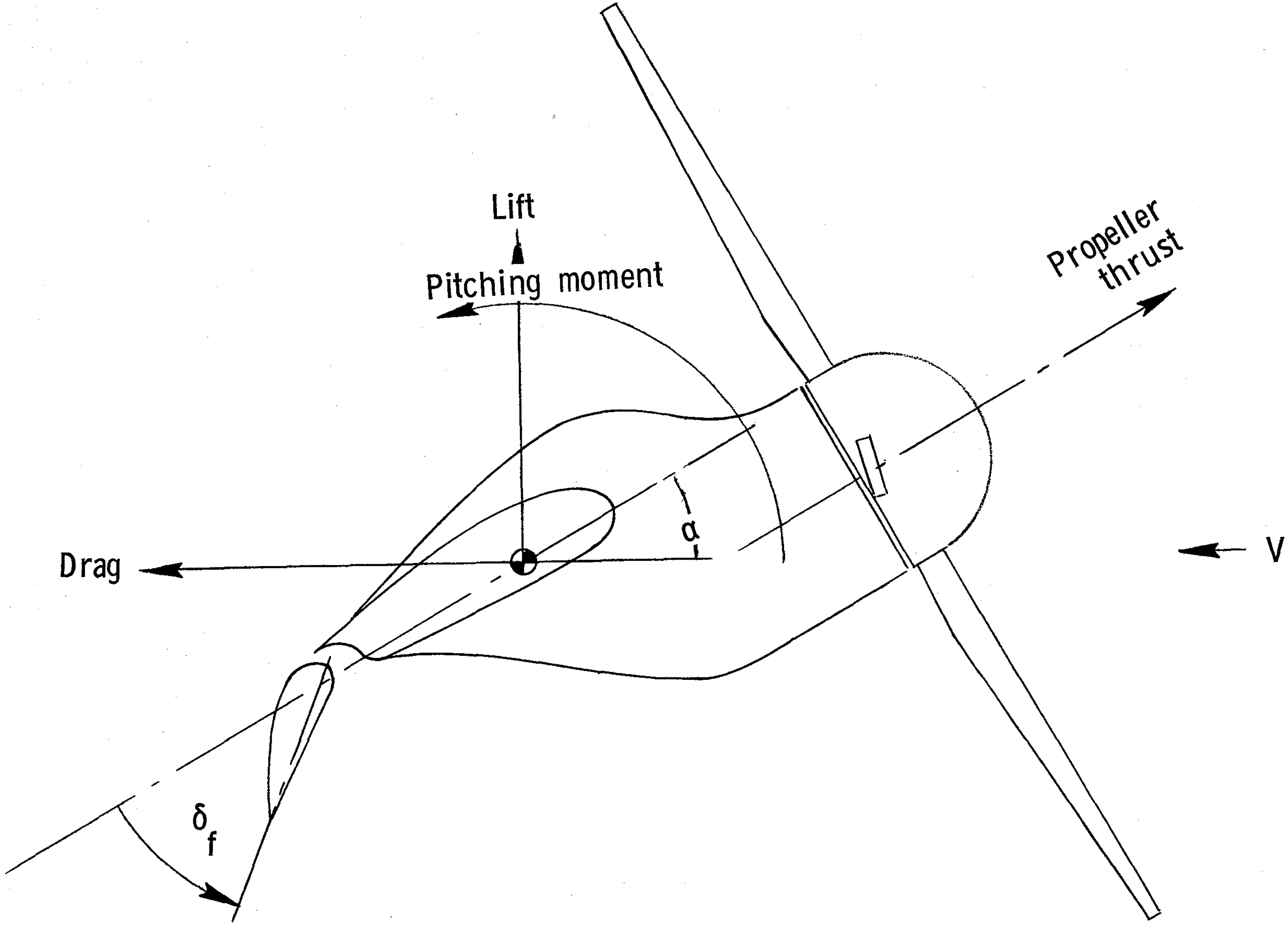

Figure 1.- The positive sense of forces, moments, and angles.

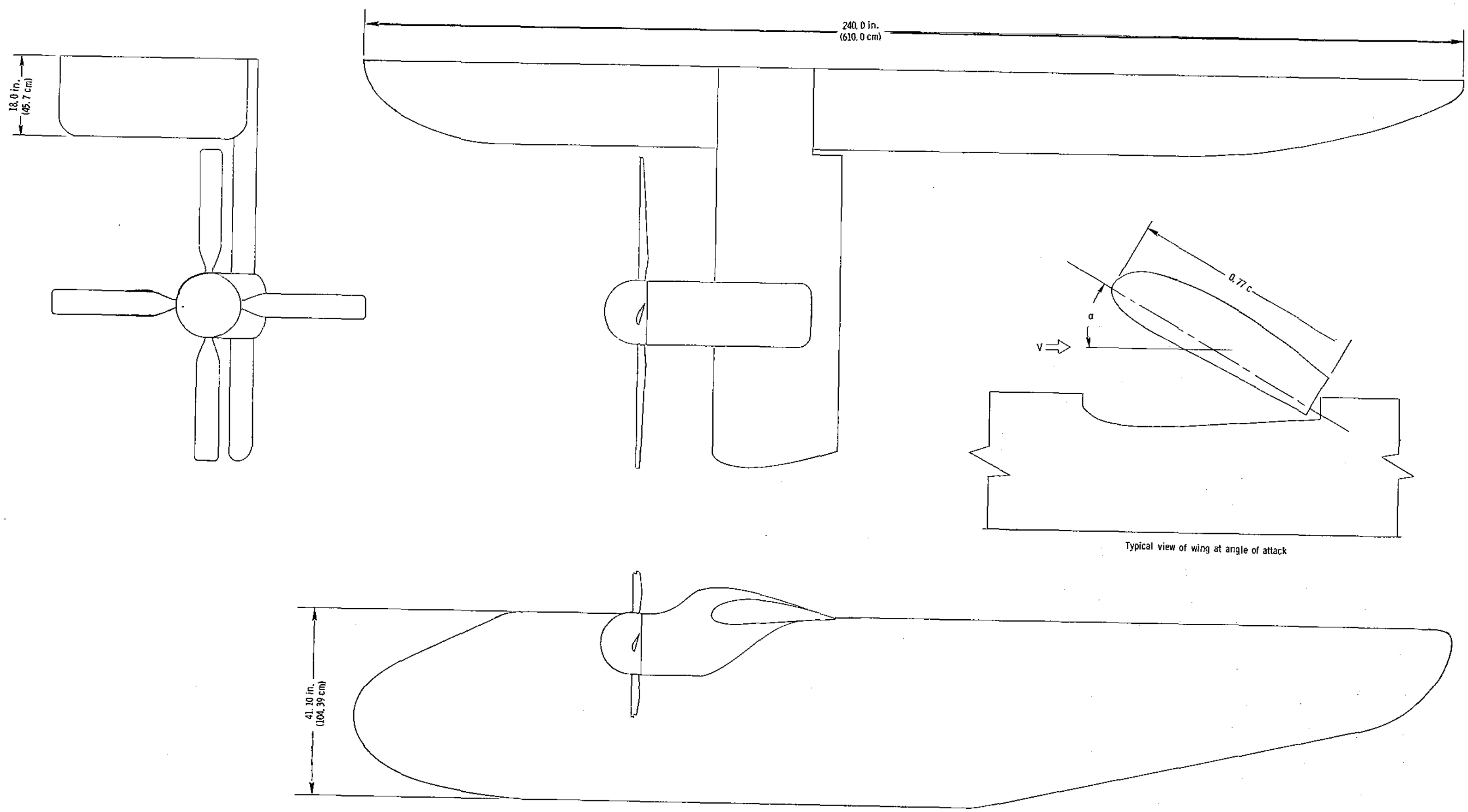

(a) Three-view drawing of the wing and fuselage.

Figure 2.- Three-view drawing and principal dimensions of the model.

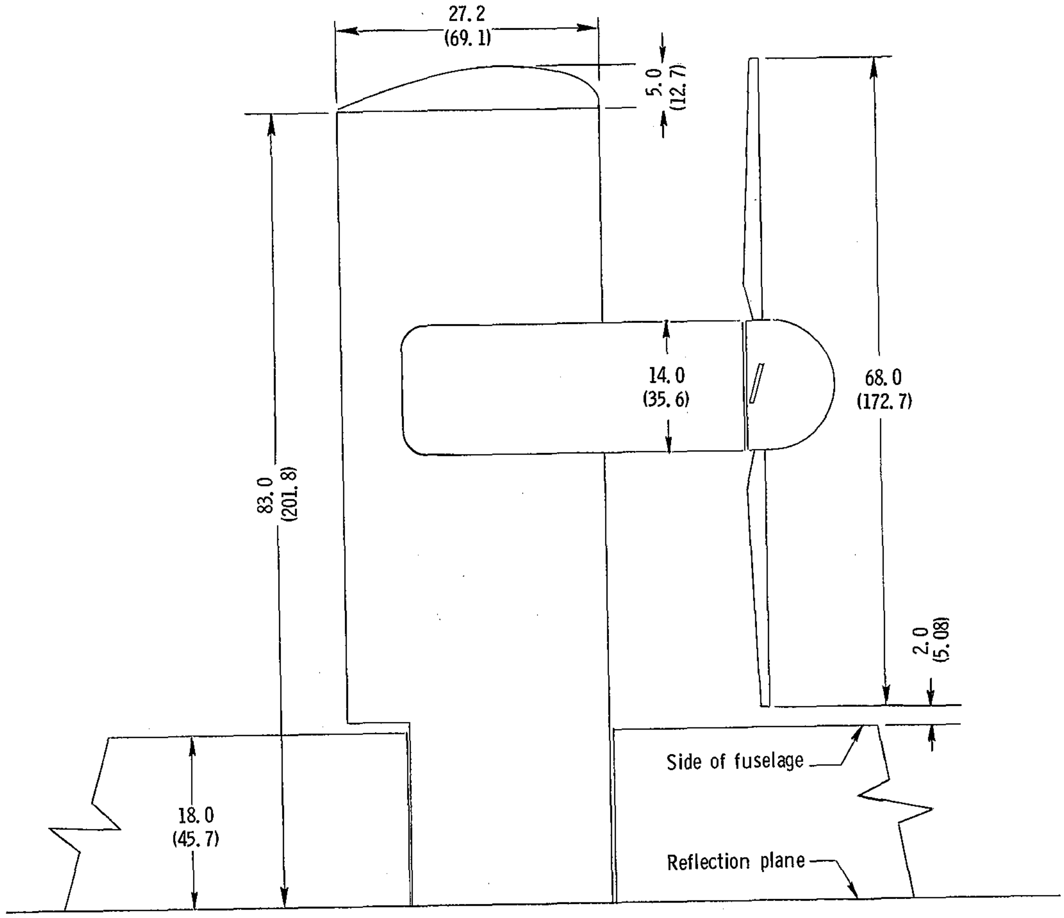

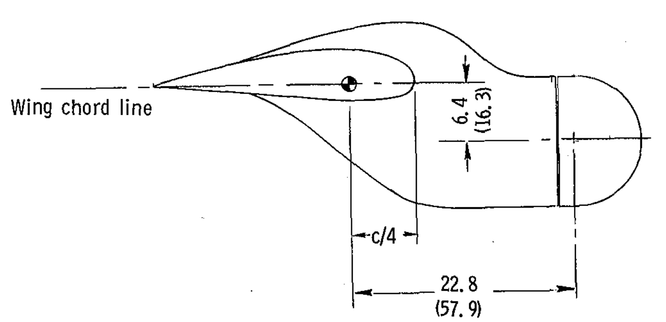

(b) Principal dimensions of wing in inches and parenthetically in centimeters.

Figure 2.- Concluded.

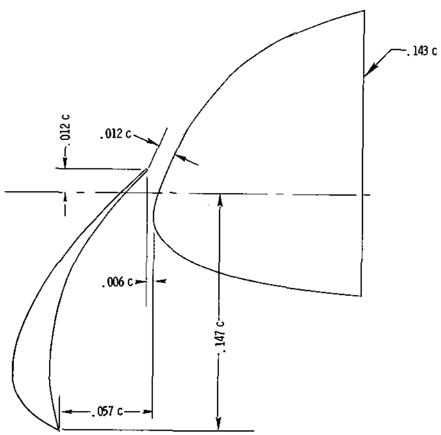

Cross section of slat

Flap nose location			Flap ordinates		
δ_f, deg	$\frac{x}{c}$	$\frac{z}{c}$	$\frac{x}{c_f}$	$\frac{y_u}{c_f}$	$\frac{y_l}{c_f}$
20	0.055	0.055	0	0	0
40	.026	.031	.013	.062	-.034
60	.005	.020	.025	.083	-.047
			.050	.114	-.066
			.075	.135	-.077
			.100	.149	-.084
			.150	.169	-.087
			.200	.182	Straight line
			.249	.188	
			.299	.192	
			.399	.186	
			.499	.170	
			.599	.146	
			.698	.116	
			.798	.083	
			.898	.045	
			.948	.027	
			.998	.005	
			1.000	.005	-.005

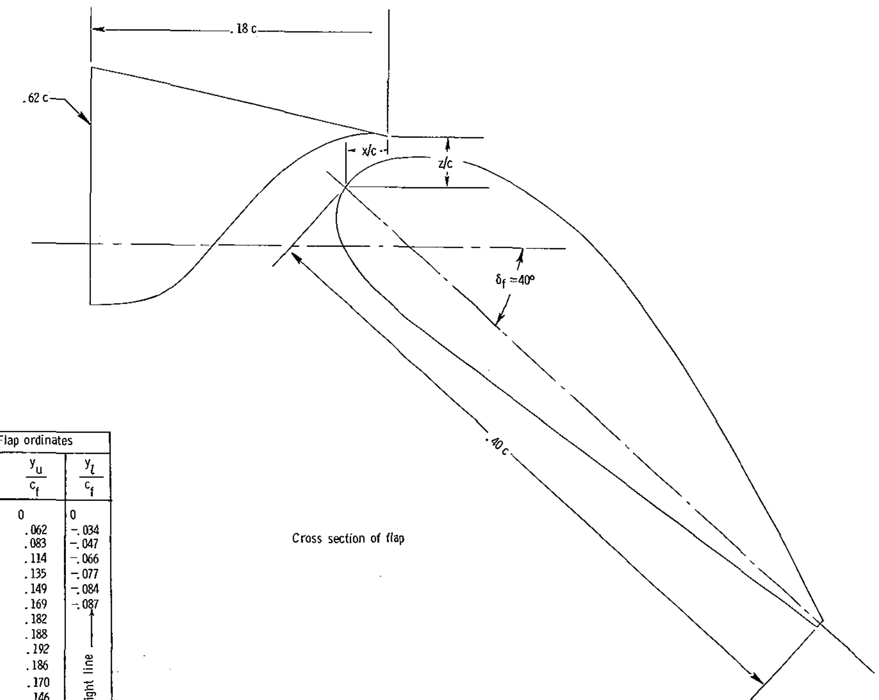

Cross section of flap

(a) Cross-sectional view of the slat and flap.

Figure 3.- Cross-sectional views of the slat, flap, and fences and fence location.

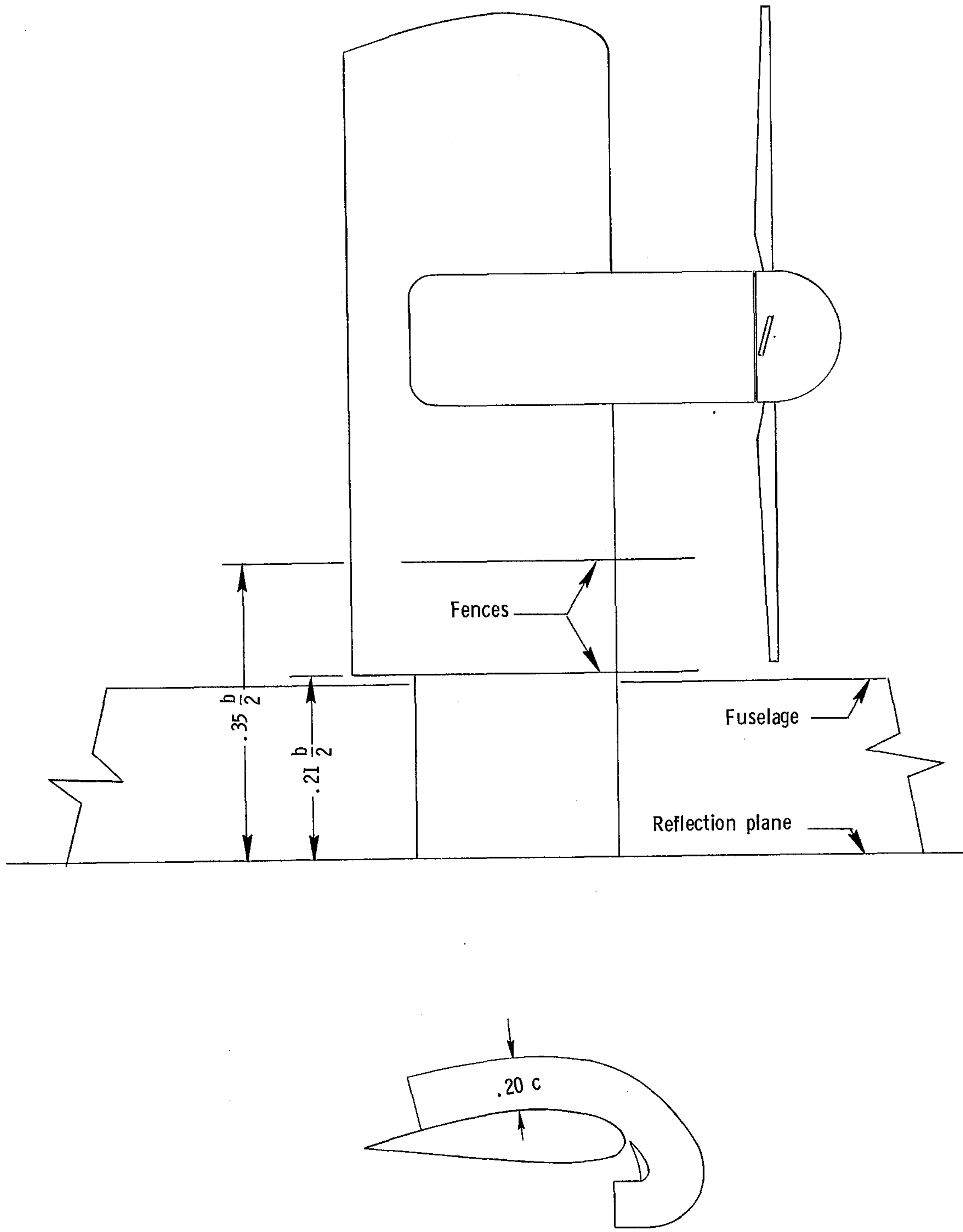

(b) Sectional view and location of fences.

Figure 3.- Concluded.

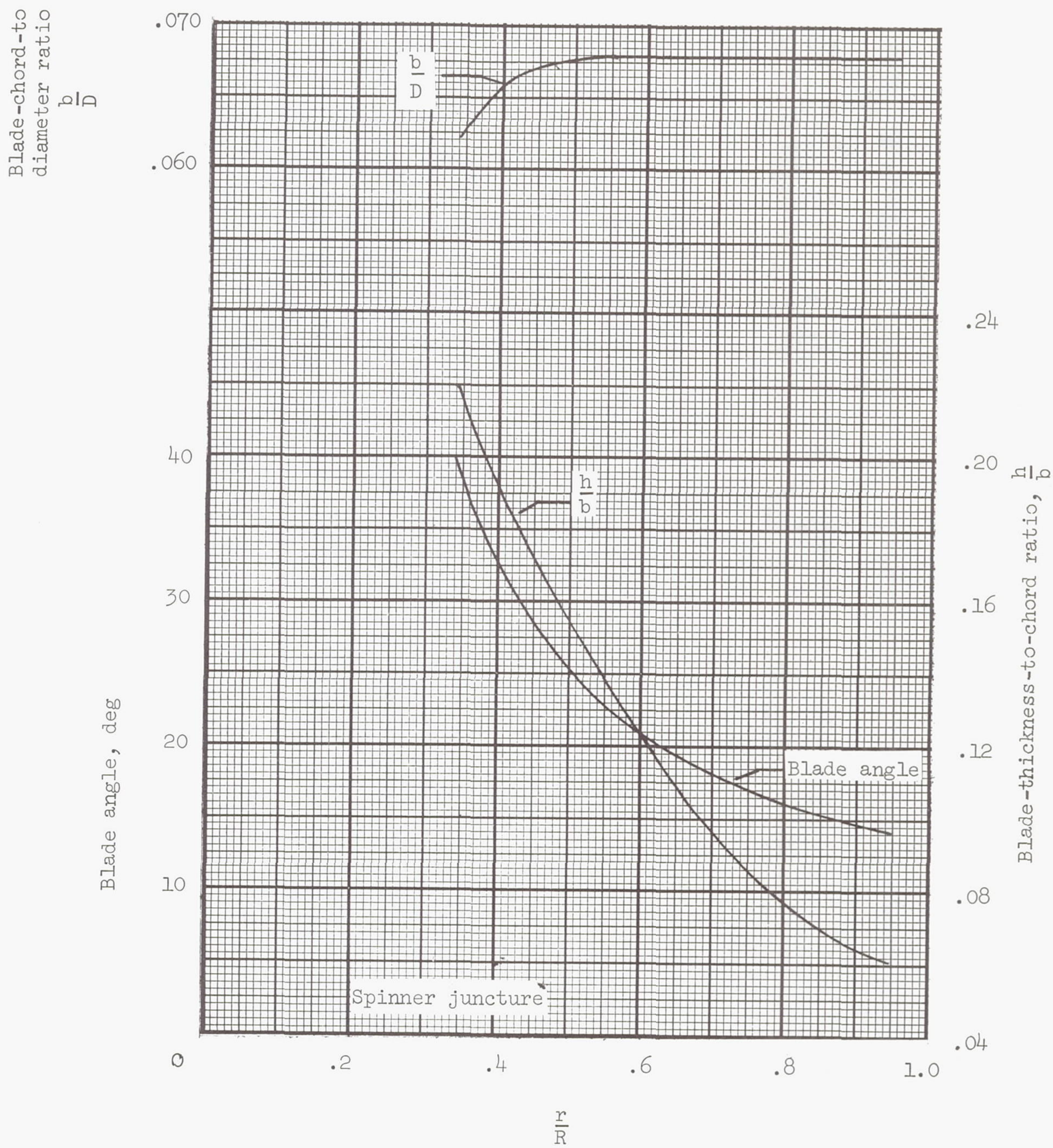

Figure 4.- Propeller blade-form curves.

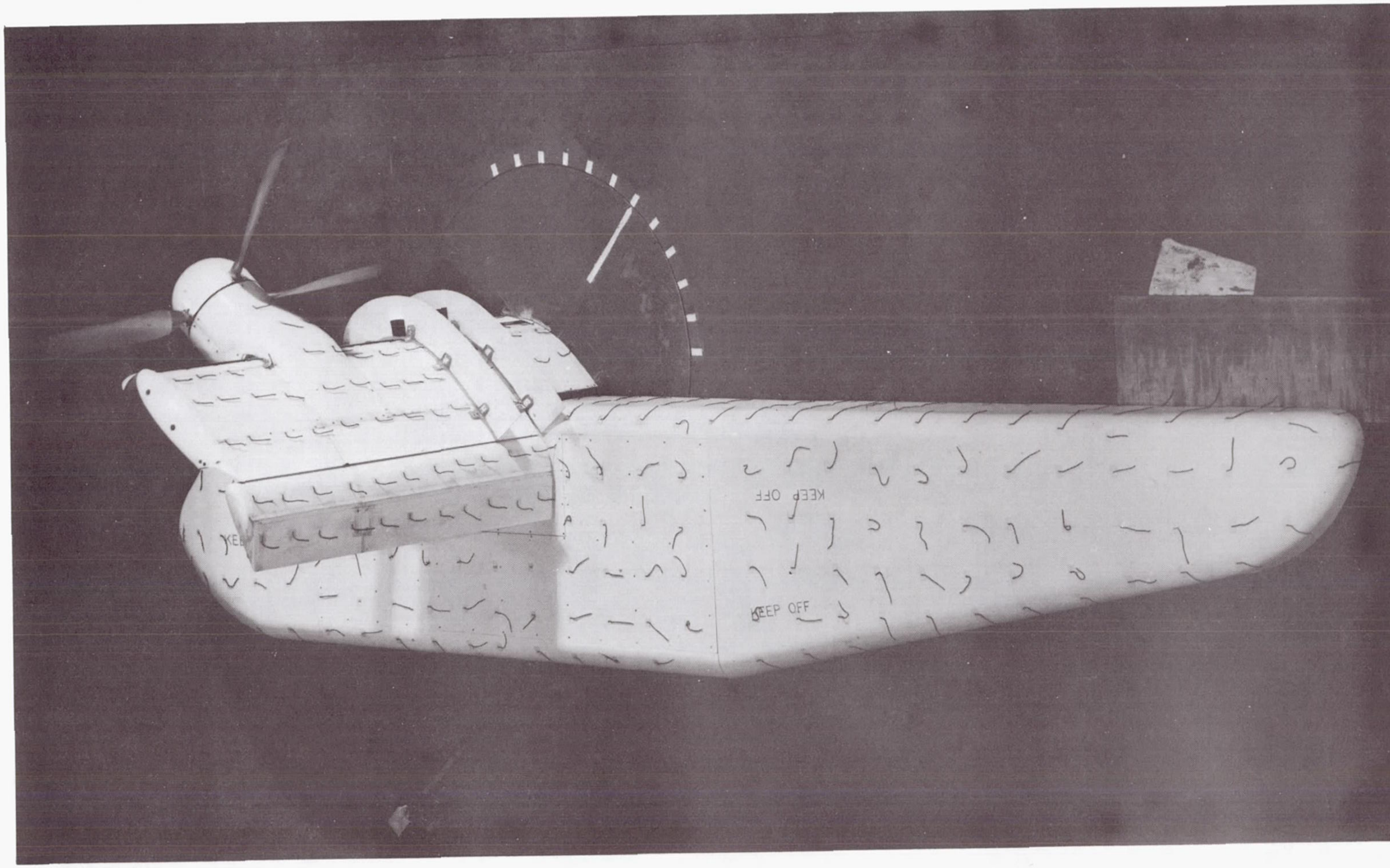

Figure 5.- Photograph of model.

L-68-10,012

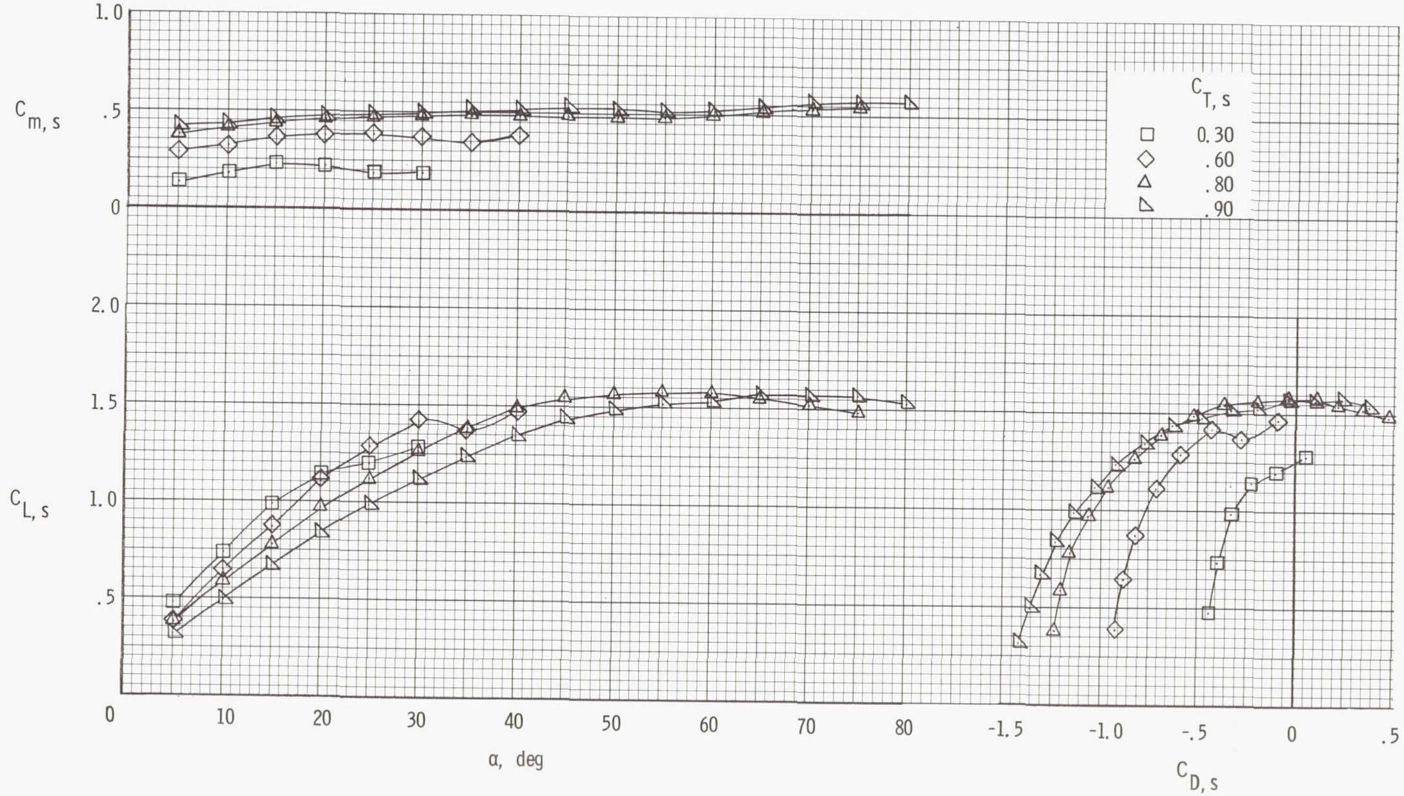

(a) Aerodynamic characteristics.

Figure 6.- Aerodynamic and flow characteristics of the wing with the propeller rotating down at the tip, basic leading edge, and $\delta_f = 0^o$.

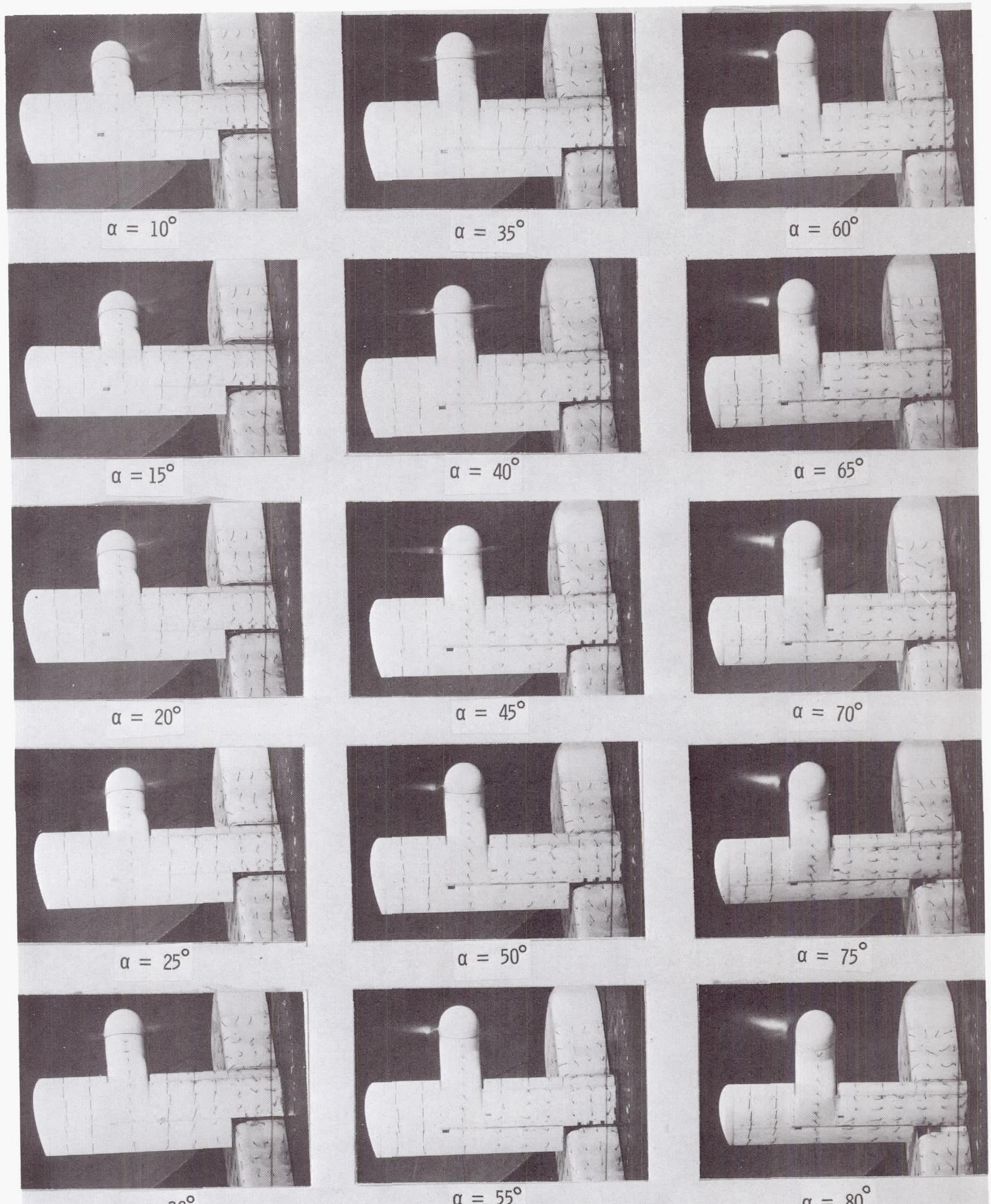

(b) Flow characteristics; $C_{T,s} = 0.90$.

Figure 6.- Continued.

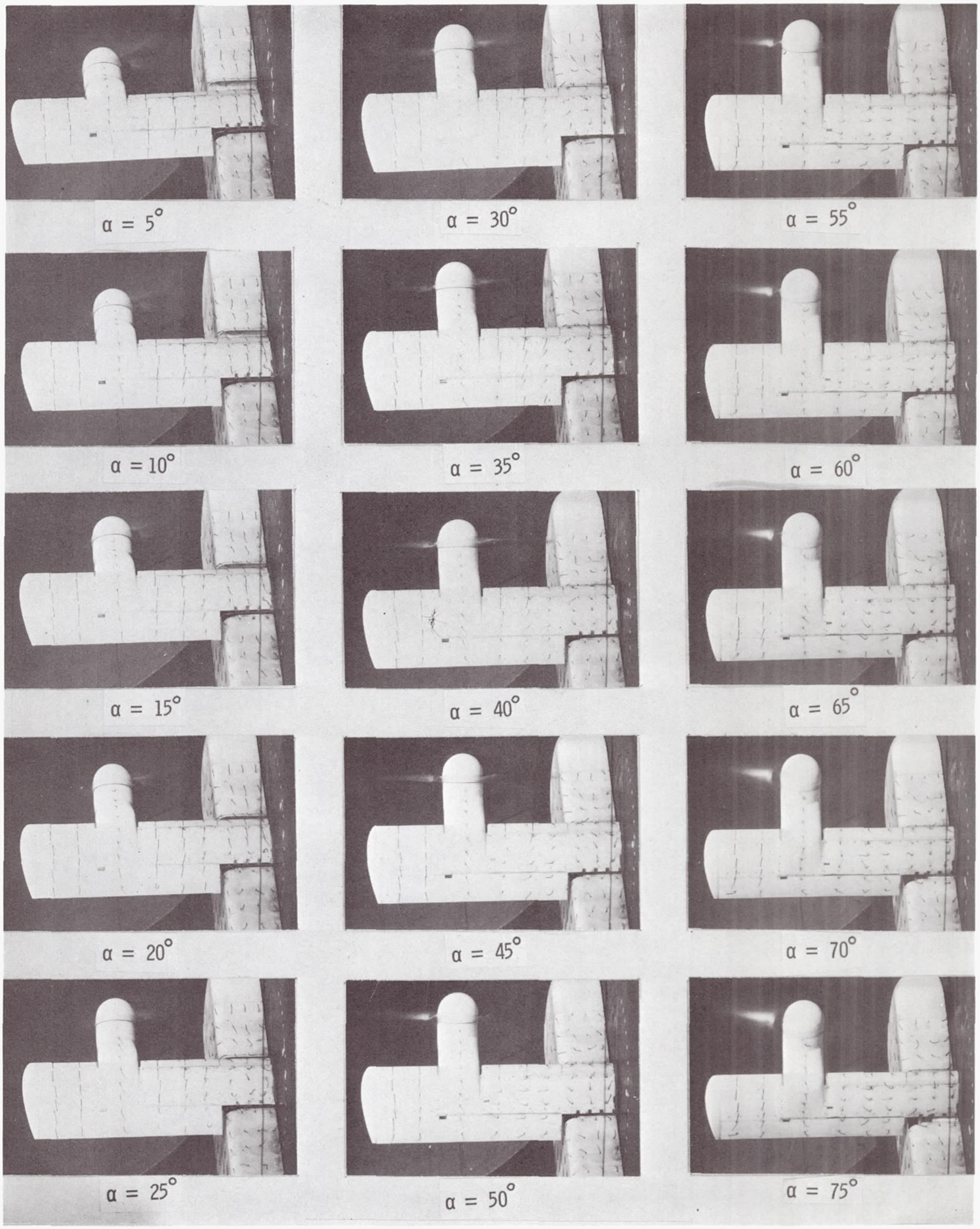

(c) Flow characteristics; $C_{T,s} = 0.80$.

Figure 6.- Continued.

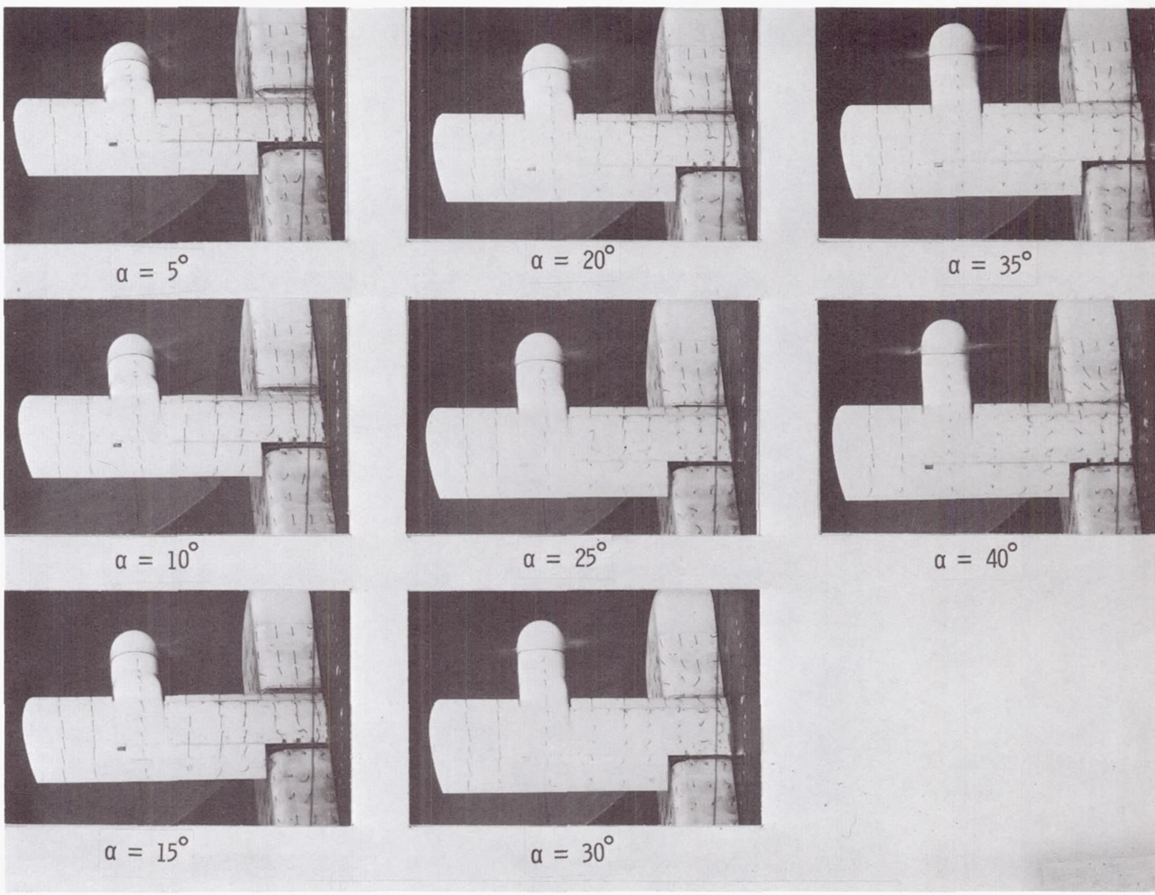

(d) Flow characteristics; $C_{T,s} = 0.60$.

Figure 6.- Continued.

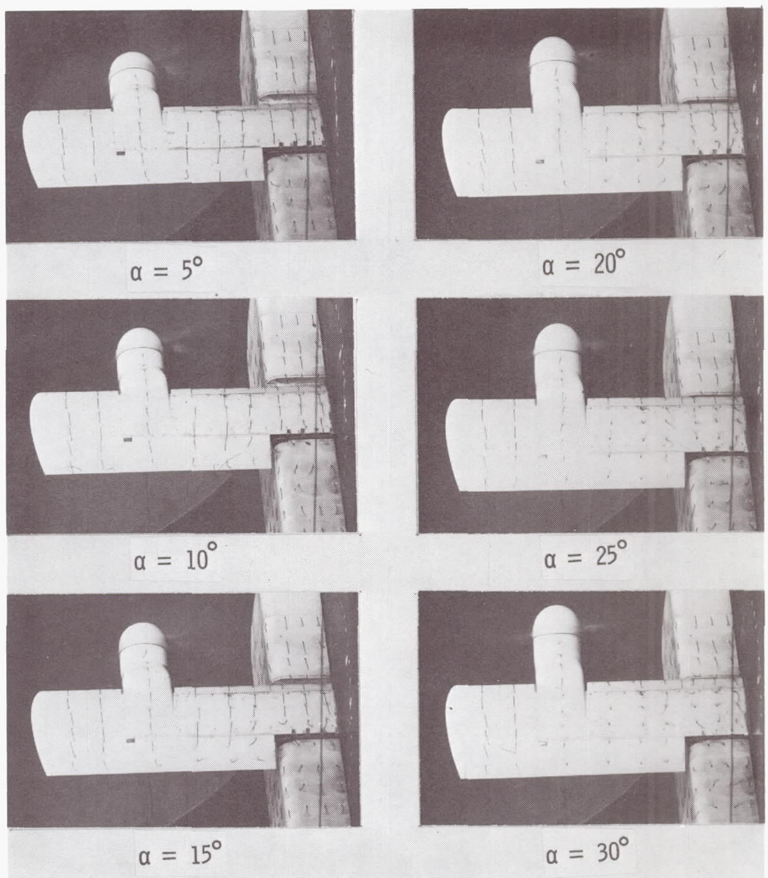

(e) Flow characteristics; $C_{T,s} = 0.30$.

Figure 6.- Concluded.

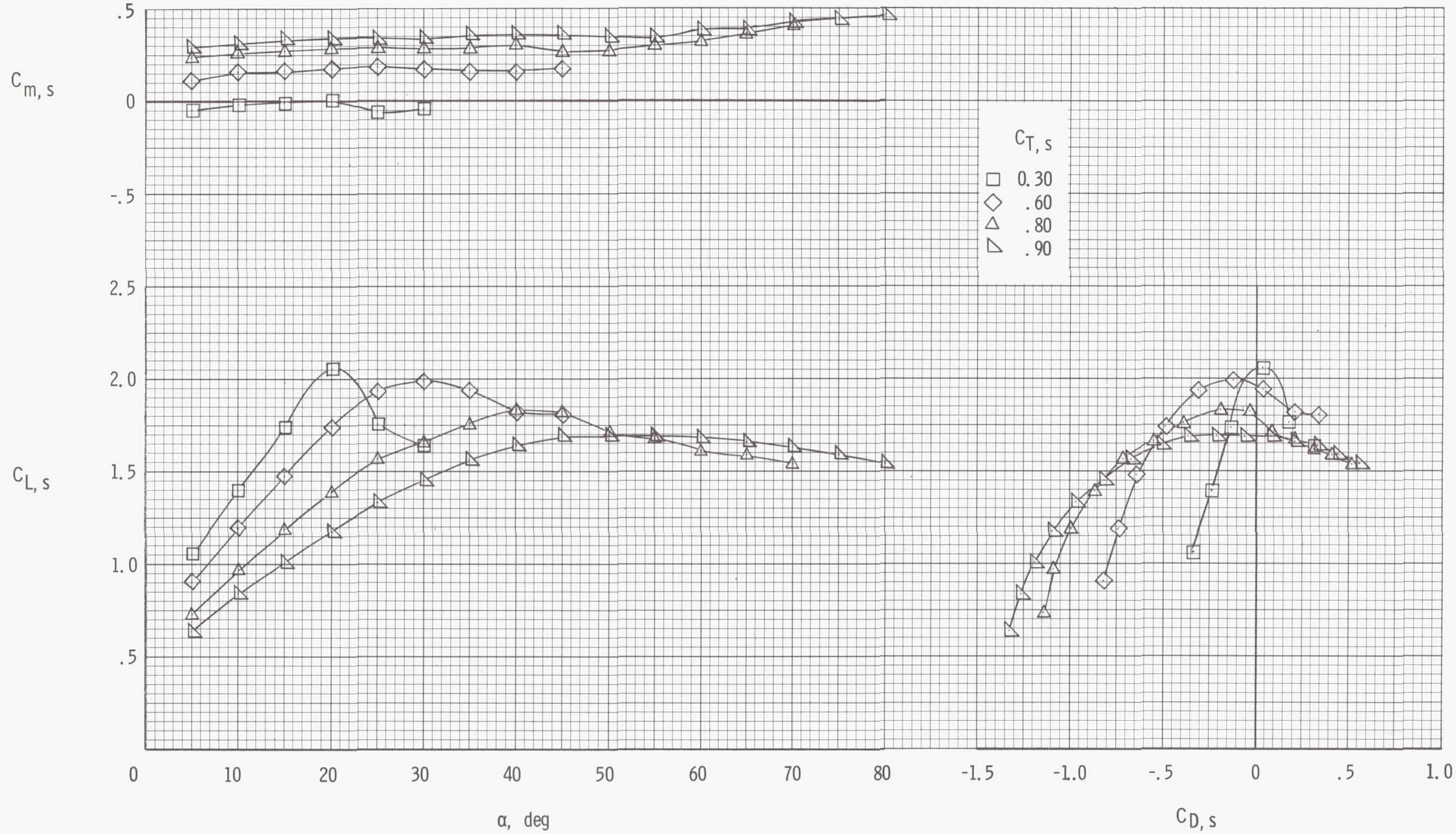

(a) Aerodynamic characteristics.

Figure 7.- Aerodynamic and flow characteristics of the wing with the propeller rotating down at the tip, basic leading edge, and $\delta_f = 20^{\circ}$.

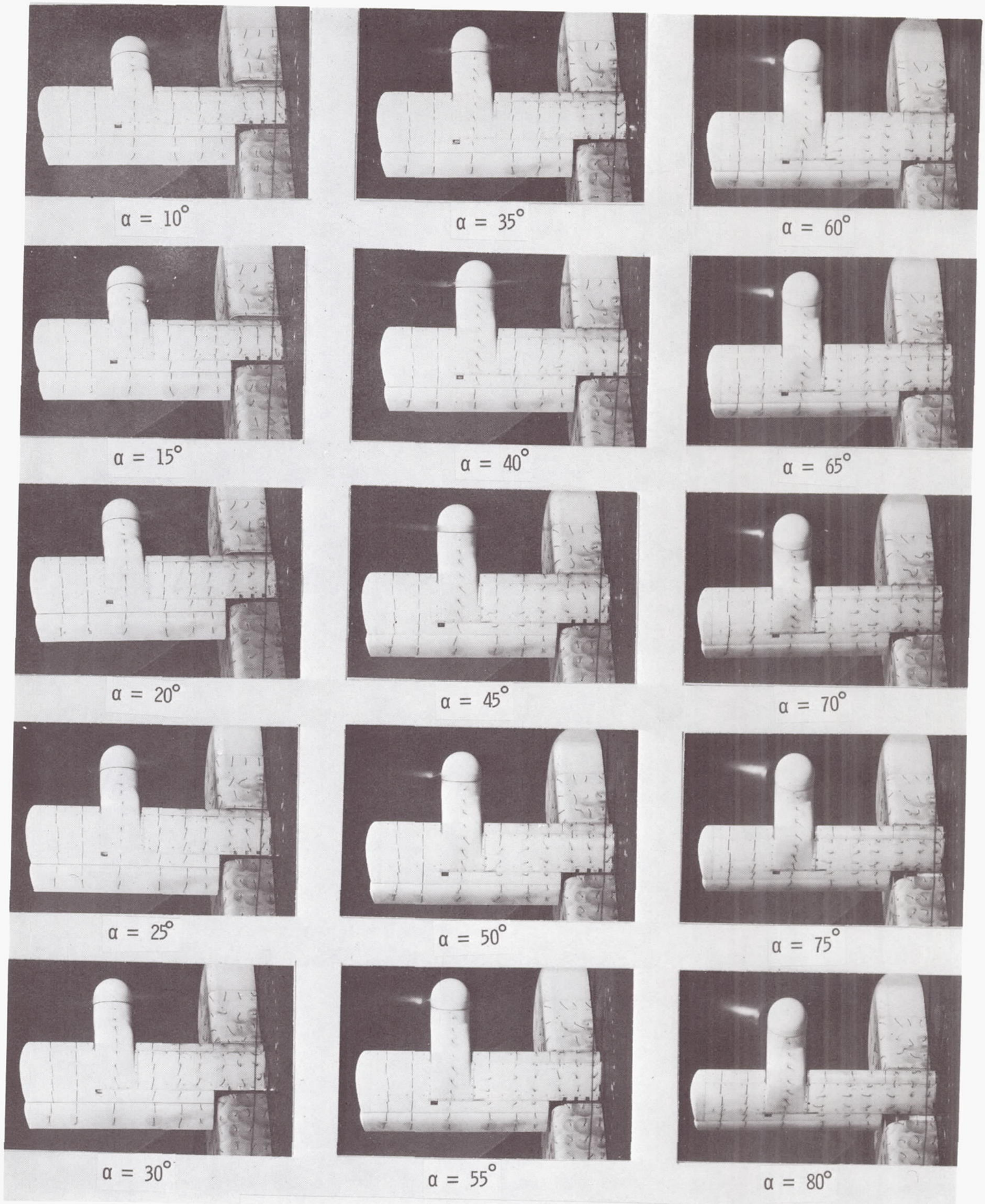

(b) Flow characteristics; $C_{T,s} = 0.90$.

Figure 7.- Continued.

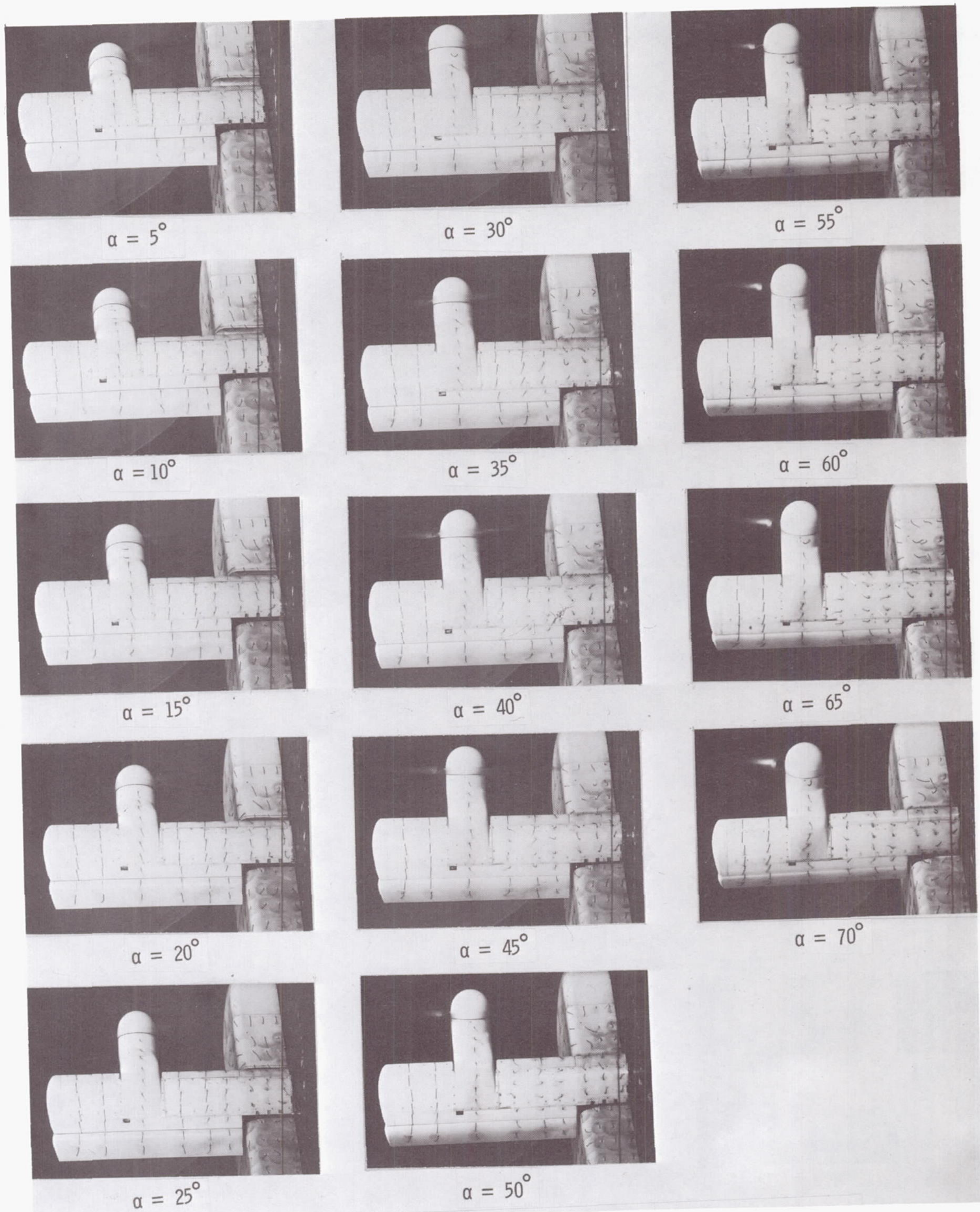

(c) Flow characteristics; $C_{T,s} = 0.80$.

Figure 7.- Continued.

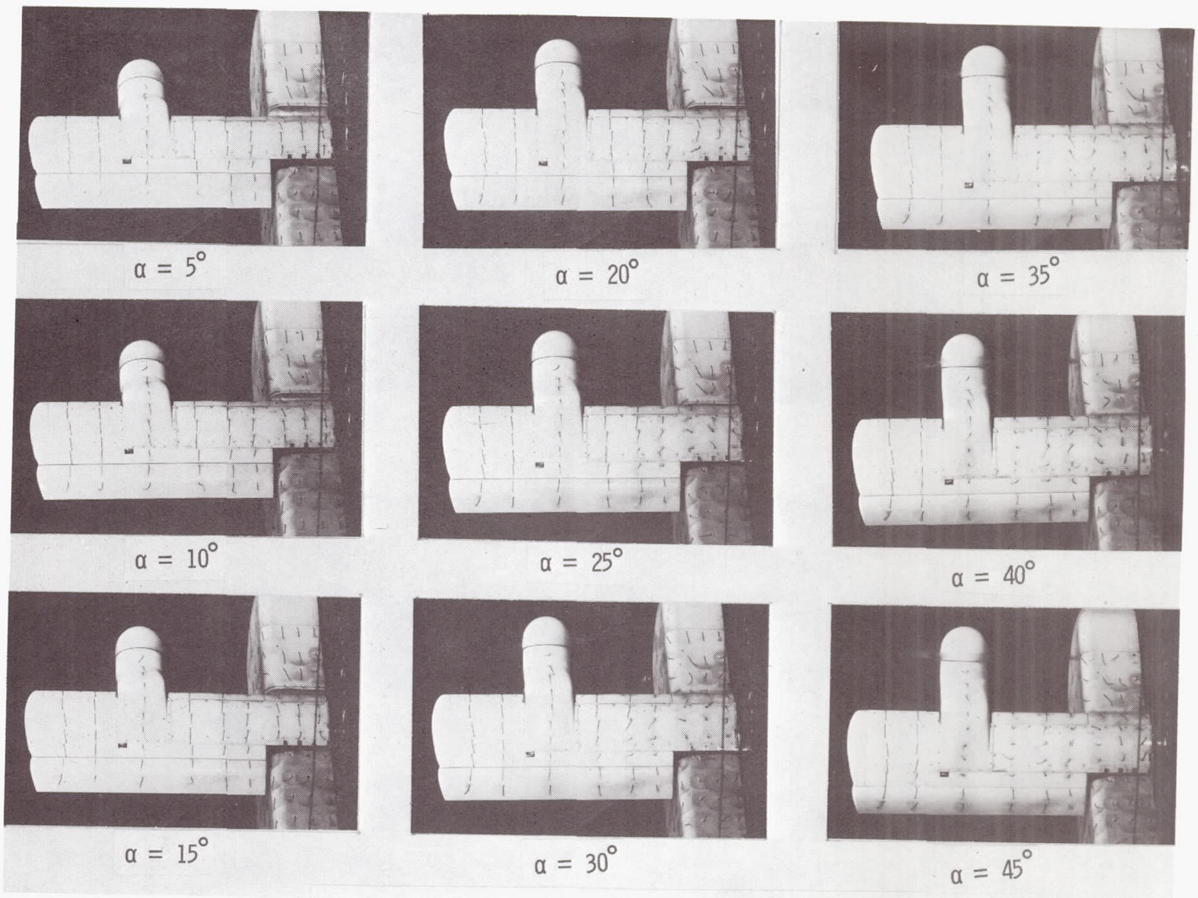

(d) Flow characteristics; $C_{T,s} = 0.60$.

Figure 7.- Continued.

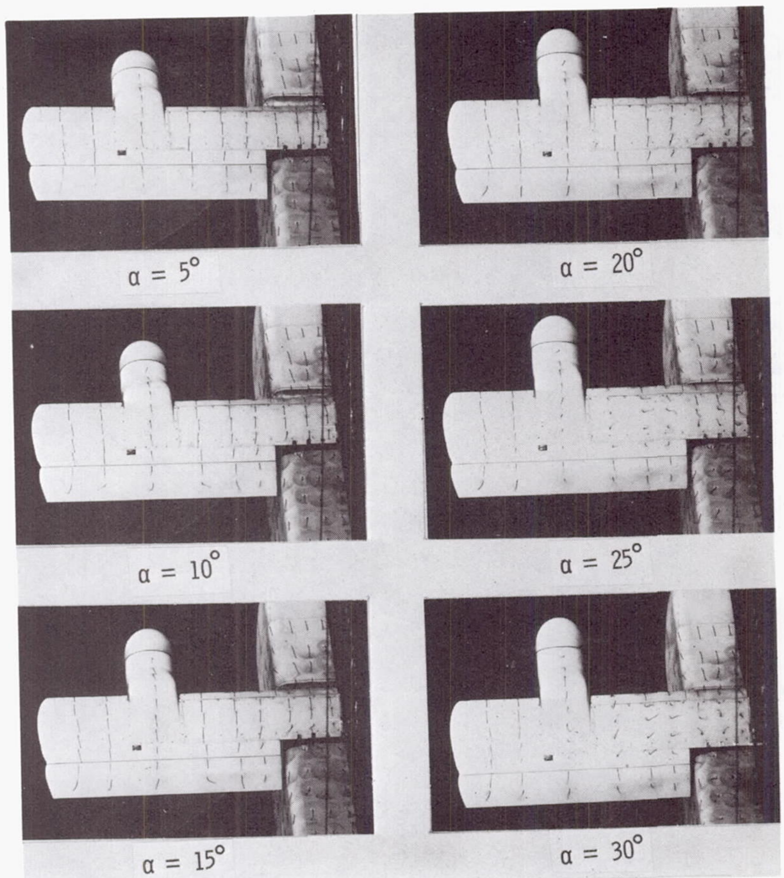

(e) Flow characteristics; $C_{T,s} = 0.30$.

Figure 7.- Concluded.

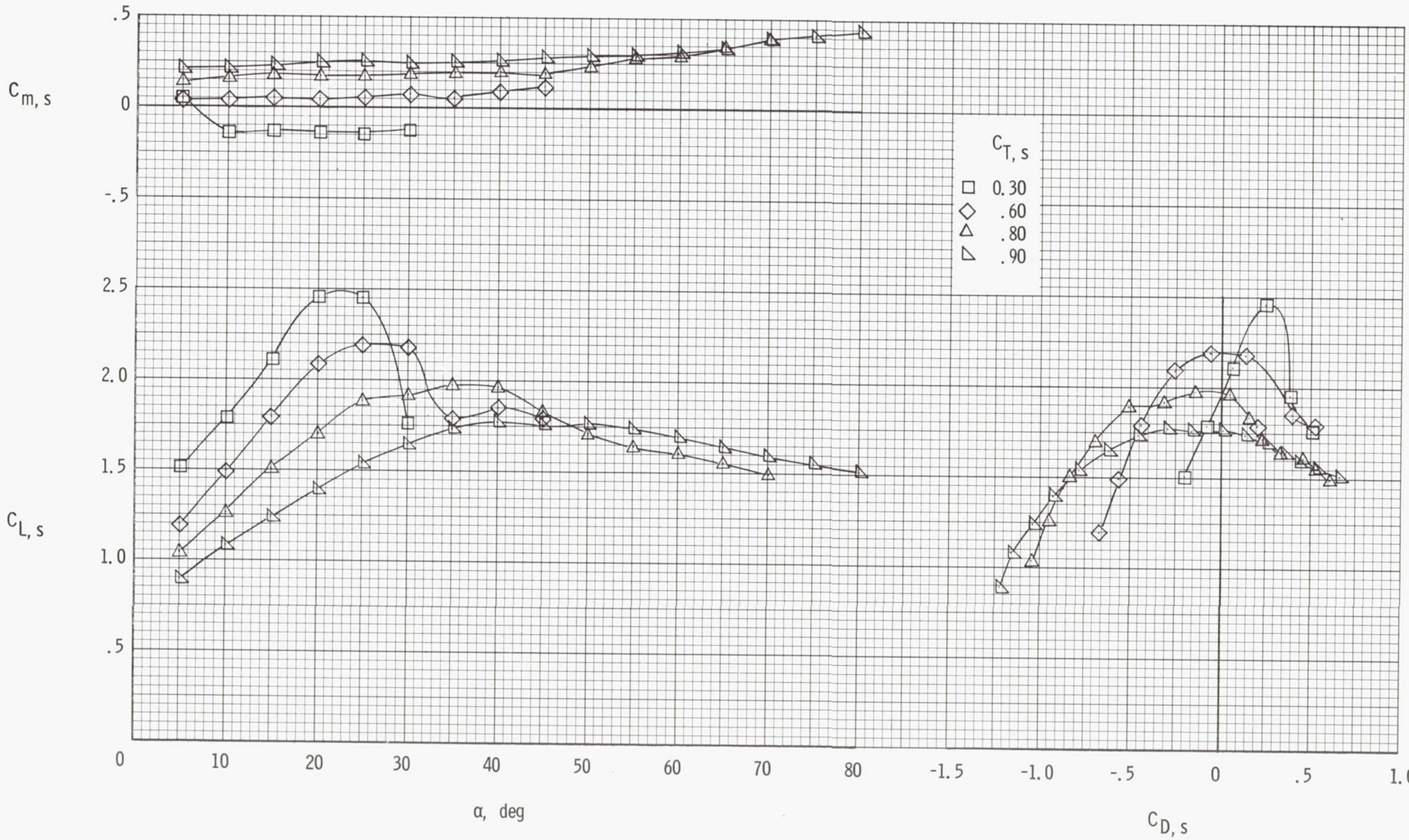

(a) Aerodynamic characteristics.

Figure 8.- Aerodynamic and flow characteristics of the wing with the propeller rotating down at the tip, basic leading edge, and $\delta_f = 40^o$.

(b) Flow characteristics; $C_{T,s} = 0.90$.

Figure 8.- Continued.

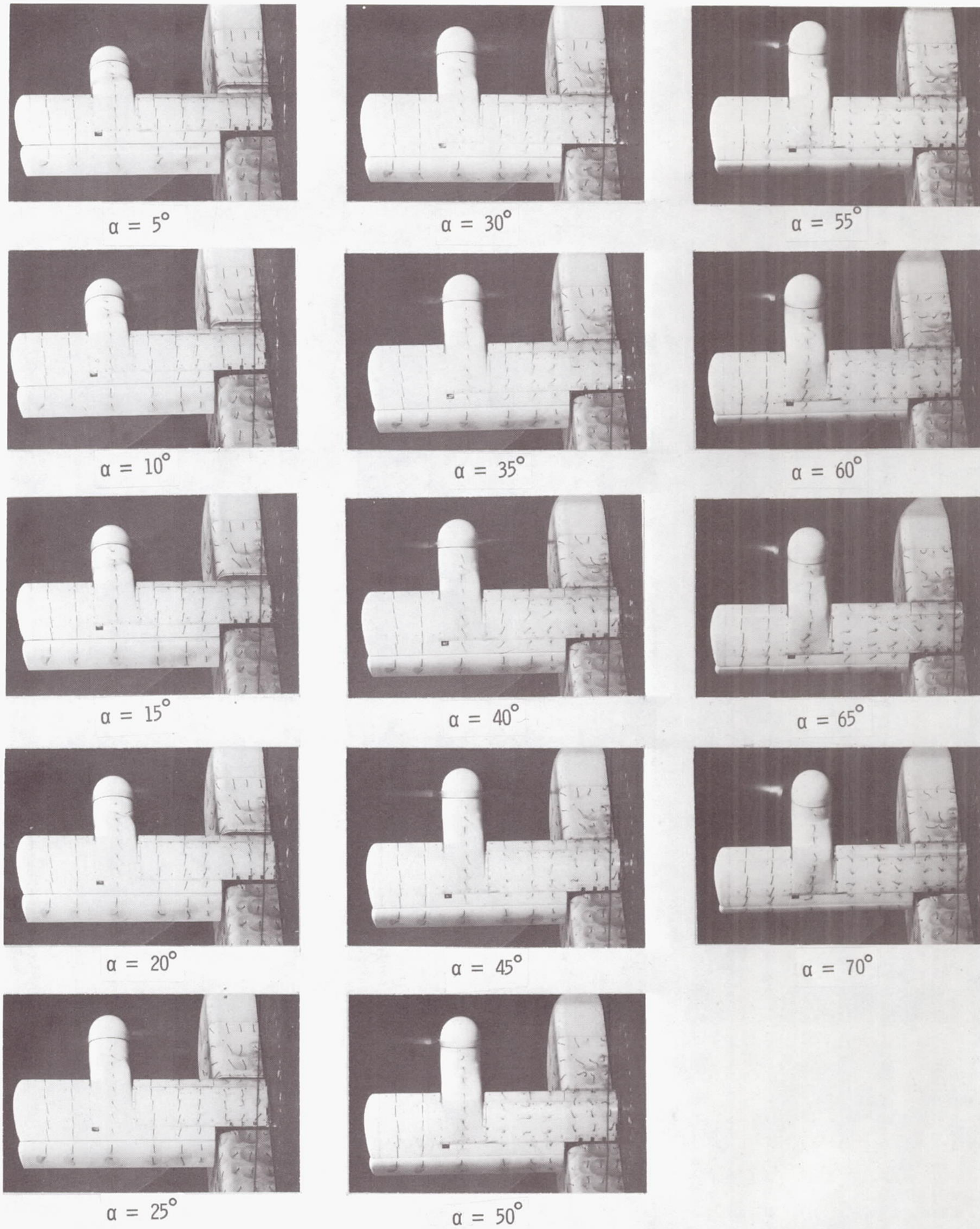

(c) Flow characteristics; $C_{T,s} = 0.80$.

Figure 8.- Continued.

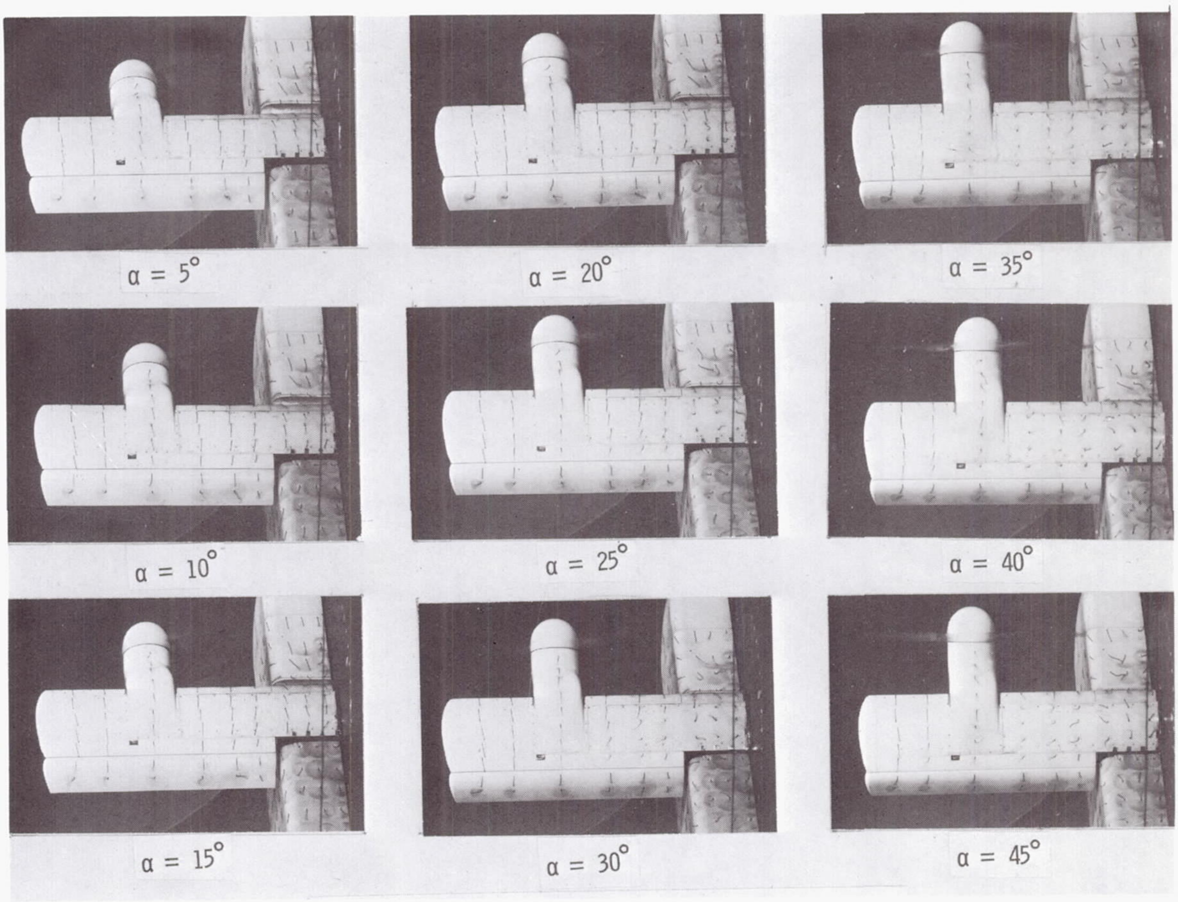

(d) Flow characteristics; $C_{T,s} = 0.60$.

Figure 8.- Continued.

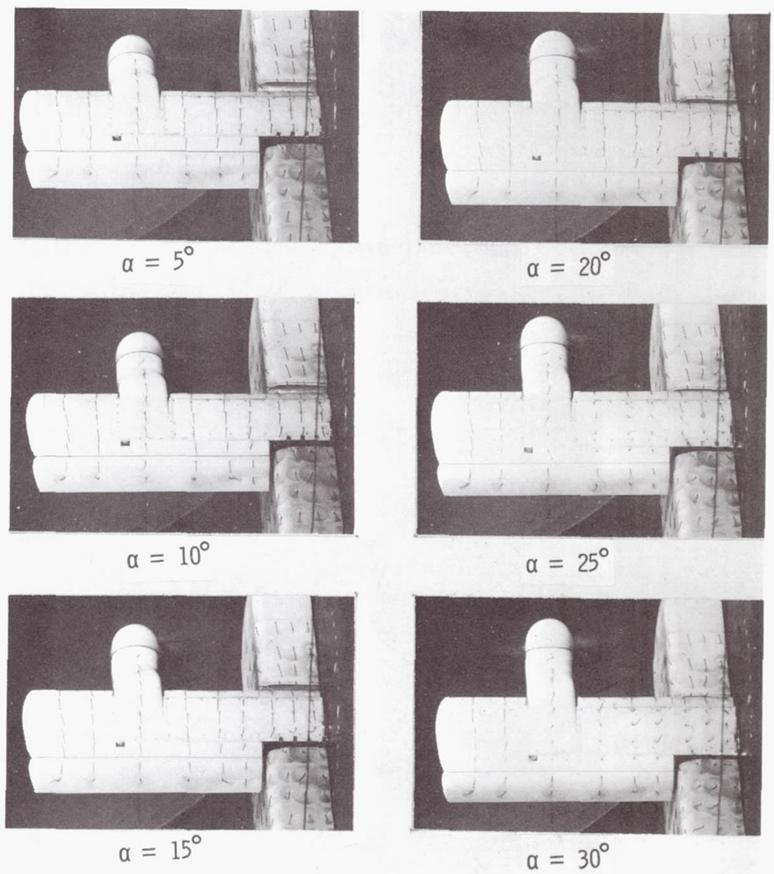

$\alpha = 5^\circ$ | $\alpha = 20^\circ$

$\alpha = 10^\circ$ | $\alpha = 25^\circ$

$\alpha = 15^\circ$ | $\alpha = 30^\circ$

(e) Flow characteristics; $C_{T,s} = 0.30$.

Figure 8.- Concluded.

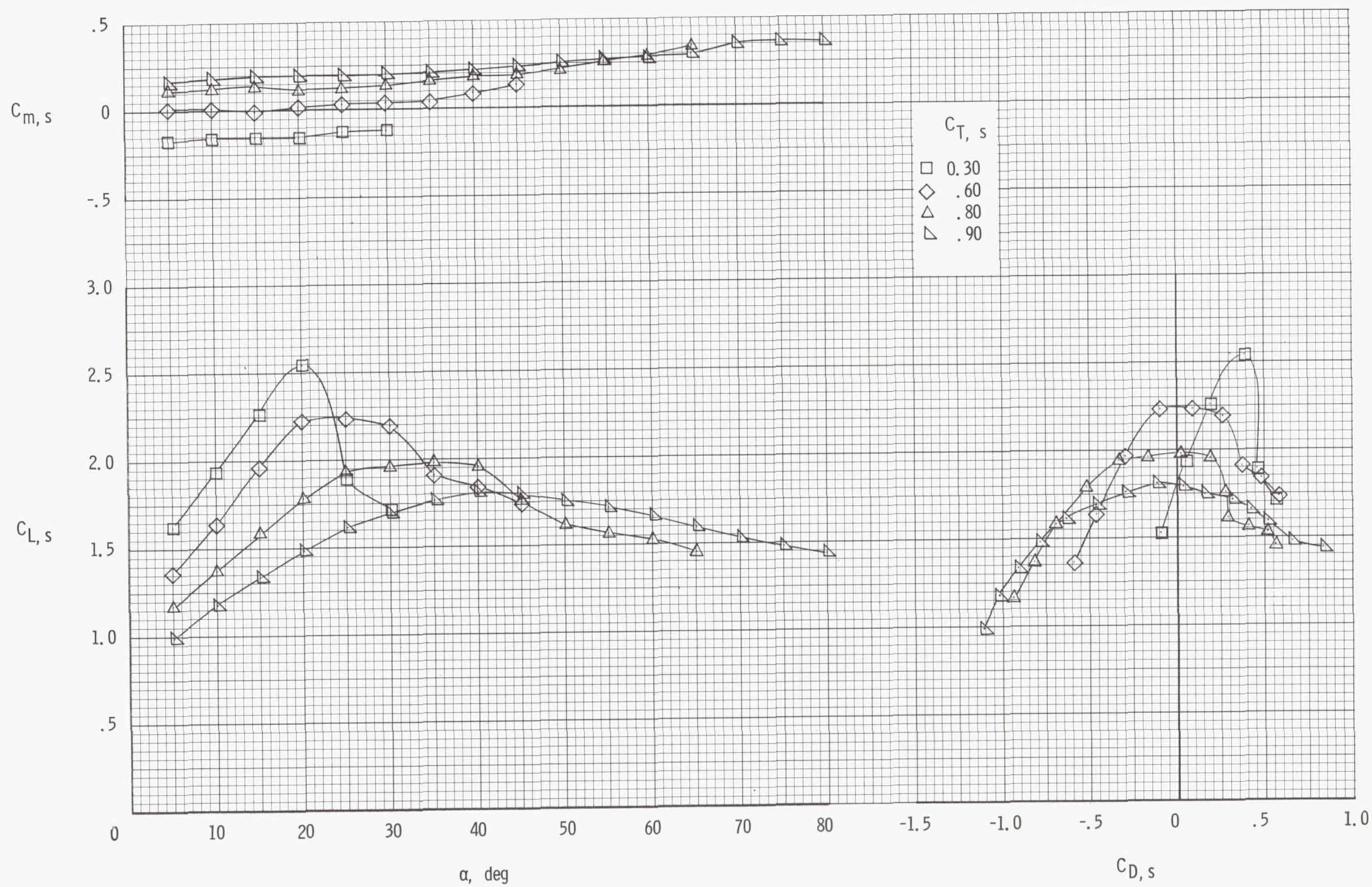

(a) Aerodynamic characteristics.

Figure 9.- Aerodynamic and flow characteristics of the wing with the propeller rotating down at the tip, basic leading edge, and $\delta_f = 60^o$.

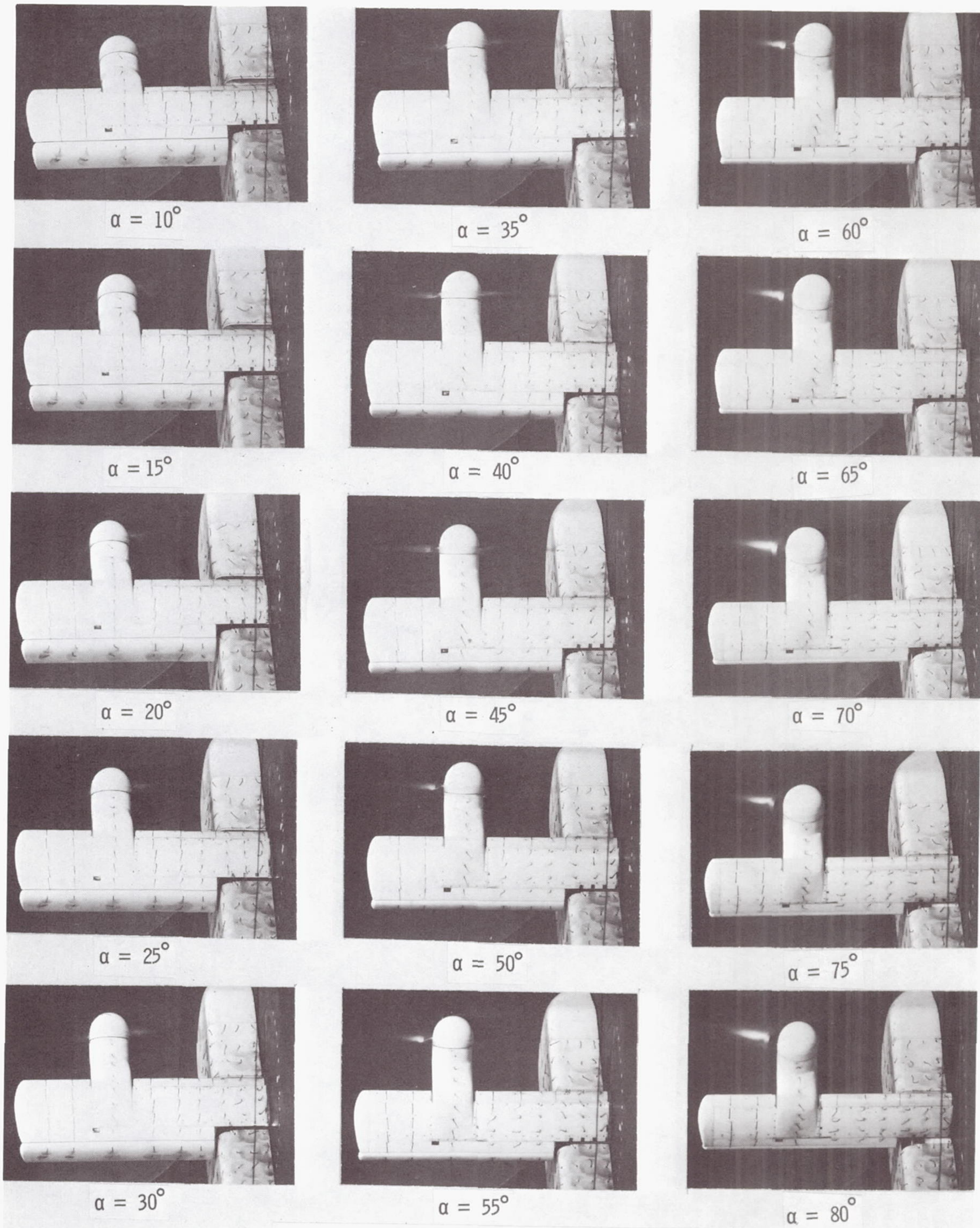

(b) Flow characteristics; $C_{T,s} = 0.90$.

Figure 9.- Continued.

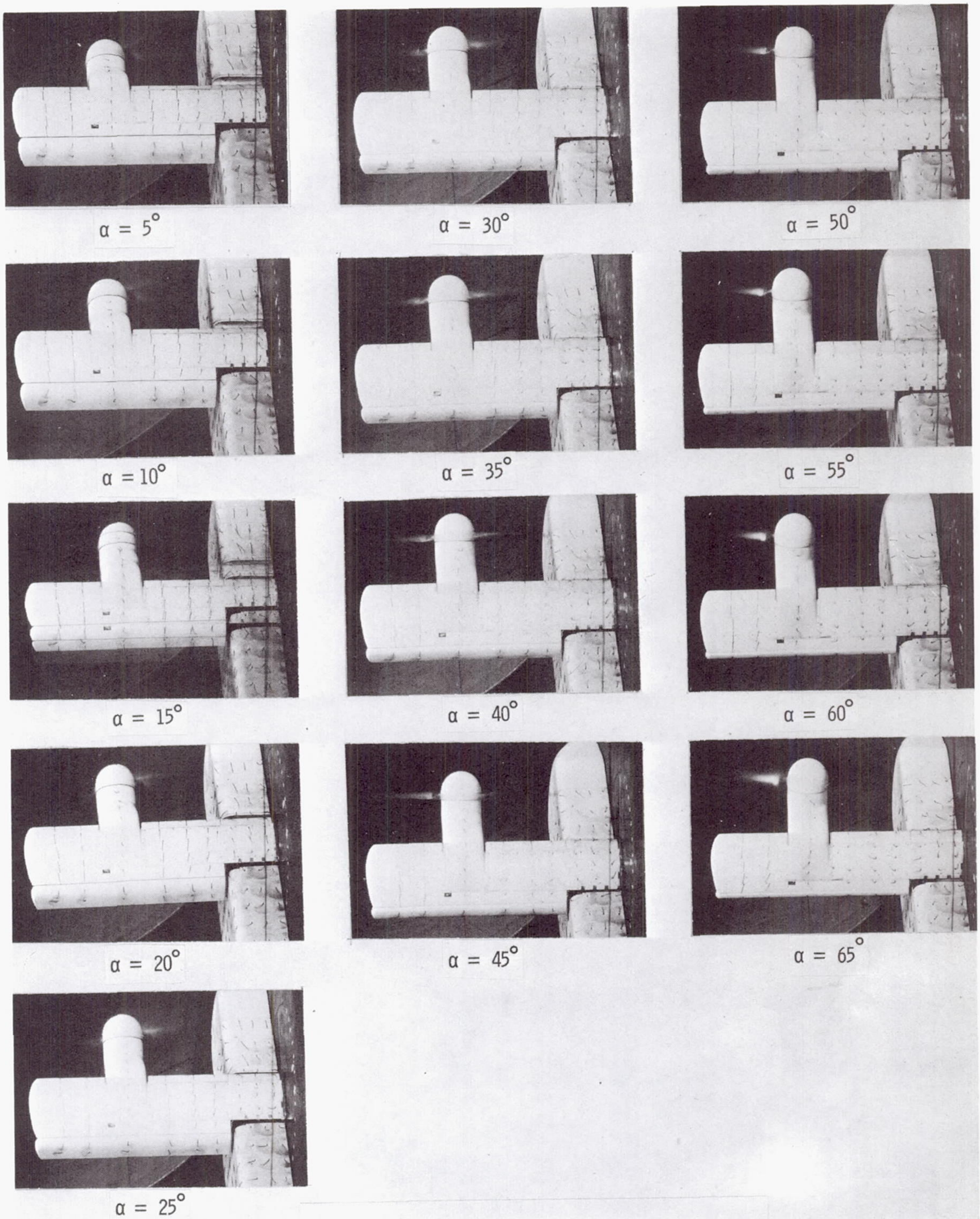

(c) Flow characteristics; $C_{T,s} = 0.80$.

Figure 9.- Continued.

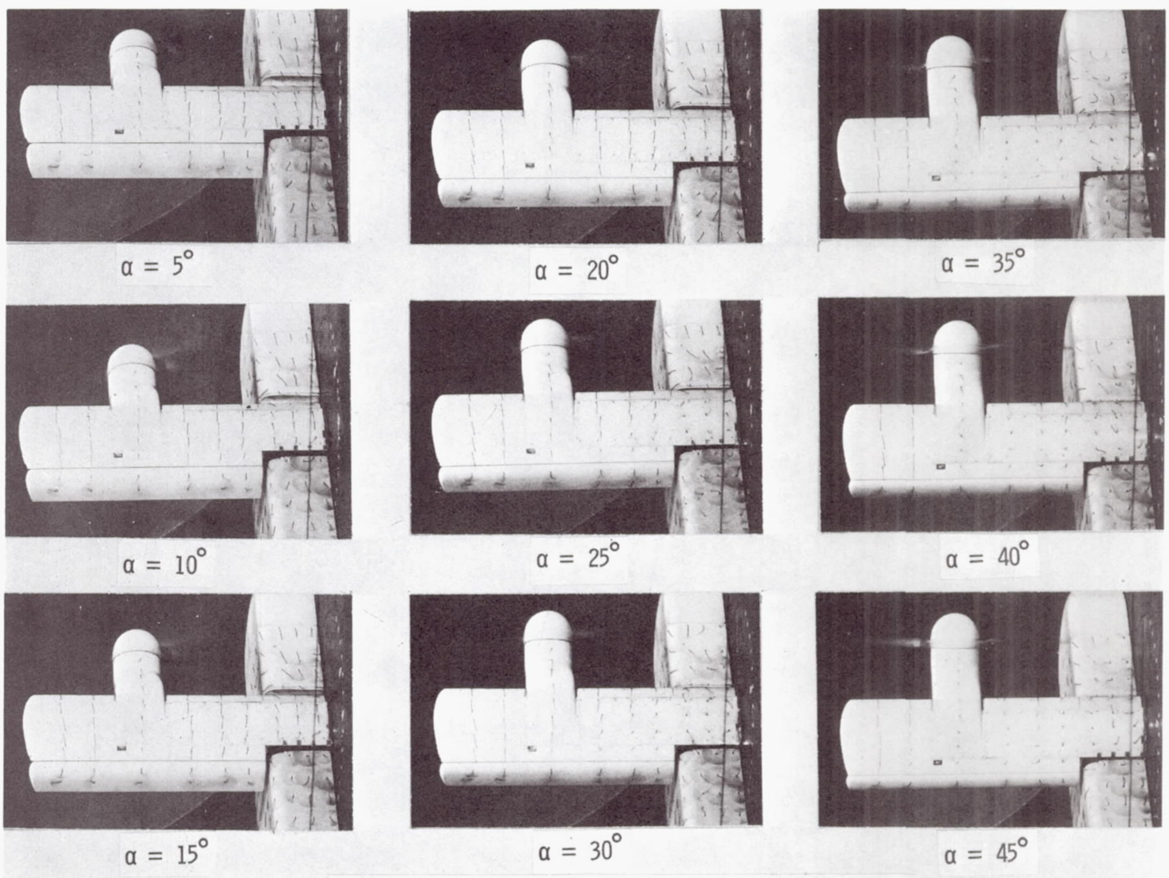

(d) Flow characteristics; $C_{T,s} = 0.60$.

Figure 9.- Continued.

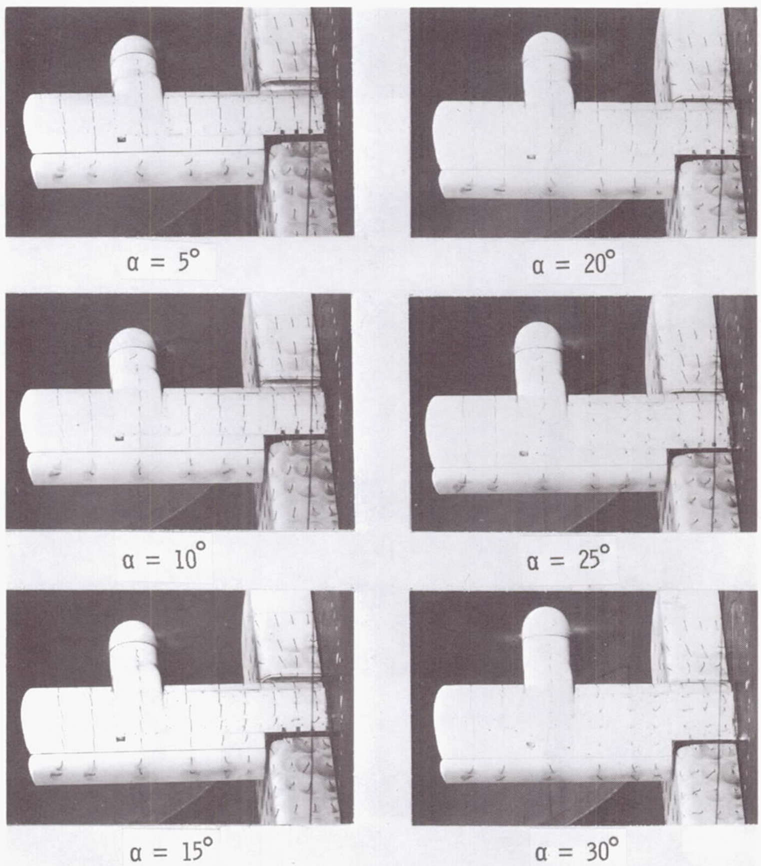

(e) Flow characteristics; $C_{T,s} = 0.30$.

Figure 9.- Concluded.

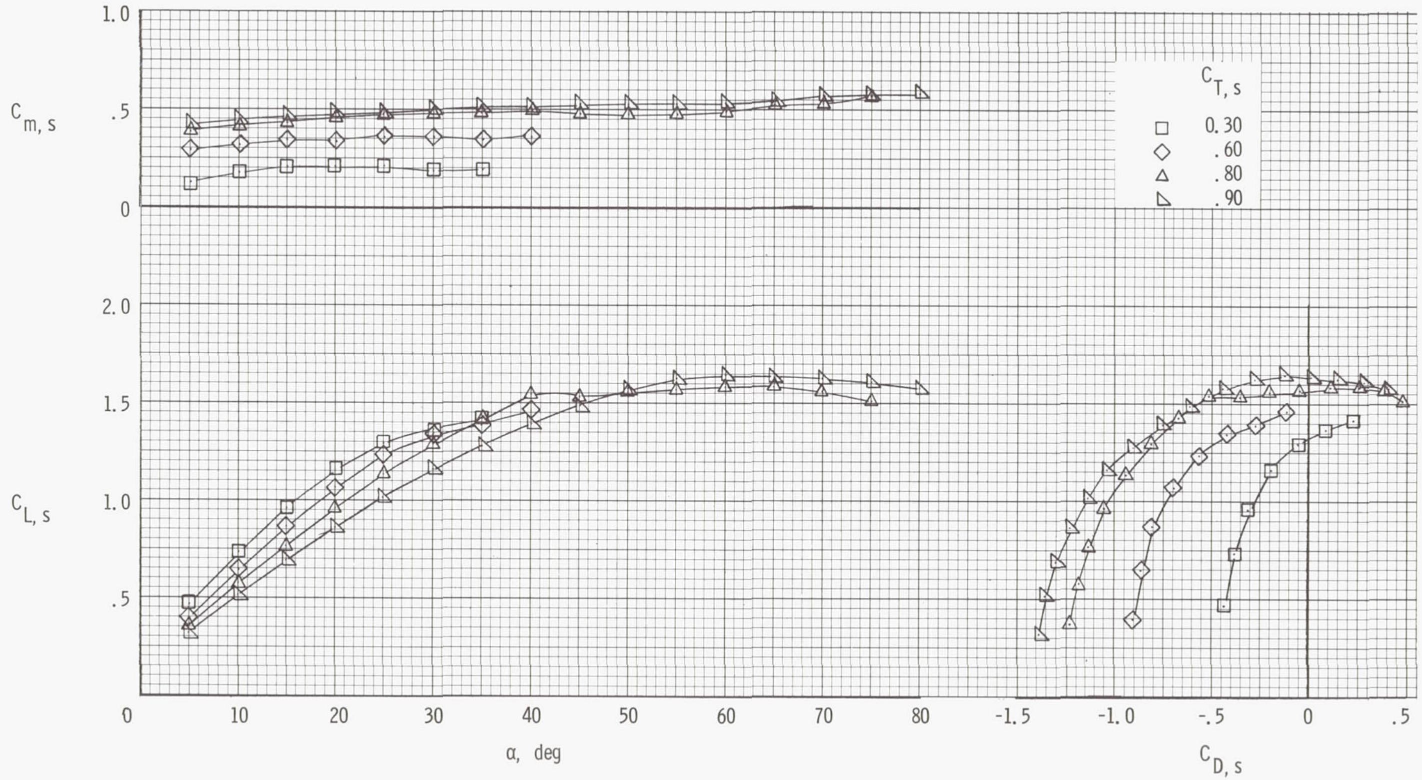

(a) Aerodynamic characteristics.

Figure 10.- Aerodynamic and flow characteristics of the wing with the propeller rotating down at the tip, basic leading edge, fences on, and $\delta_f = 0^o$.

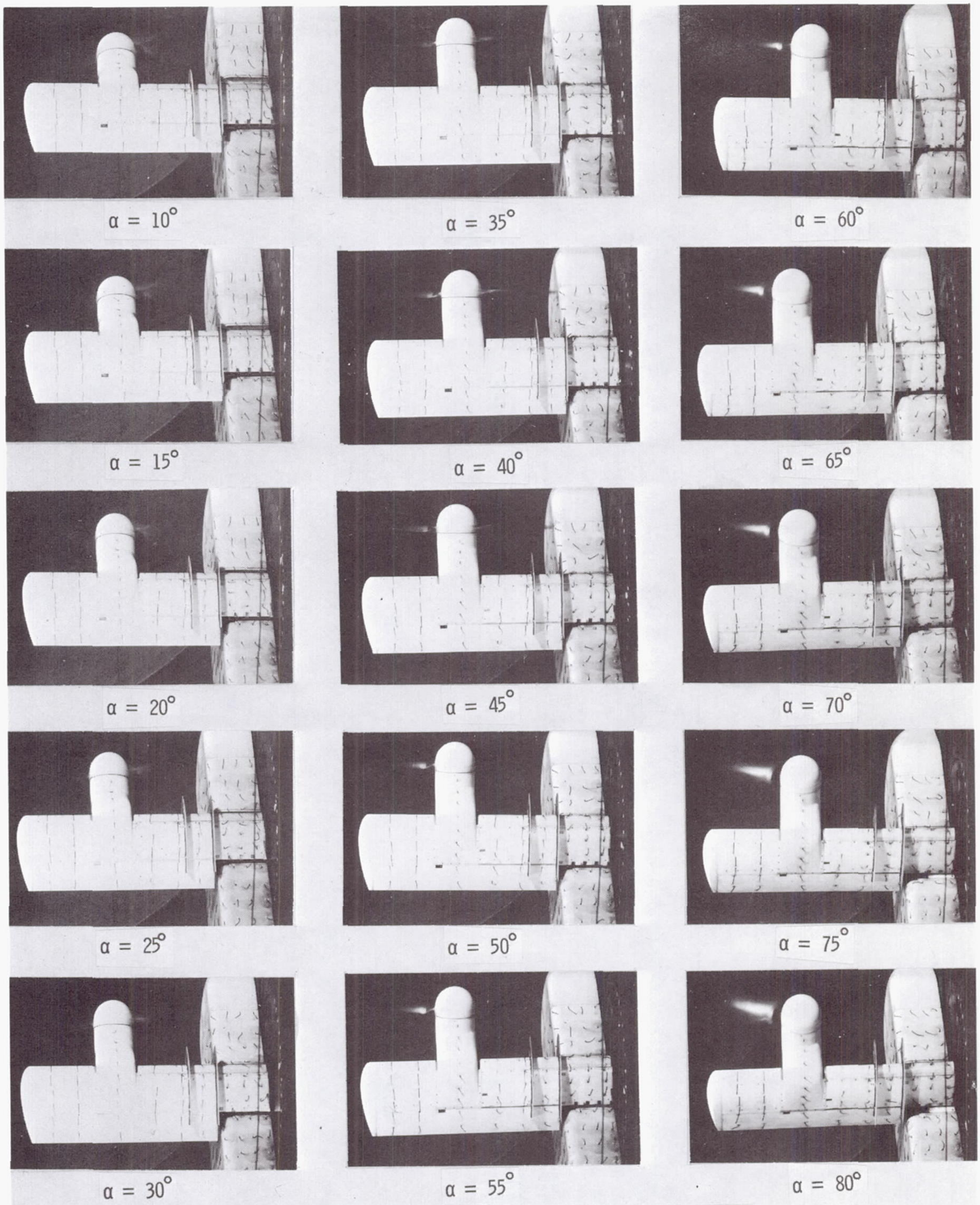

(b) Flow characteristics; $C_{T,s} = 0.90$.

Figure 10.- Continued.

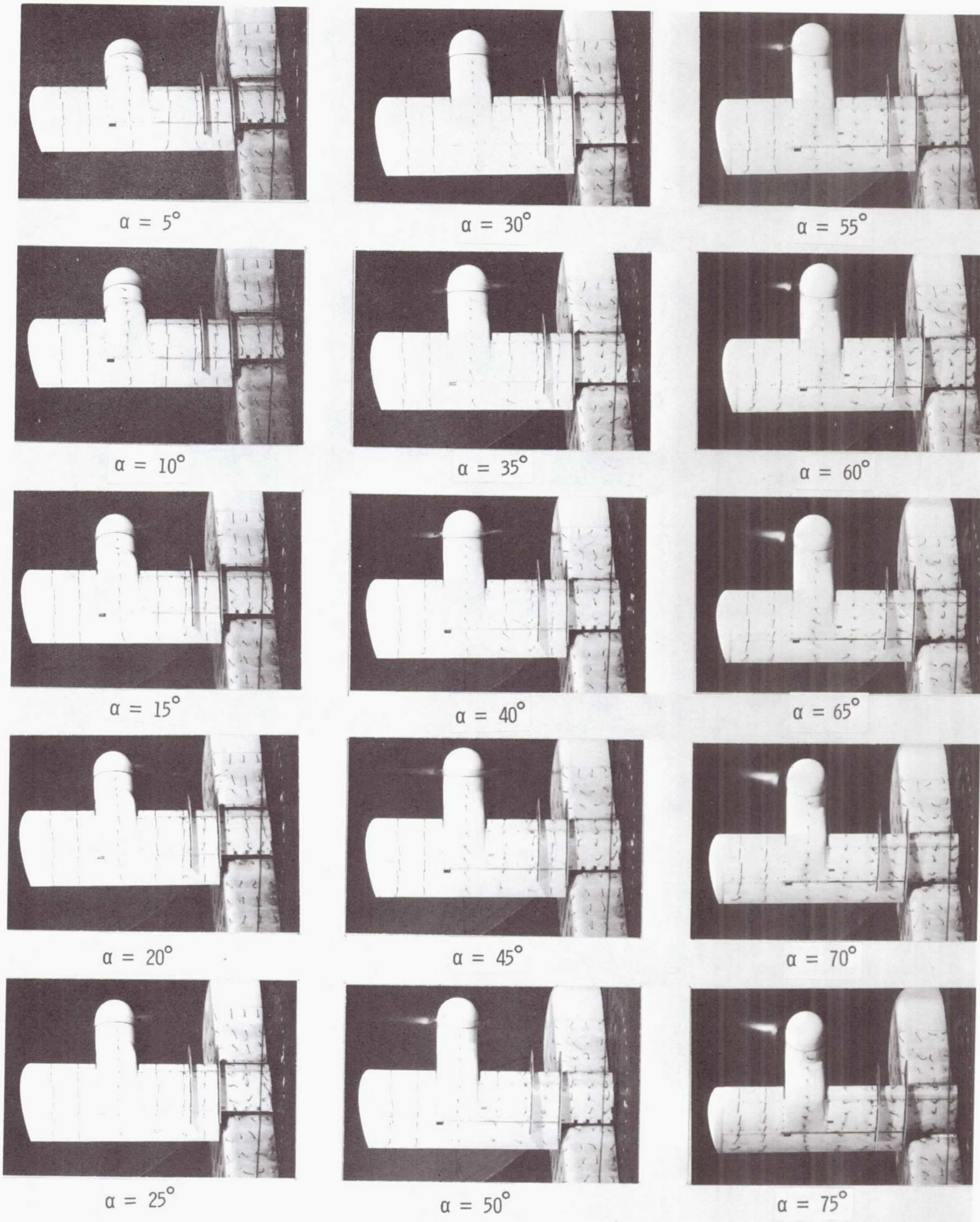

(c) Flow characteristics; $C_{T,s} = 0.80$.

Figure 10.- Continued.

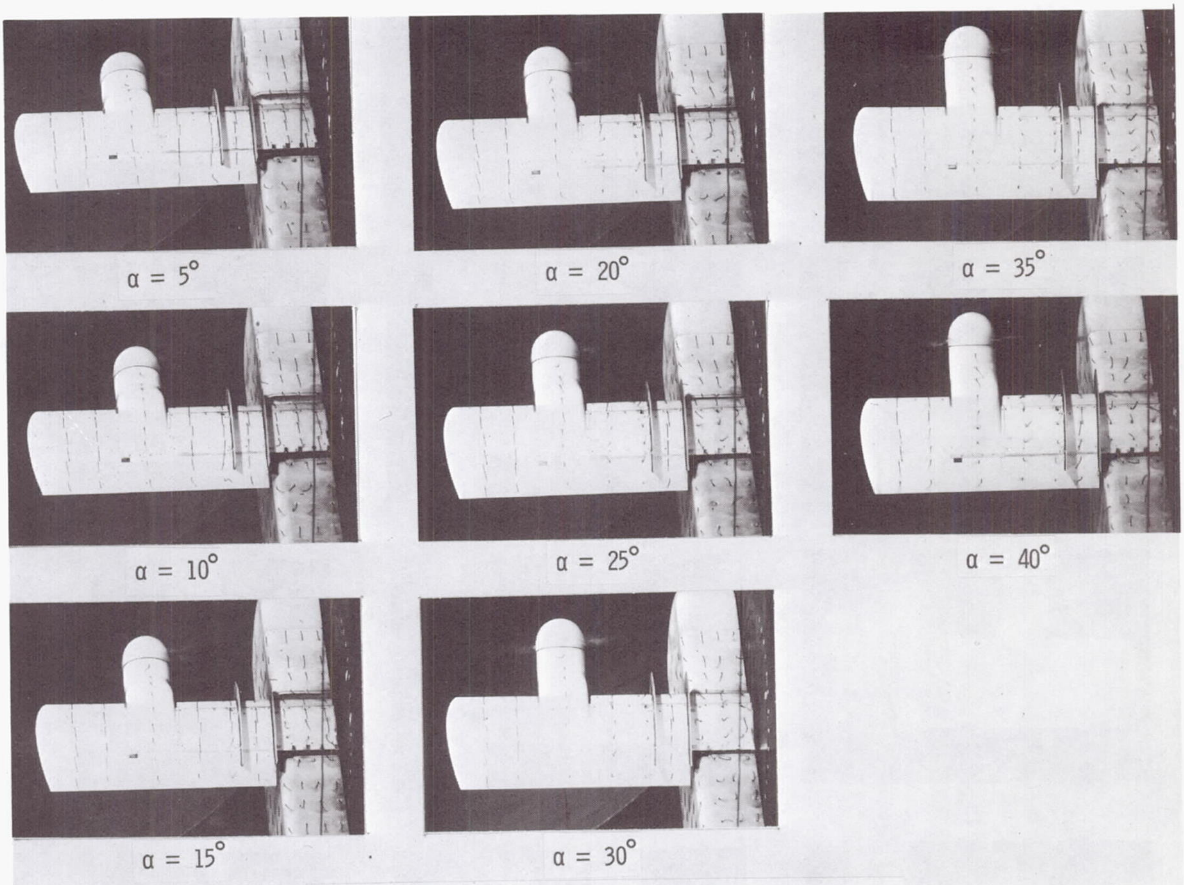

(d) Flow characteristics; $C_{T,s} = 0.60$.

Figure 10.- Continued.

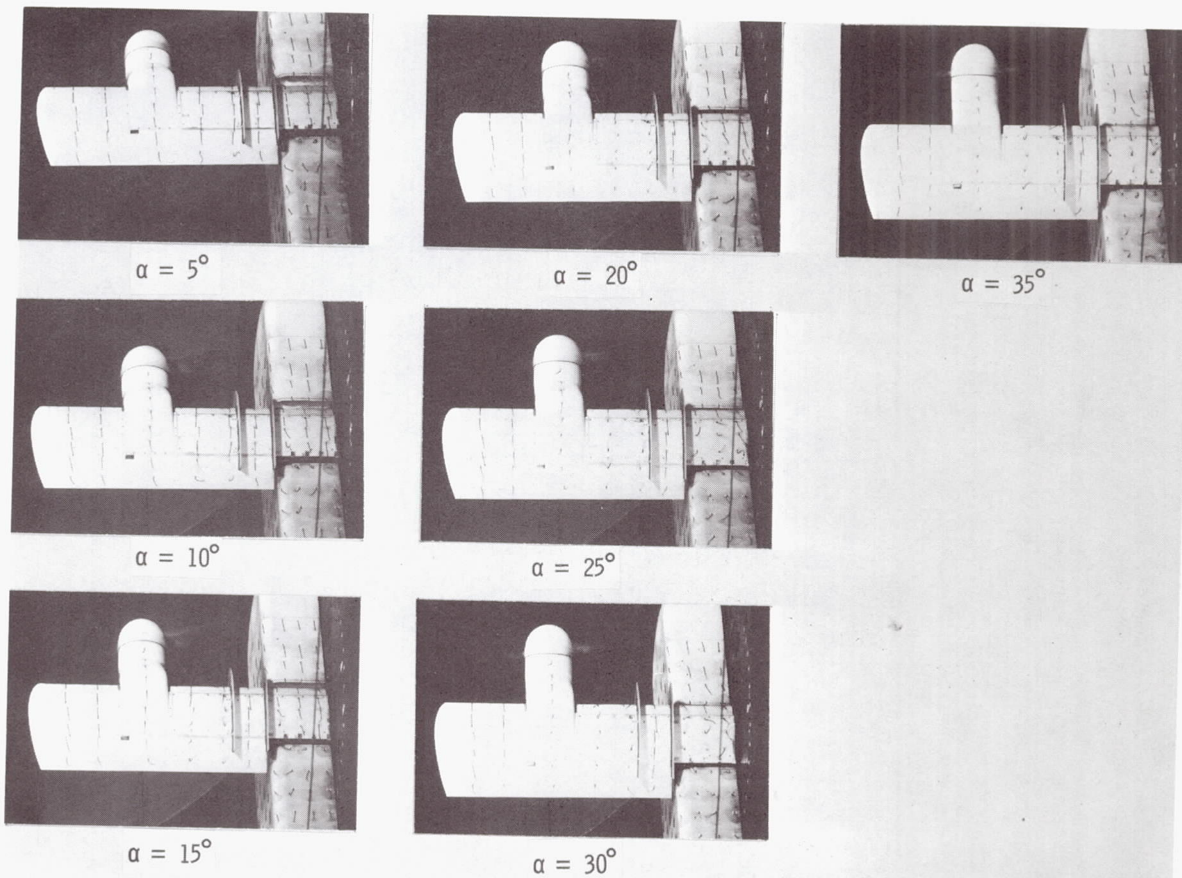

(e) Flow characteristics; $C_{T,s} = 0.30$.

Figure 10.- Concluded.

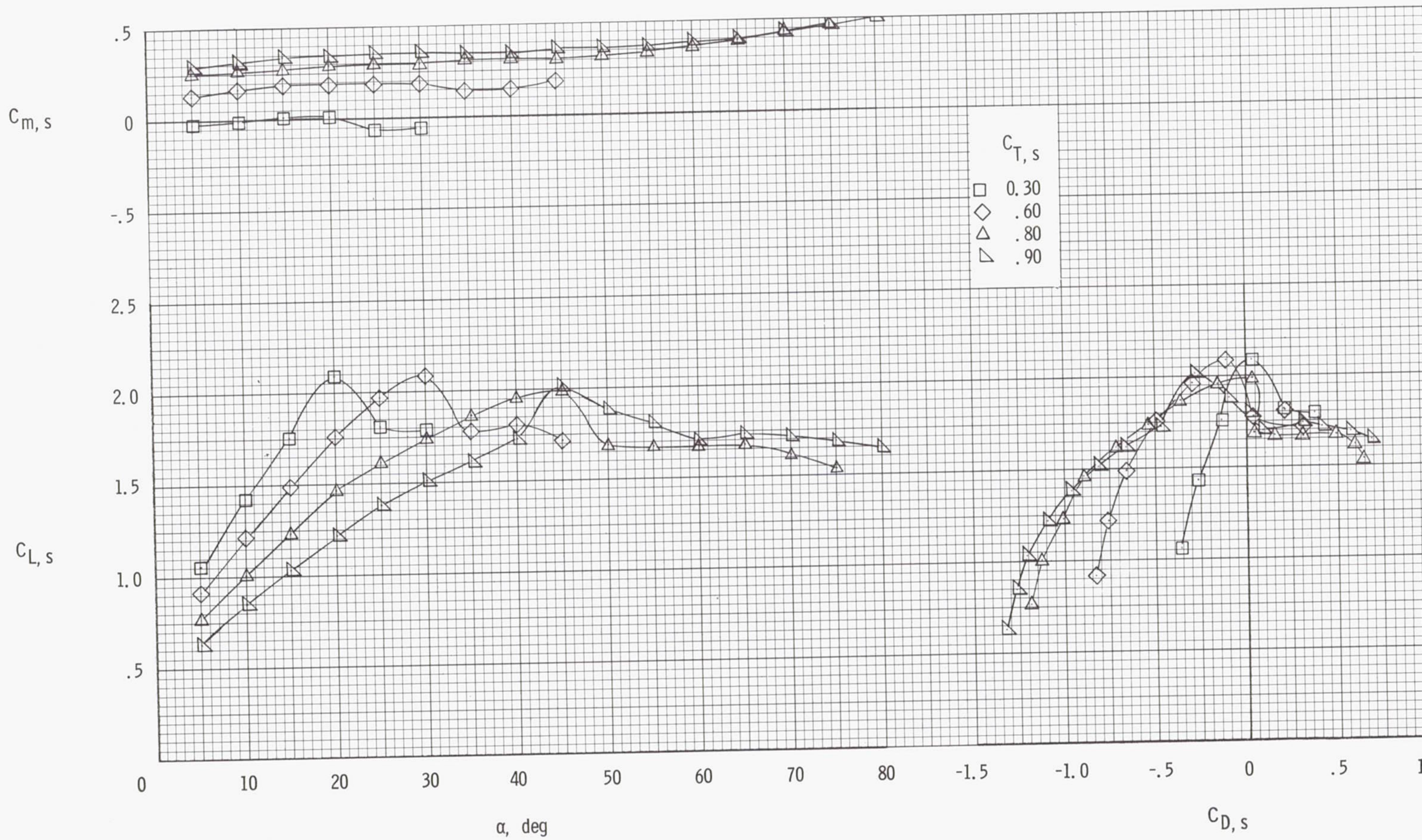

(a) Aerodynamic characteristics.

Figure 11.- Aerodynamic and flow characteristics of the wing with the propeller rotating down at the tip, basic leading edge, fences on, and $\delta_f = 20^o$.

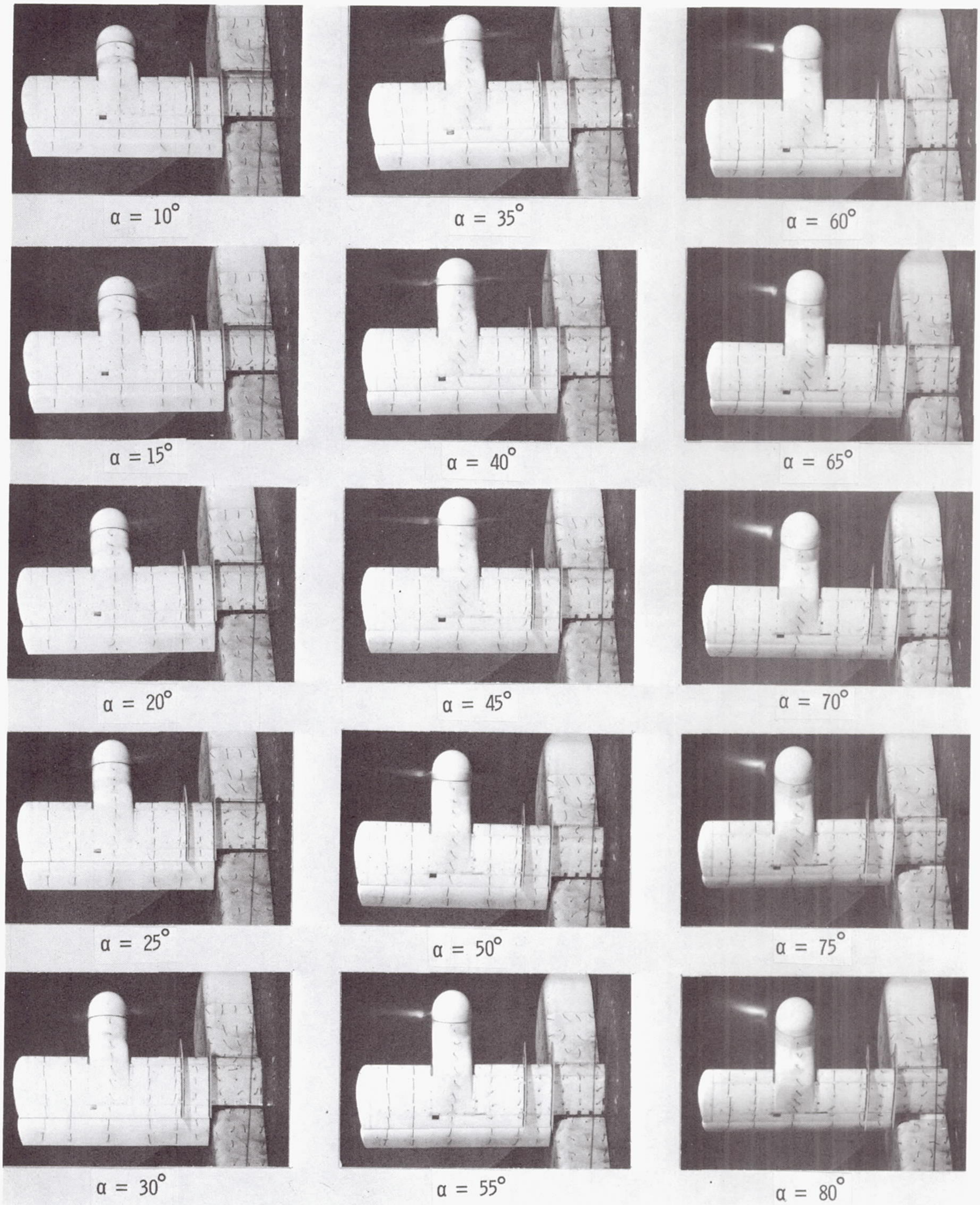

(b) Flow characteristics; $C_{T,s} = 0.90$.

Figure 11.- Continued.

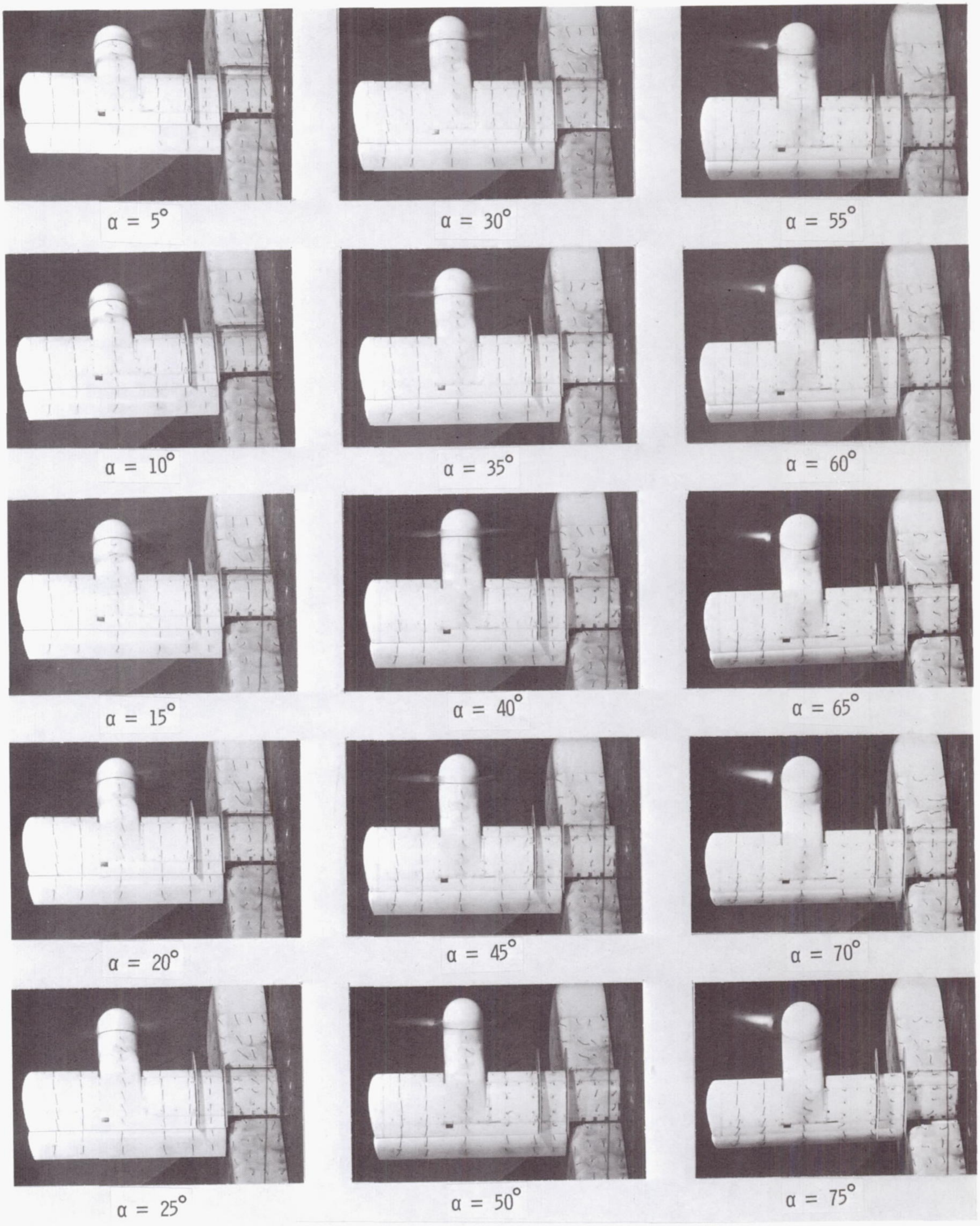

(c) Flow characteristics; $C_{T,s} = 0.80$.

Figure 11.- Continued.

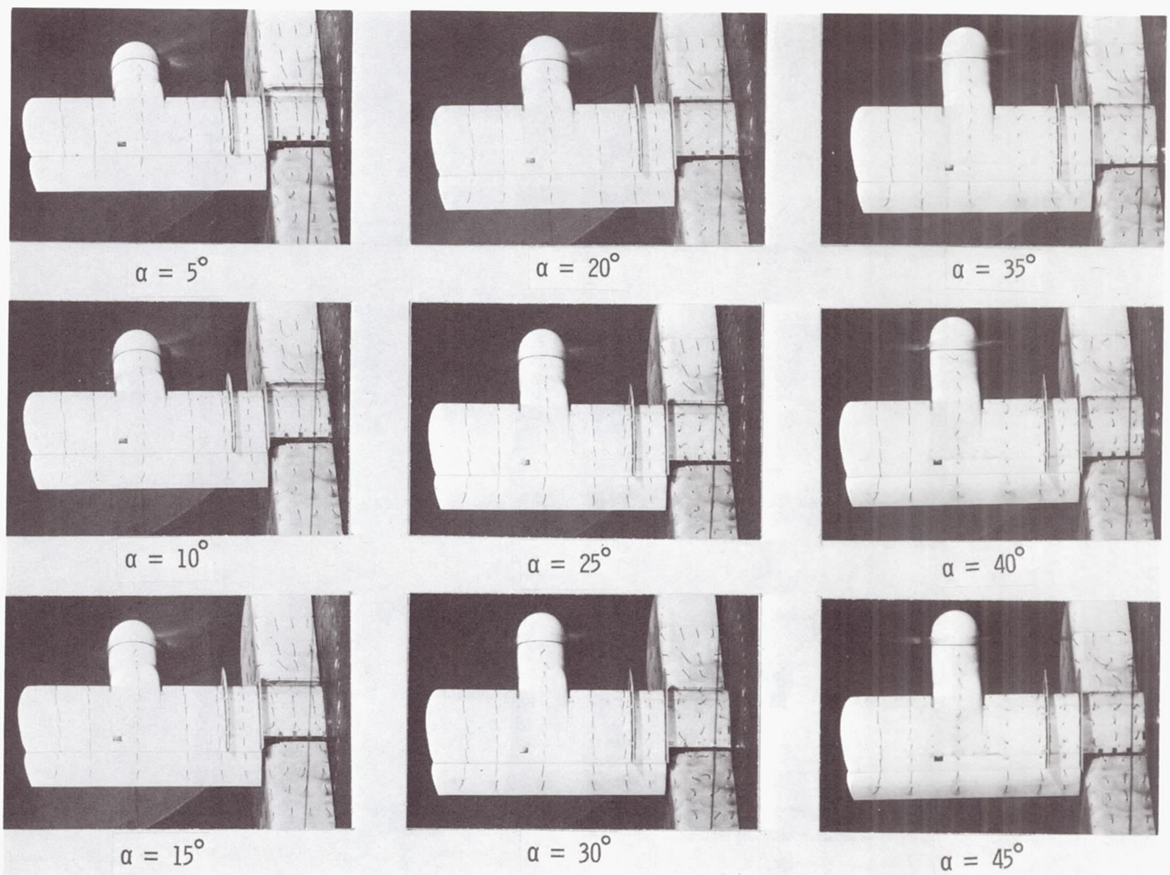

(d) Flow characteristics; $C_{T,s} = 0.60$.

Figure 11.- Continued.

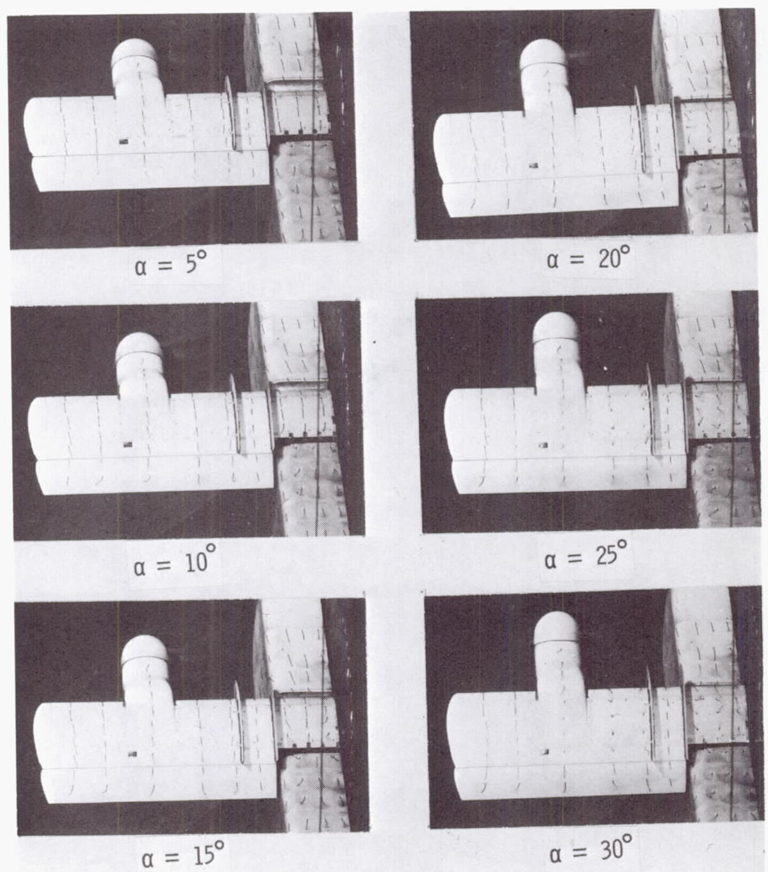

(e) Flow characteristics; $C_{T,s} = 0.30$.

Figure 11.- Concluded.

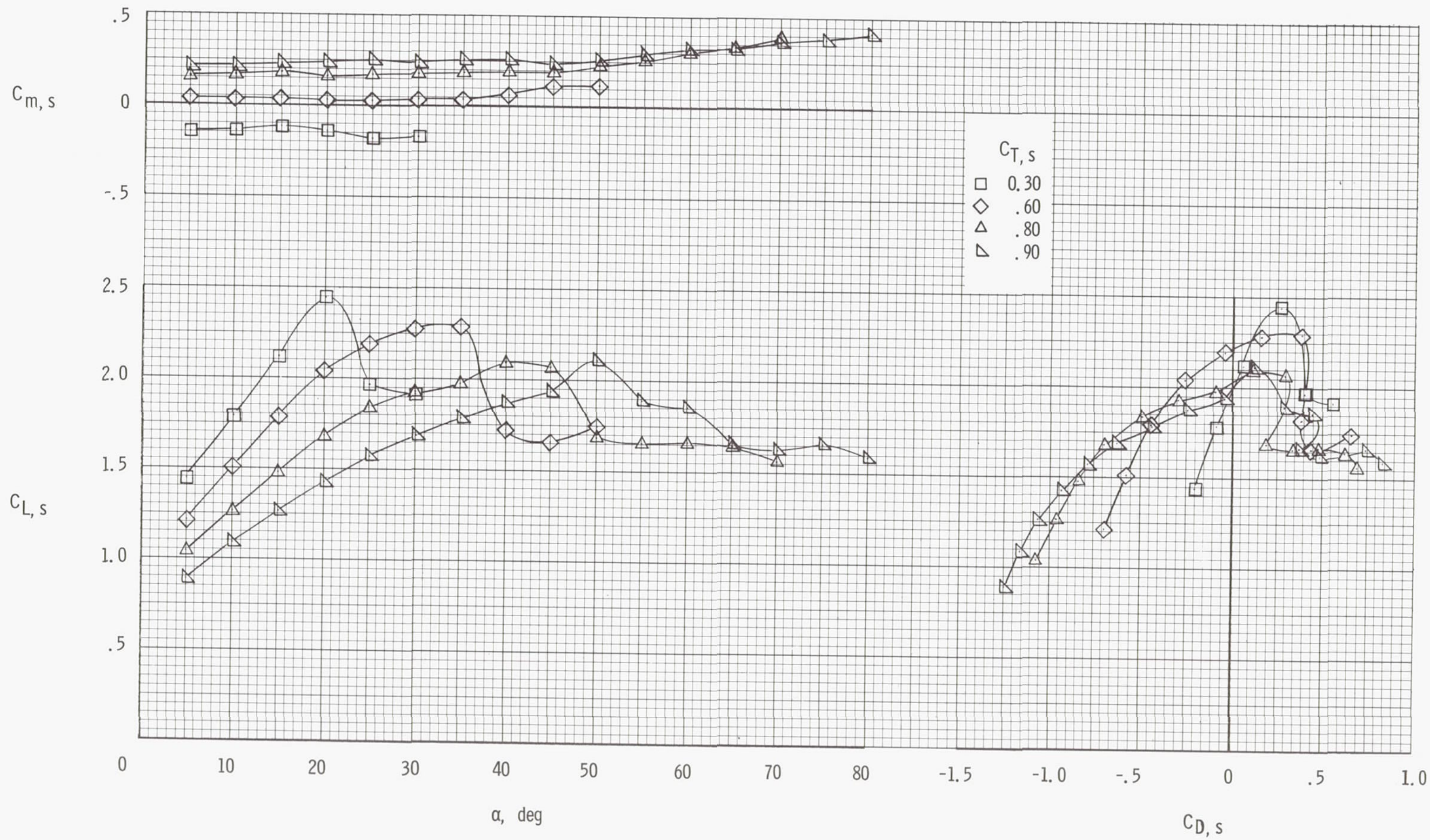

(a) Aerodynamic characteristics.

Figure 12.- Aerodynamic and flow characteristics of the wing with the propeller rotating down at the tip, basic leading edge, fences on, and $\delta_f = 40^o$.

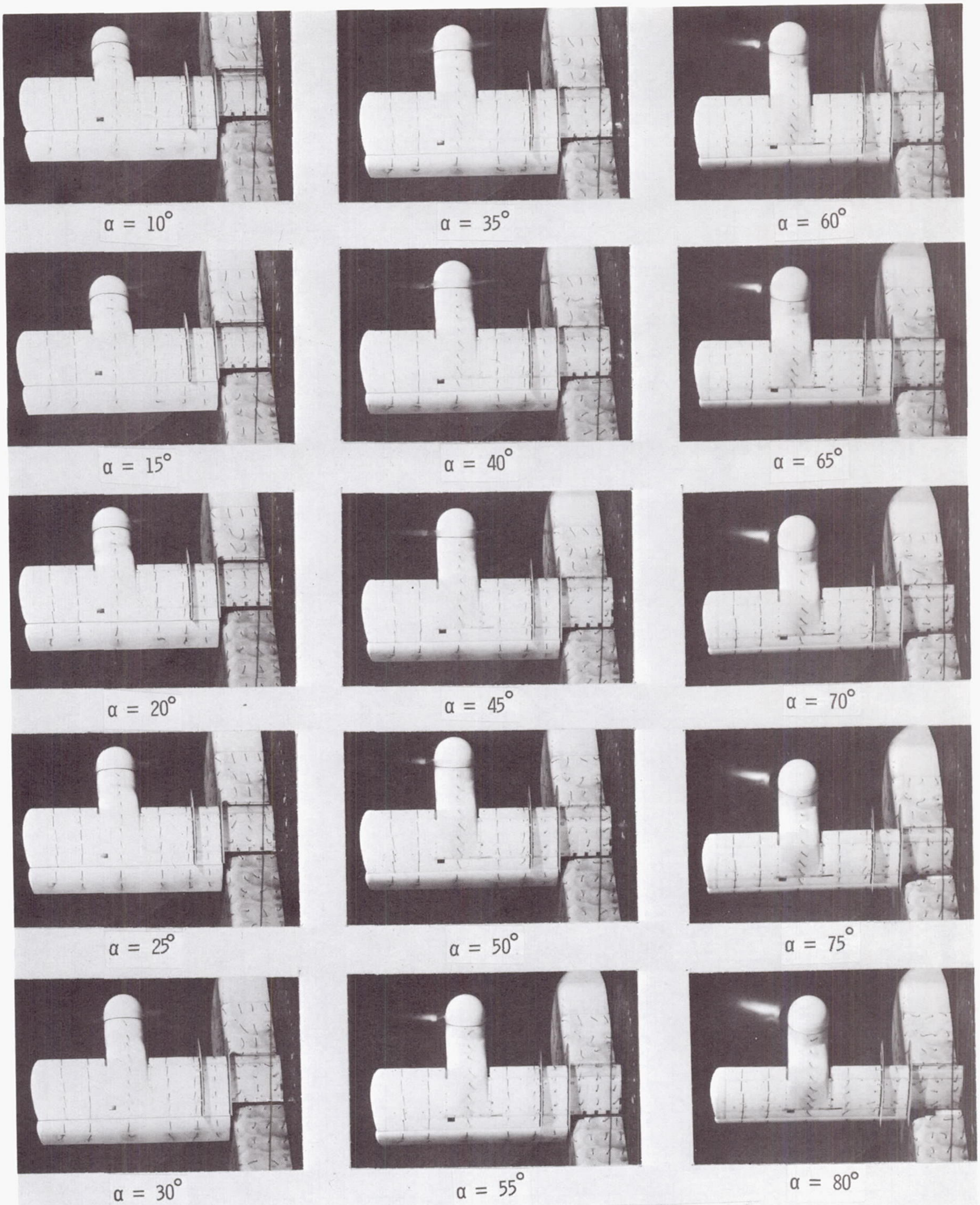

(b) Flow characteristics; $C_{T,s} = 0.90$.

Figure 12.- Continued.

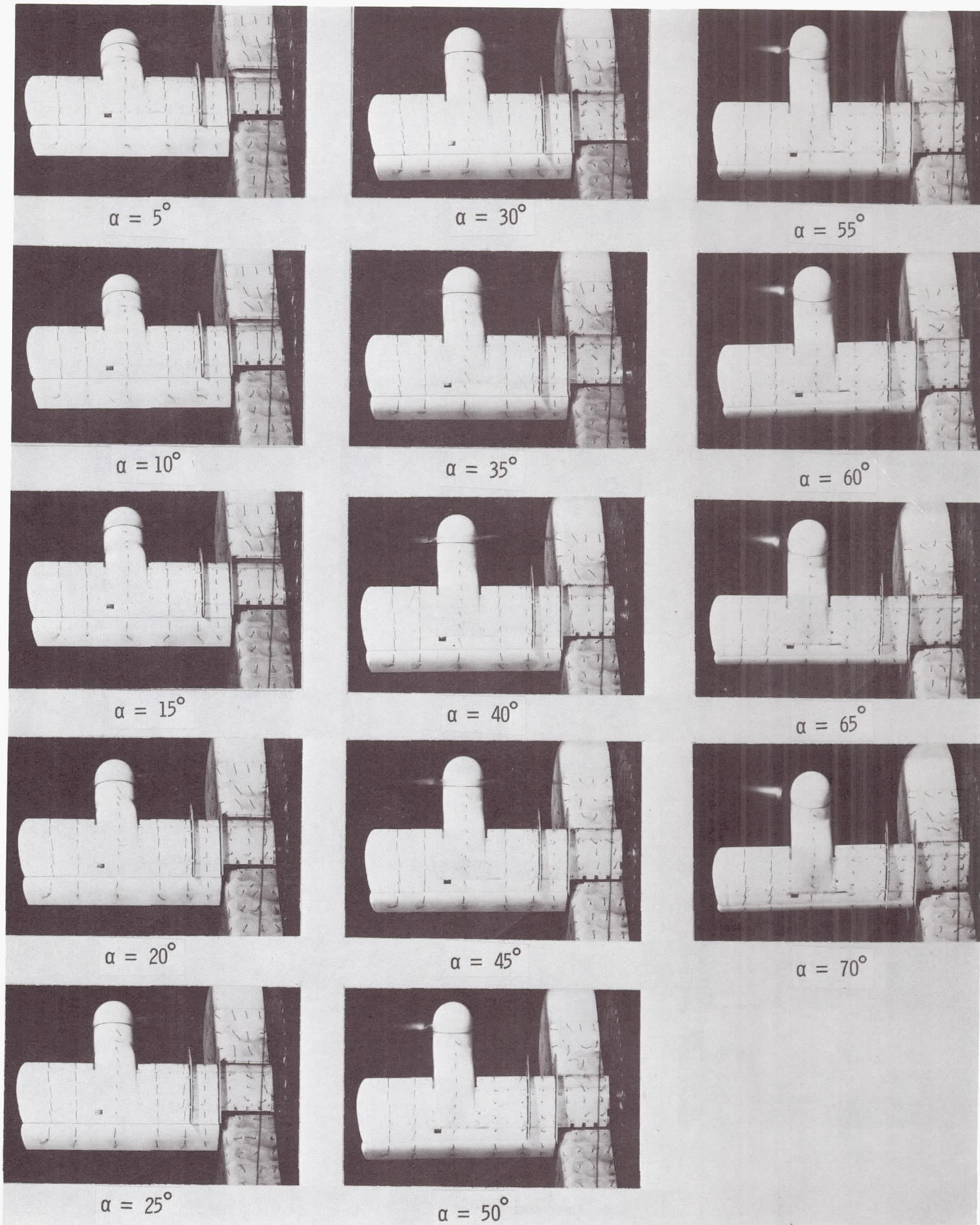

(c) Flow characteristics; $C_{T,s} = 0.80$.

Figure 12.- Continued.

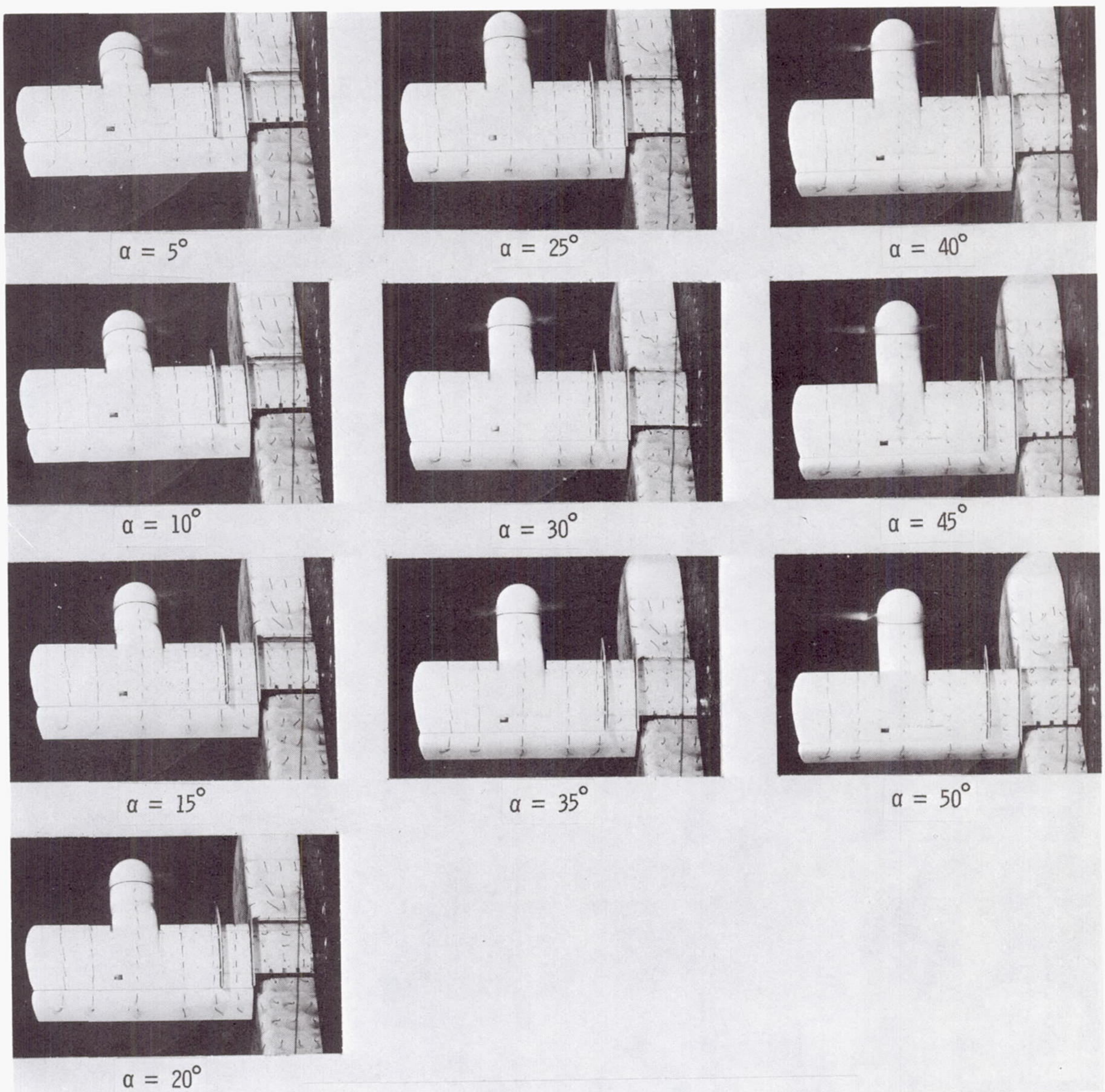

(d) Flow characteristics; $C_{T,s} = 0.60$.

Figure 12.- Continued.

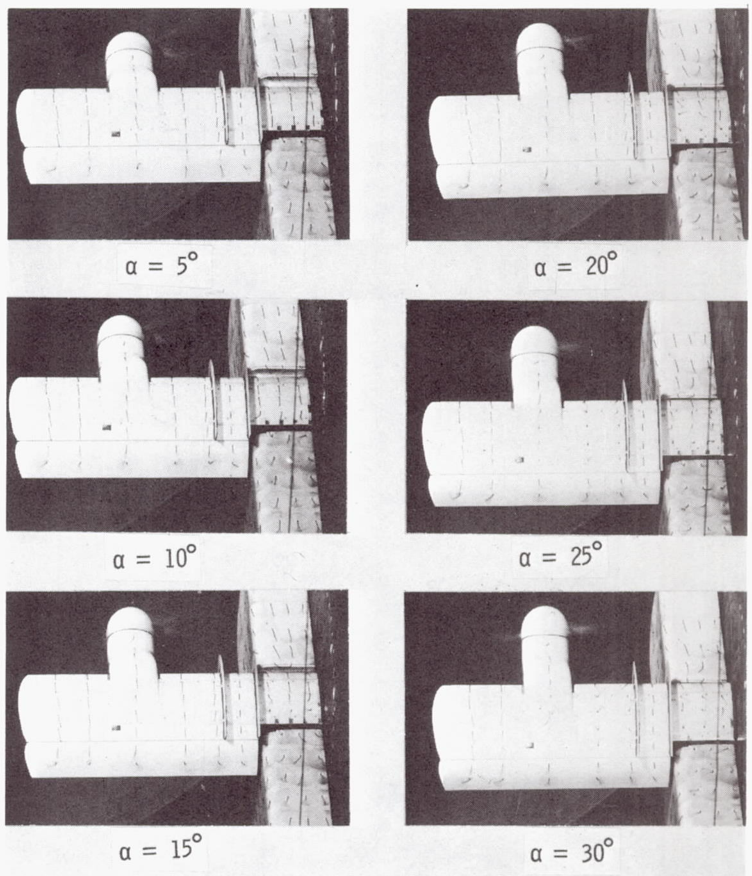

(e) Flow characteristics; $C_{T,s} = 0.30$.

Figure 12.- Concluded.

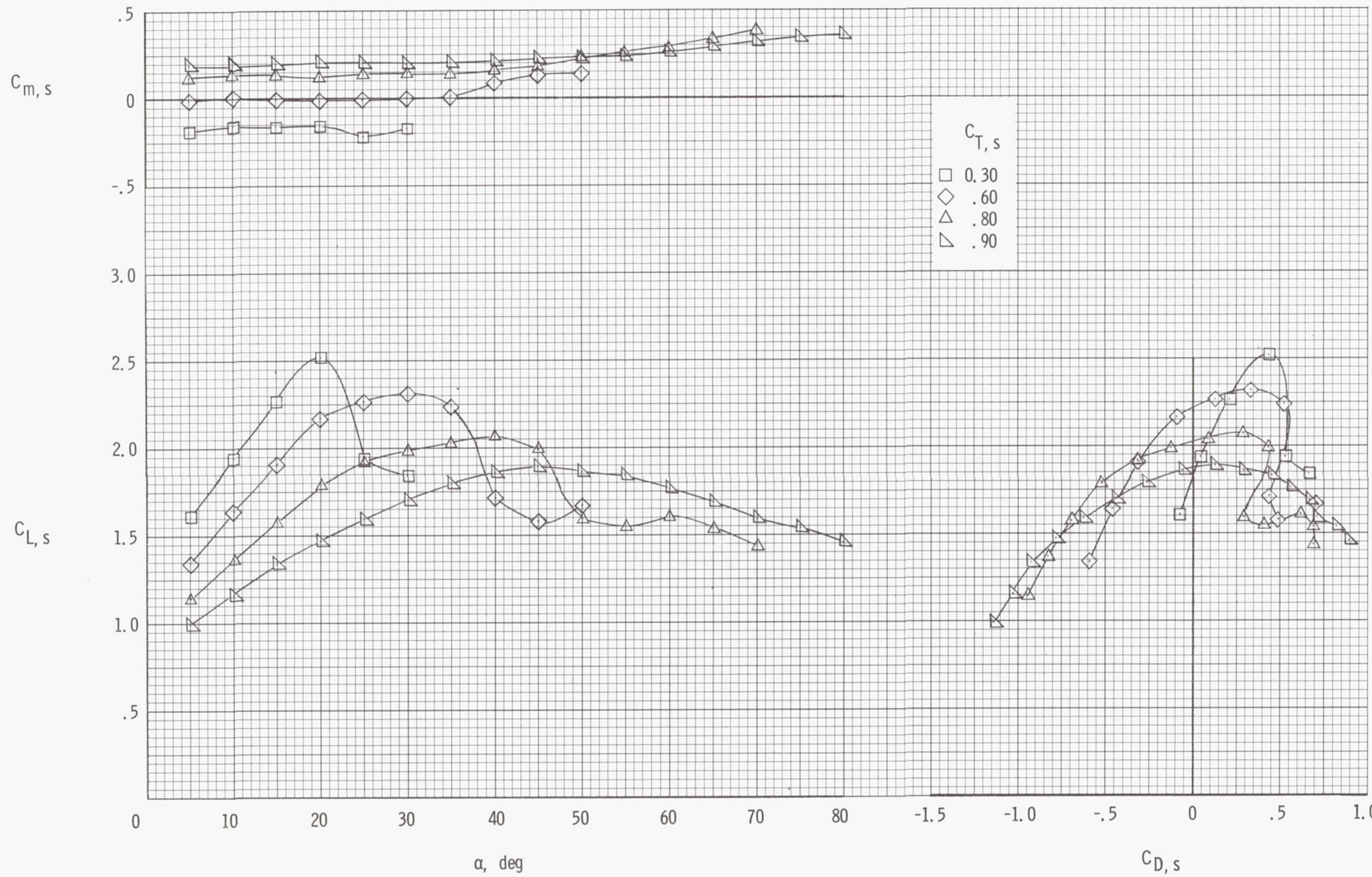

(a) Aerodynamic characteristics.

Figure 13.- Aerodynamic and flow characteristics of the wing with the propeller rotating down at the tip, basic leading edge, fences on, and $\delta_f = 60^o$.

(b) Flow characteristics; $C_{T,s} = 0.90$.

Figure 13.- Continued.

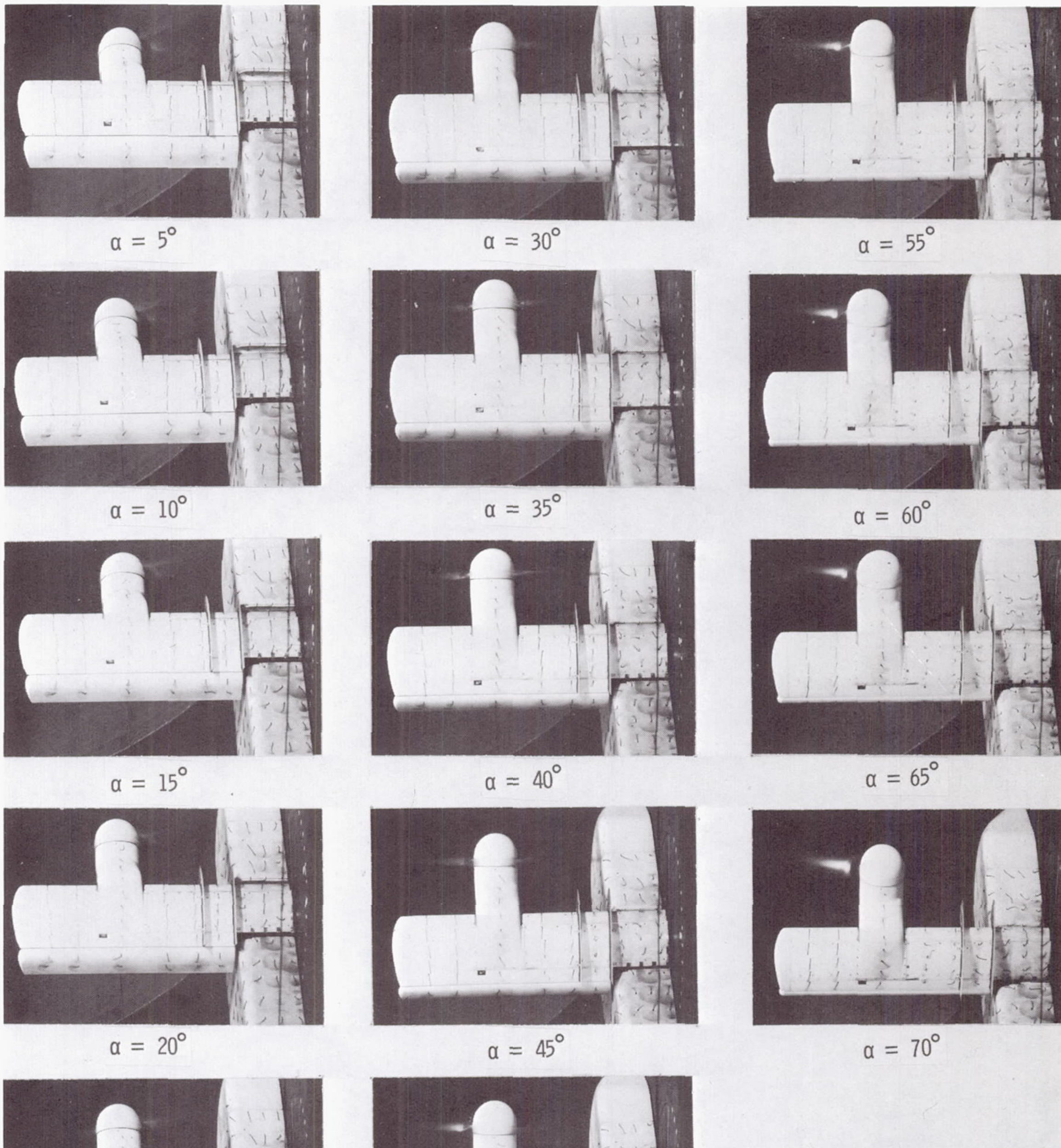

(c) Flow characteristics; $C_{T,s} = 0.80$.

Figure 13.- Continued.

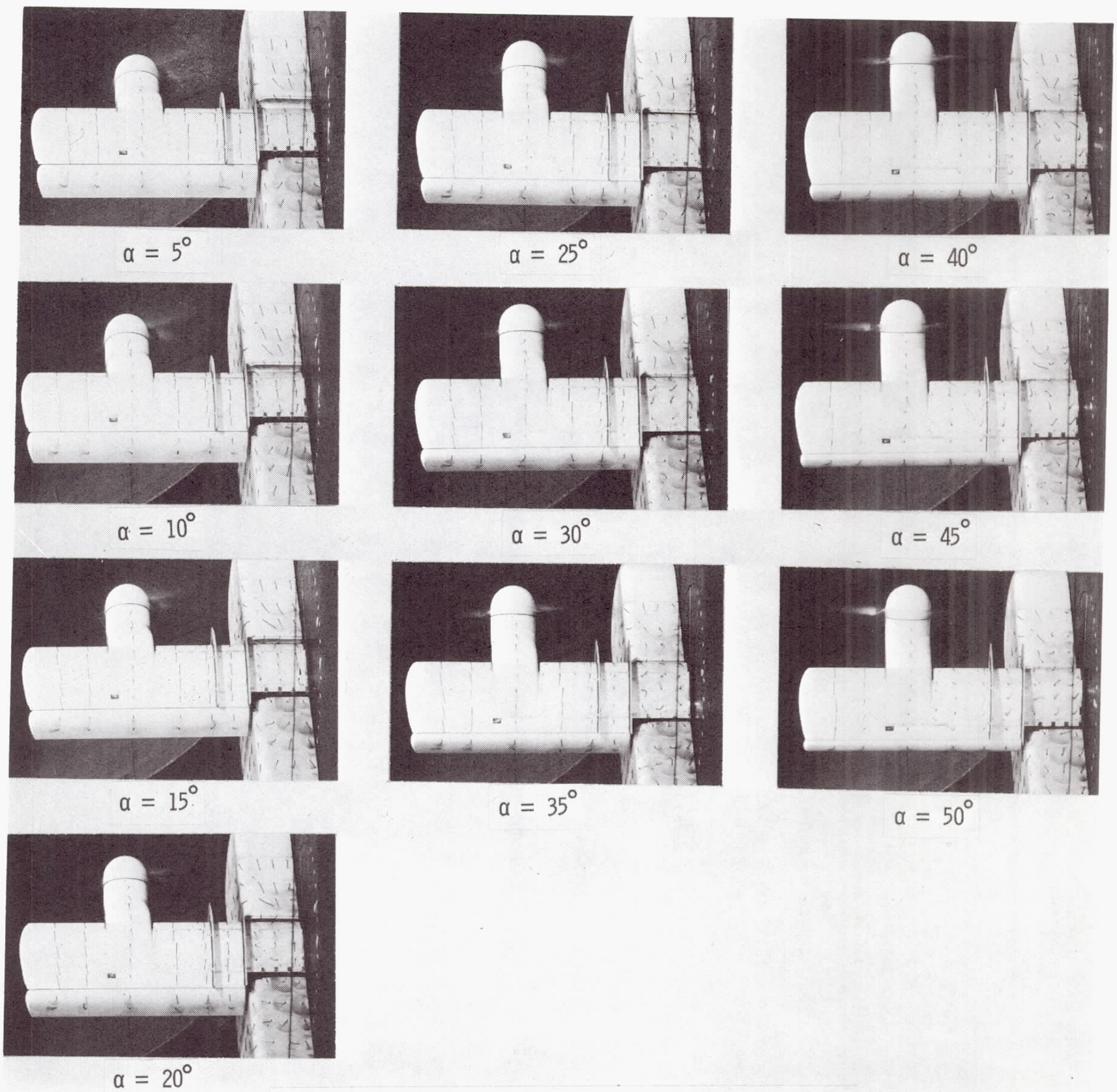

(d) Flow characteristics; $C_{T,s} = 0.60$.

Figure 13.- Continued.

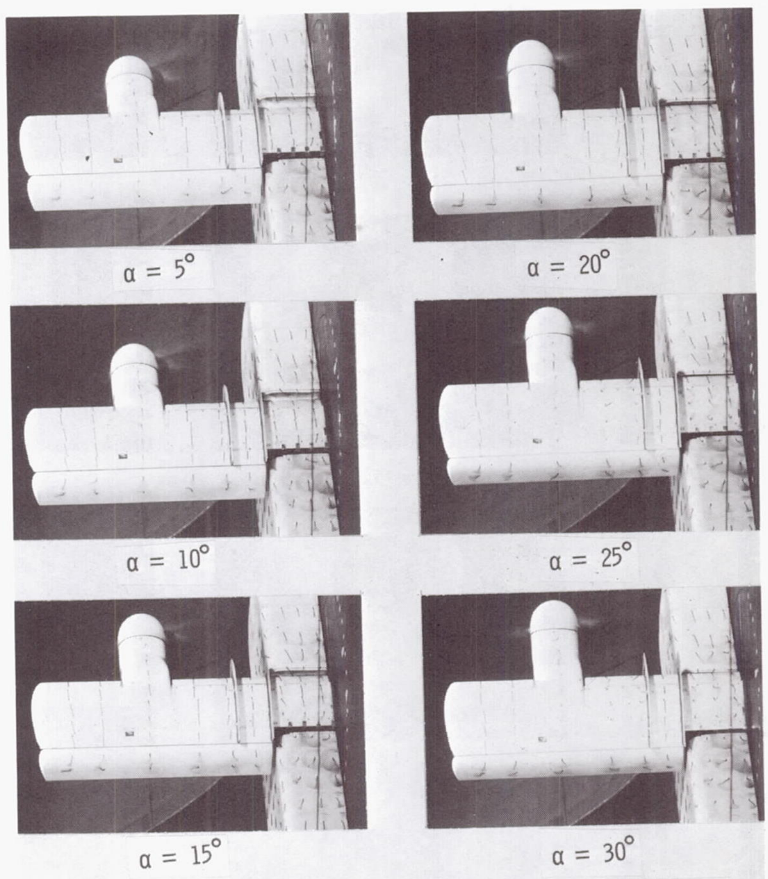

(e) Flow characteristics; $C_{T,s} = 0.30$.

Figure 13.- Concluded.

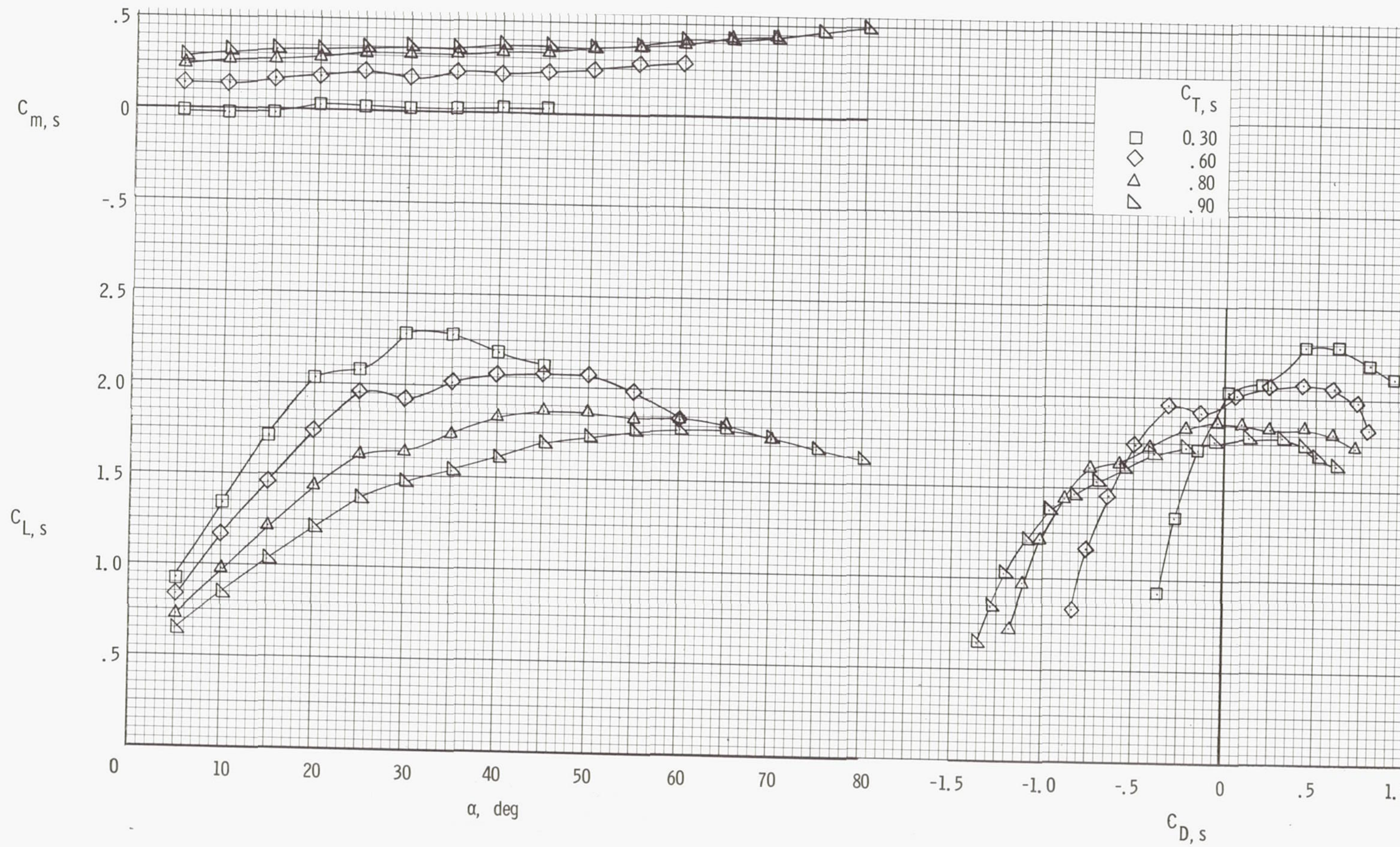

(a) Aerodynamic characteristics.

Figure 14.- Aerodynamic and flow characteristics of the wing with the propeller rotating down at the tip, inboard slat on, and $\delta_f = 20^o$.

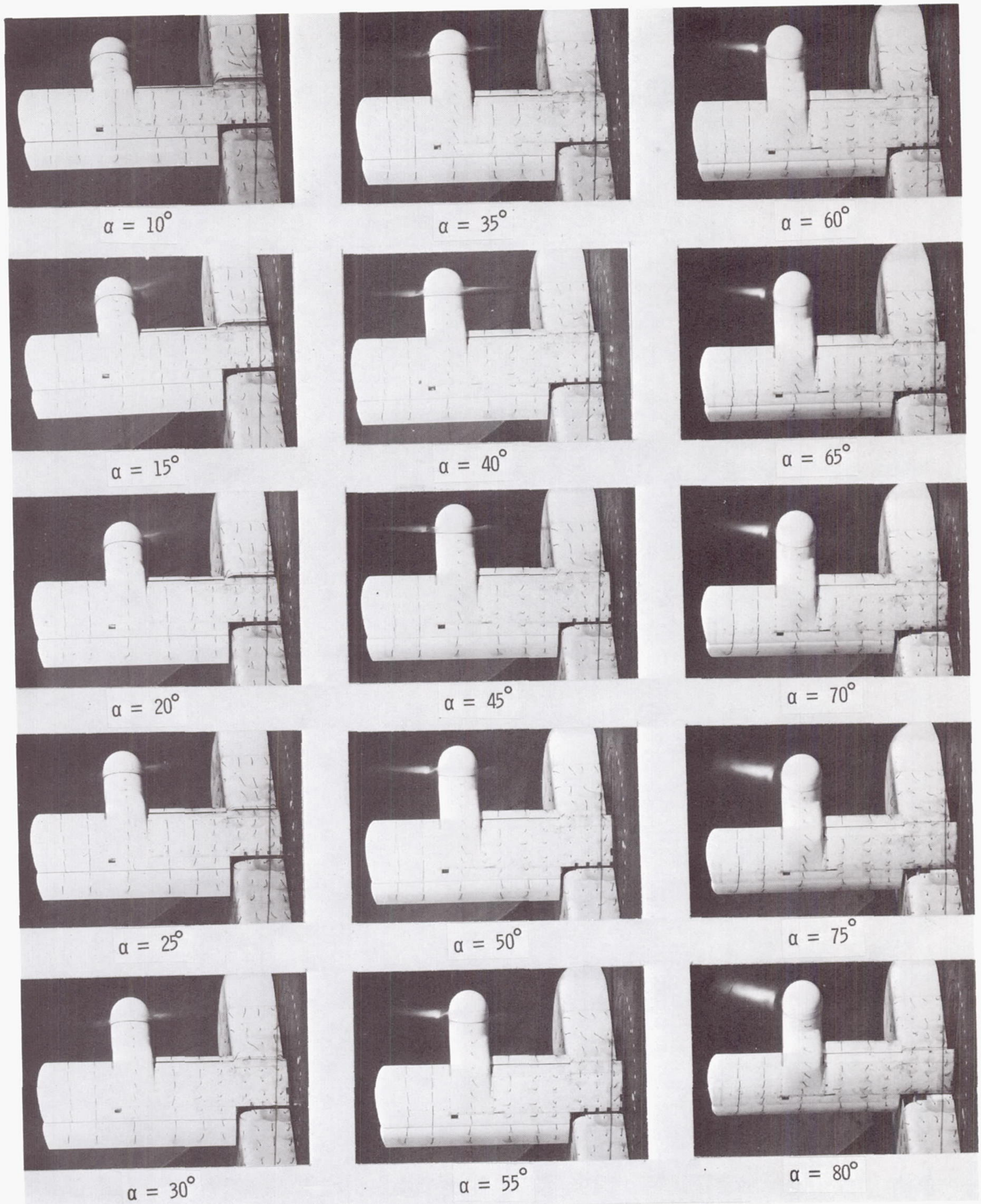

(b) Flow characteristics; $C_{T,s} = 0.90$.

Figure 14.- Continued.

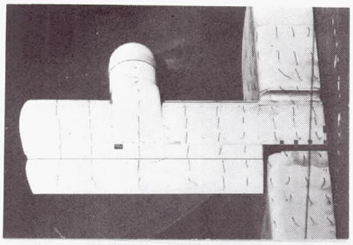

α = 5°

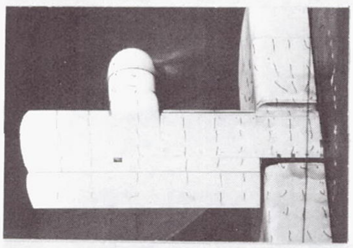

α = 10°

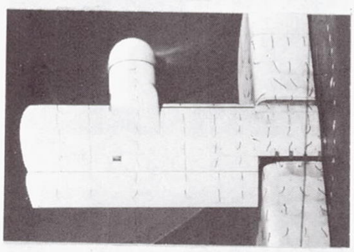

α = 15°

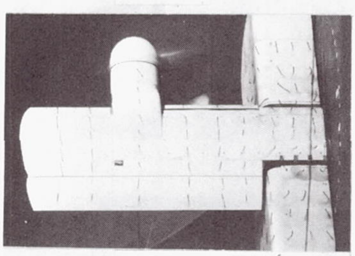

α = 20°

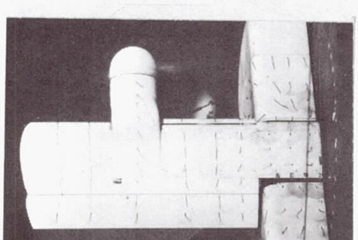

α = 25°

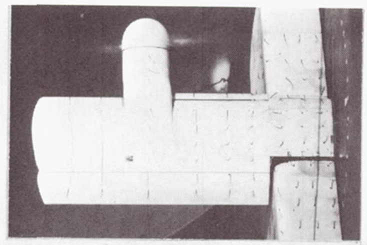

α = 30°

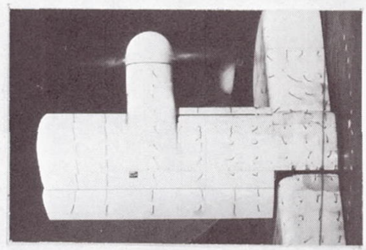

α = 35°

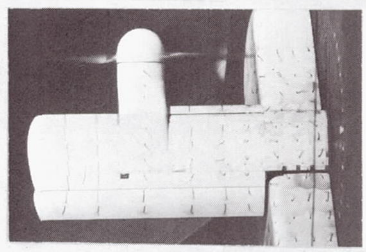

α = 40°

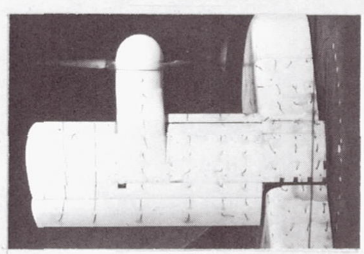

α = 45°

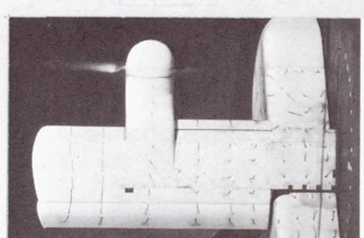

α = 50°

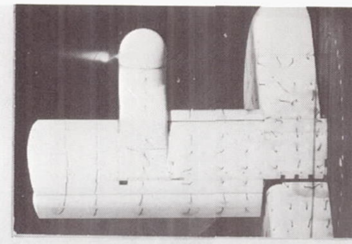

α = 55°

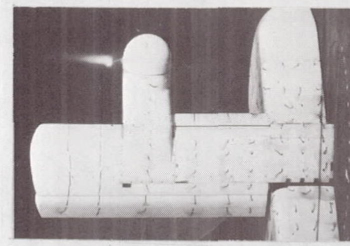

α = 60°

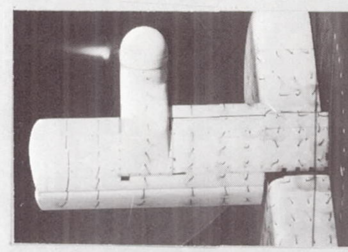

α = 65°

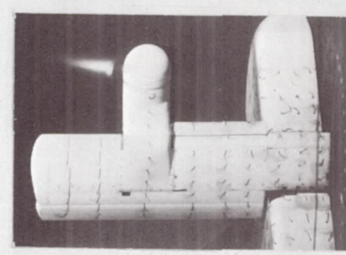

α = 70°

(c) Flow characteristics; $C_{T,s} = 0.80$.

Figure 14.- Continued.

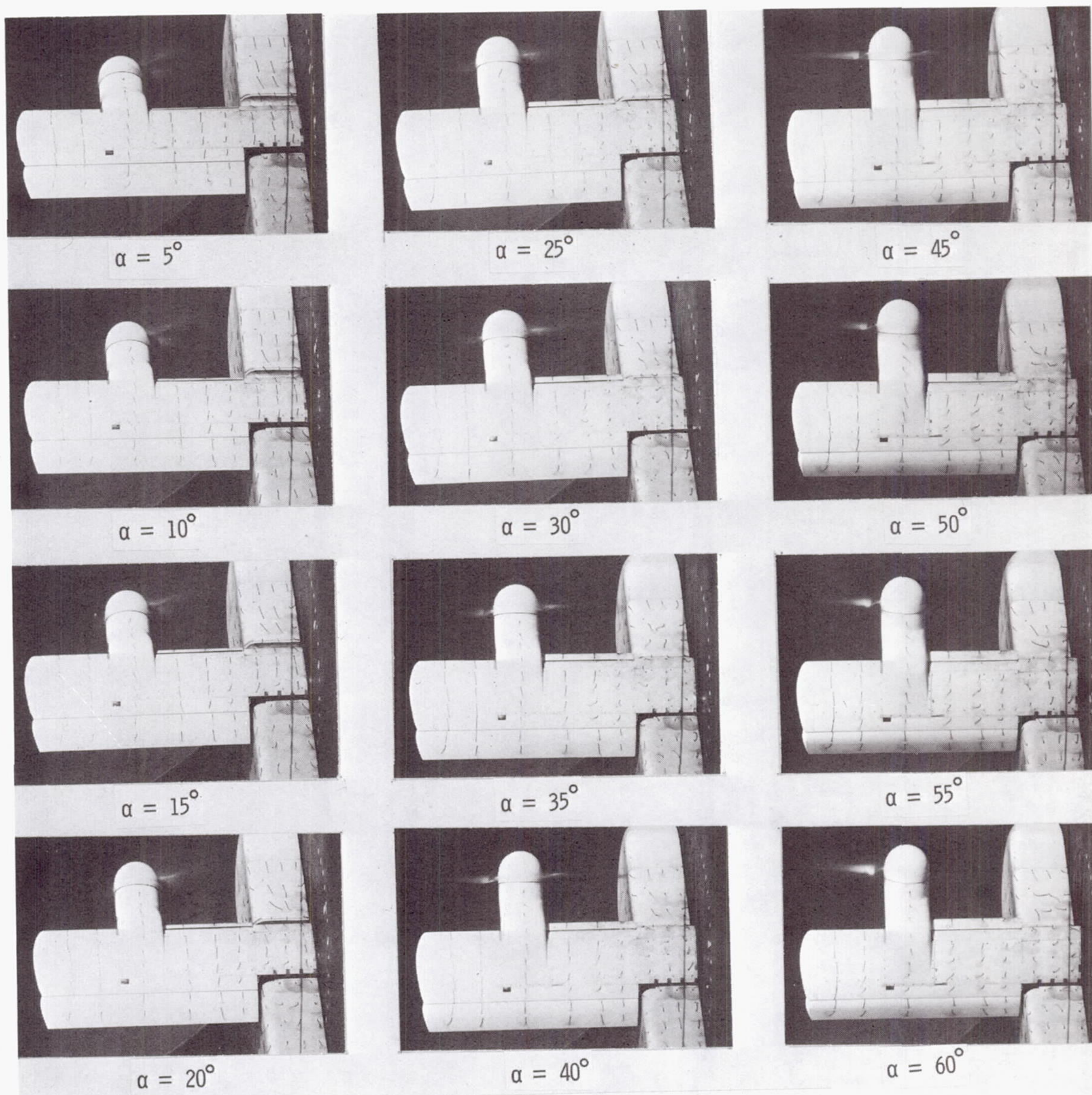

(d) Flow characteristics; $C_{T,s} = 0.60$.

Figure 14.- Continued.

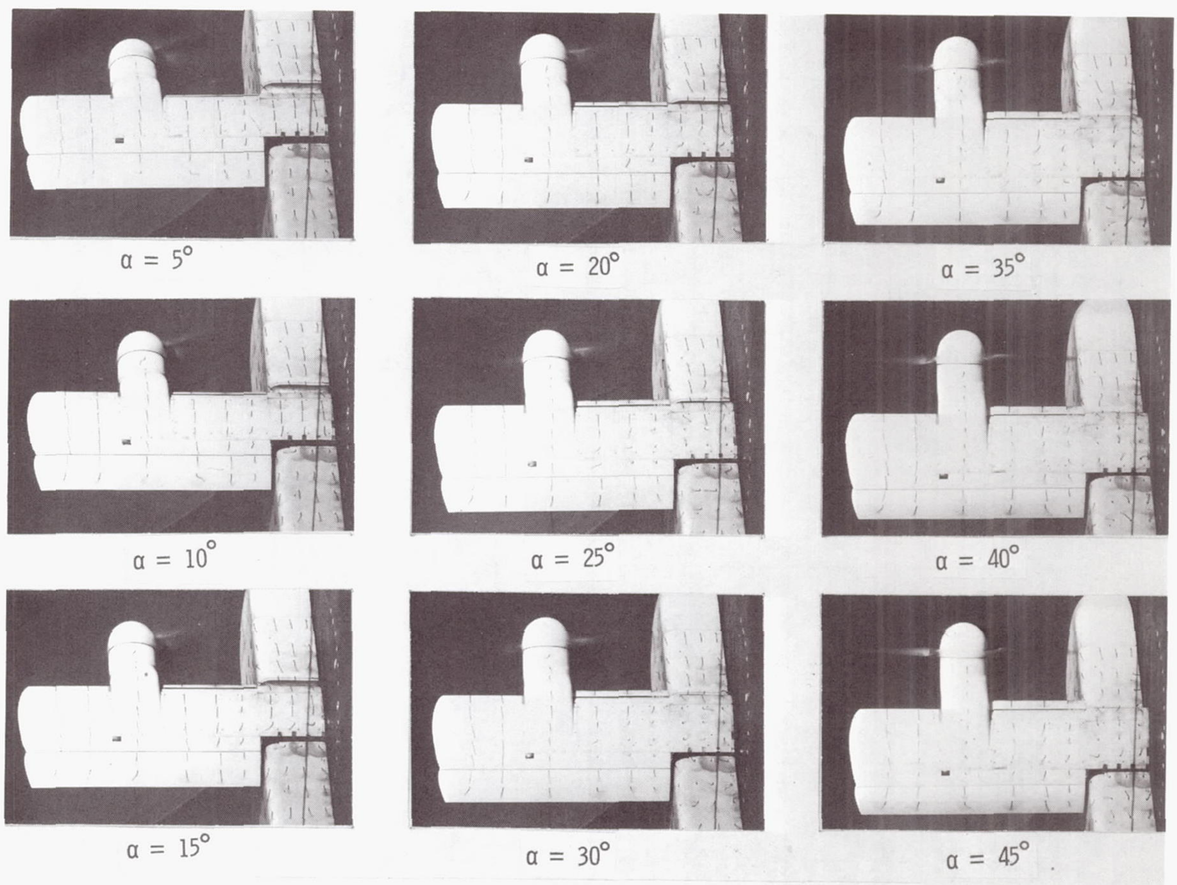

(e) Flow characteristics; $C_{T,s} = 0.30$.

Figure 14.- Concluded.

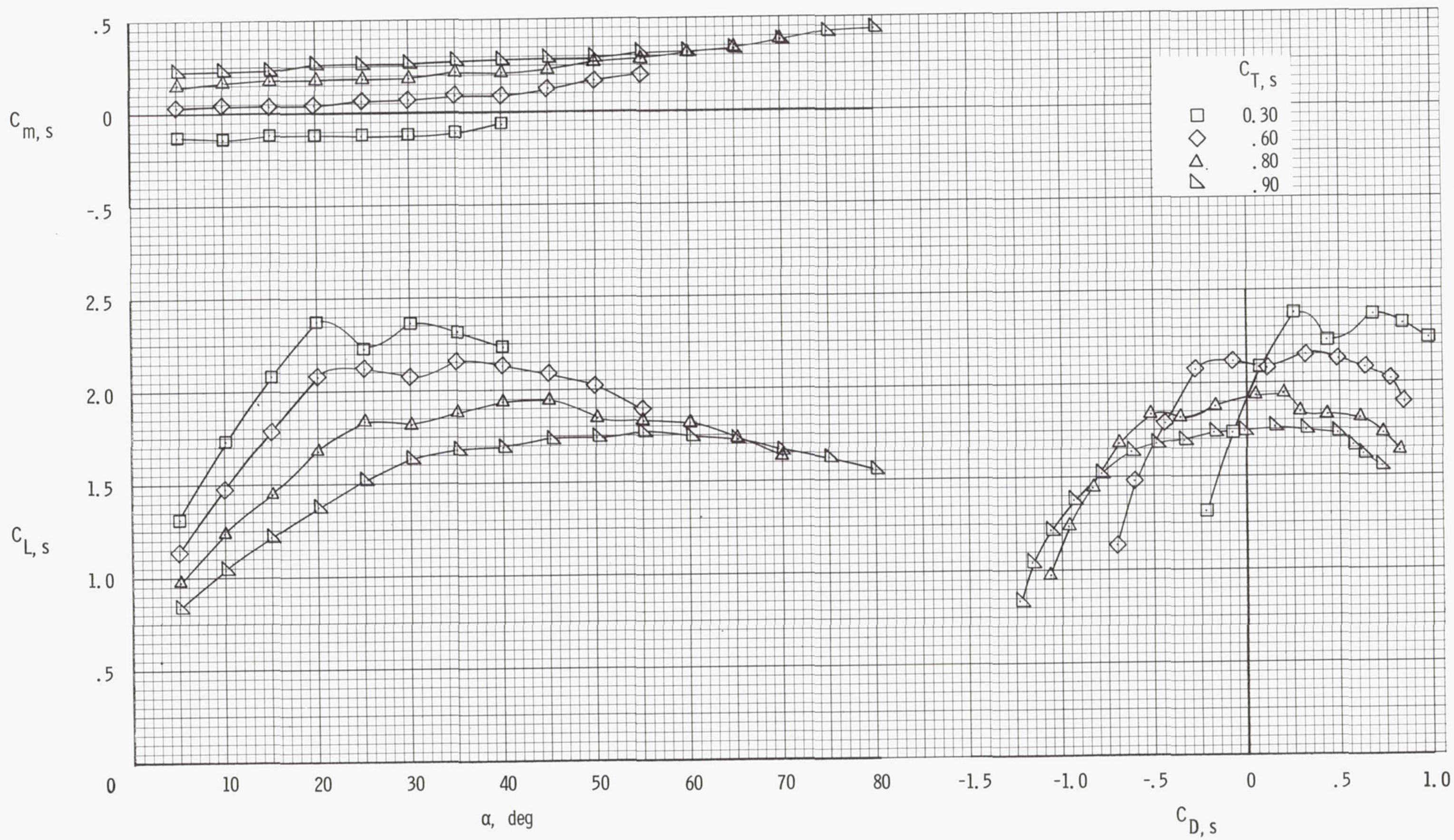

(a) Aerodynamic characteristics.

Figure 15.- Aerodynamic and flow characteristics of the wing with the propeller rotating down at the tip, inboard slat on, and $\delta_f = 40^o$.

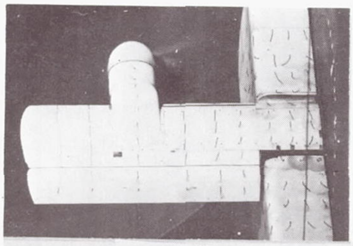

$\alpha = 10^\circ$

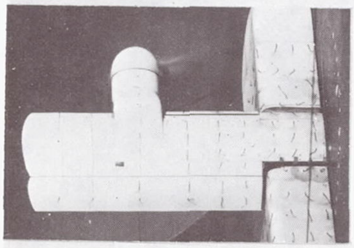

$\alpha = 15^\circ$

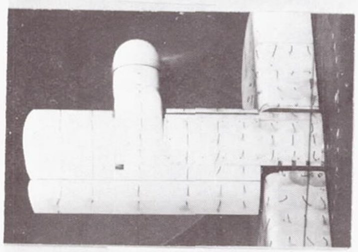

$\alpha = 20^\circ$

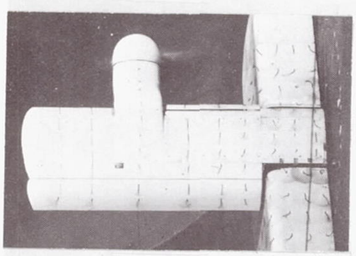

$\alpha = 25^\circ$

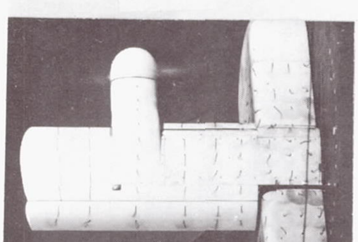

$\alpha = 30^\circ$

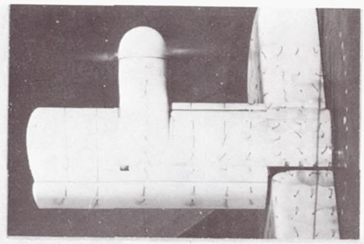

$\alpha = 35^\circ$

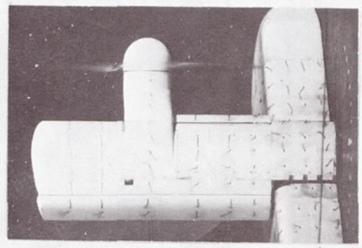

$\alpha = 40^\circ$

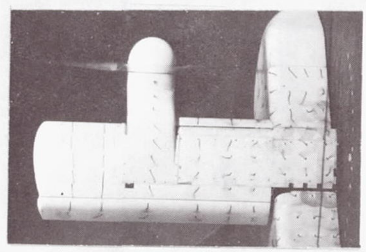

$\alpha = 45^\circ$

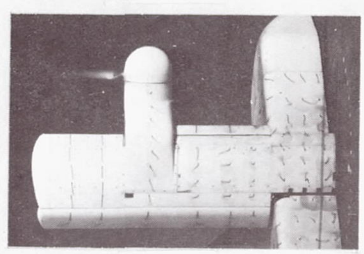

$\alpha = 50^\circ$

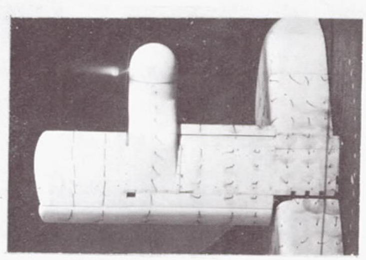

$\alpha = 55^\circ$

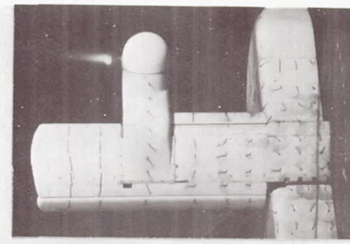

$\alpha = 60^\circ$

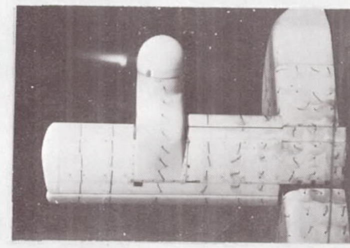

$\alpha = 65^\circ$

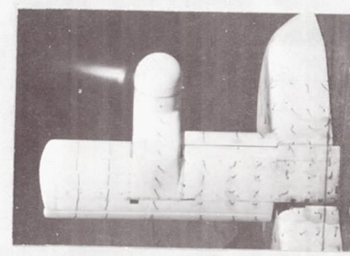

$\alpha = 70^\circ$

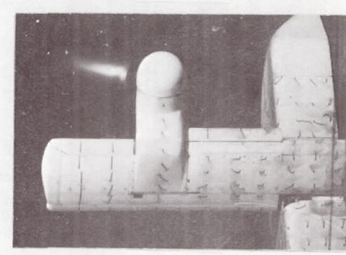

$\alpha = 75^\circ$

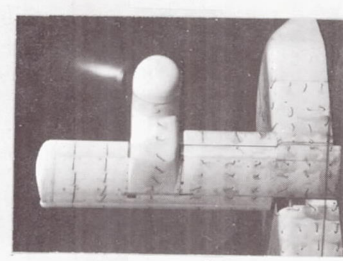

$\alpha = 80^\circ$

(b) Flow characteristics; $C_{T,s} = 0.90$.

Figure 15.- Continued.

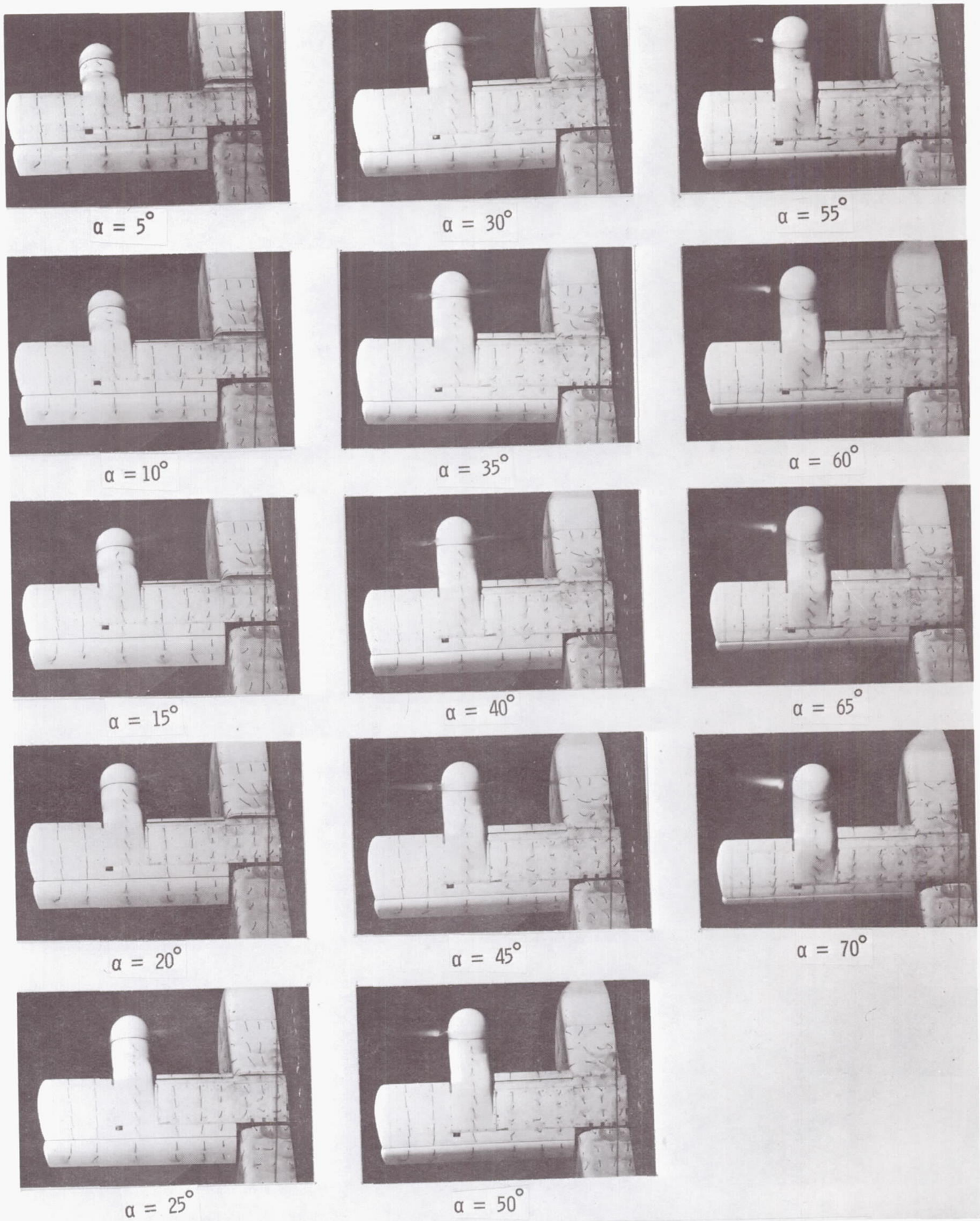

(c) Flow characteristics; $C_{T,s} = 0.80$.

Figure 15.- Continued.

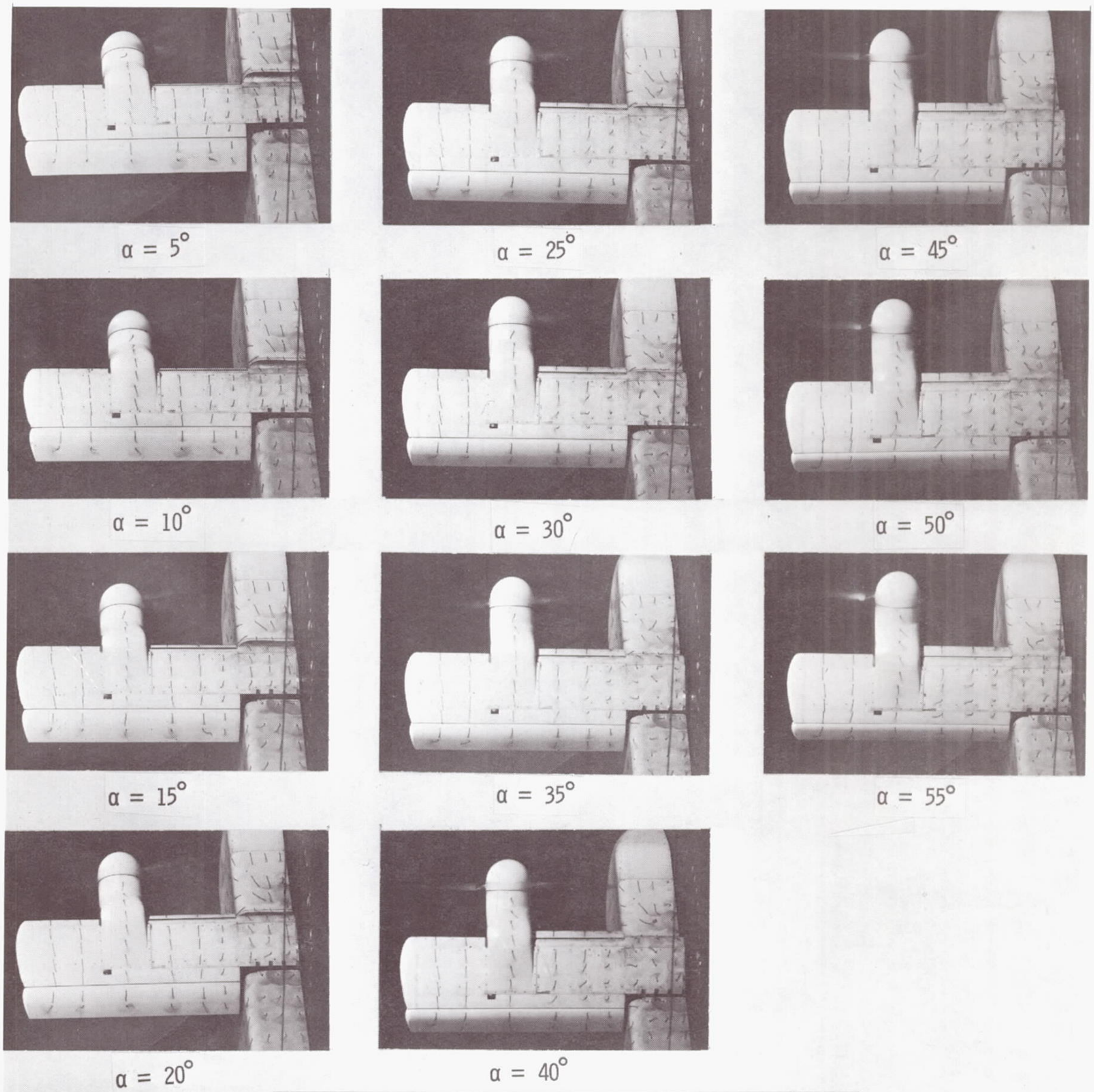

(d) Flow characteristics; $C_{T,s} = 0.60$.

Figure 15.- Continued.

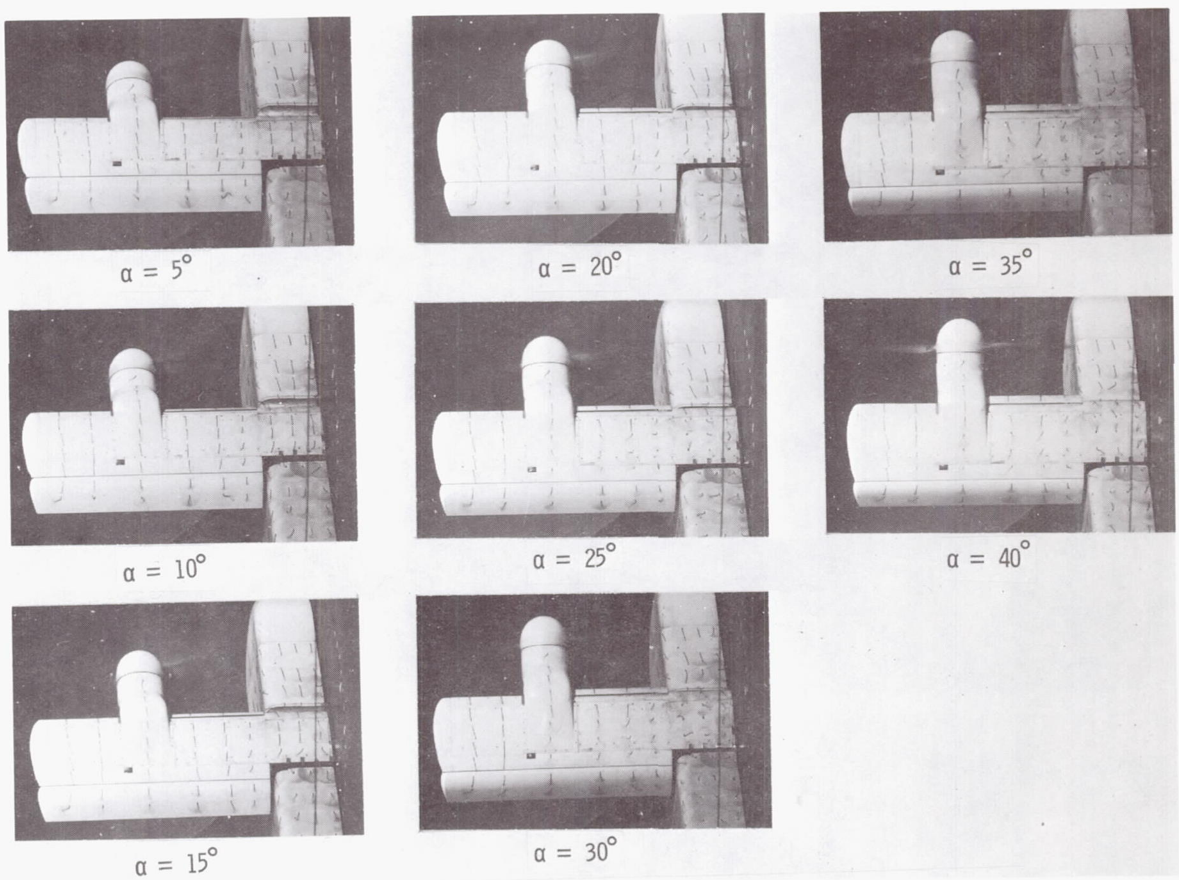

(e) Flow characteristics; $C_{T,s} = 0.30$.

Figure 15.- Concluded.

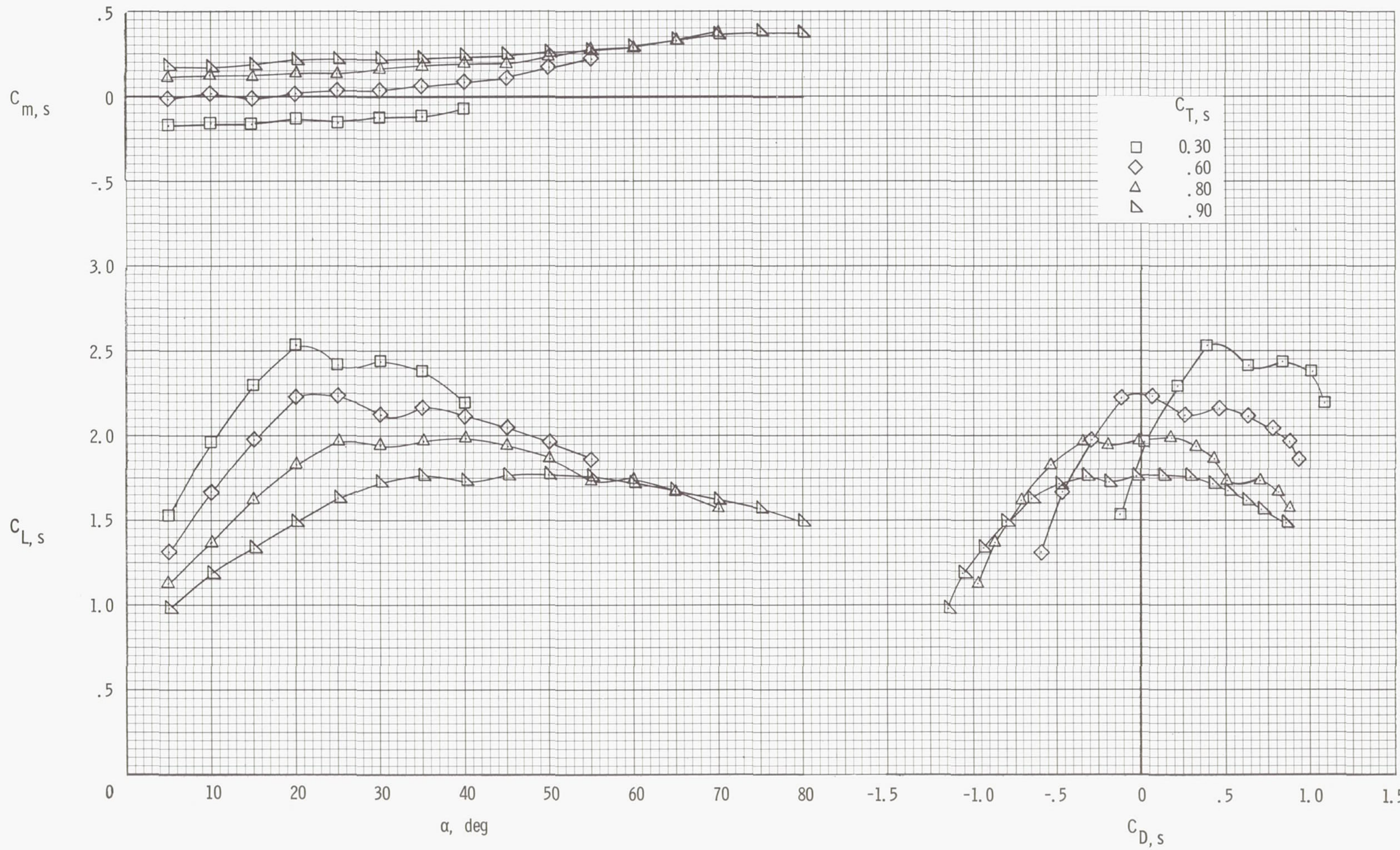

(a) Aerodynamic characteristics.

Figure 16.- Aerodynamic and flow characteristics of the wing with the propeller rotating down at the tip, inboard slat on, and $\delta_f = 60^o$.

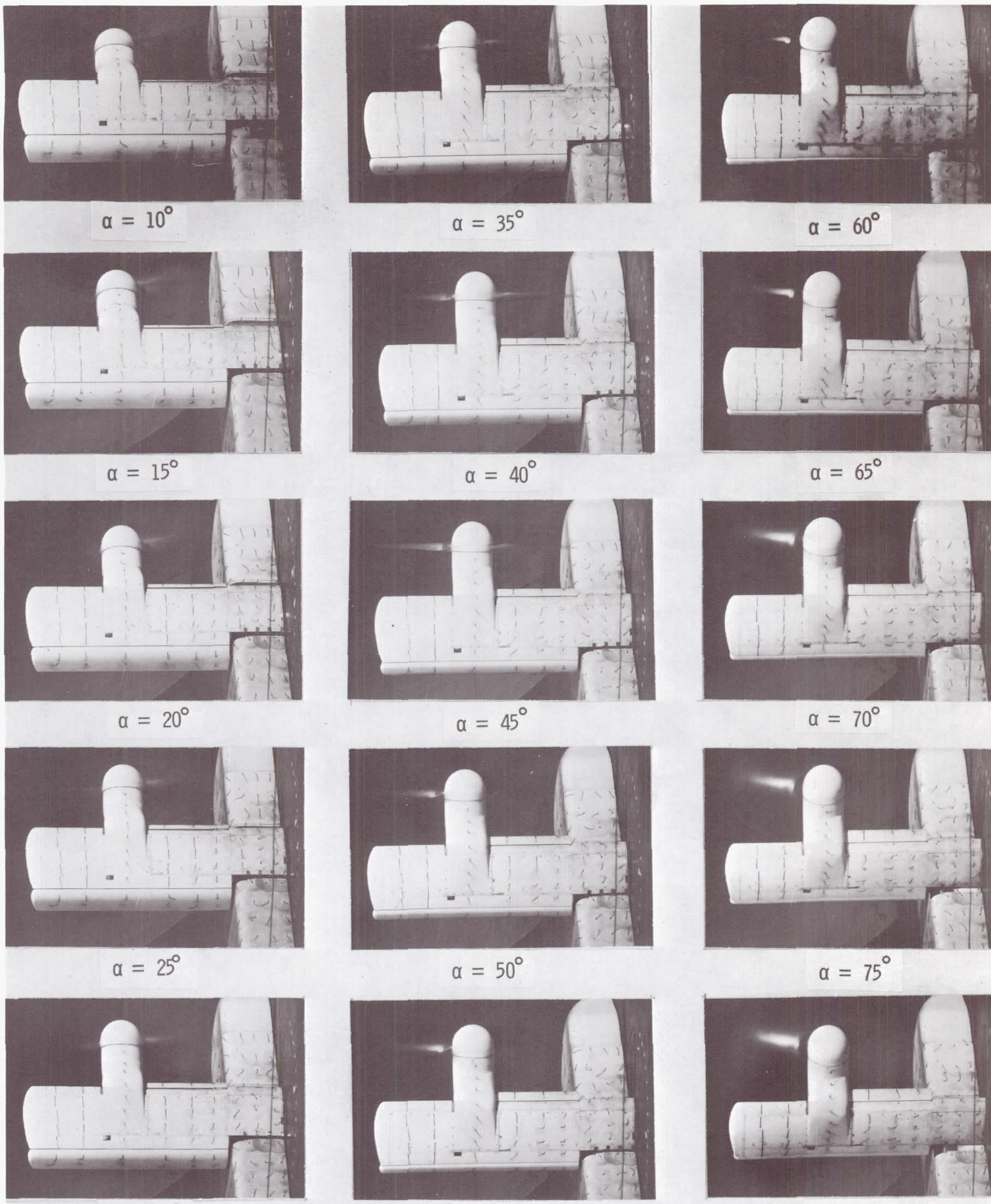

(b) Flow characteristics; $C_{T,s} = 0.90$.

Figure 16.- Continued.

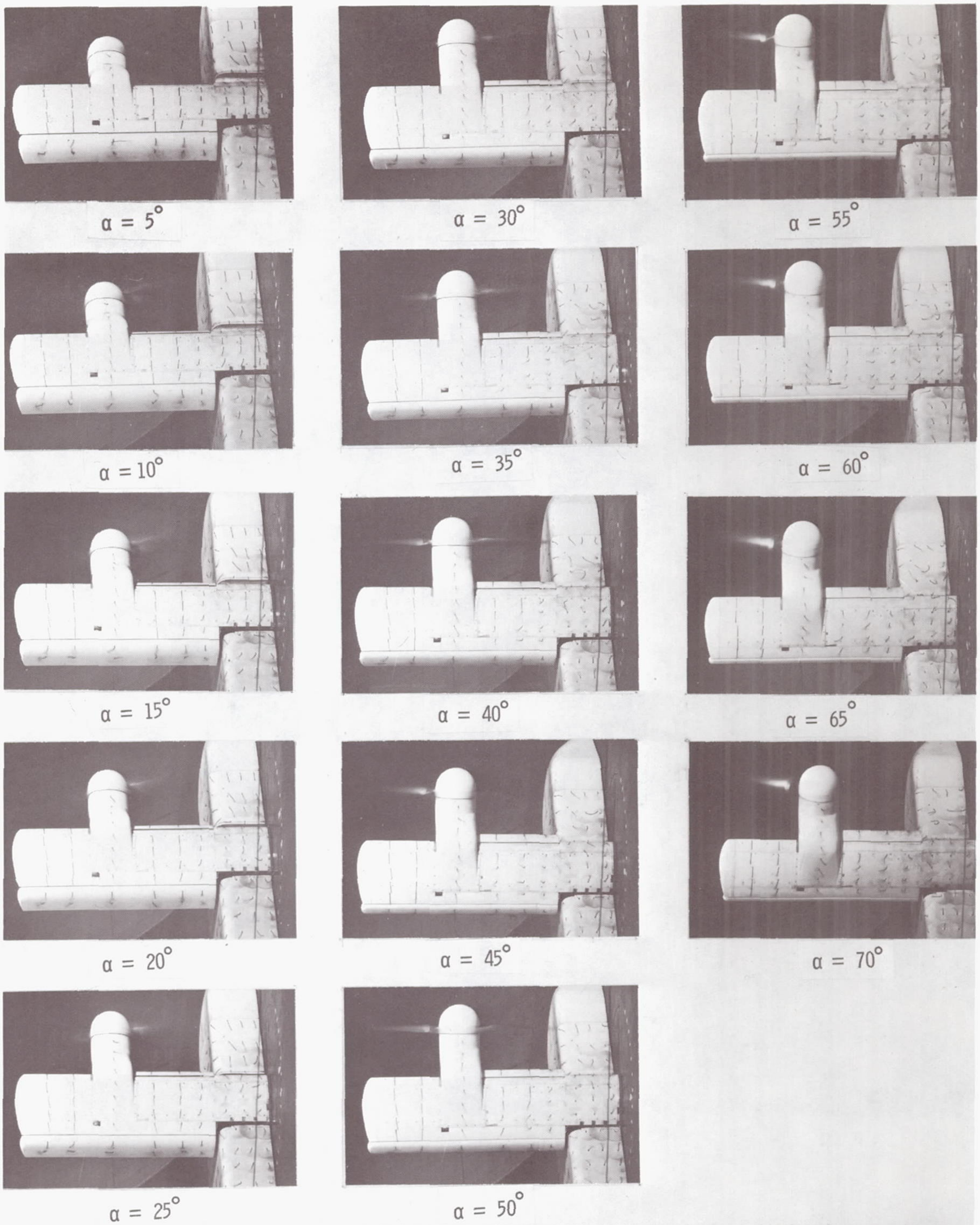

(c) Flow characteristics; $C_{T,s} = 0.80$.

Figure 16.- Continued.

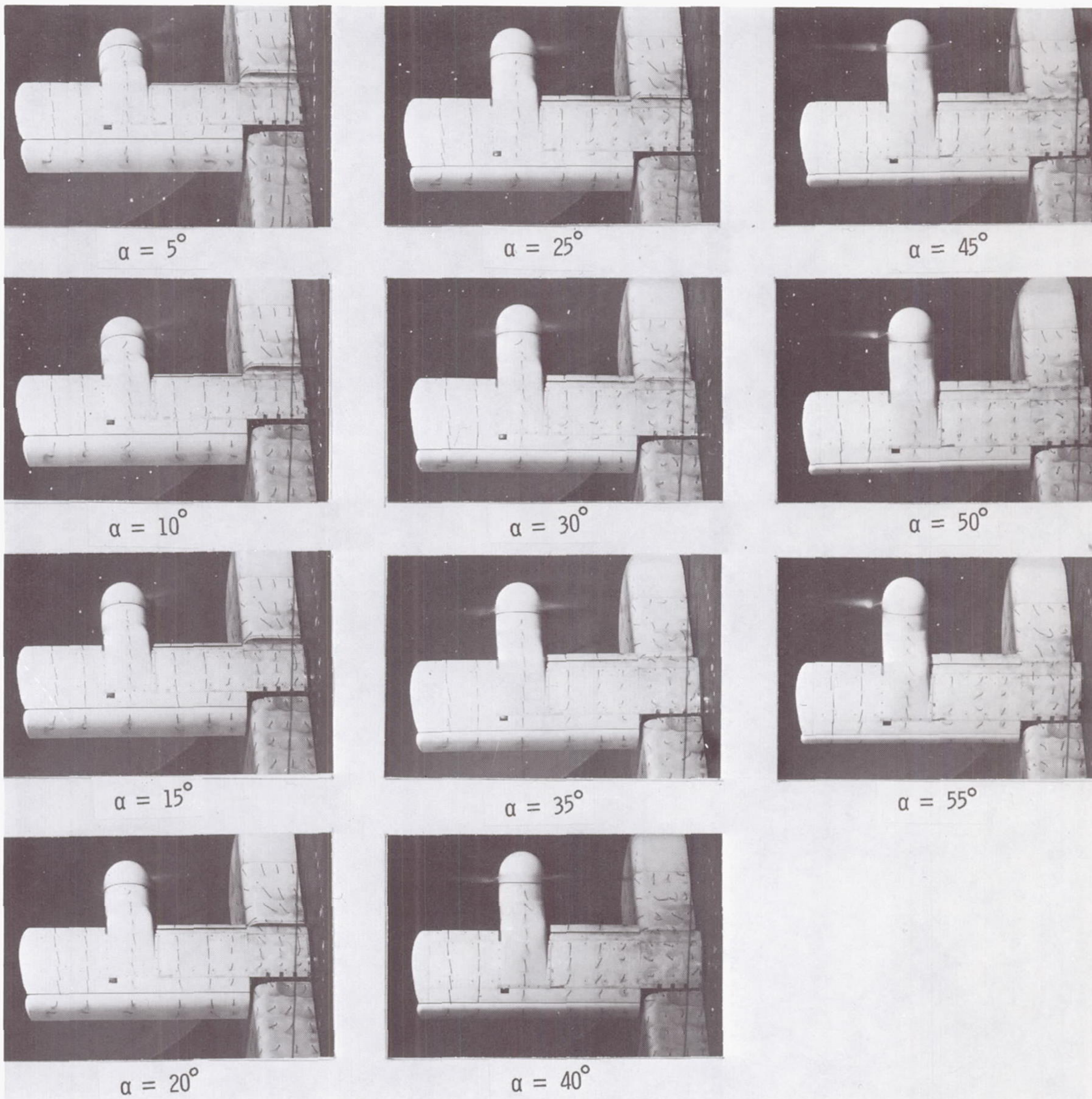

(d) Flow characteristics; $C_{T,s} = 0.60$.

Figure 16.- Continued.

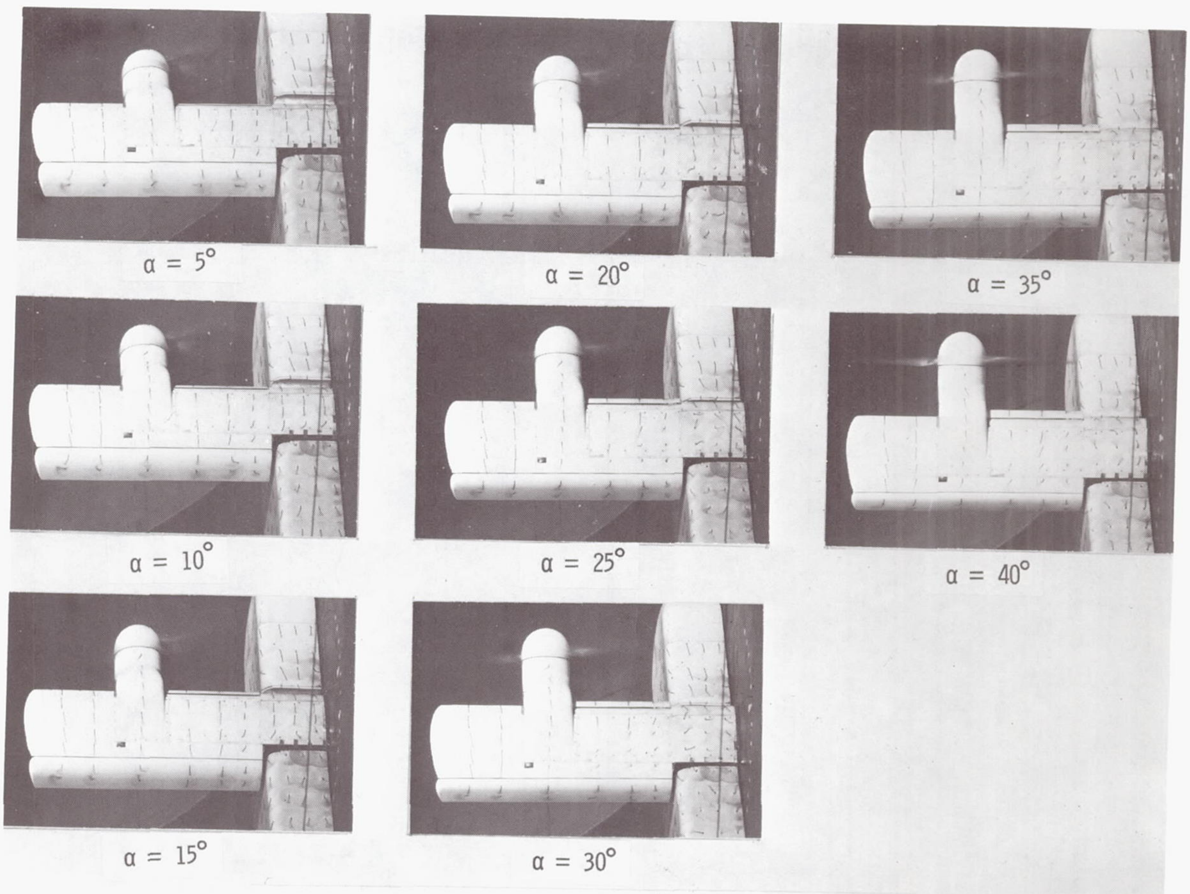

(e) Flow characteristics; $C_{T,s} = 0.30$.

Figure 16.- Concluded.

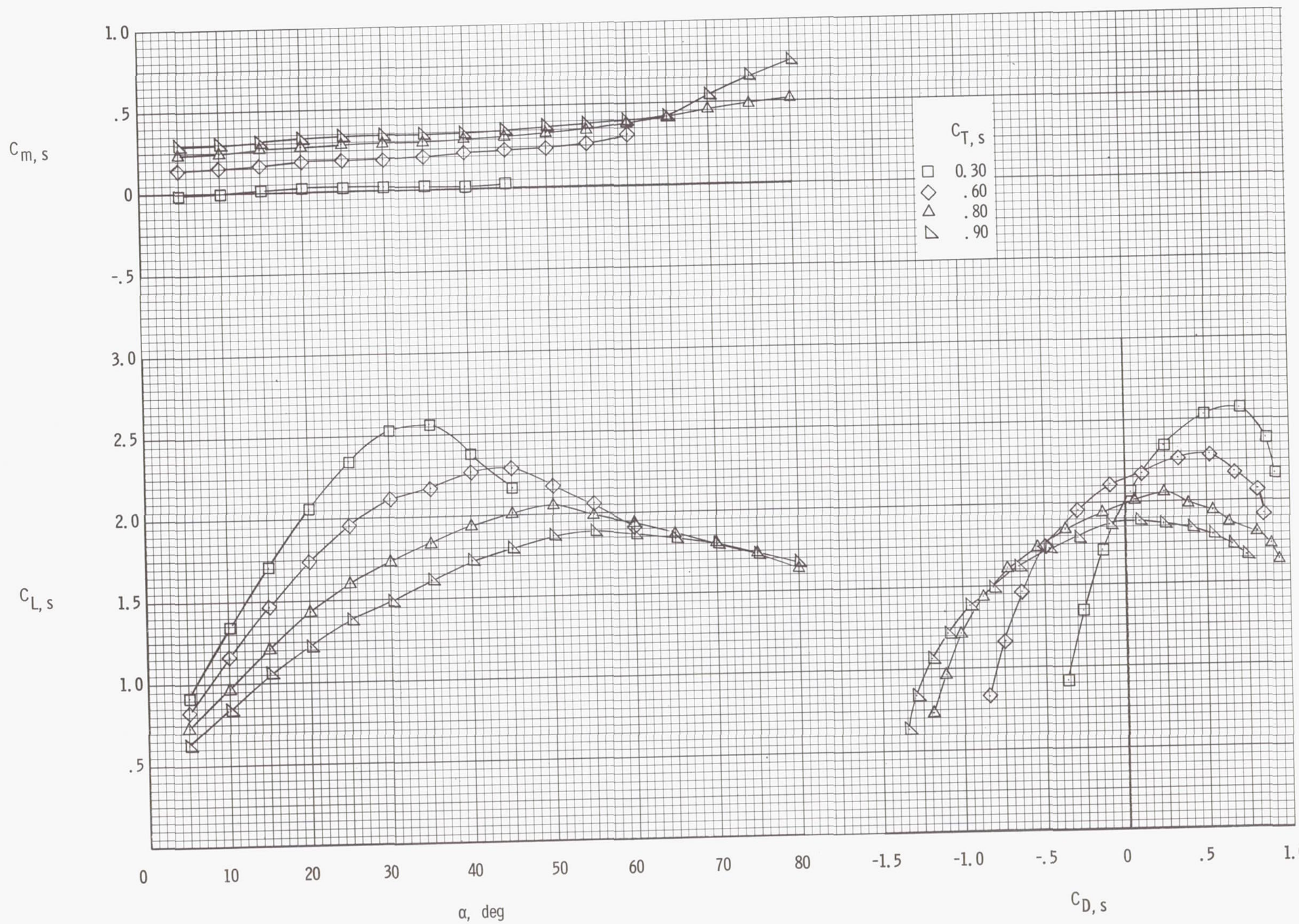

(a) Aerodynamic characteristics.

Figure 17.- Aerodynamic and flow characteristics of the wing with the propeller rotating down at the tip, inboard slat on, fences on, and $\delta_f = 20^{\circ}$.

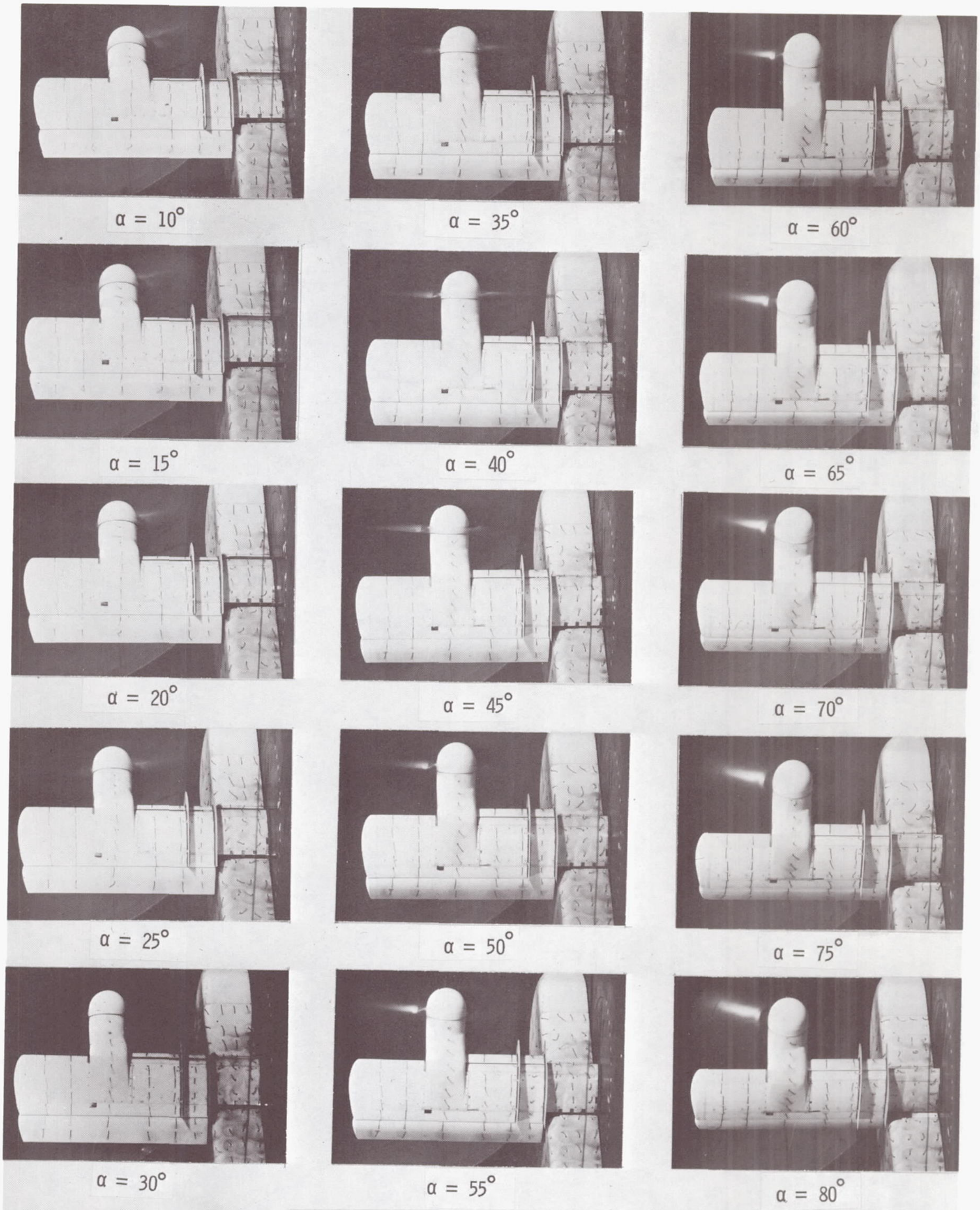

(b) Flow characteristics; $C_{T,s} = 0.90$.

Figure 17.- Continued.

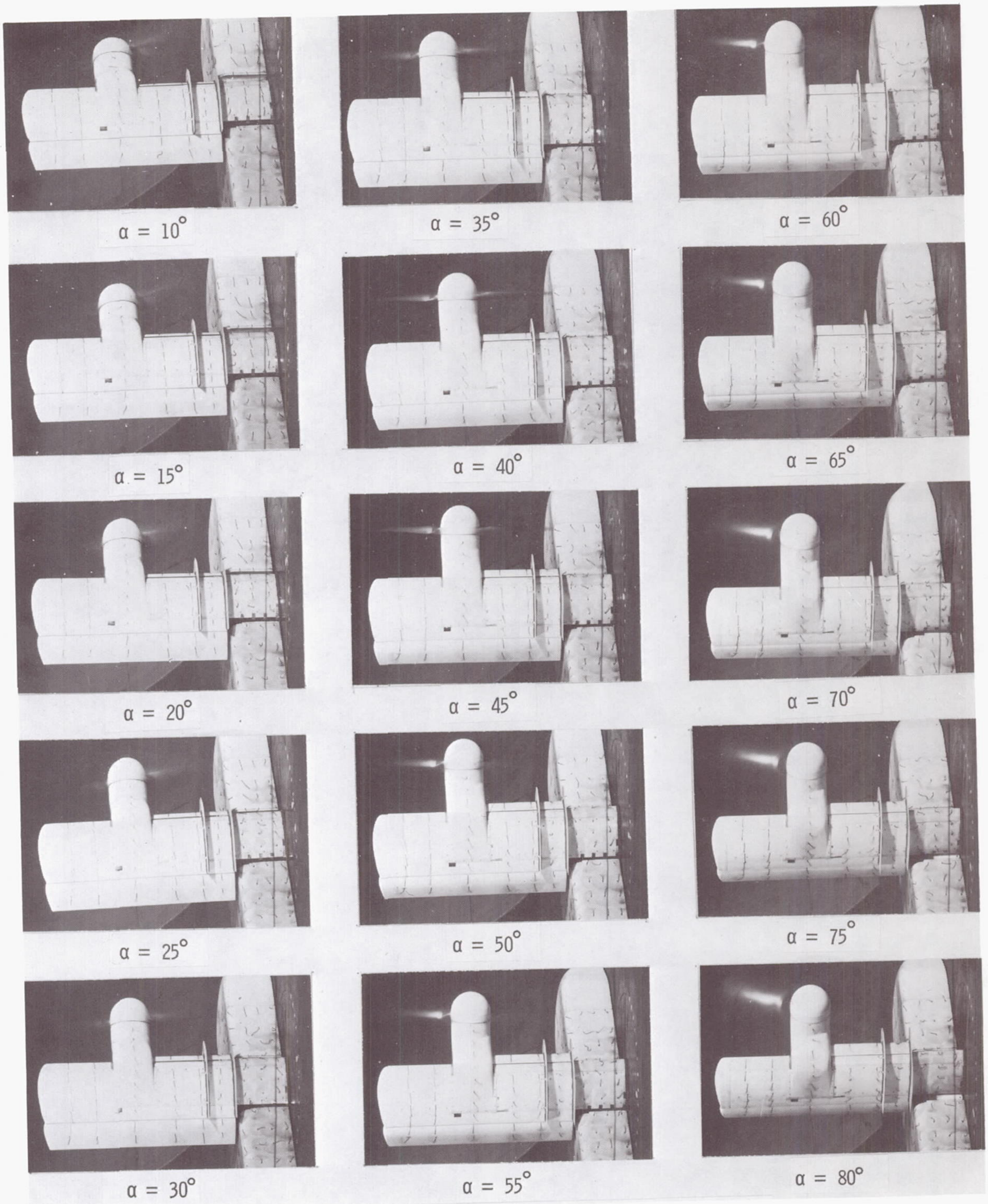

(c) Flow characteristics; $C_{T,s} = 0.80$.

Figure 17.- Continued.

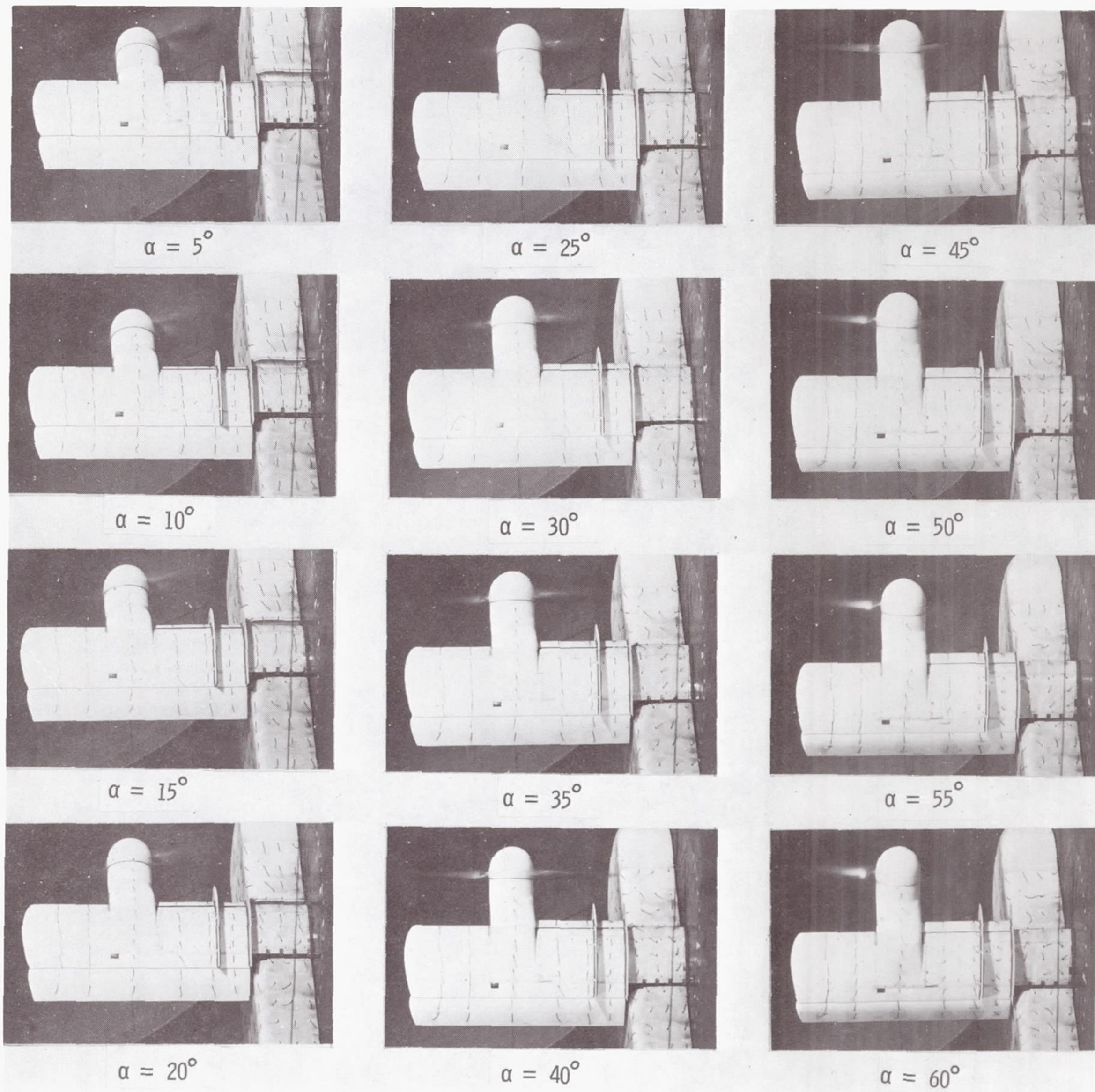

(d) Flow characteristics; $C_{T,s} = 0.60$.

Figure 17.- Continued.

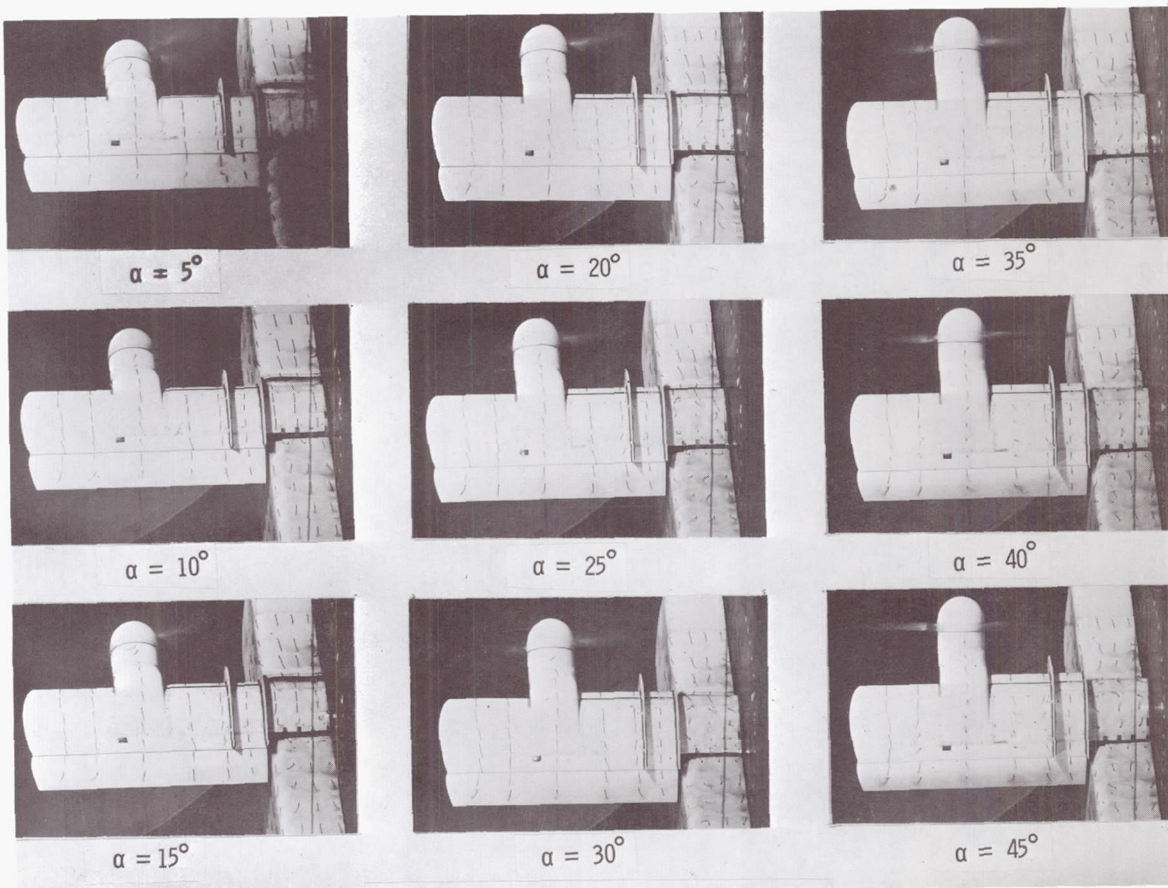

(e) Flow characteristics; $C_{T,s} = 0.30$.

Figure 17.- Concluded.

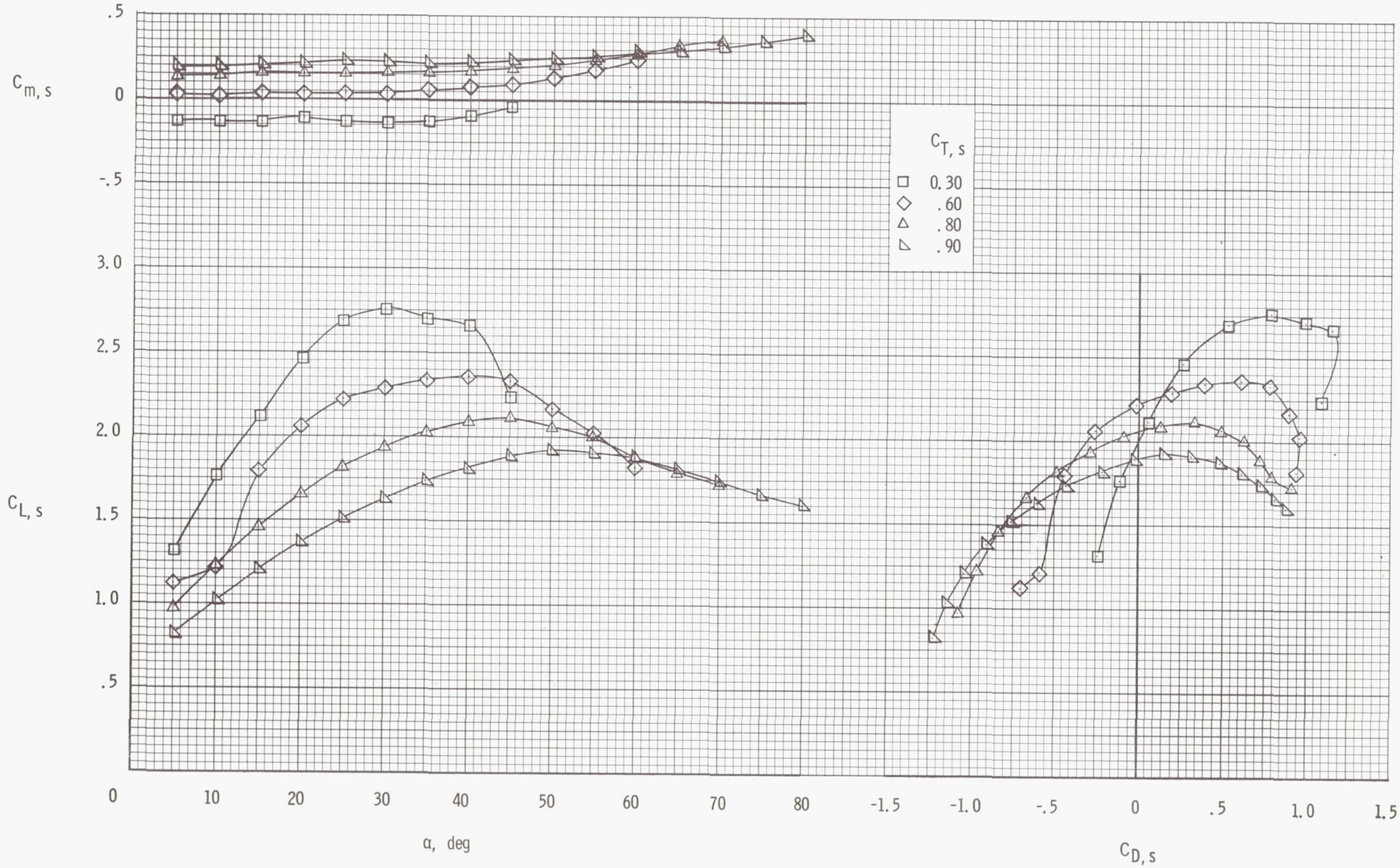

(a) Aerodynamic characteristics.

Figure 18.- Aerodynamic and flow characteristics of the wing with the propeller rotating down at the tip, inboard slat on, fences on, and $\delta_f = 40^o$.

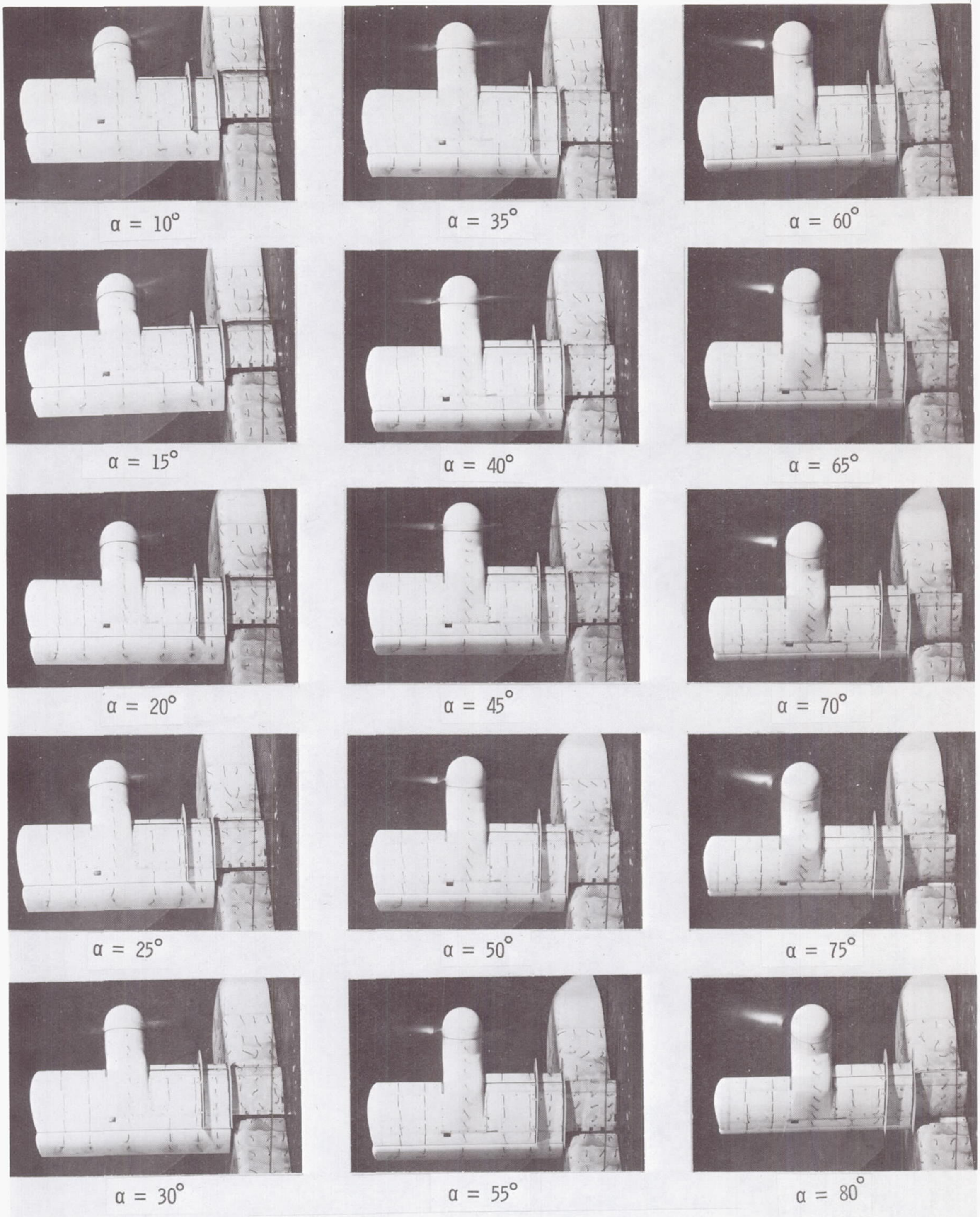

(b) Flow characteristics; $C_{T,s} = 0.90$.

Figure 18.- Continued.

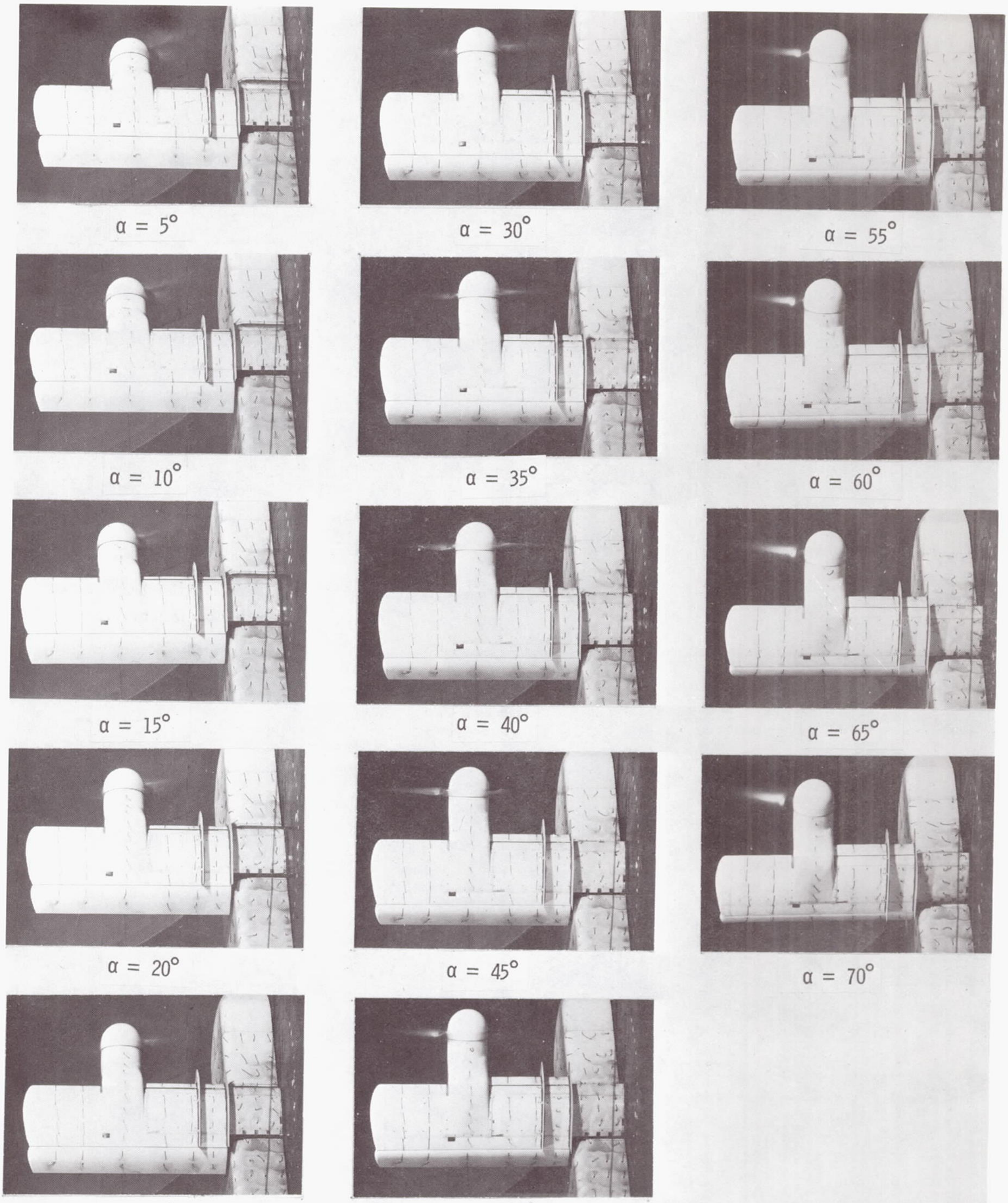

$\alpha = 5^\circ$ $\alpha = 10^\circ$ $\alpha = 15^\circ$ $\alpha = 20^\circ$ $\alpha = 25^\circ$

$\alpha = 30^\circ$ $\alpha = 35^\circ$ $\alpha = 40^\circ$ $\alpha = 45^\circ$ $\alpha = 50^\circ$

$\alpha = 55^\circ$ $\alpha = 60^\circ$ $\alpha = 65^\circ$ $\alpha = 70^\circ$

(c) Flow characteristics; $C_{T,s} = 0.80$.

Figure 18.- Continued.

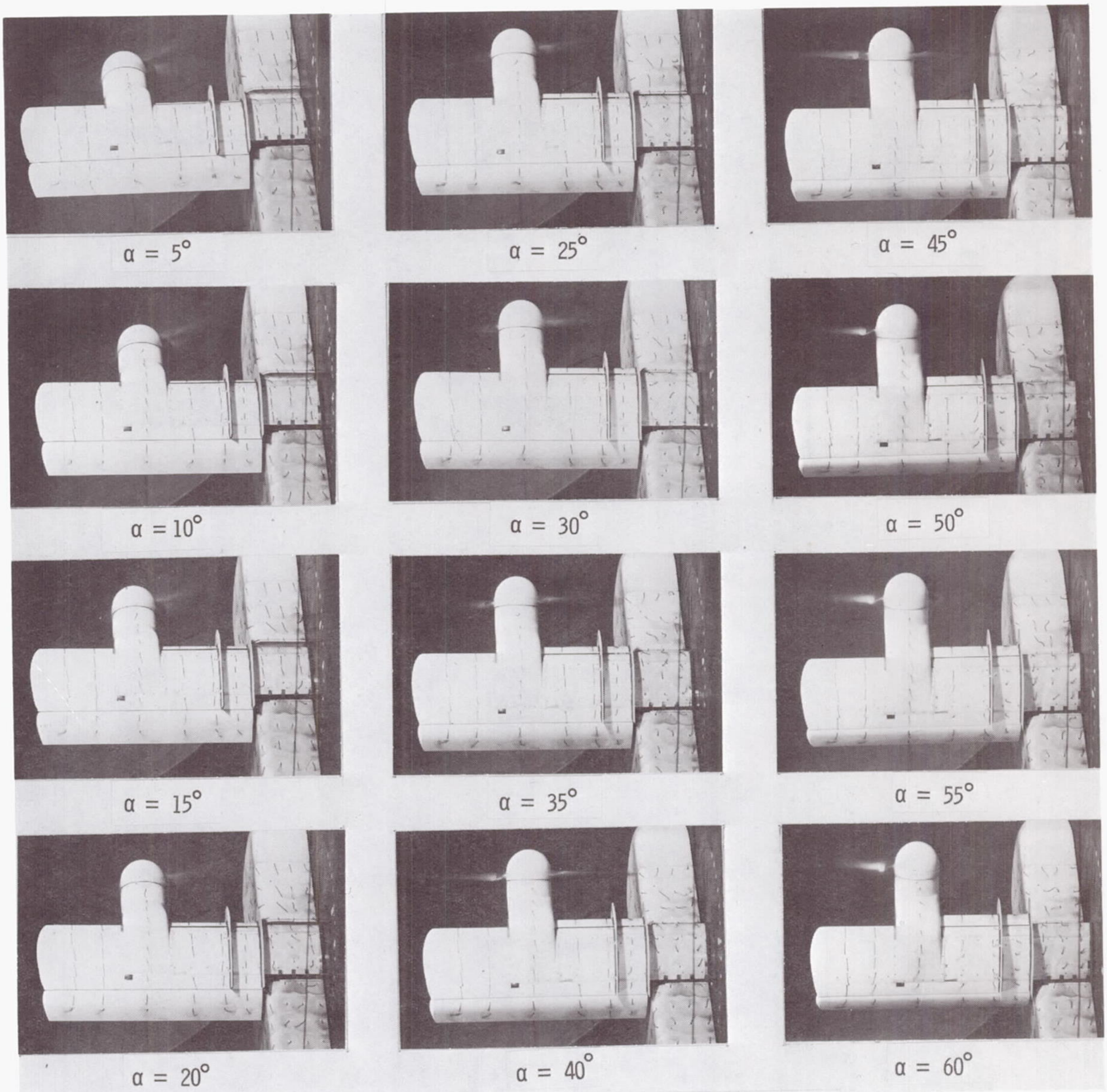

(d) Flow characteristics; $C_{T,s} = 0.60$.

Figure 18.- Continued.

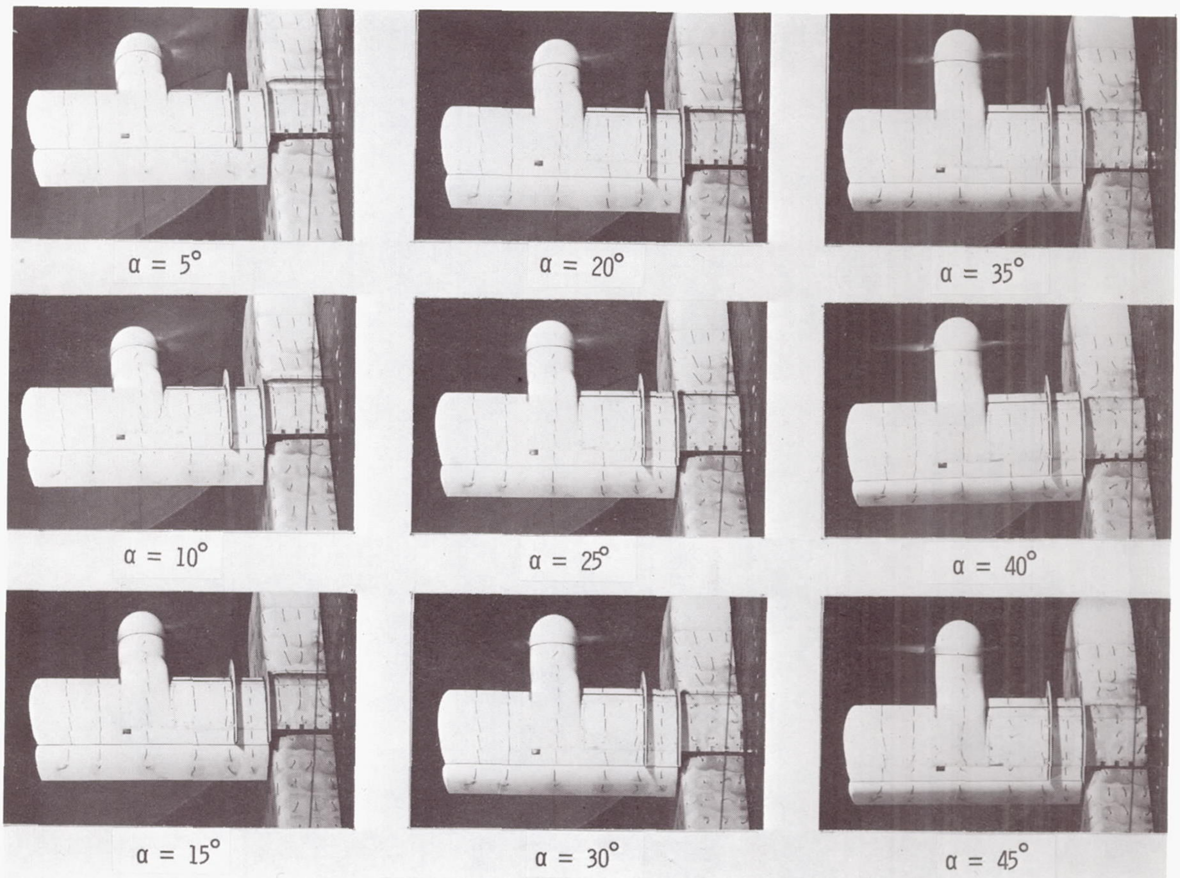

(e) Flow characteristics; $C_{T,s} = 0.30$.

Figure 18.- Concluded.

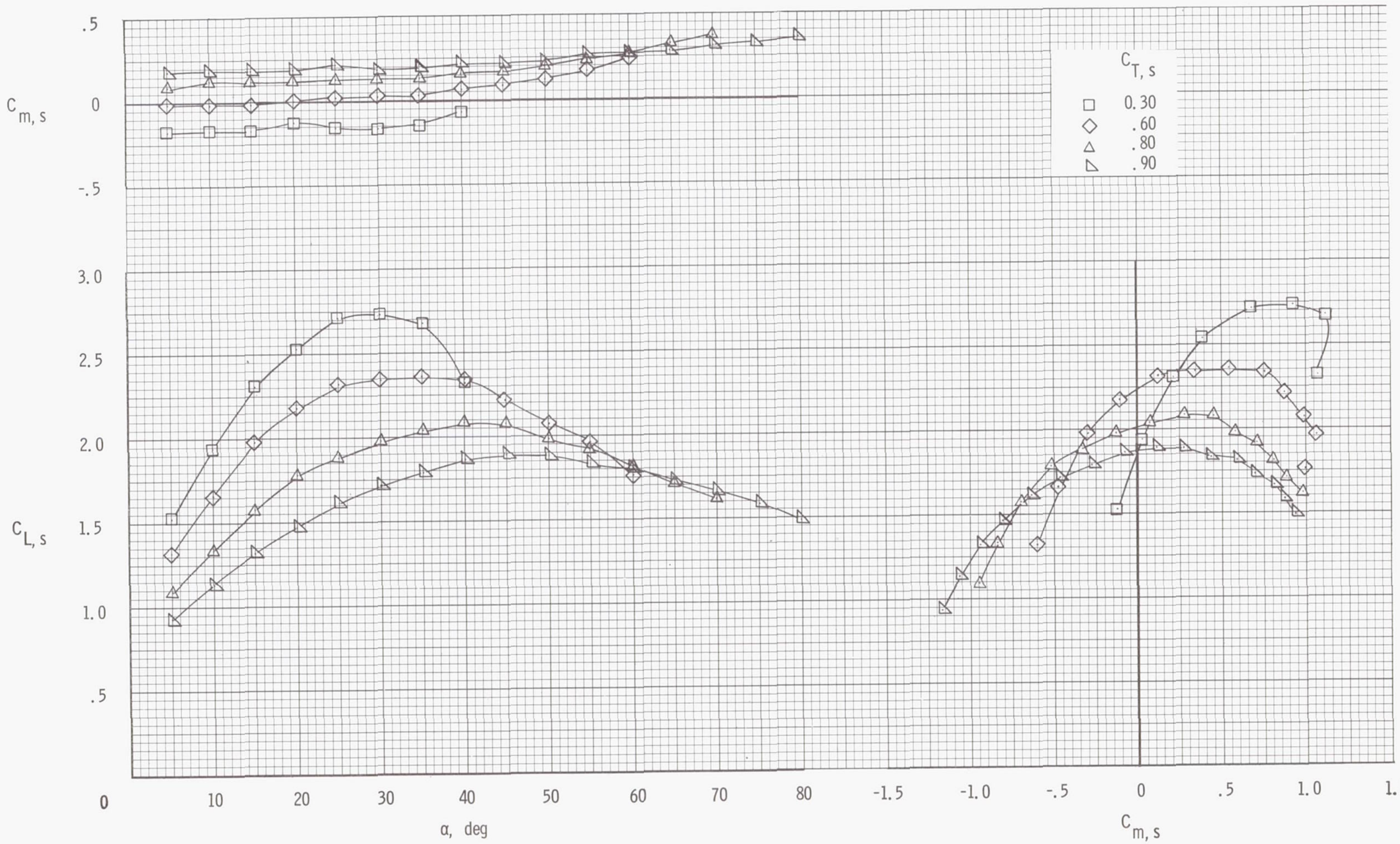

(a) Aerodynamic characteristics.

Figure 19.- Aerodynamic and flow characteristics of the wing with the propeller rotating down at the tip, inboard slat on, fences on, and $\delta_f = 60^o$.

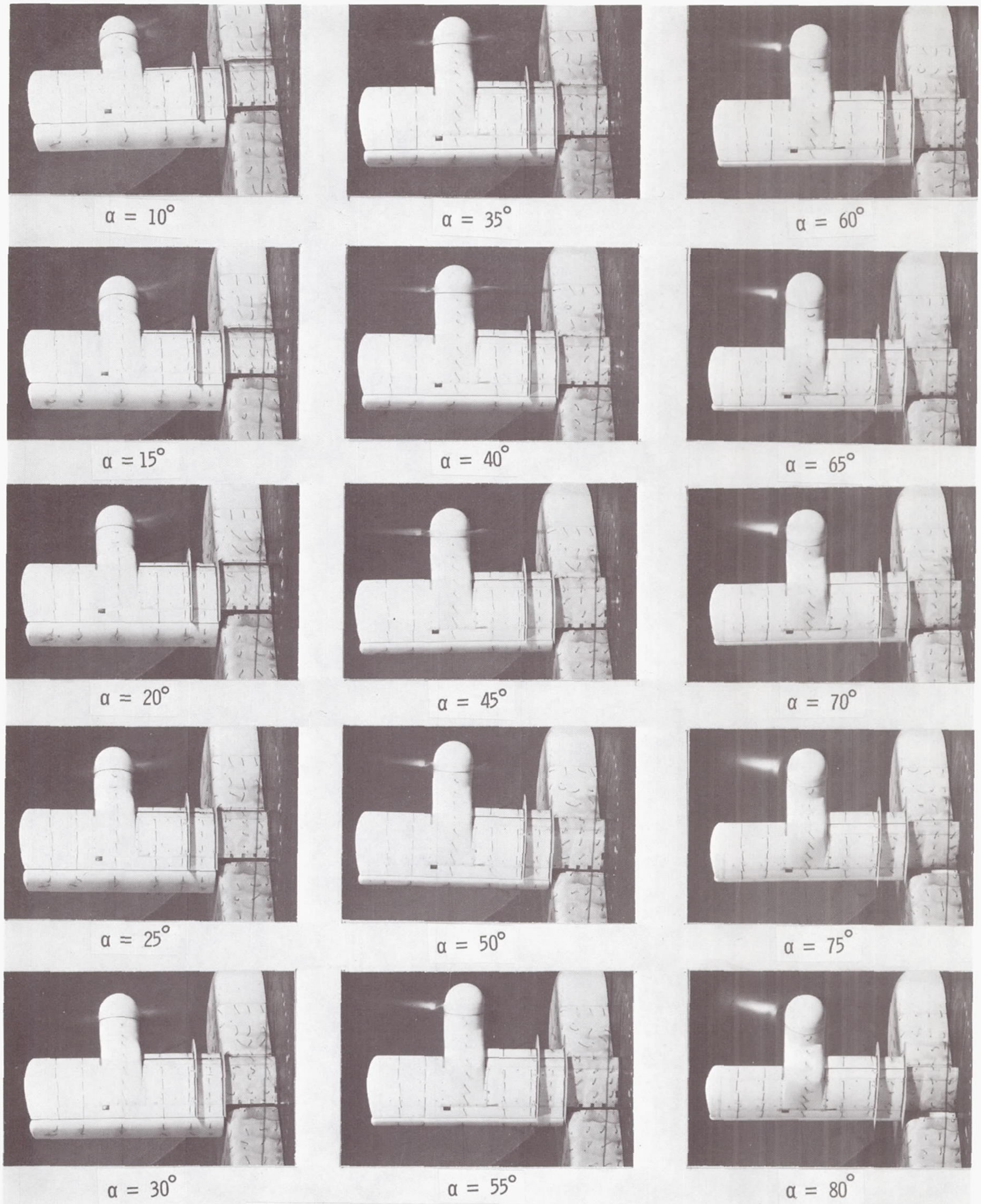

(b) Flow characteristics; $C_{T,s} = 0.90$.

Figure 19.- Continued.

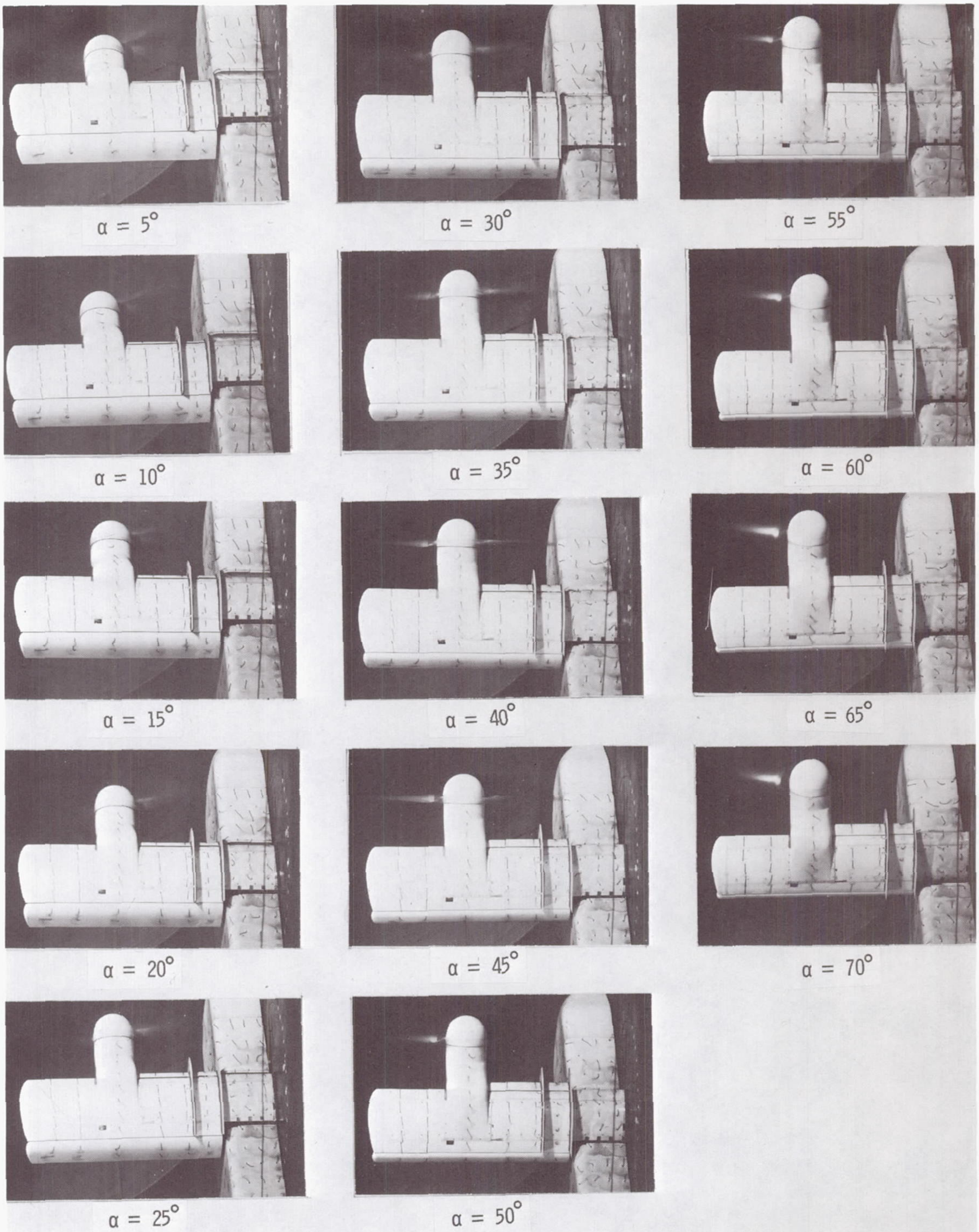

(c) Flow characteristics; $C_{T,s} = 0.80$.

Figure 19.- Continued.

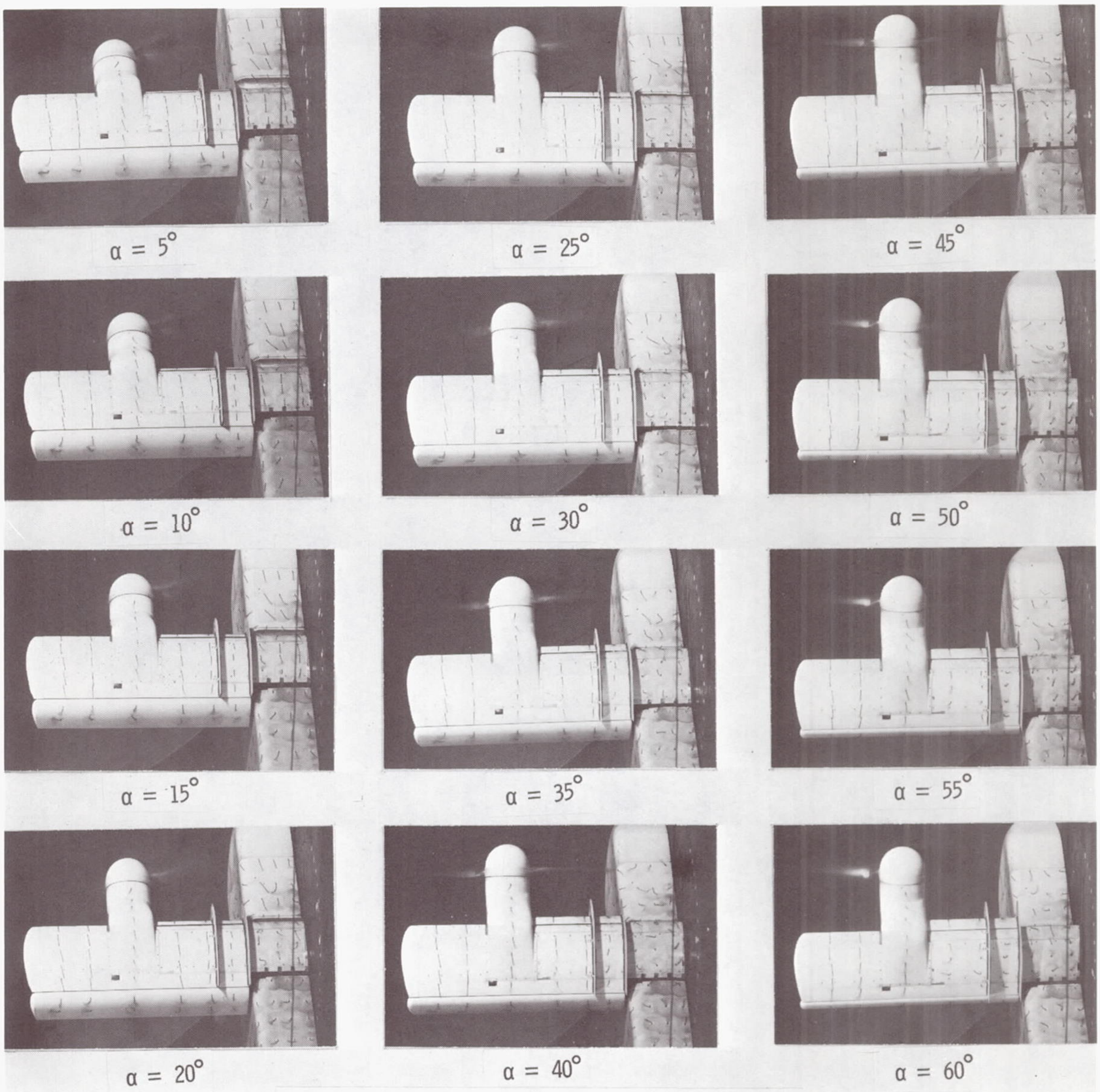

(d) Flow characteristics; $C_{T,s} = 0.60$.

Figure 19.- Continued.

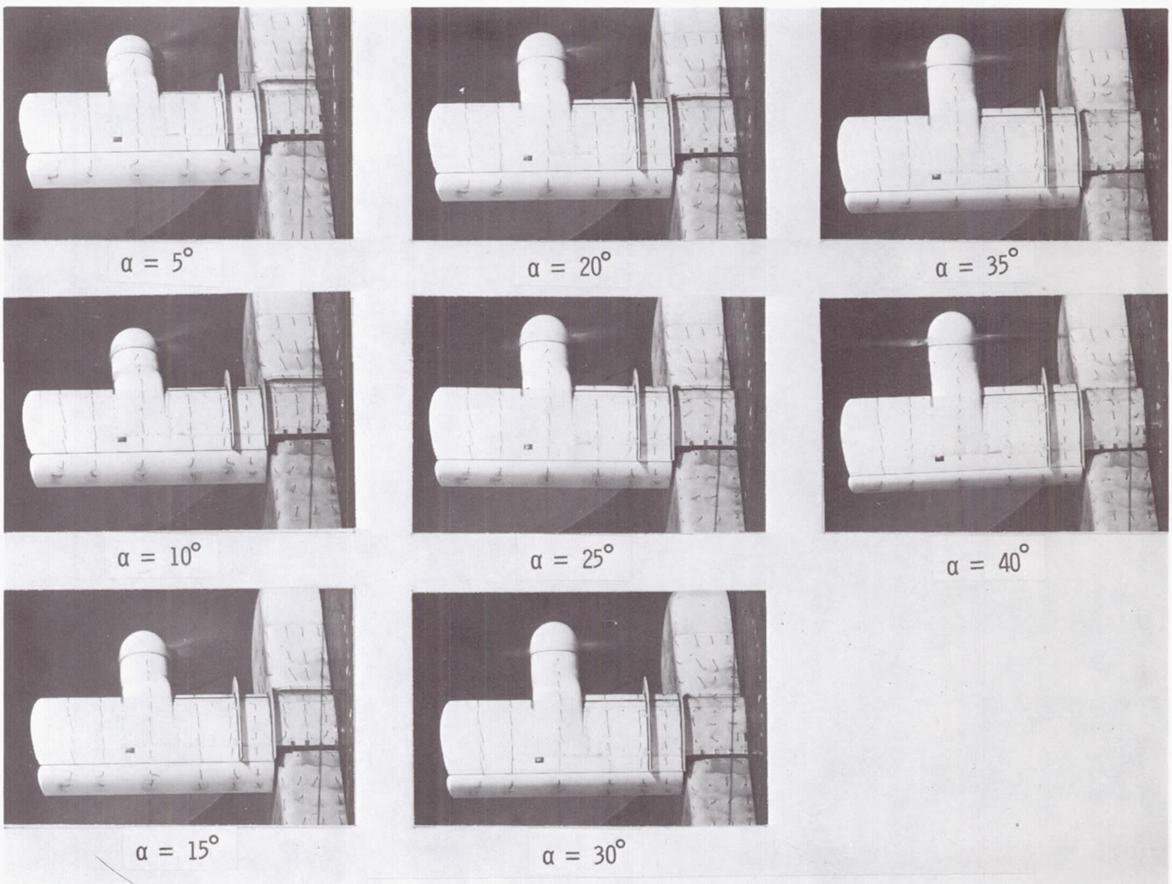

(e) Flow characteristics; $C_{T,s} = 0.30$.

Figure 19.- Concluded.

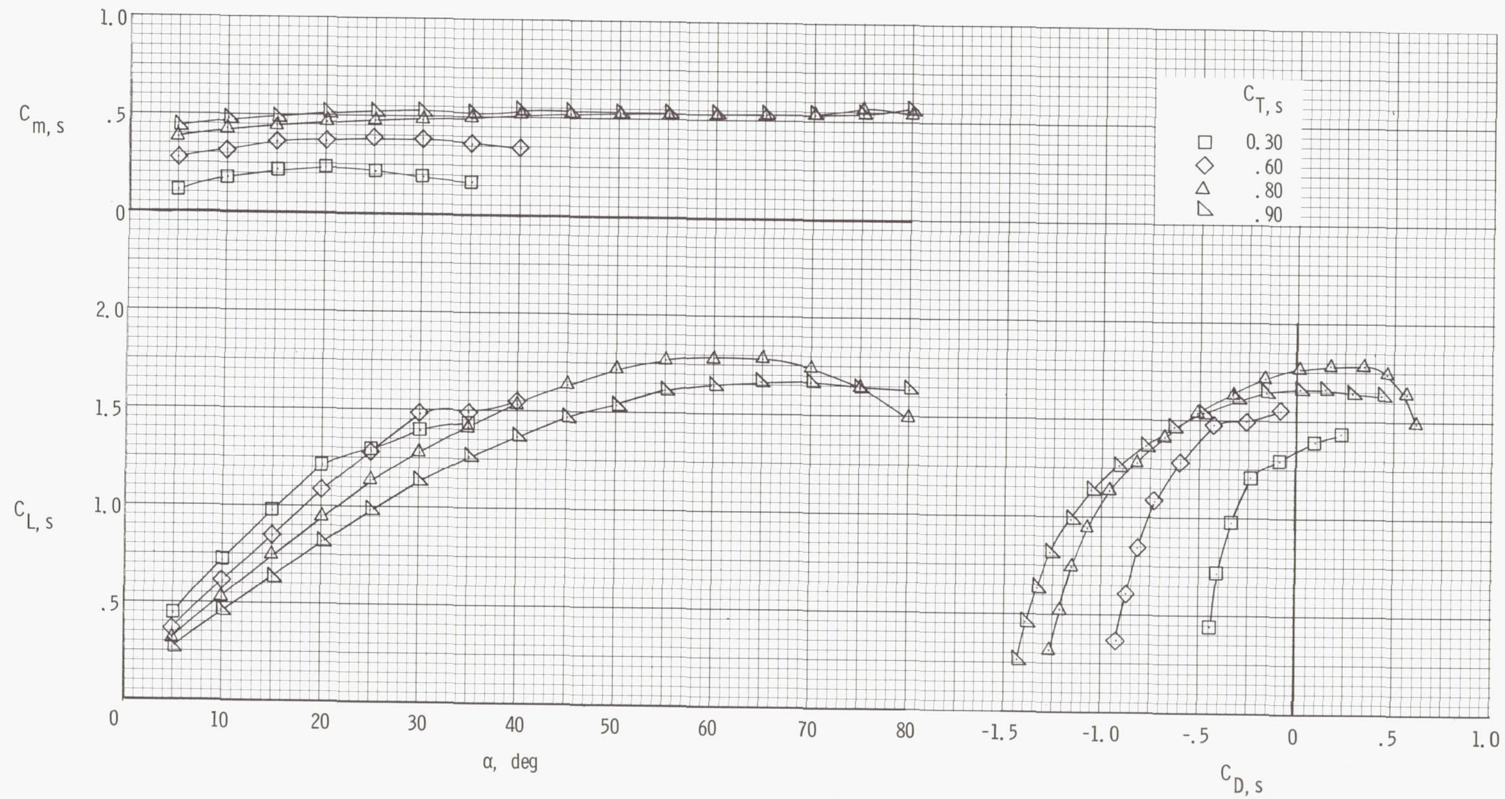

(a) Aerodynamic characteristics.

Figure 20.- Aerodynamic and flow characteristics of the wing with the propeller rotating up at the tip, basic leading edge, and $\delta_f = 0^o$.

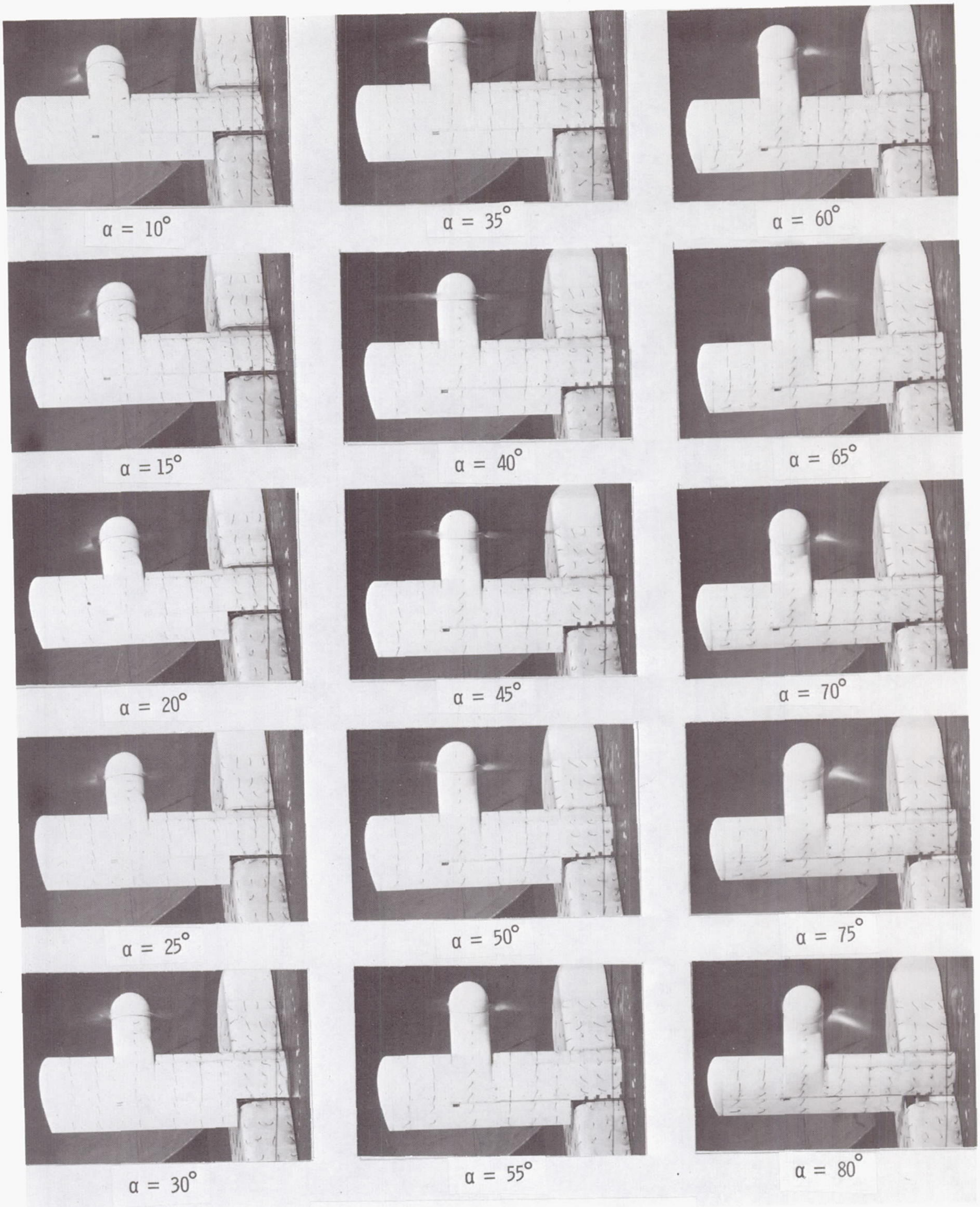

(b) Flow characteristics; $C_{T,s} = 0.90$.

Figure 20.- Continued.

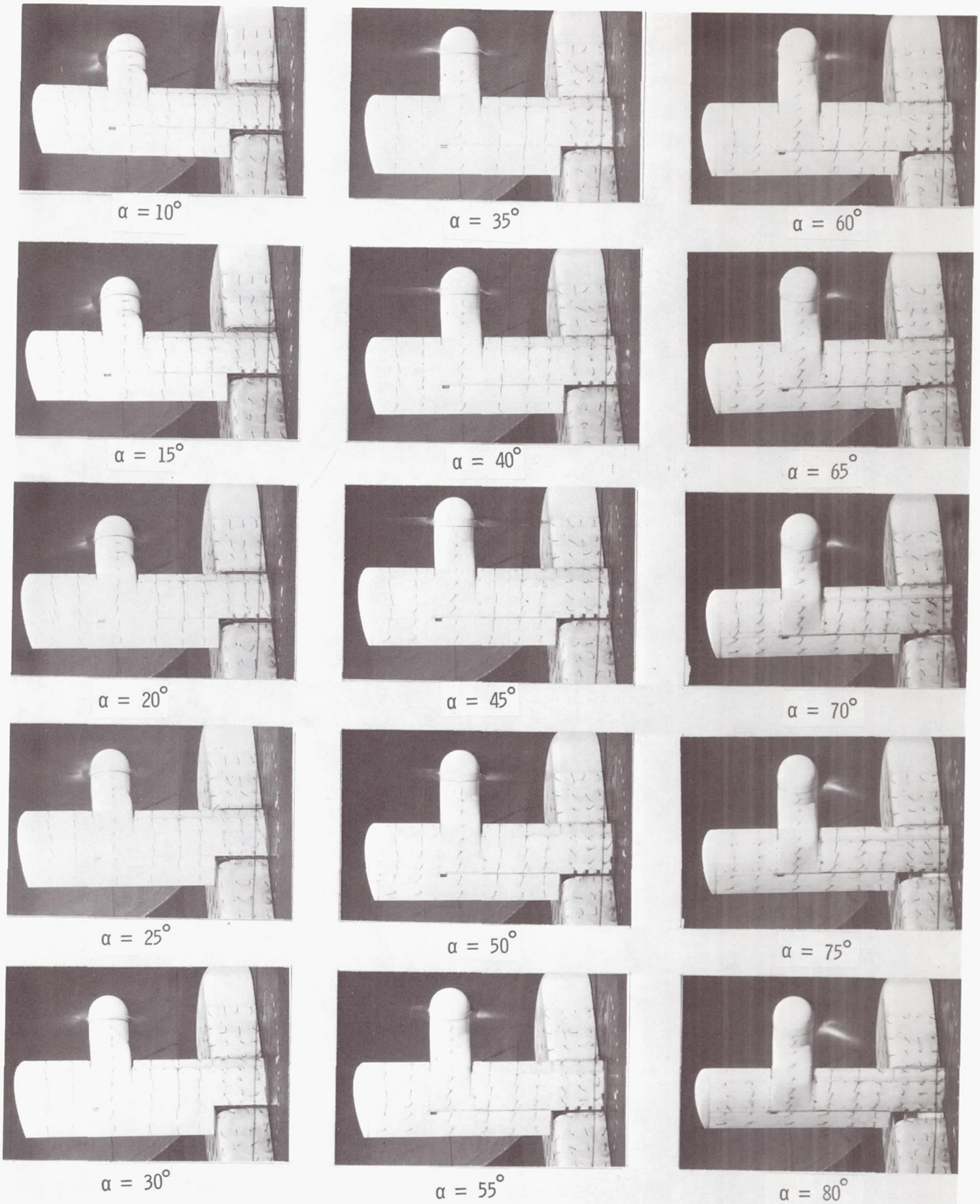

(c) Flow characteristics; $C_{T,s} = 0.80$.

Figure 20.- Continued.

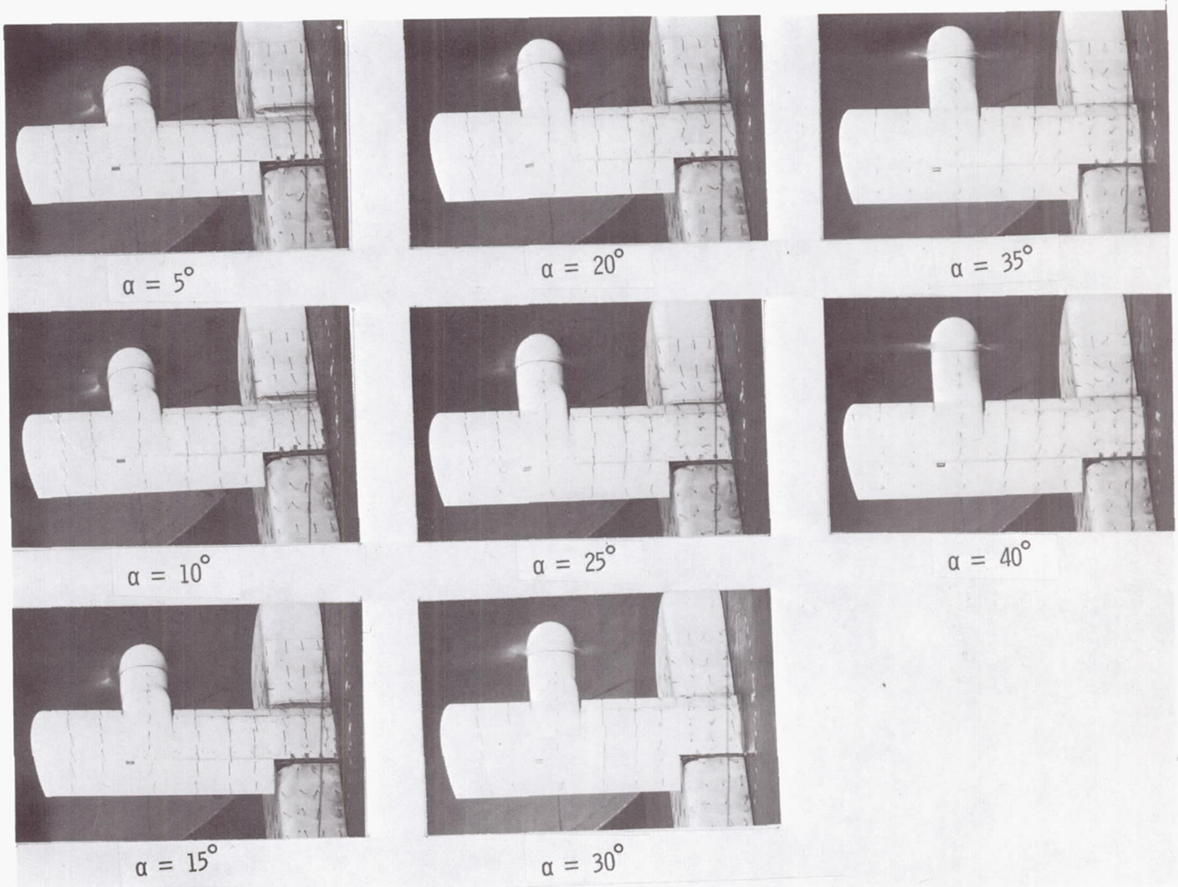

(d) Flow characteristics; $C_{T,s} = 0.60$.

Figure 20.- Continued.

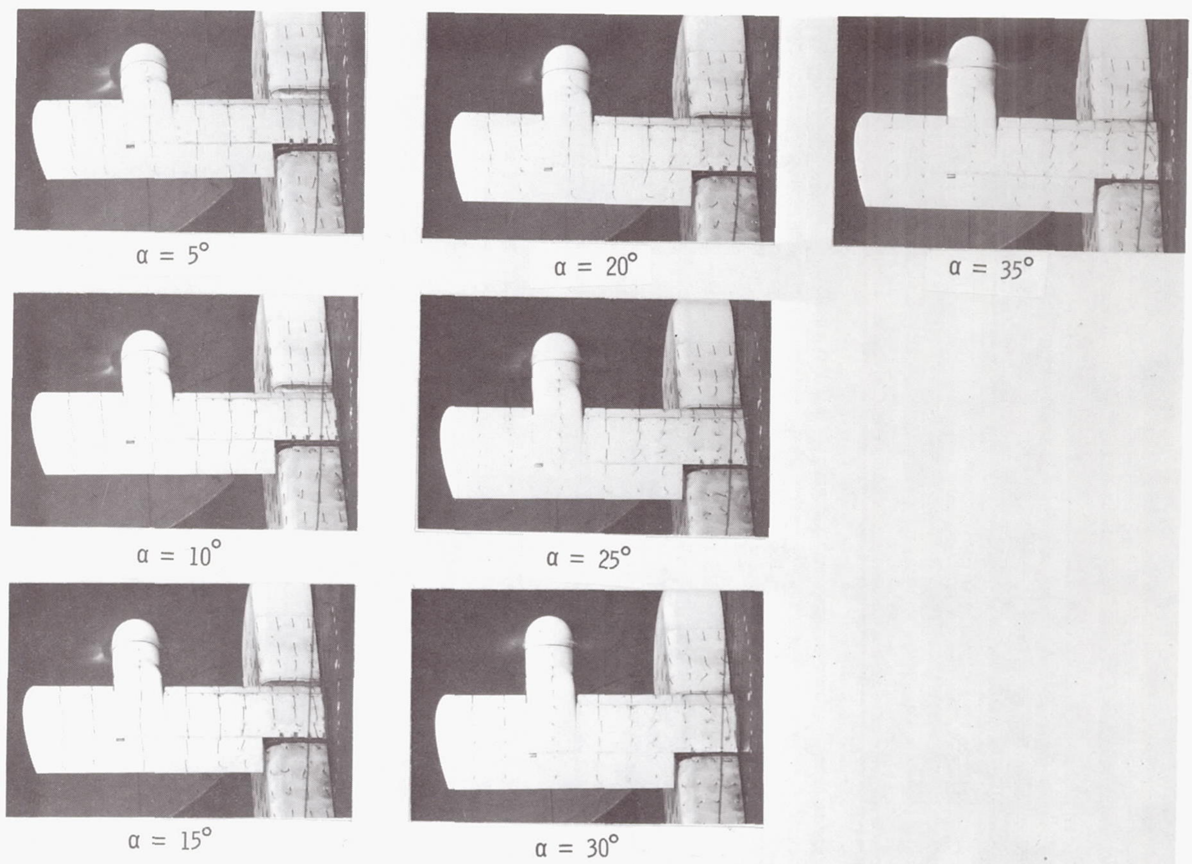

(e) Flow characteristics; $C_{T,s} = 0.30$.

Figure 20.- Concluded.

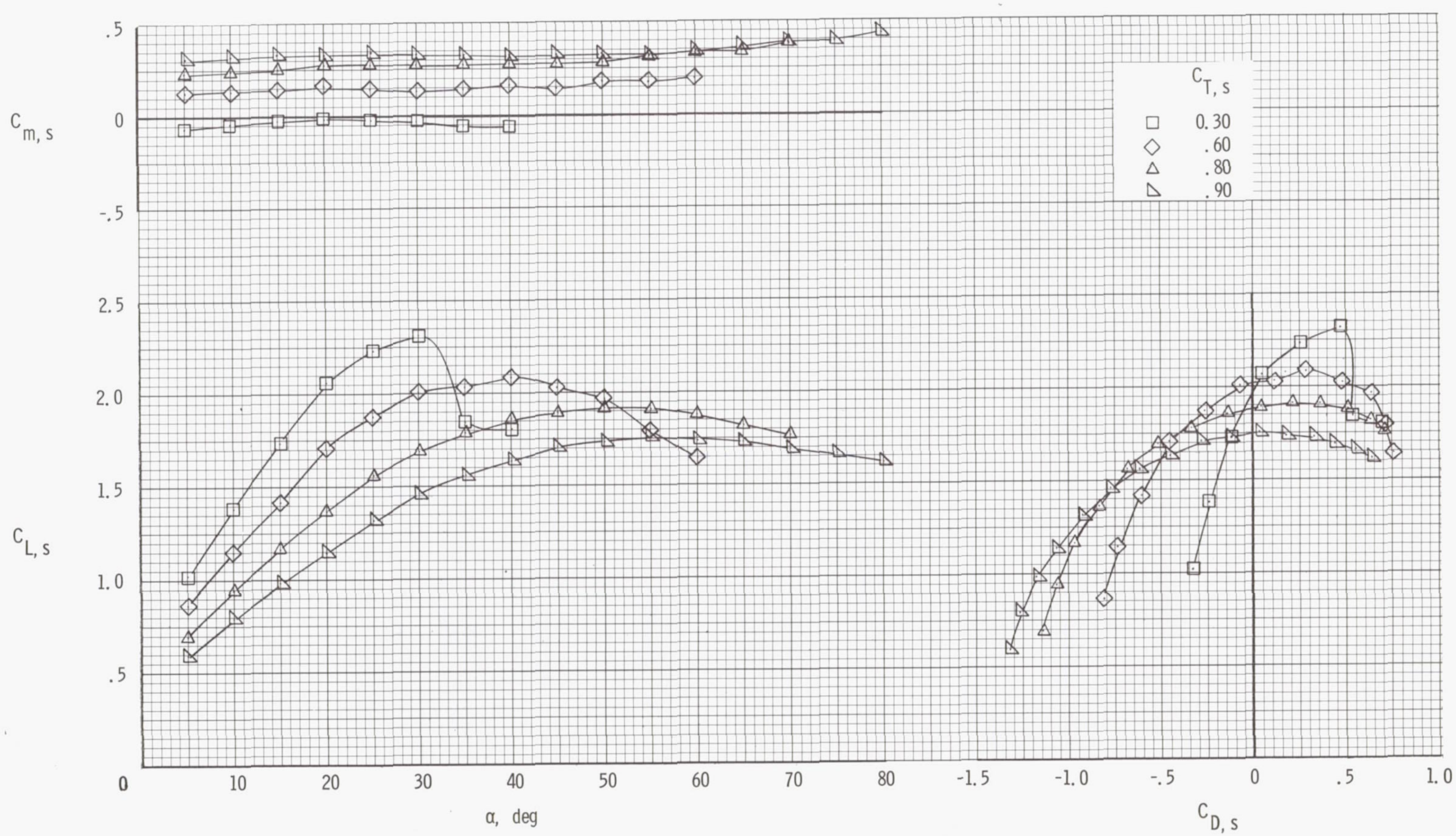

(a) Aerodynamic characteristics.

Figure 21.- Aerodynamic and flow characteristics of the wing with the propeller rotating up at the tip, basic leading edge, and $\delta_f = 20^{\circ}$.

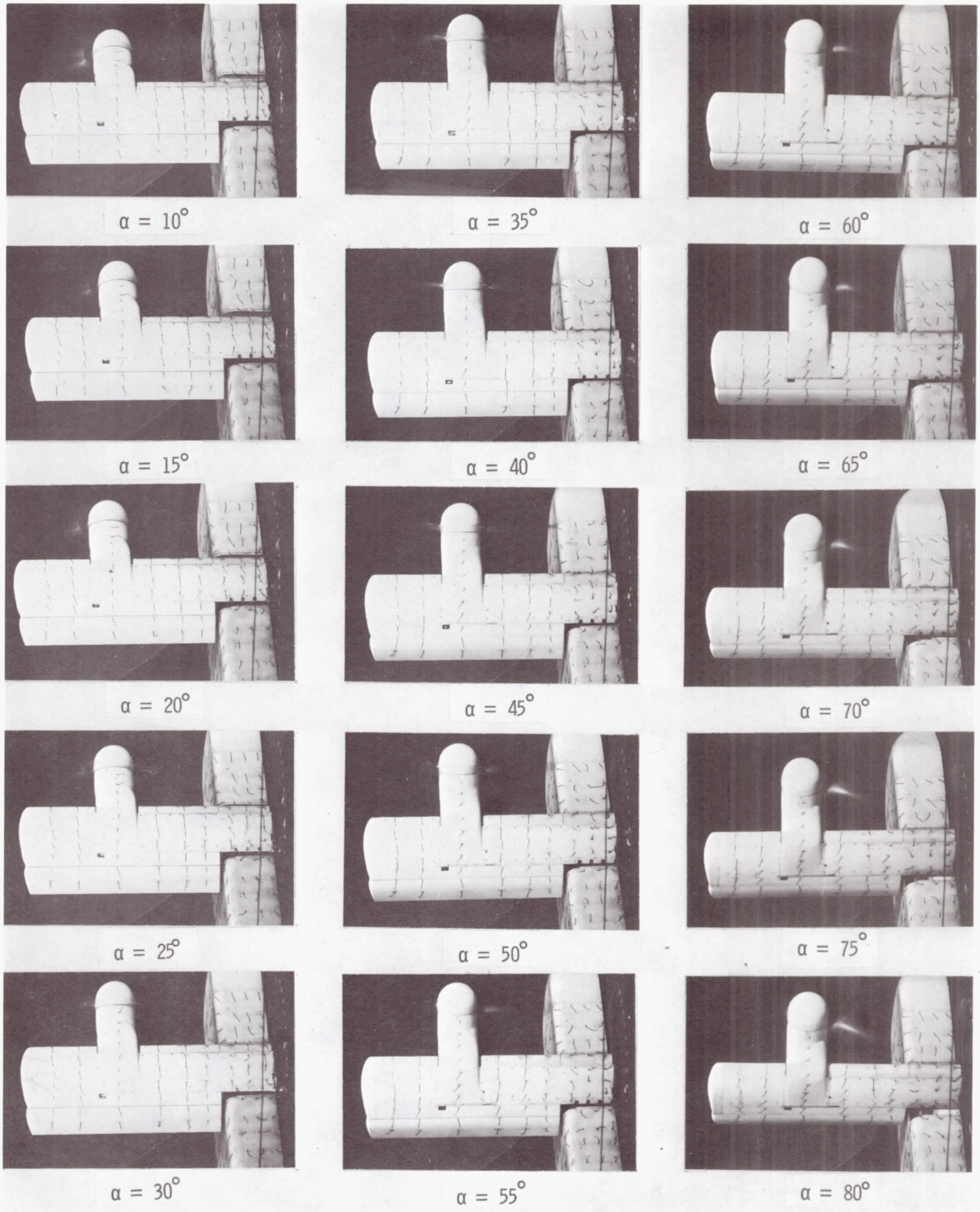

(b) Flow characteristics; $C_{T,s} = 0.90$.

Figure 21.- Continued.

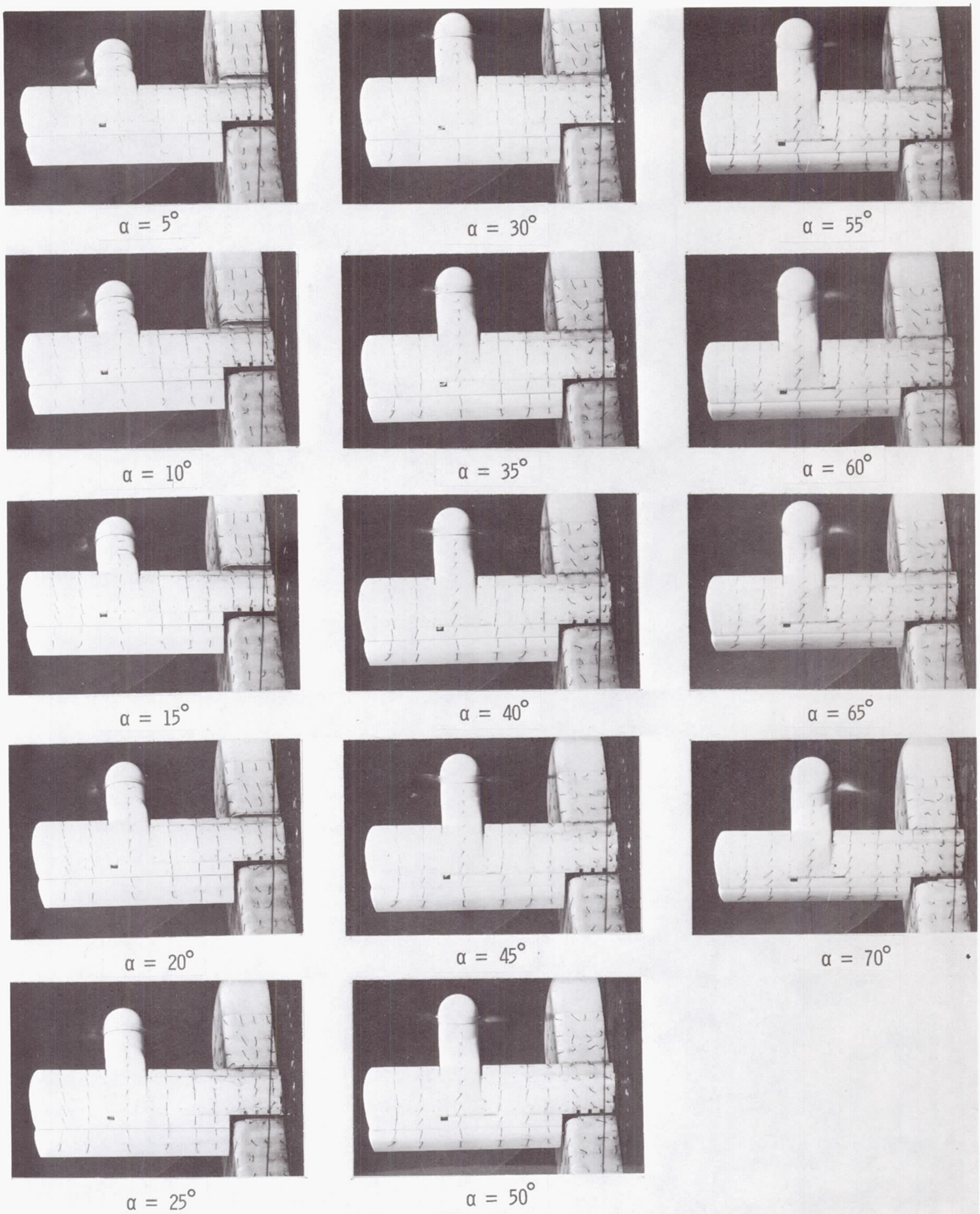

(c) Flow characteristics; $C_{T,s} = 0.80$.

Figure 21.- Continued.

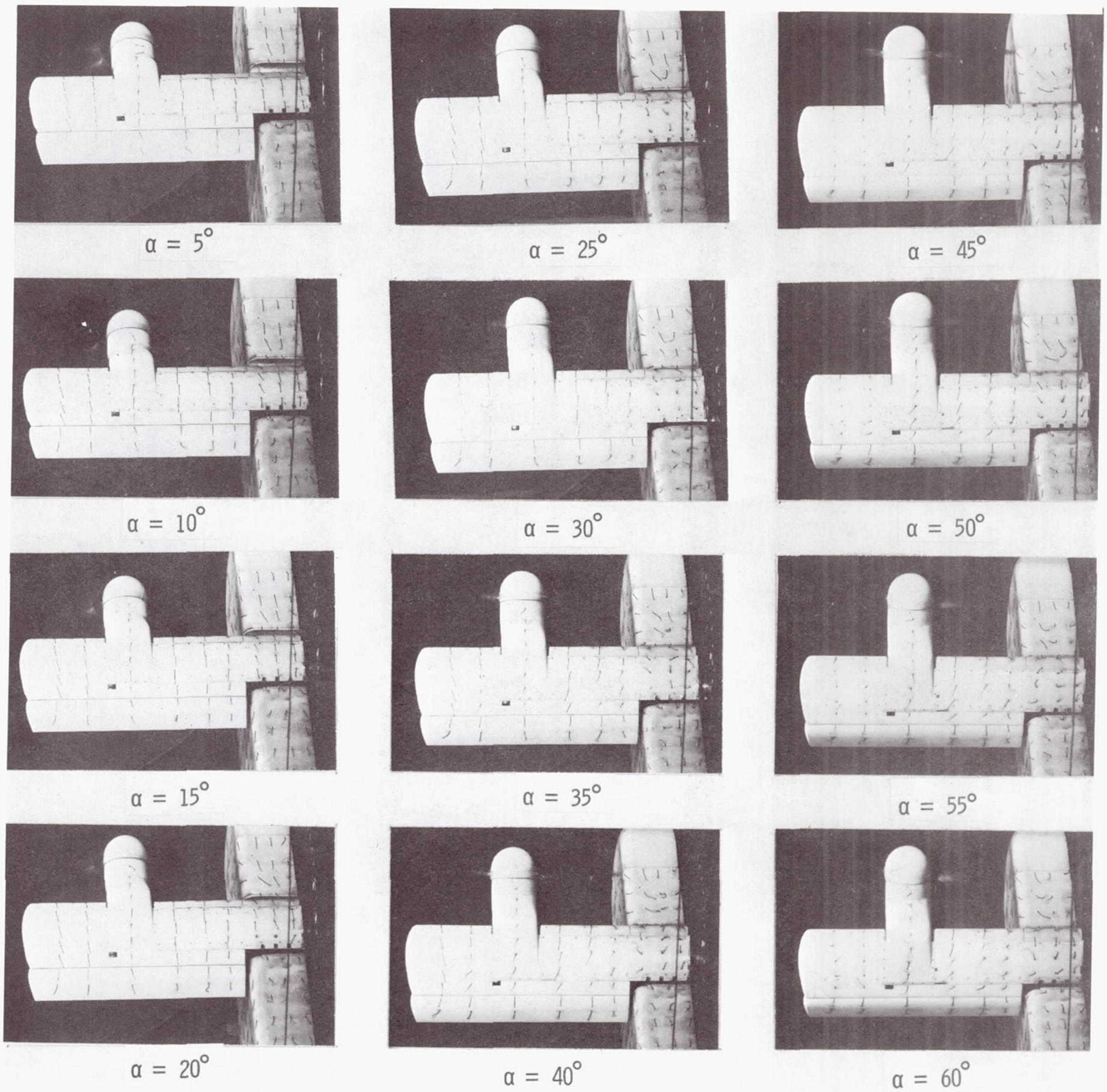

(d) Flow characteristics; $C_{T,s} = 0.60$.

Figure 21.- Continued.

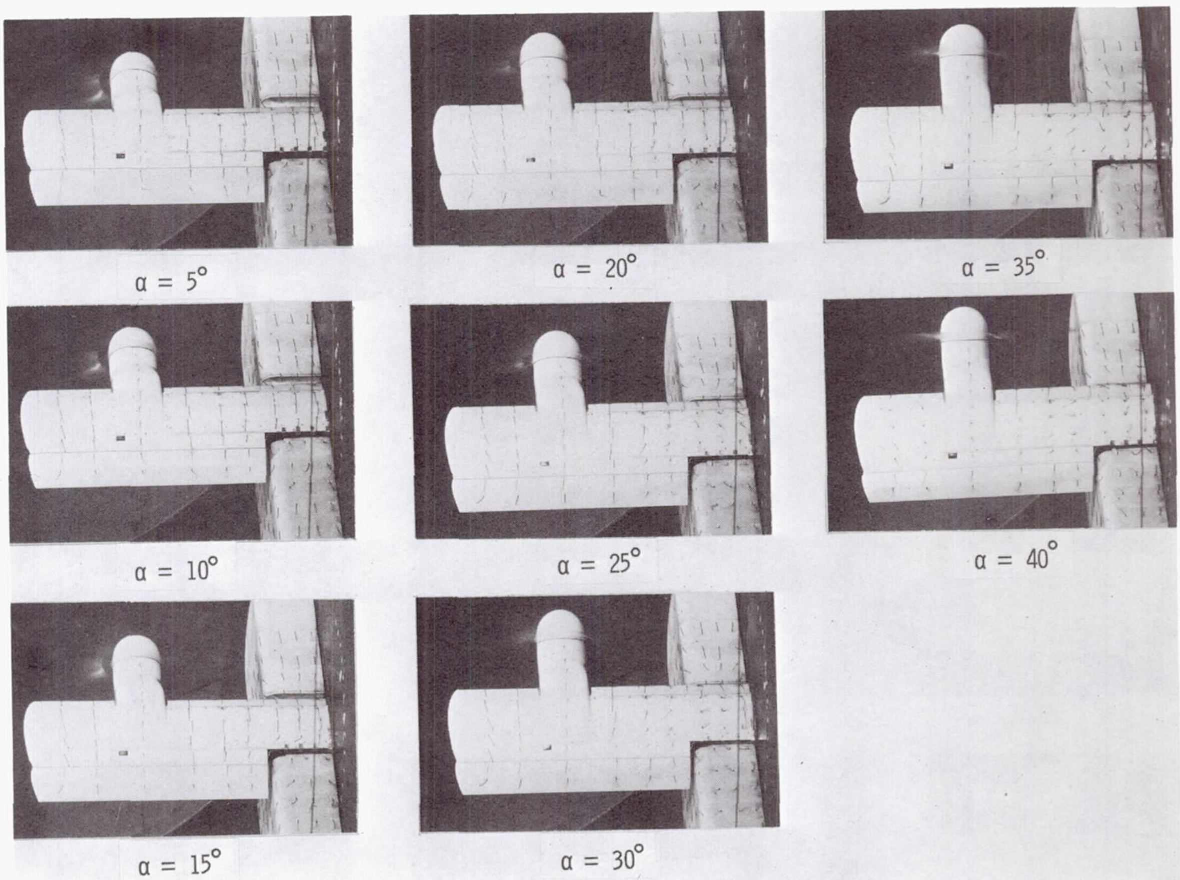

(e) Flow characteristics; $C_{T,s} = 0.30$.

Figure 21.- Concluded.

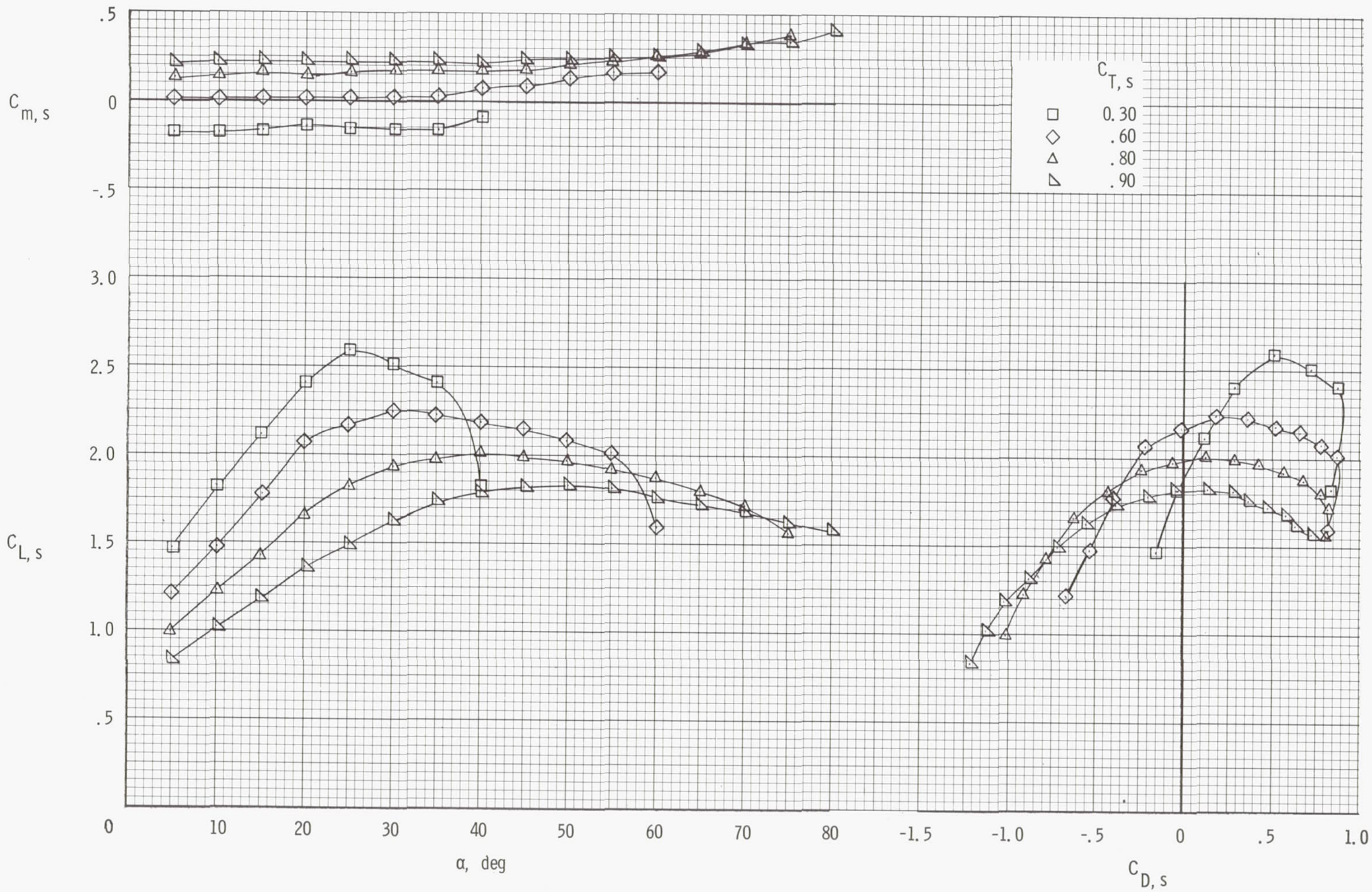

(a) Aerodynamic characteristics.

Figure 22.- Aerodynamic and flow characteristics of the wing with the propeller rotating up at the tip, basic leading edge, and $\delta_f = 40^o$.

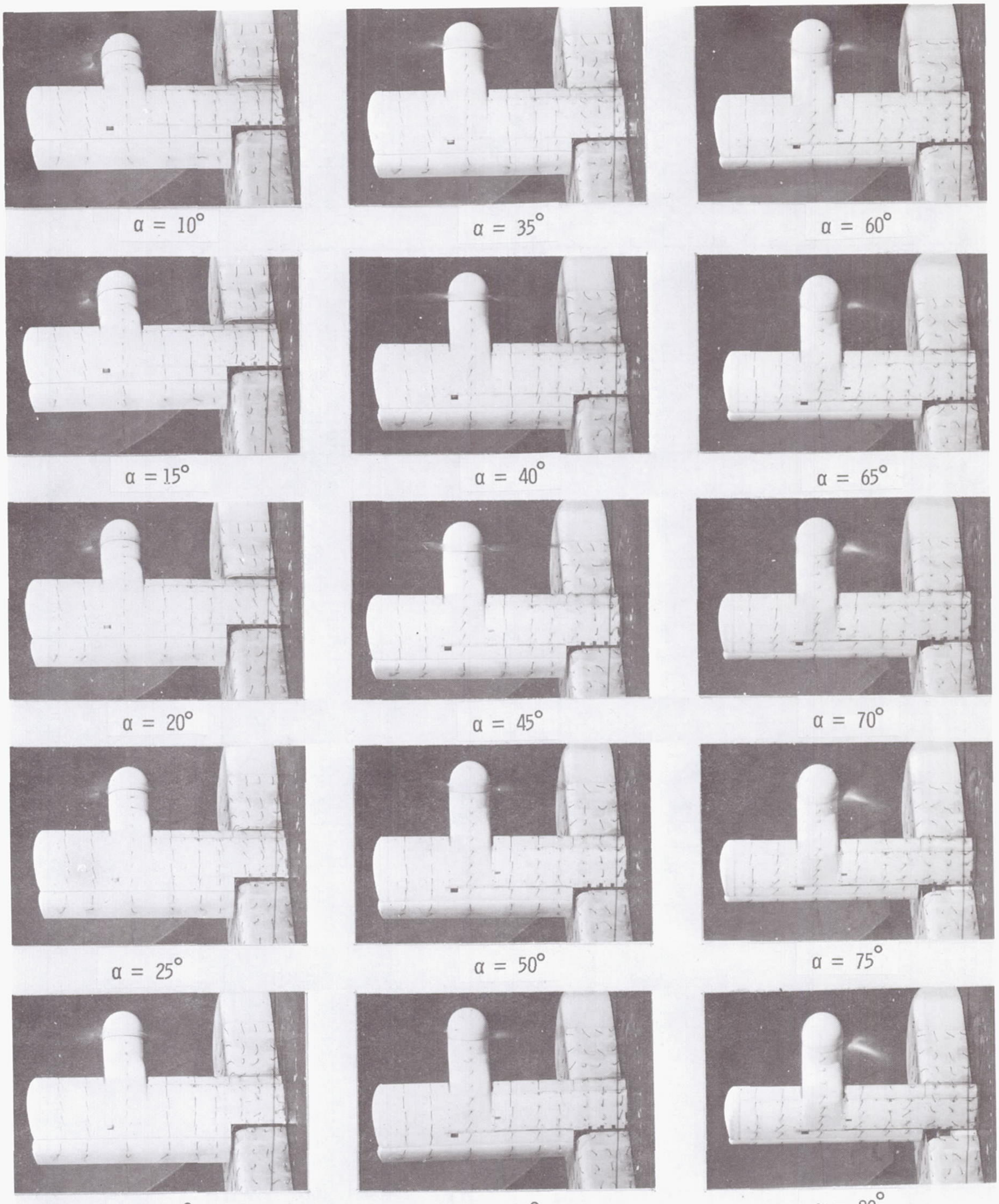

(b) Flow characteristics; $C_{T,s} = 0.90$.

Figure 22.- Continued.

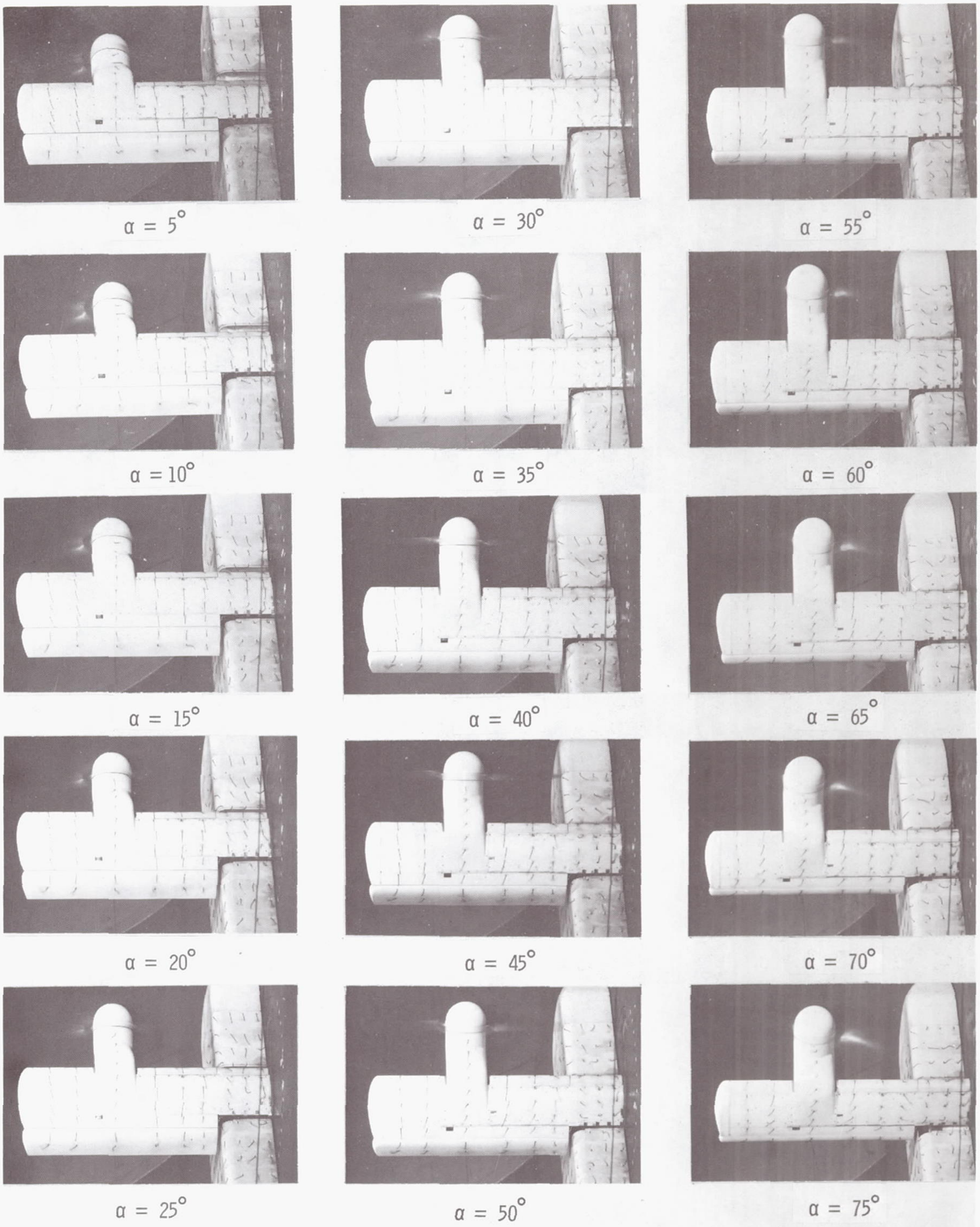

(c) Flow characteristics; $C_{T,s} = 0.80$.

Figure 22.- Continued.

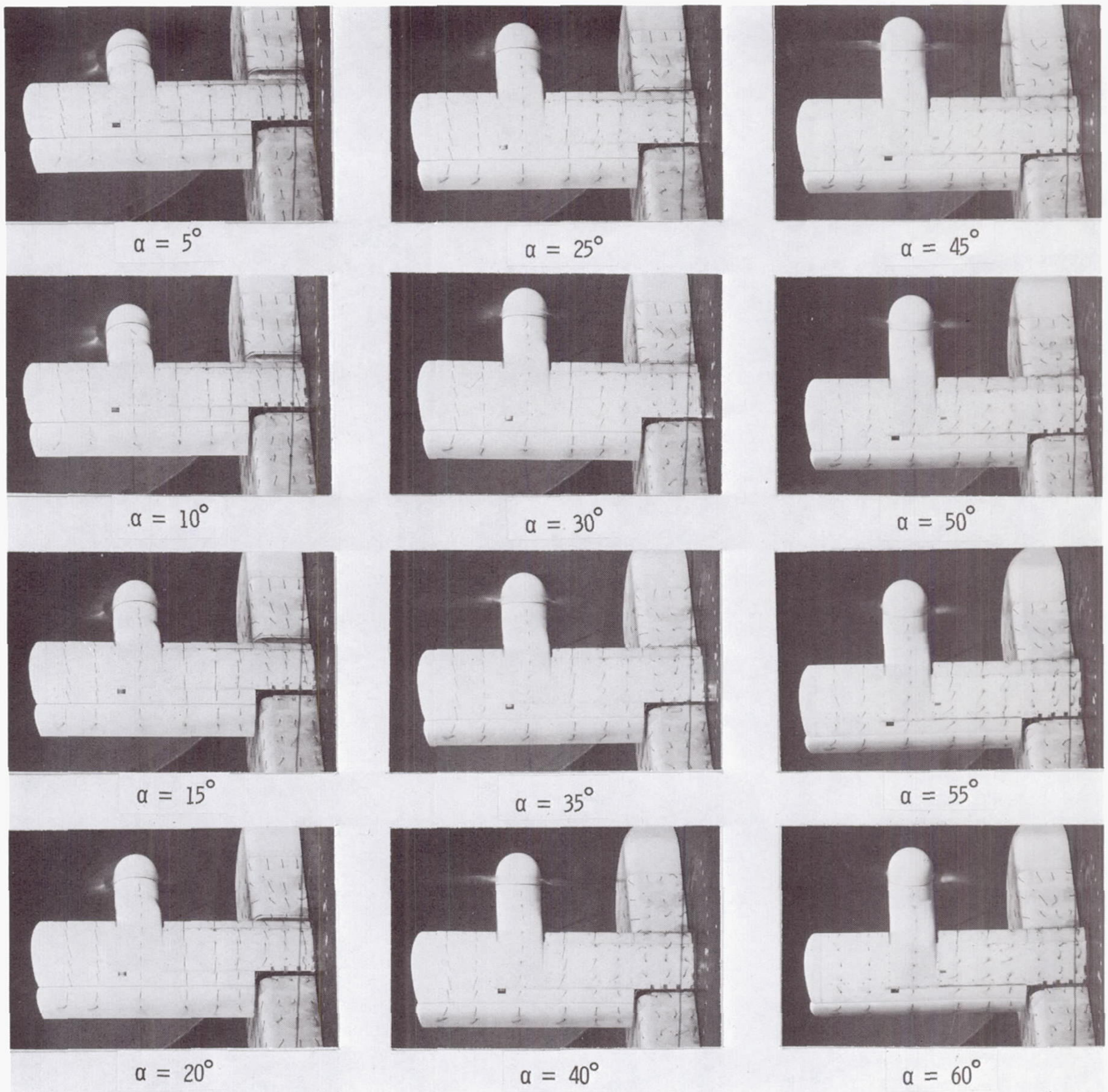

(d) Flow characteristics; $C_{T,s} = 0.60$.

Figure 22.- Continued.

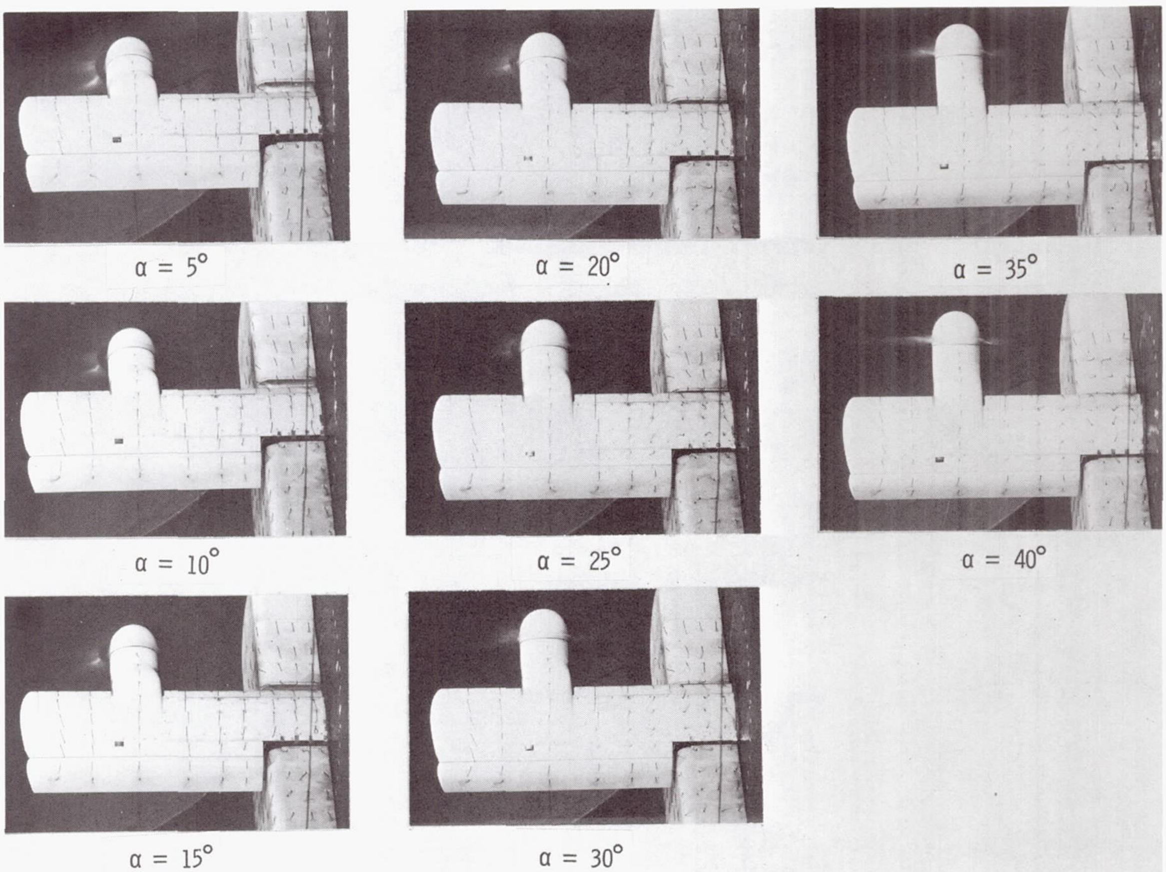

$\alpha = 5^\circ$ $\alpha = 20^\circ$ $\alpha = 35^\circ$

$\alpha = 10^\circ$ $\alpha = 25^\circ$ $\alpha = 40^\circ$

$\alpha = 15^\circ$ $\alpha = 30^\circ$

(e) Flow characteristics; $C_{T,s} = 0.30$.

Figure 22.- Concluded.

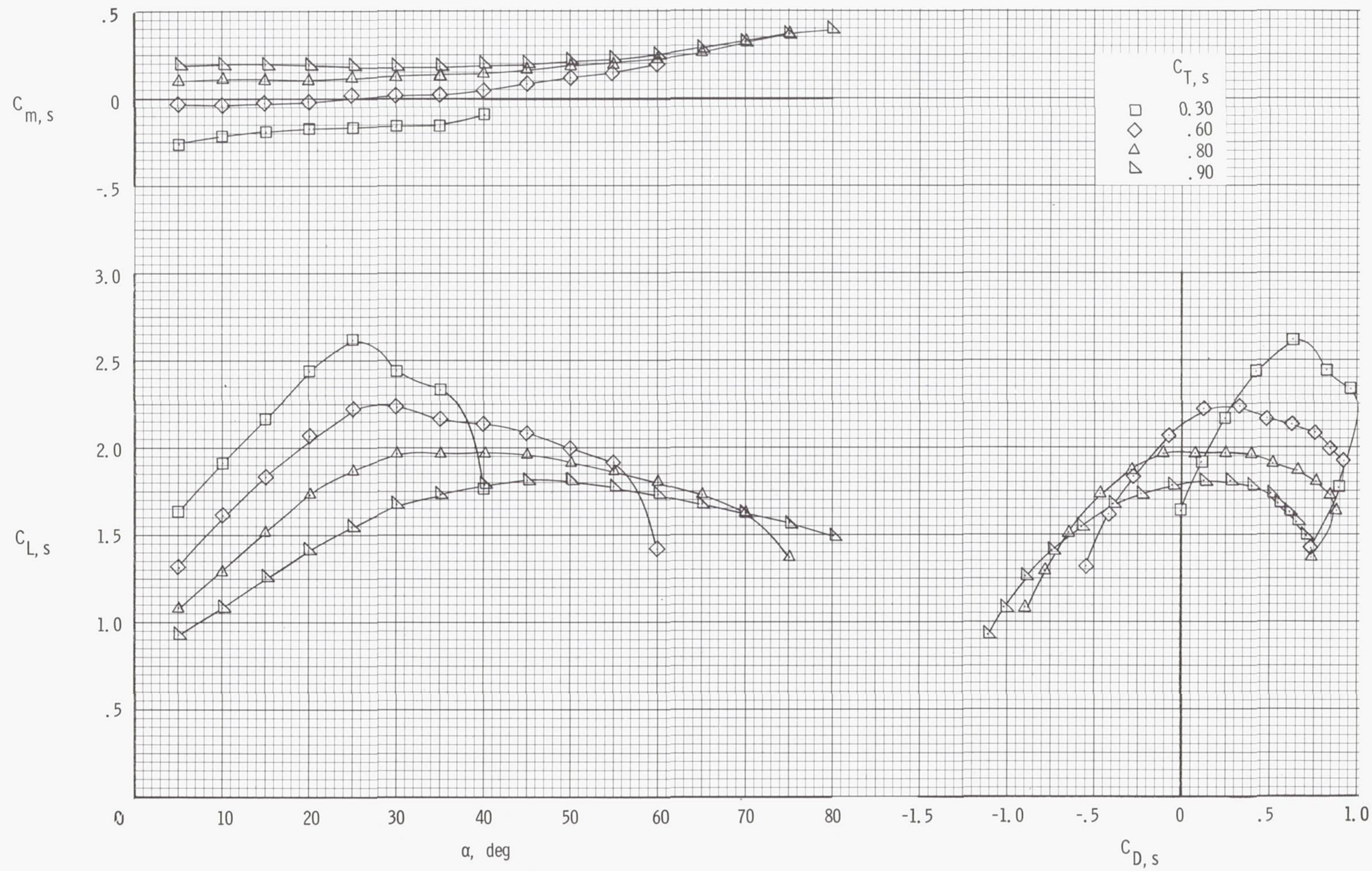

(a) Aerodynamic characteristics.

Figure 23.- Aerodynamic and flow characteristics of the wing with the propeller rotating up at the tip, basic leading edge, and $\delta_f = 60^o$.

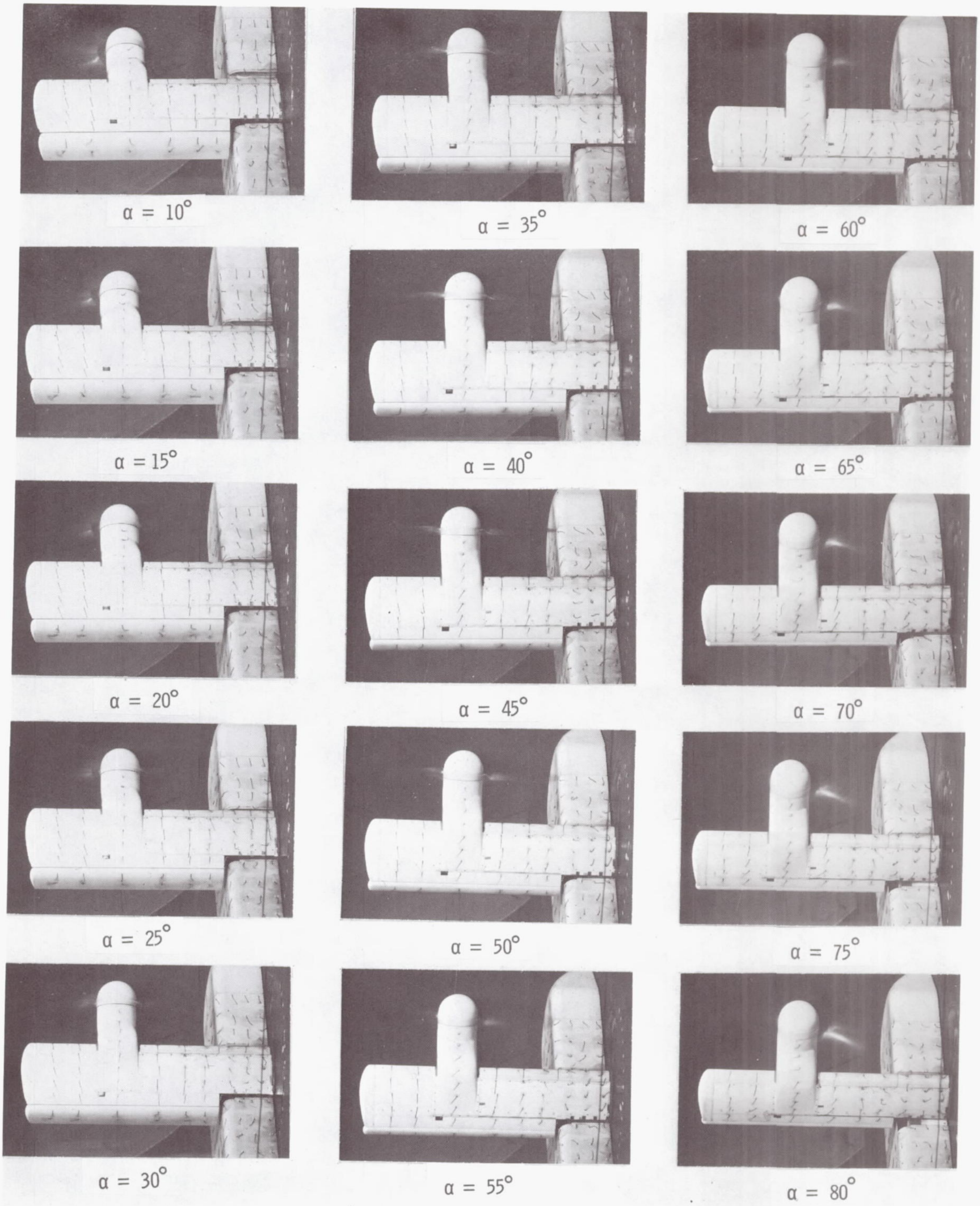

(b) Flow characteristics; $C_{T,s} = 0.90$.

Figure 23.- Continued.

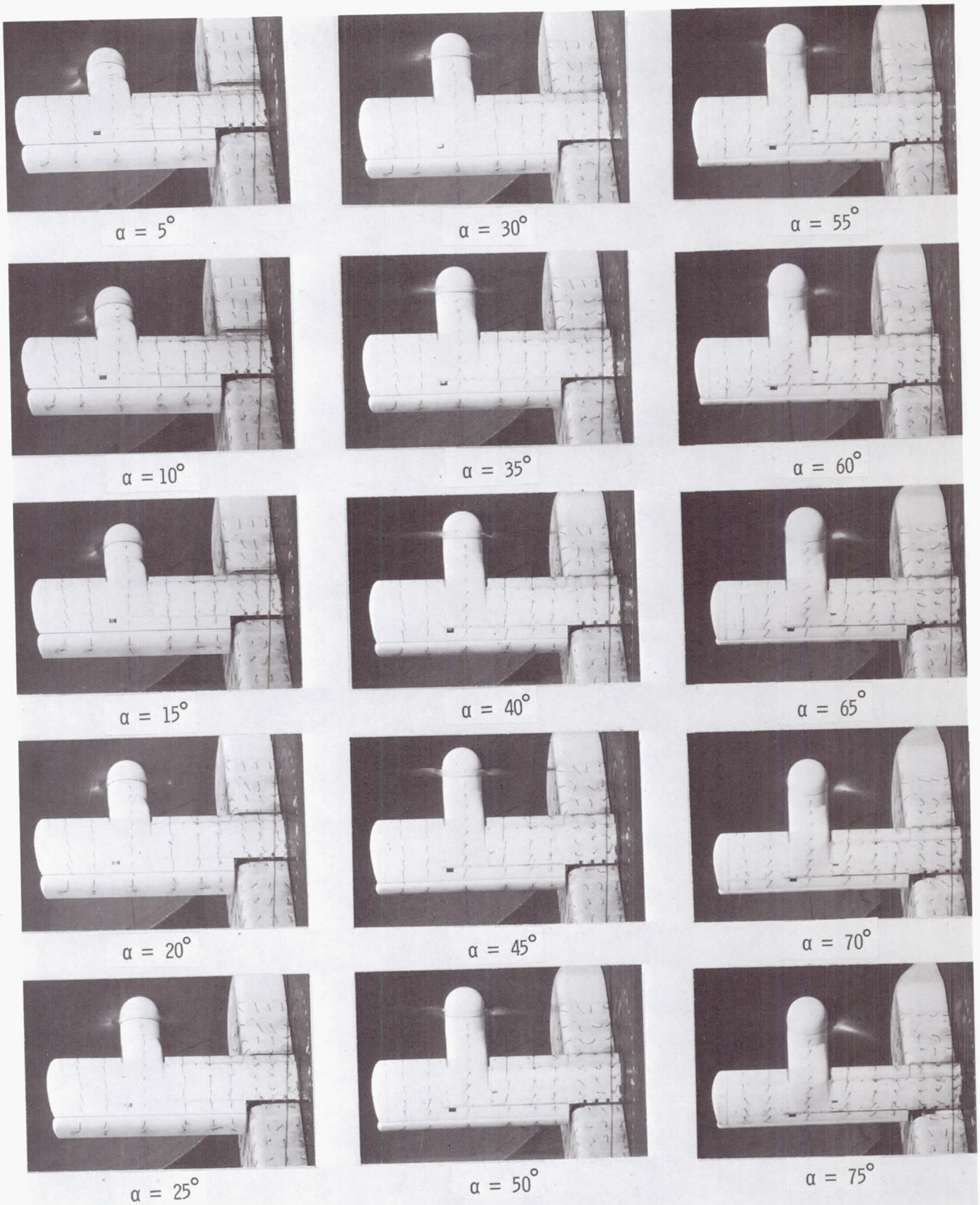

(c) Flow characteristics; $C_{T,s} = 0.80$.

Figure 23.- Continued.

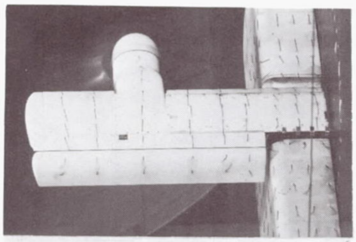

α = 5°

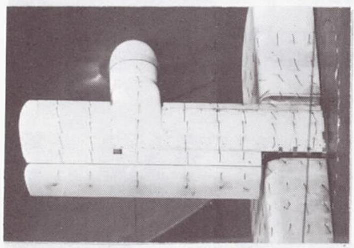

α = 10°

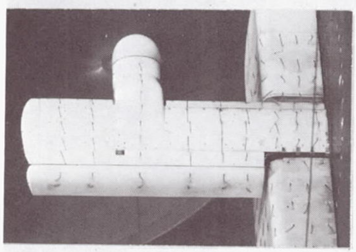

α = 15°

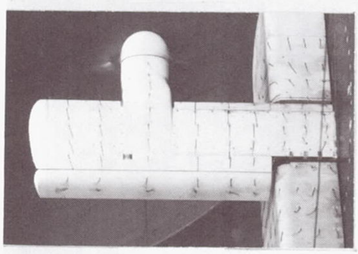

α = 20°

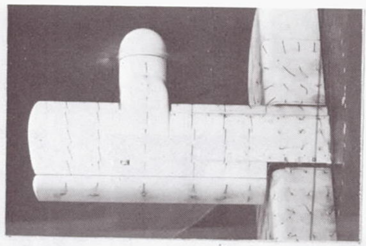

α = 25°

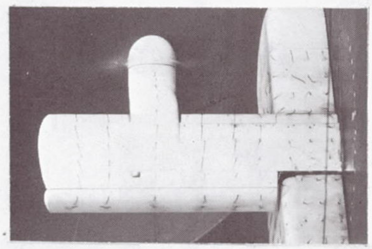

α = 30°

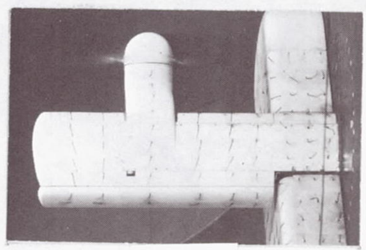

α = 35°

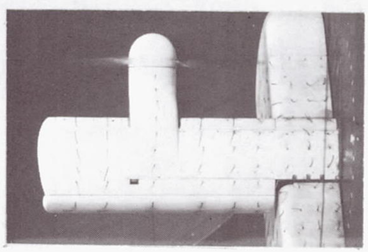

α = 40°

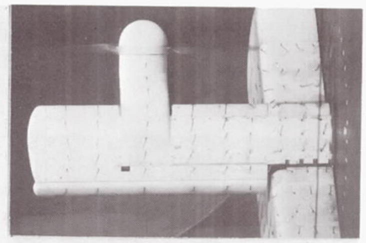

α = 45°

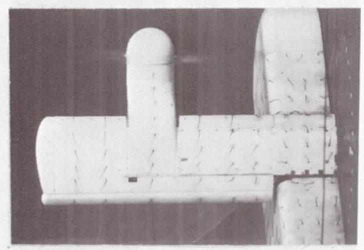

α = 50°

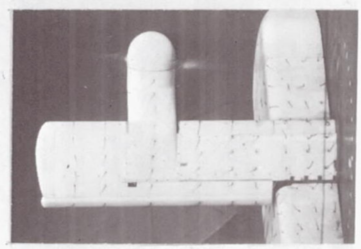

α = 55°

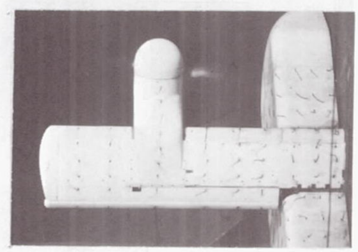

α = 60°

(d) Flow characteristics; $C_{T,s} = 0.60$.

Figure 23.- Continued.

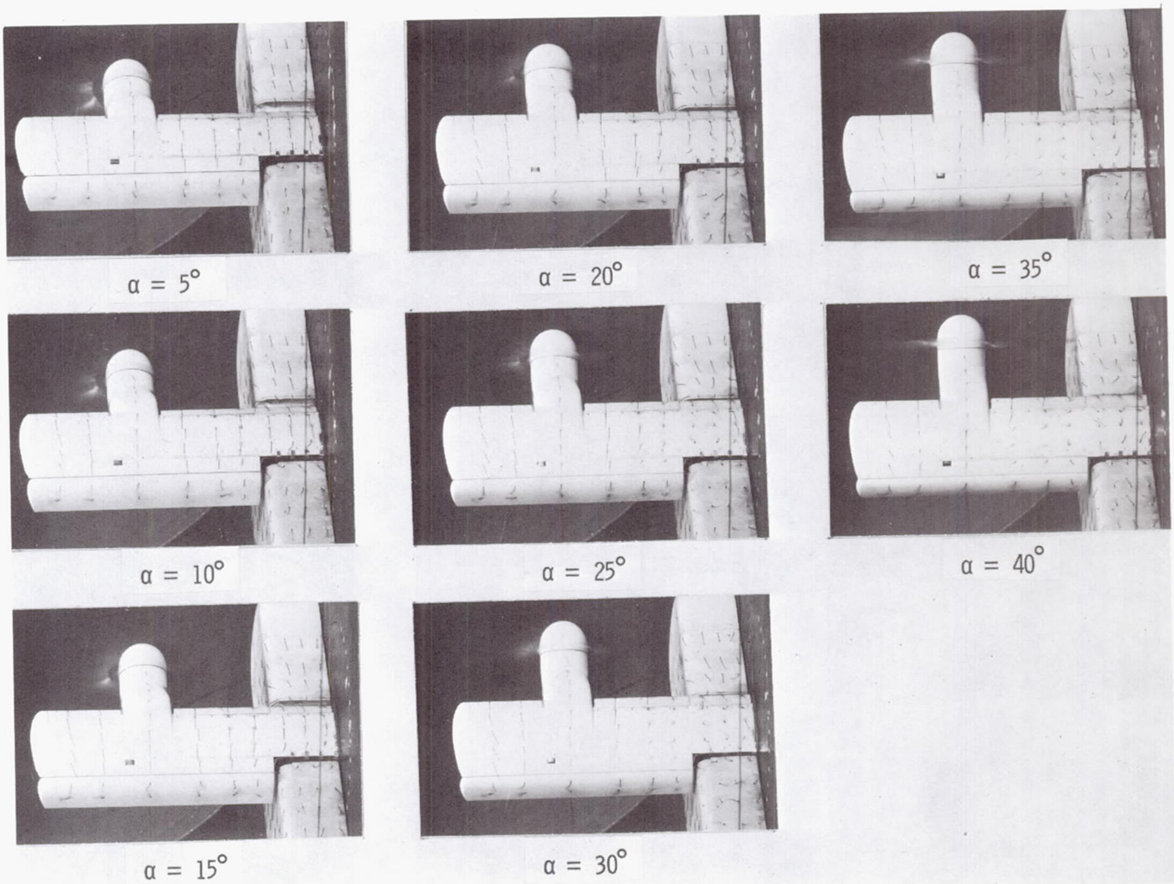

(e) Flow characteristics; $C_{T,s} = 0.30$.

Figure 23.- Concluded.

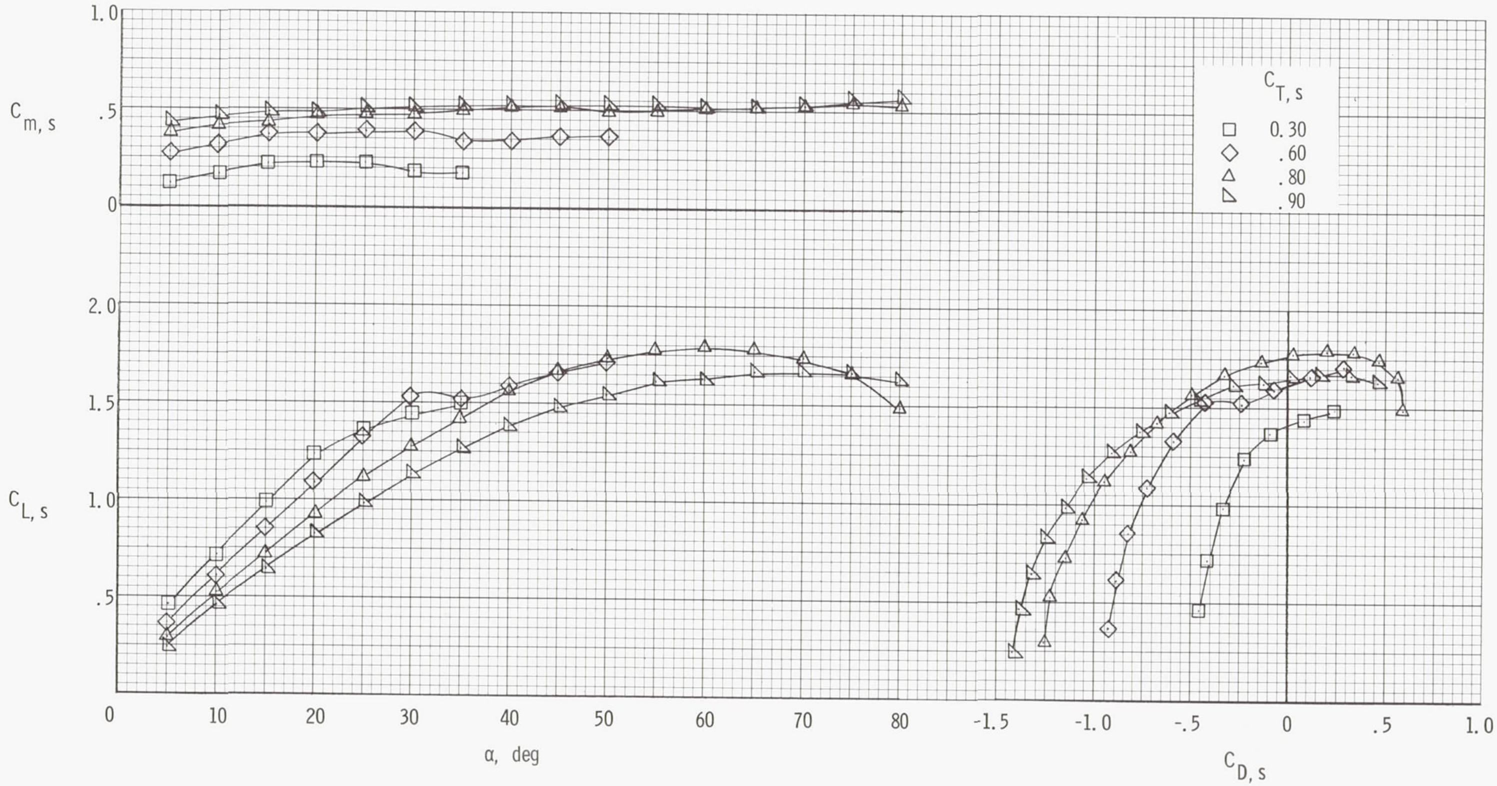

(a) Aerodynamic characteristics.

Figure 24.- Aerodynamic and flow characteristics of the wing with the propeller rotating up at the tip, basic leading edge, fences on, and $\delta_f = 0^{\circ}$.

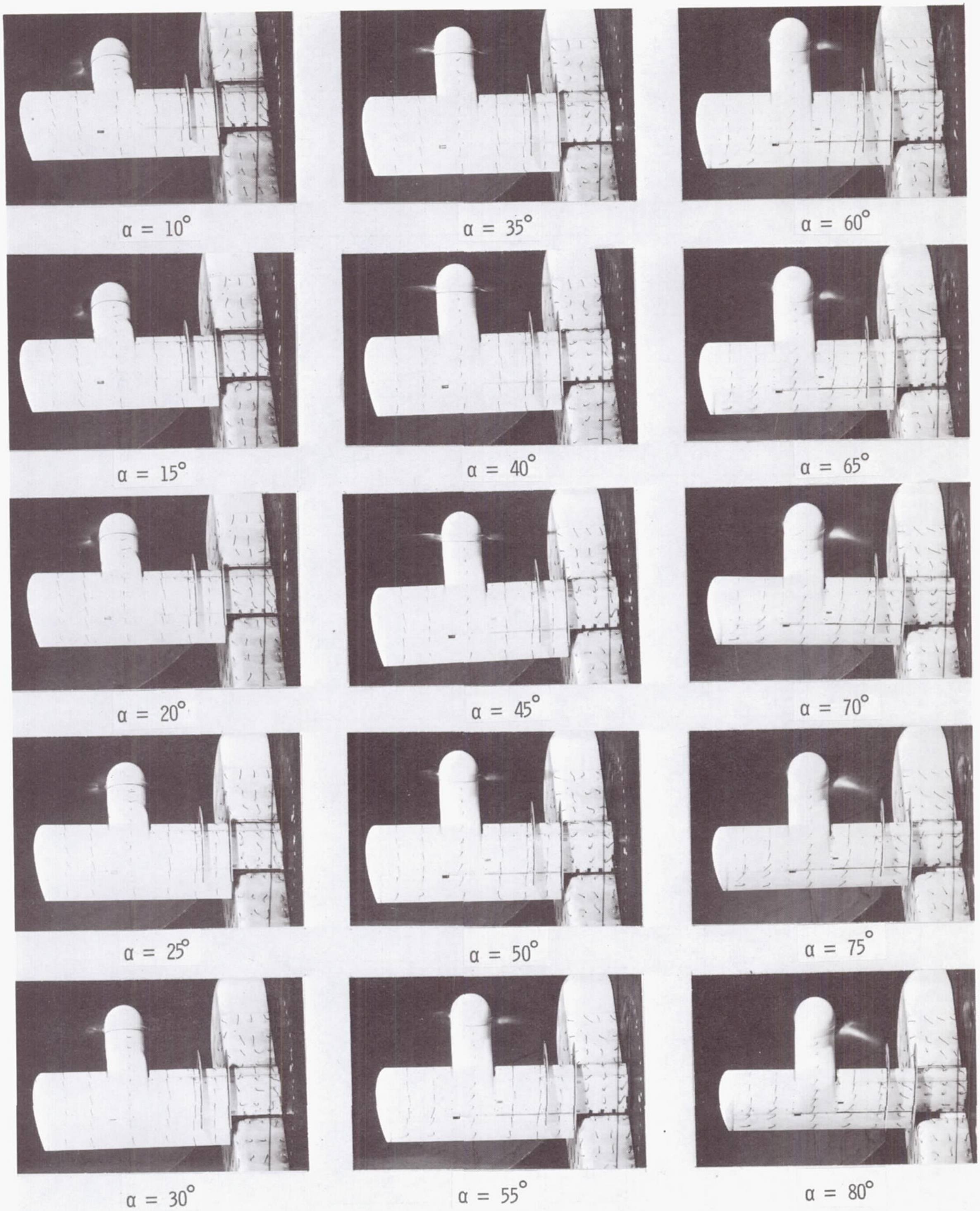

(b) Flow characteristics; $C_{T,s} = 0.90$.

Figure 24.- Continued.

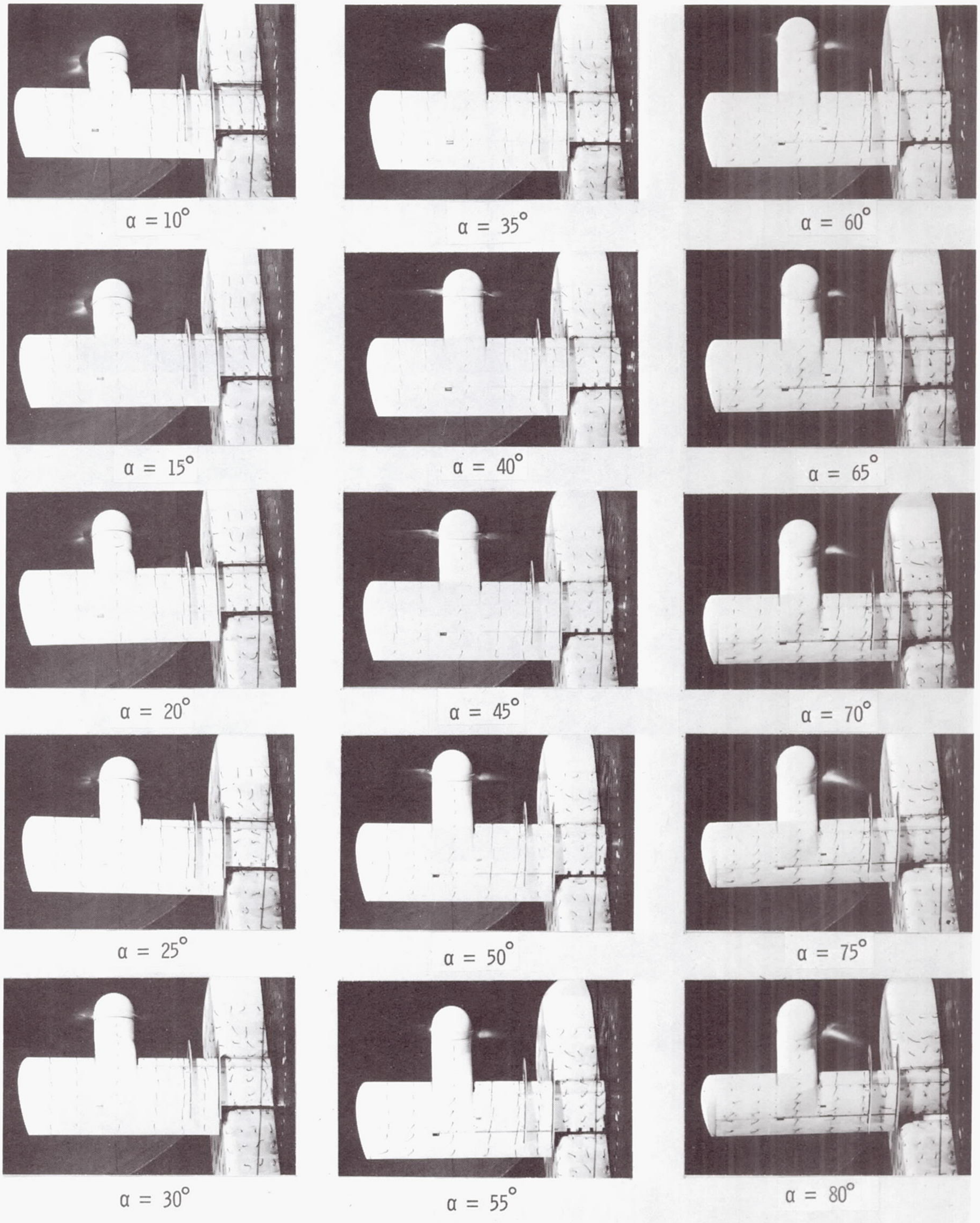

(c) Flow characteristics; $C_{T,s} = 0.80$.

Figure 24.- Continued.

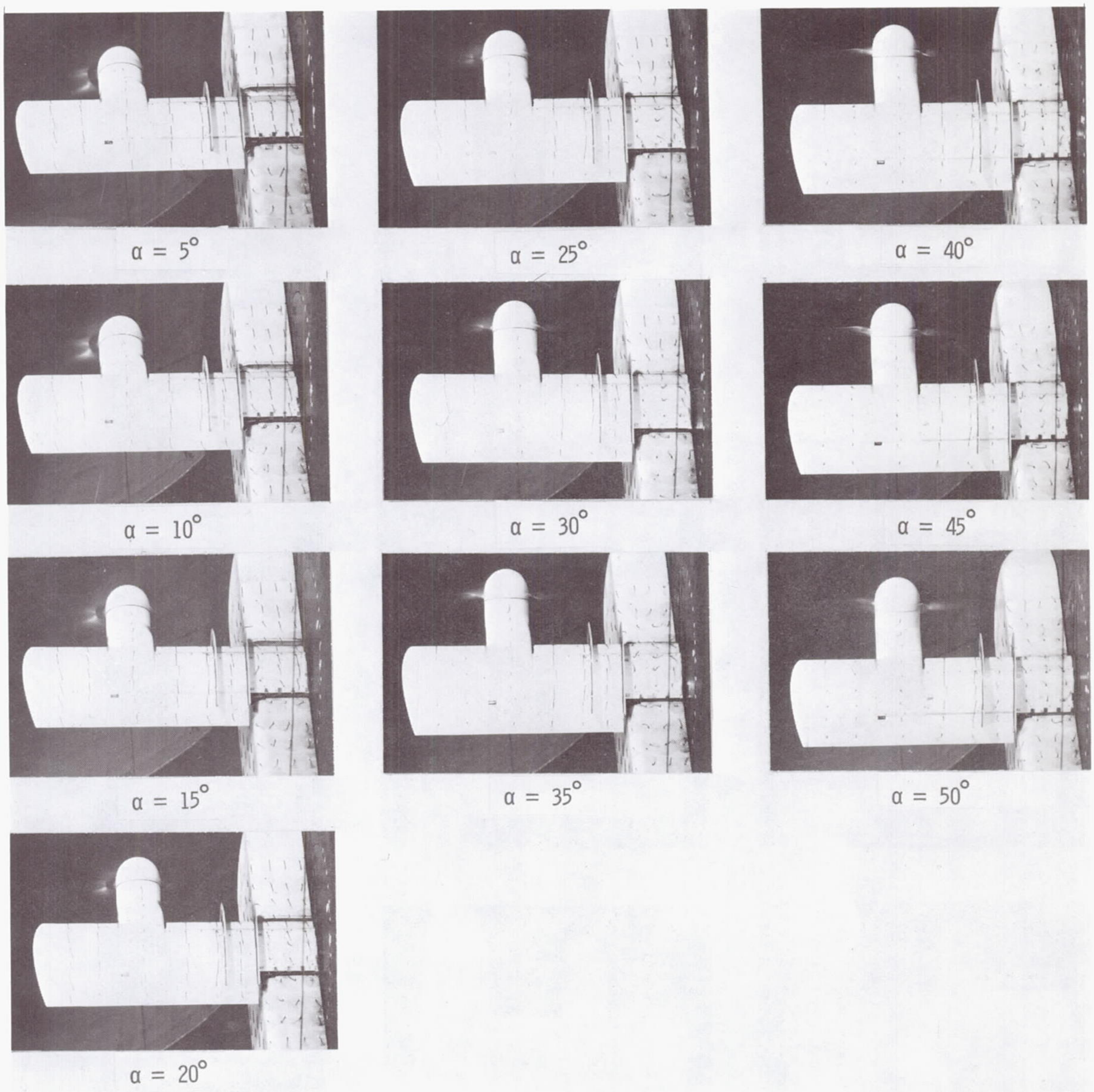

(d) Flow characteristics; $C_{T,s} = 0.60$.

Figure 24.- Continued.

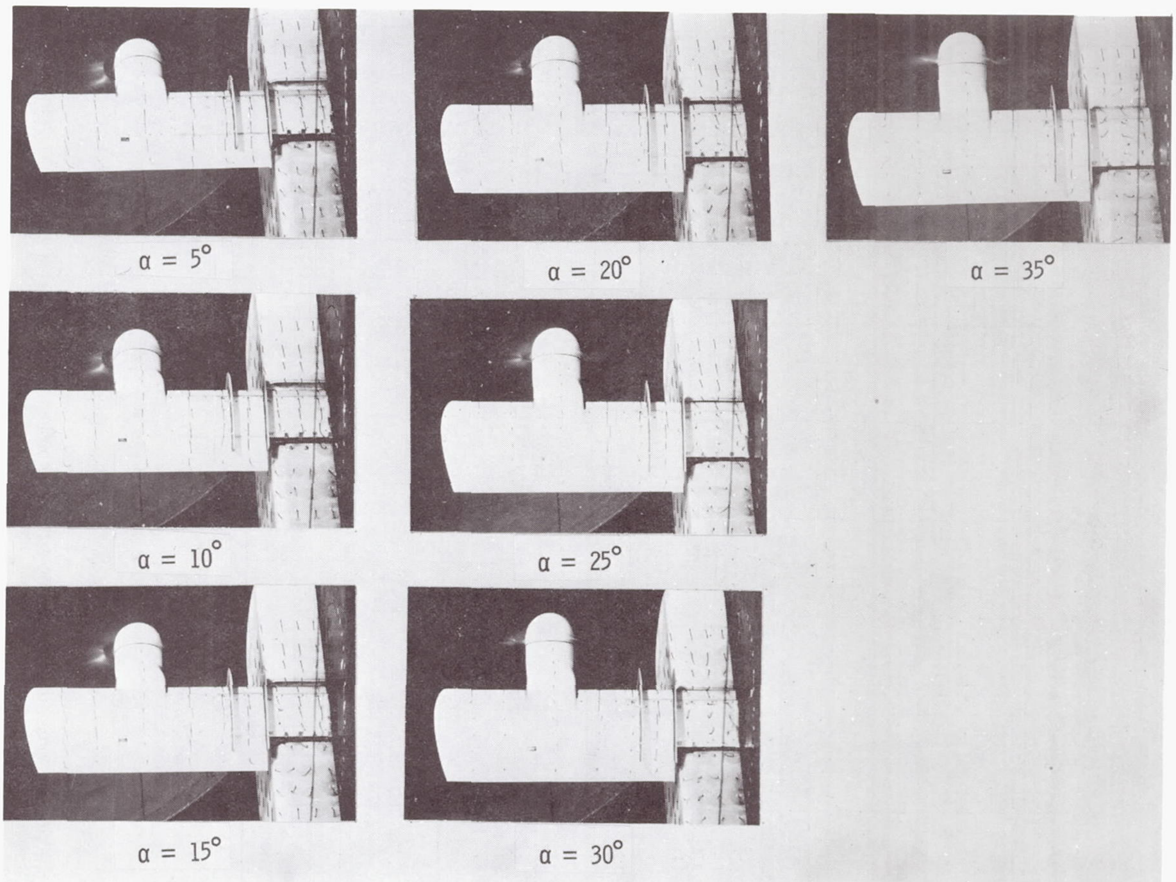

(e) Flow characteristics; $C_{T,s} = 0.30$.

Figure 24.- Concluded.

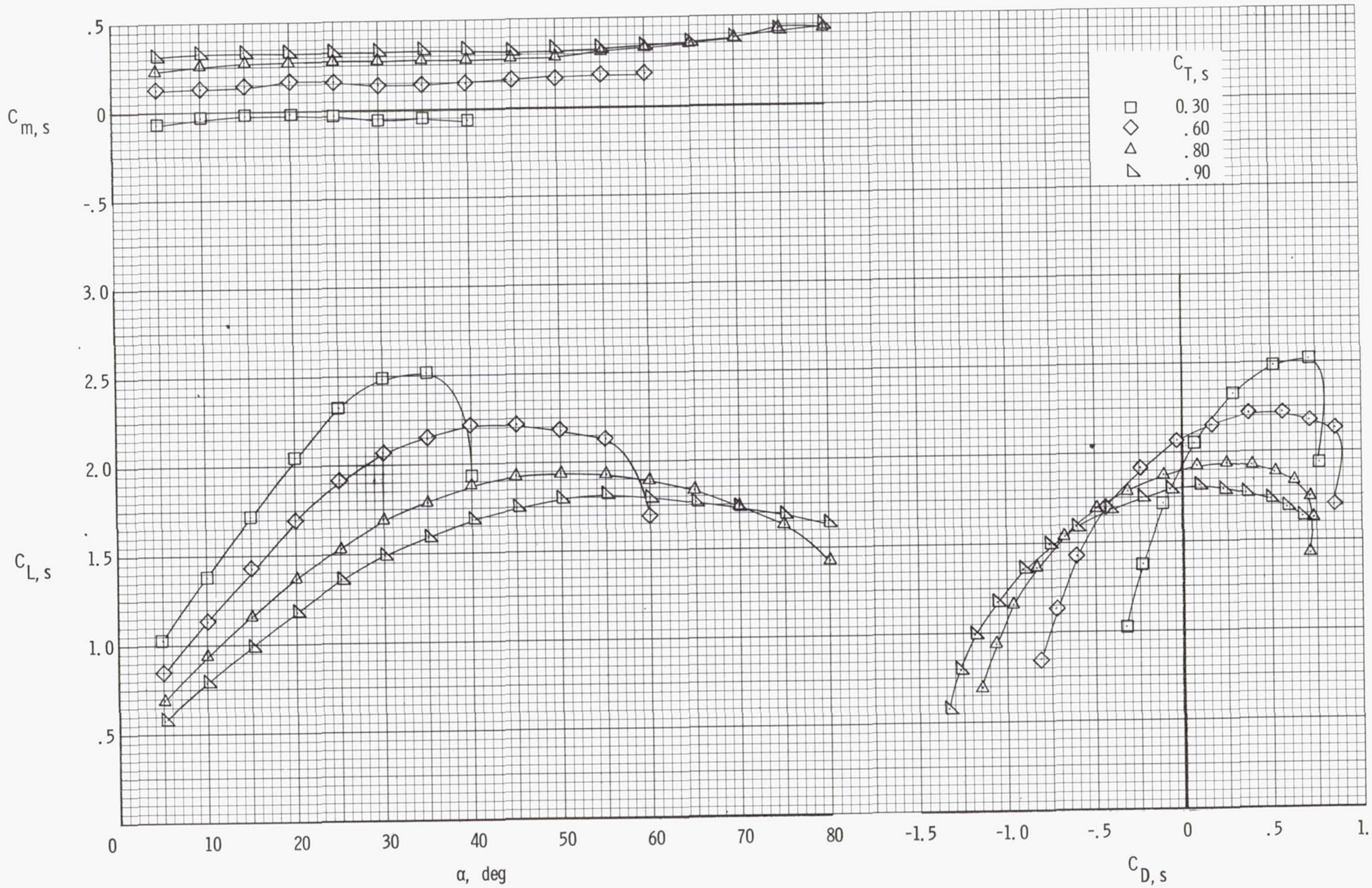

(a) Aerodynamic characteristics.

Figure 25.- **Aerodynamic** and flow characteristics of the wing with the propeller rotating up at the tip, basic leading edge, fences on, and $\delta_f = 20^{\circ}$.

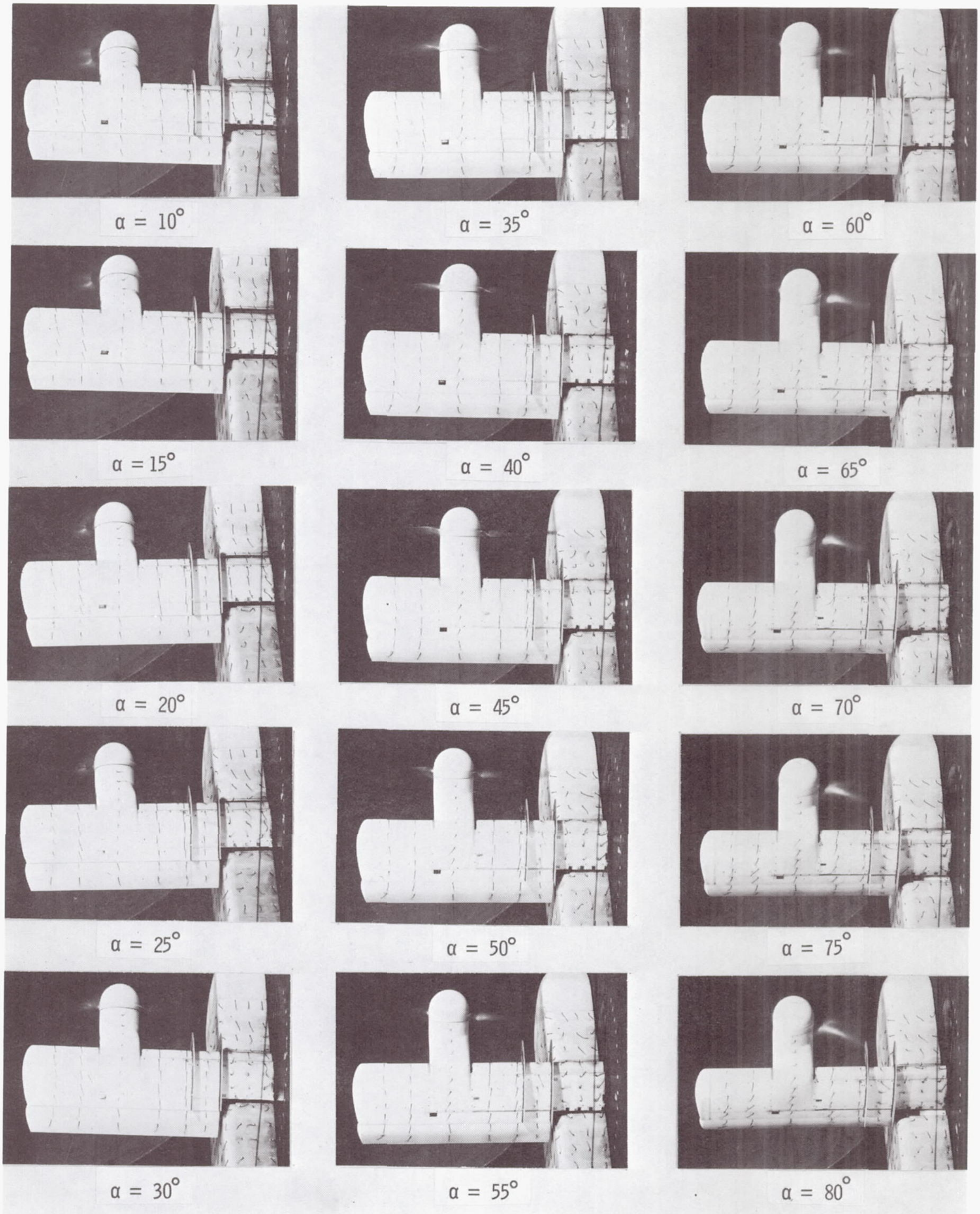

α = 10° α = 35° α = 60°
α = 15° α = 40° α = 65°
α = 20° α = 45° α = 70°
α = 25° α = 50° α = 75°
α = 30° α = 55° α = 80°

(b) Flow characteristics; $C_{T,s} = 0.90$.

Figure 25.- Continued.

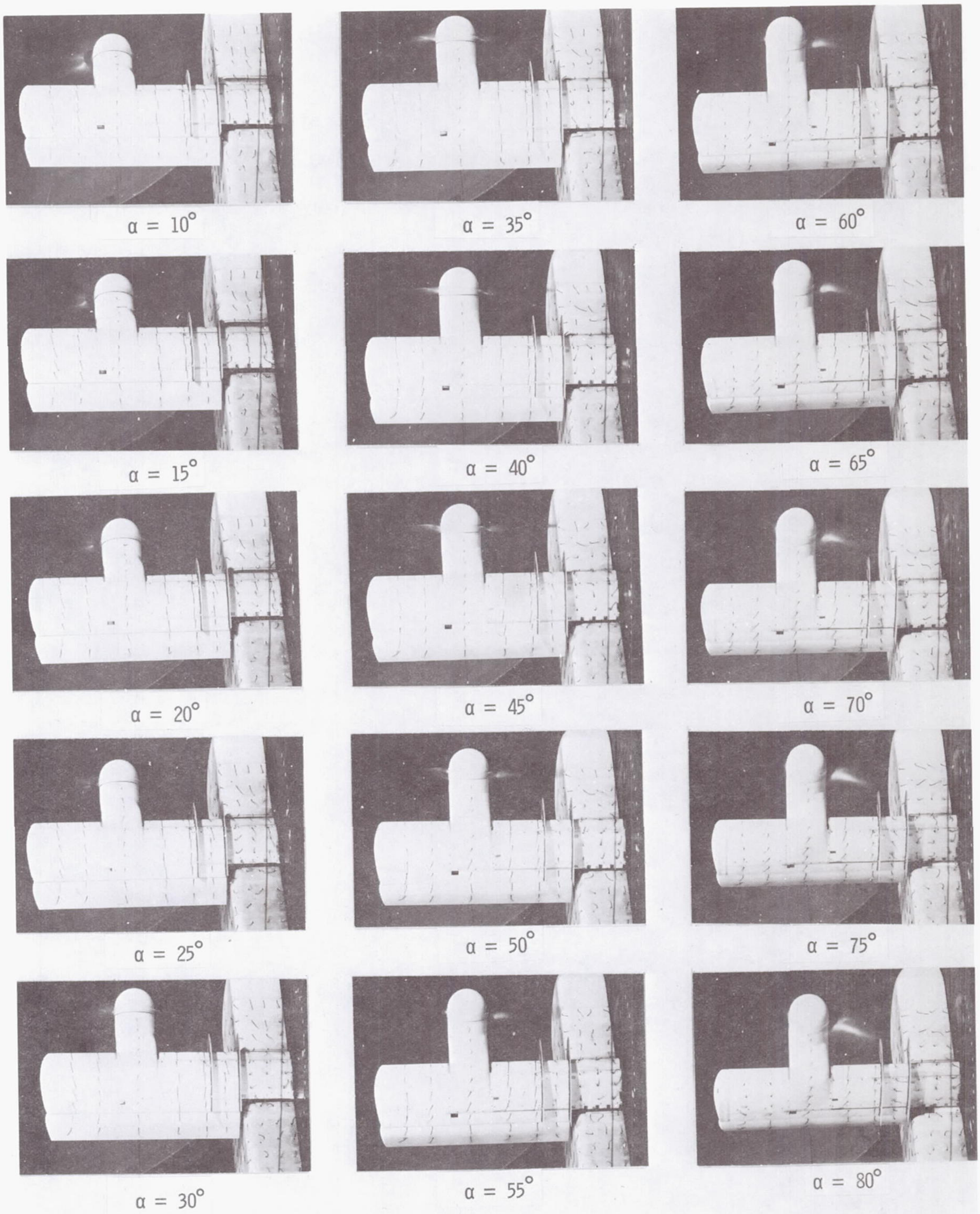

(c) Flow characteristics; $C_{T,s} = 0.80$.

Figure 25.- Continued.

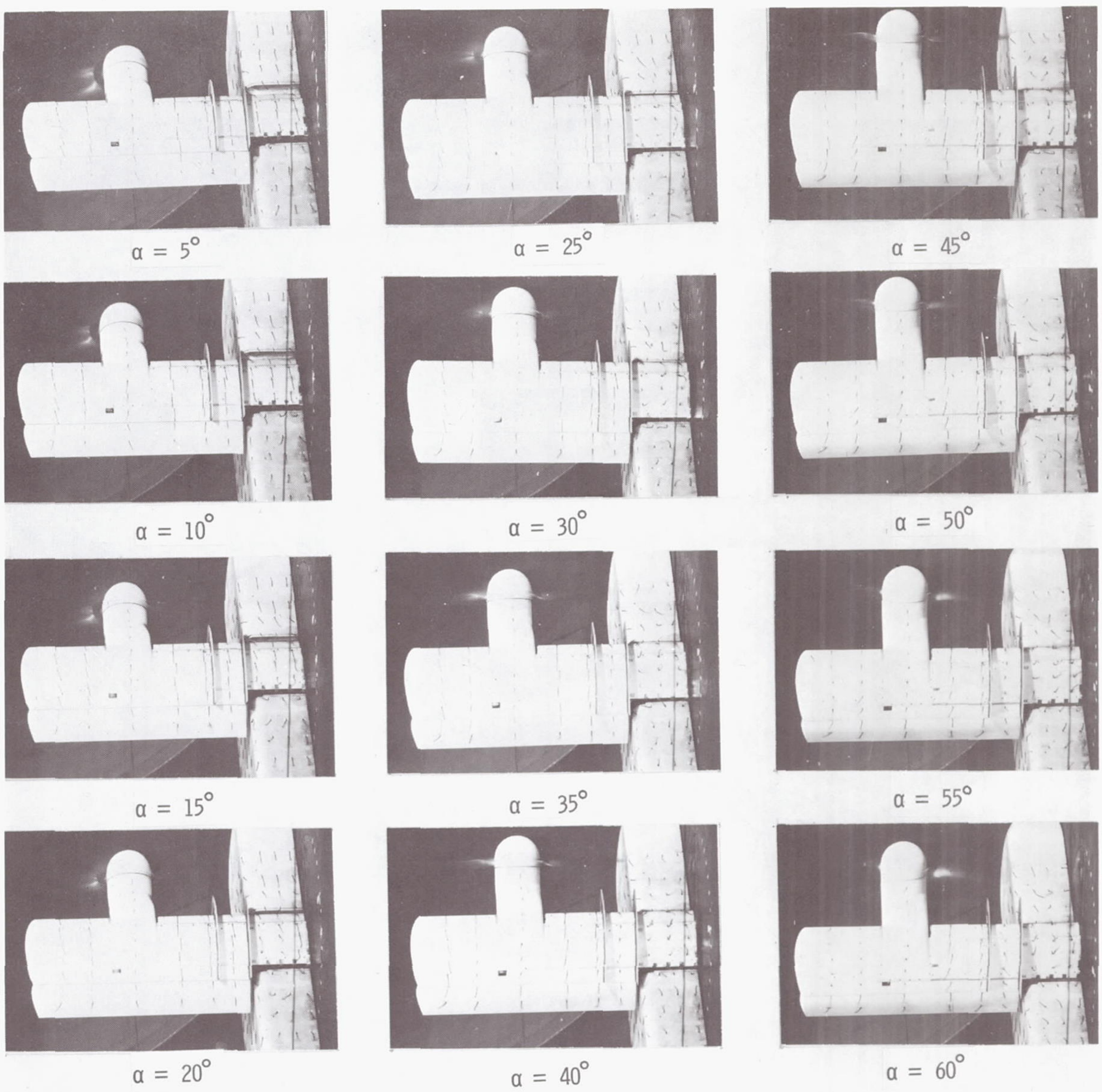

(d) Flow characteristics; $C_{T,s} = 0.60$.

Figure 25.- Continued.

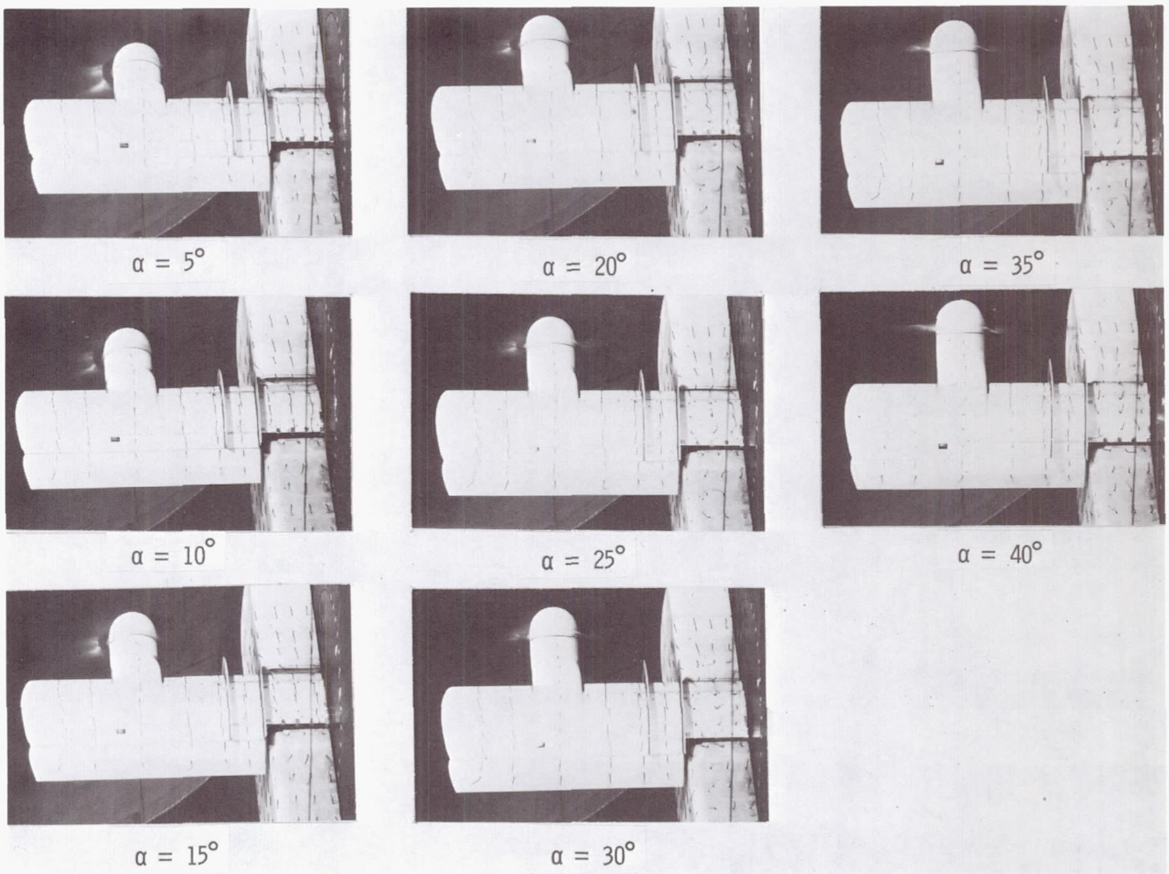

(e) Flow characteristics; $C_{T,s} = 0.30$.

Figure 25.- Concluded.

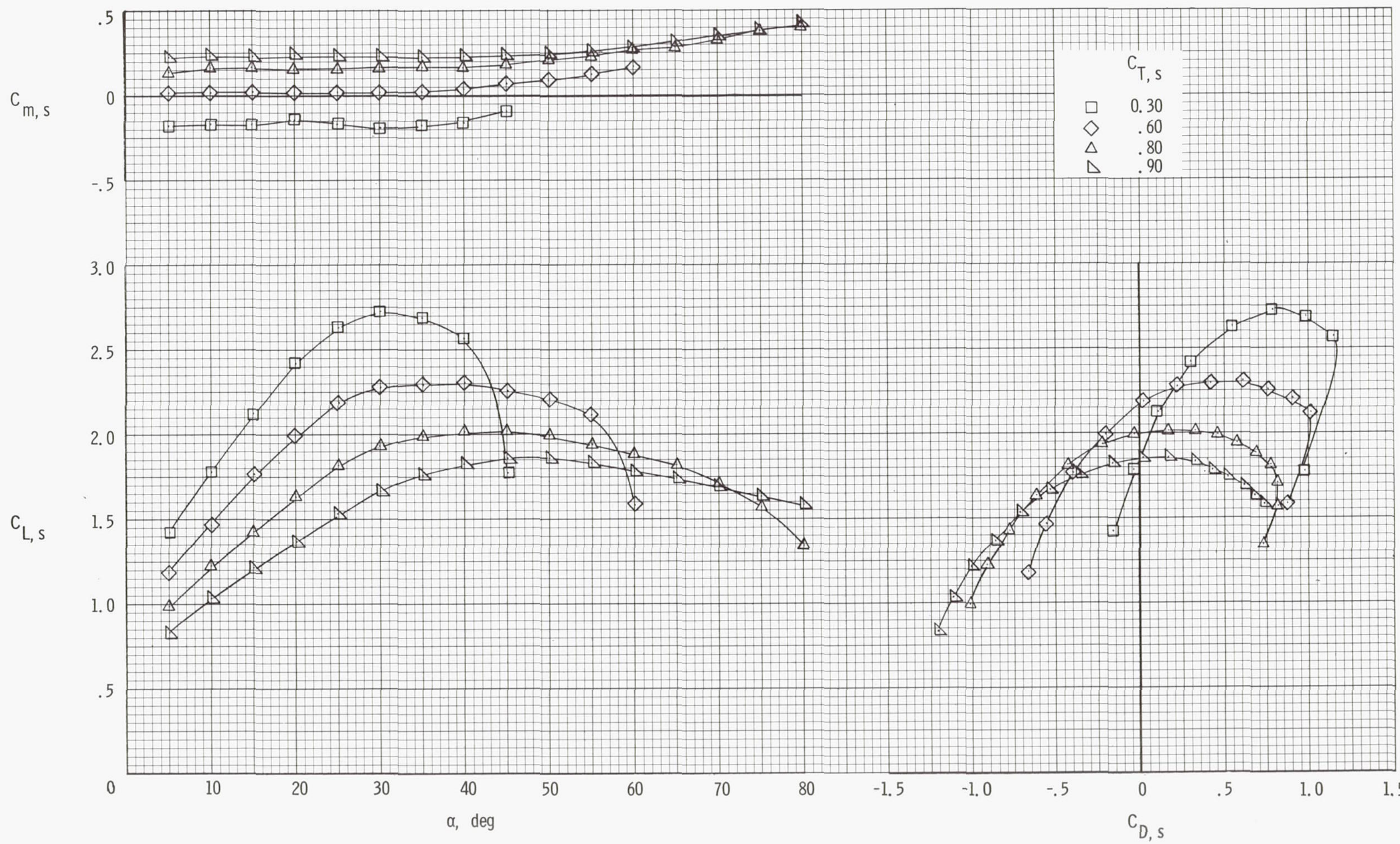

(a) Aerodynamic characteristics.

Figure 26.- Aerodynamic and flow characteristics of the wing with the propeller rotating up at the tip, basic leading edge, fences on, and $\delta_f = 40^0$.

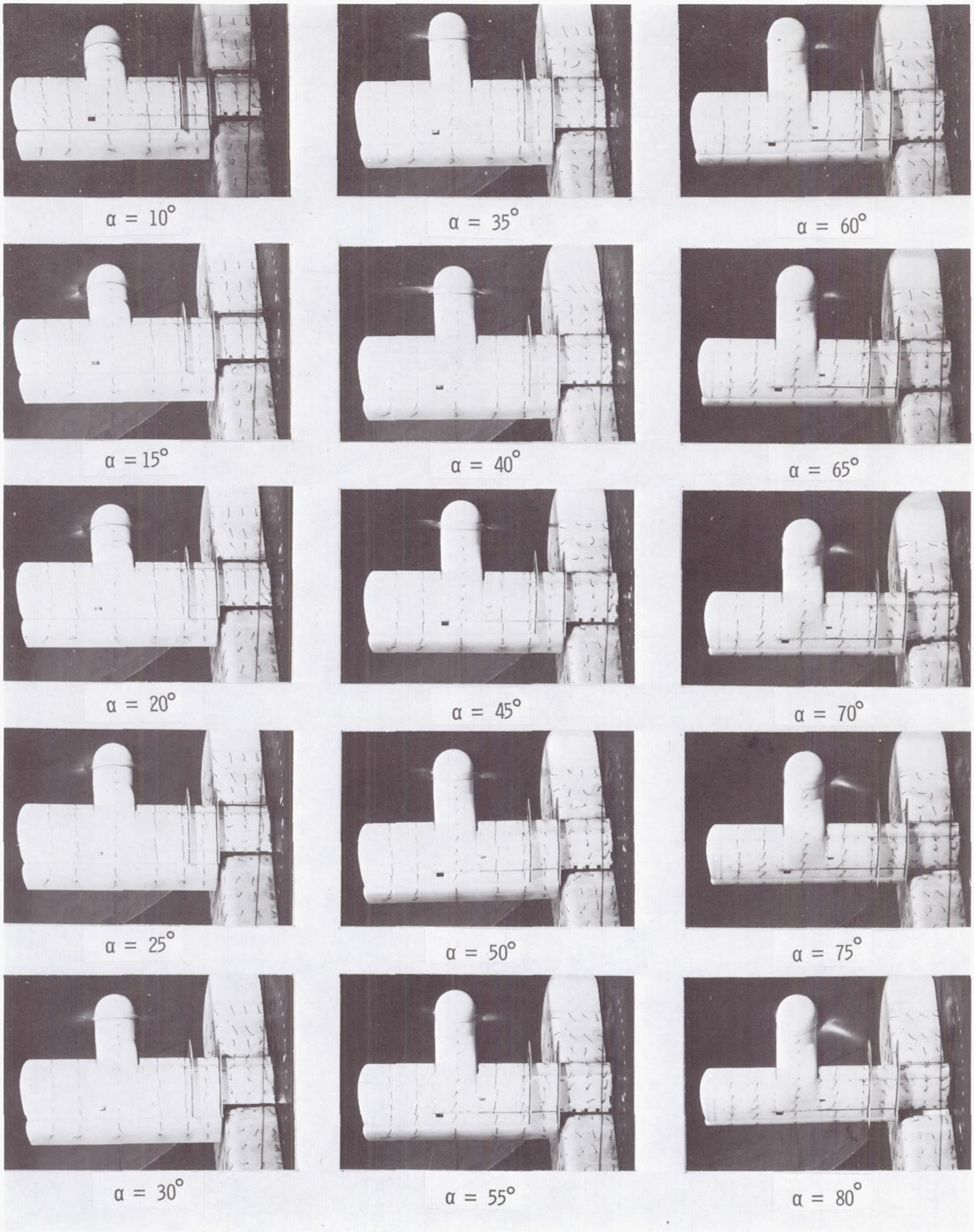

(b) Flow characteristics; $C_{T,s} = 0.90$.

Figure 26.- Continued.

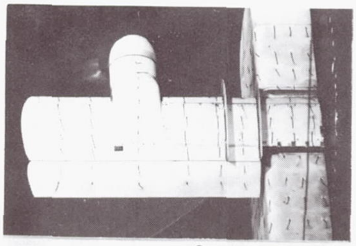
α = 10°

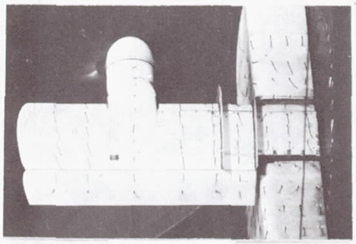
α = 15°

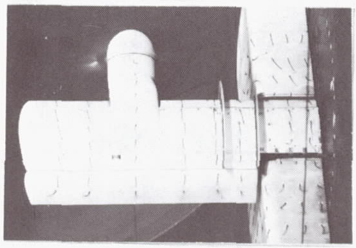
α = 20°

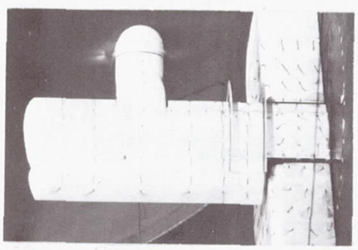
α = 25°

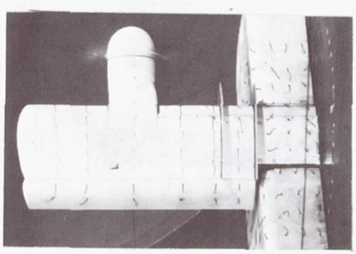
α = 30°

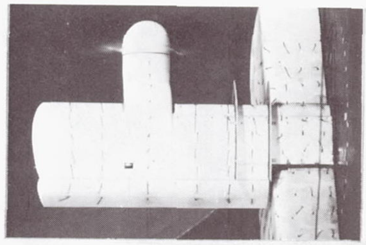
α = 35°

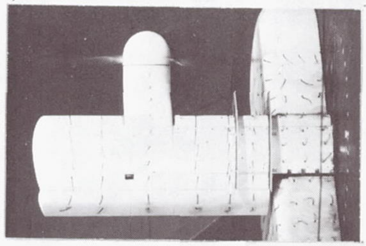
α = 40°

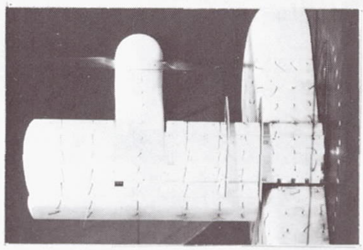
α = 45°

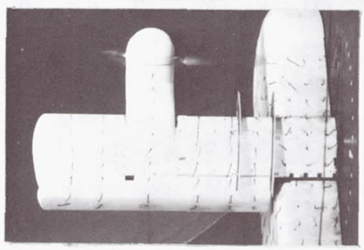
α = 50°

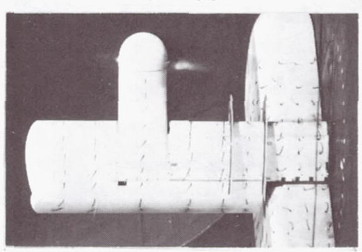
α = 55°

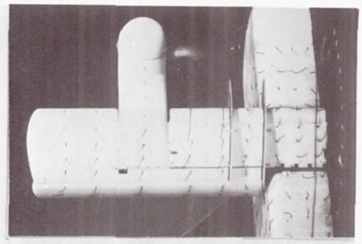
α = 60°

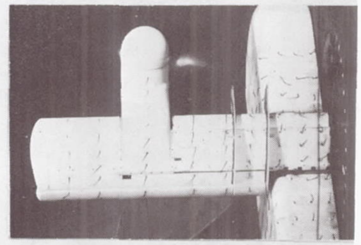
α = 65°

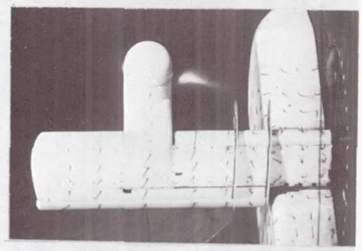
α = 70°

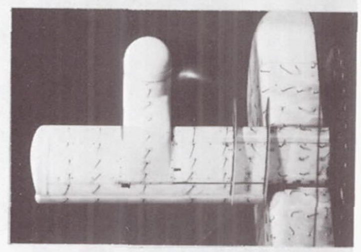
α = 75°


α = 80°

(c) Flow characteristics; $C_{T,s} = 0.80$.

Figure 26.- Continued.

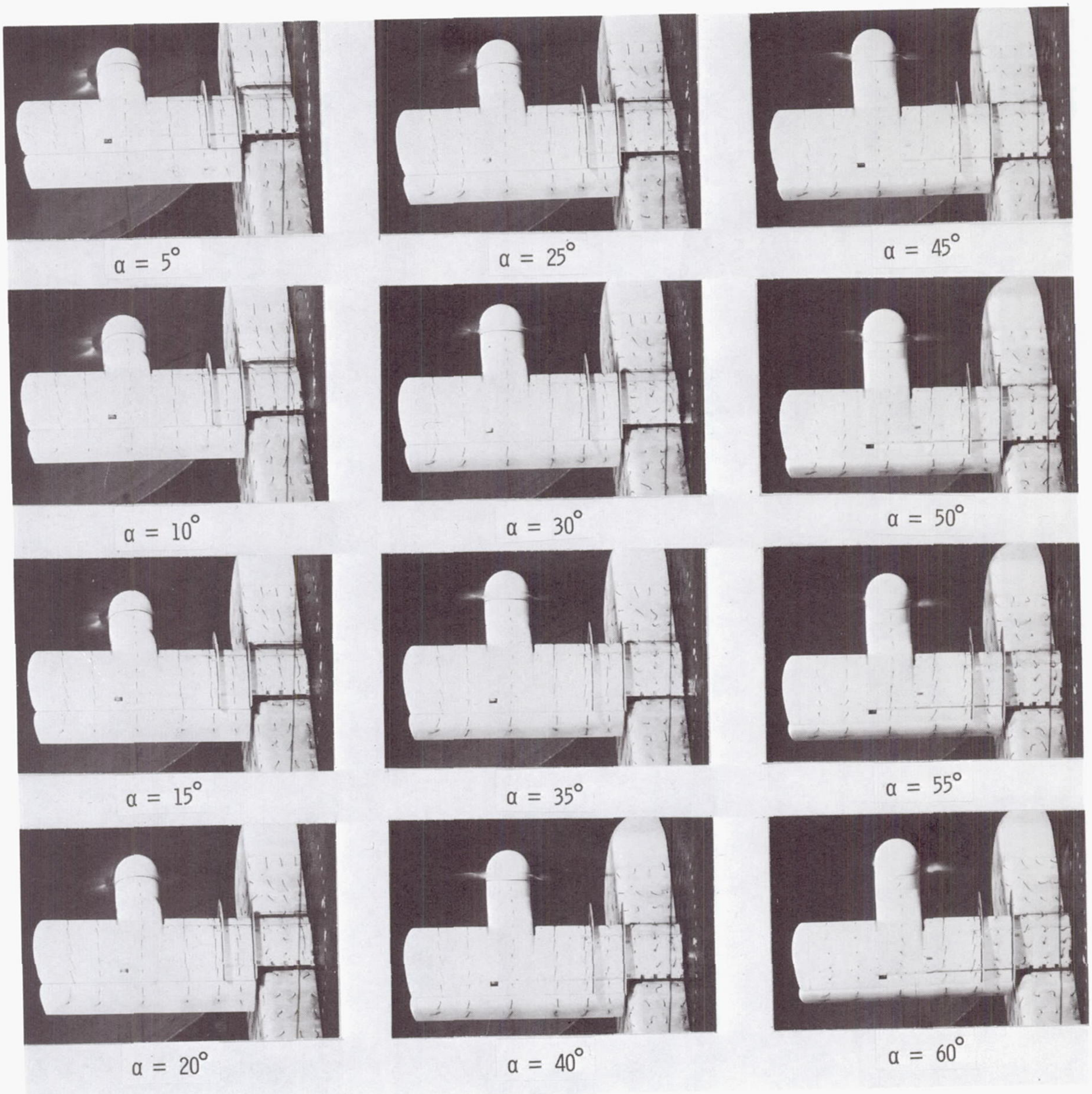

(d) Flow characteristics; $C_{T,s} = 0.60$.

Figure 26.- Continued.

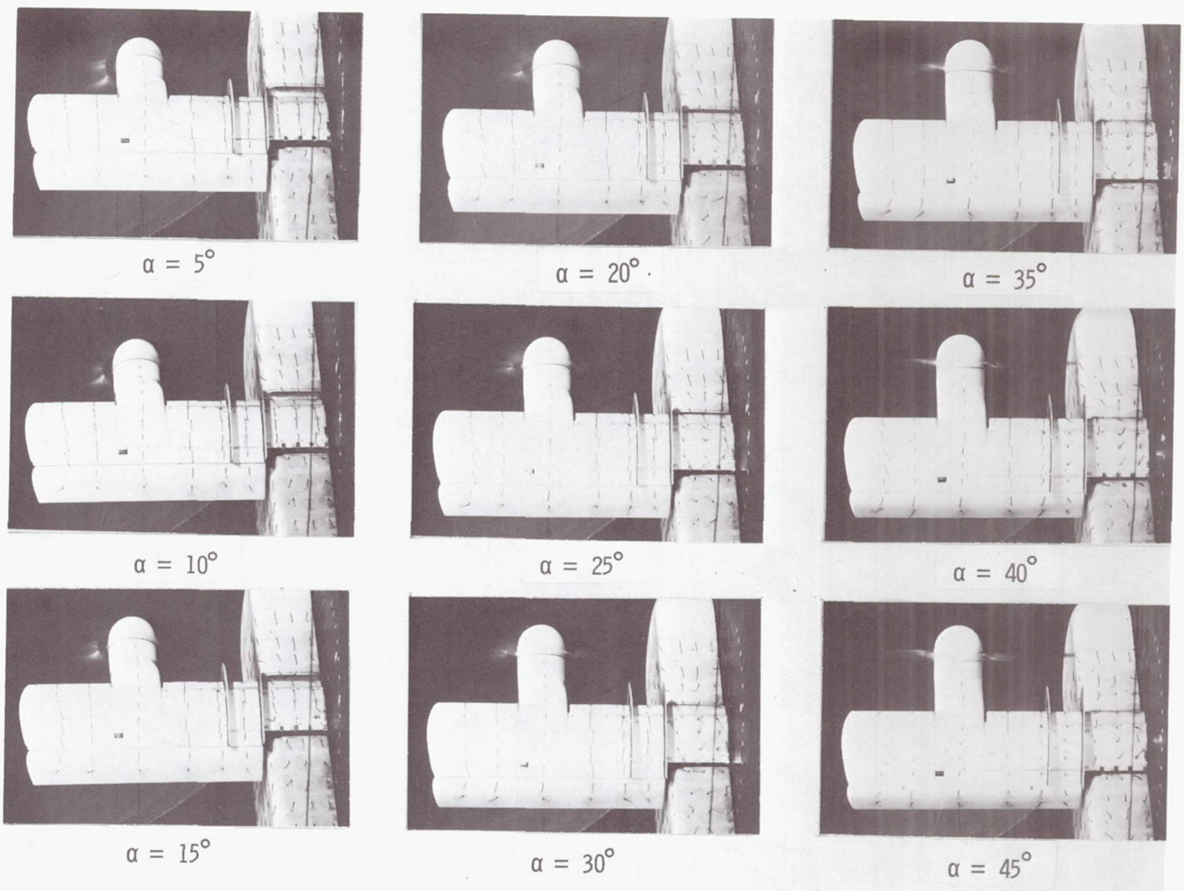

(e) Flow characteristics; $C_{T,s} = 0.30$.

Figure 26.- Concluded.

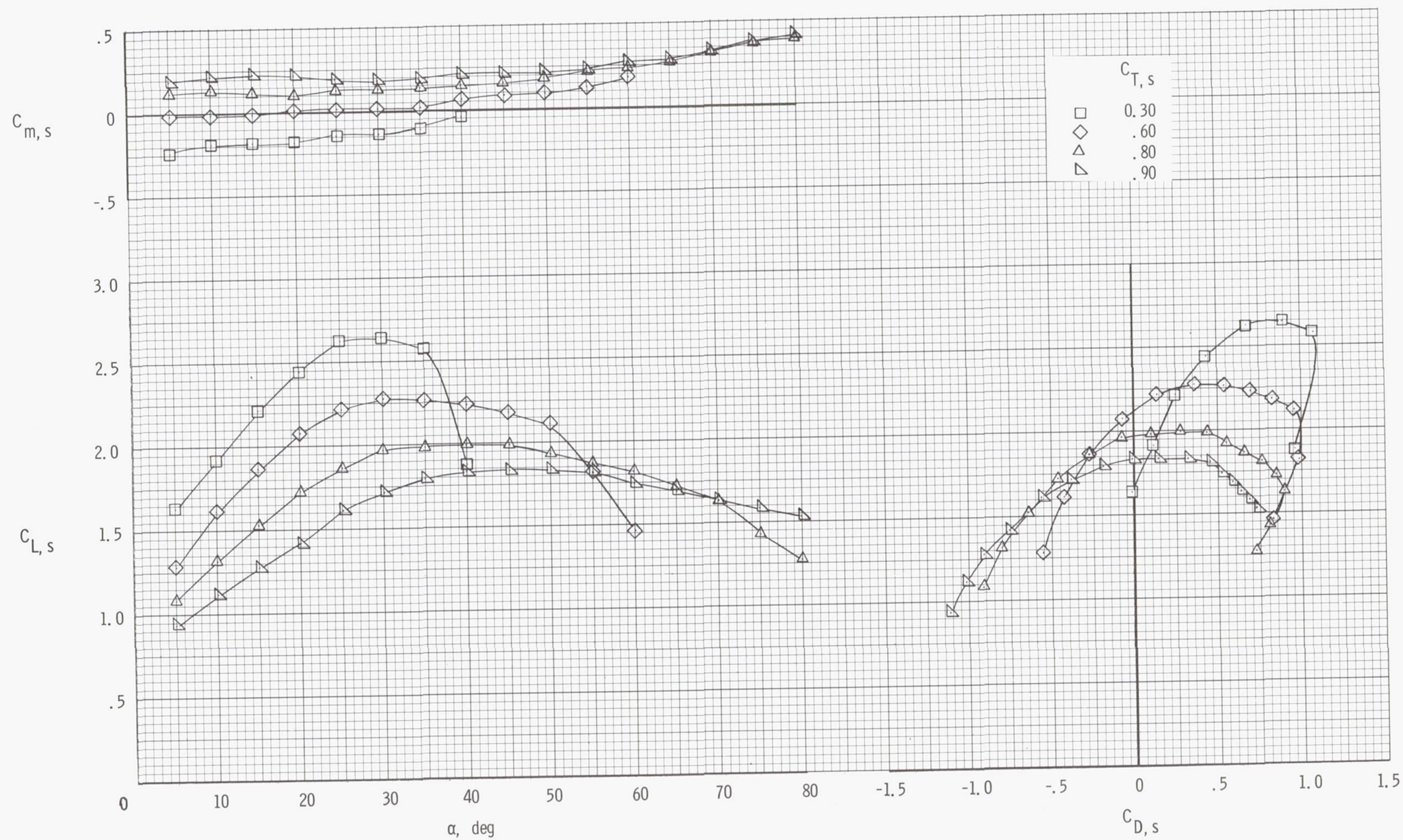

(a) Aerodynamic characteristics.

Figure 27.- Aerodynamic and flow characteristics of the wing with the propeller rotating up at the tip, basic leading edge, fences on, and $\delta_f = 60^0$.

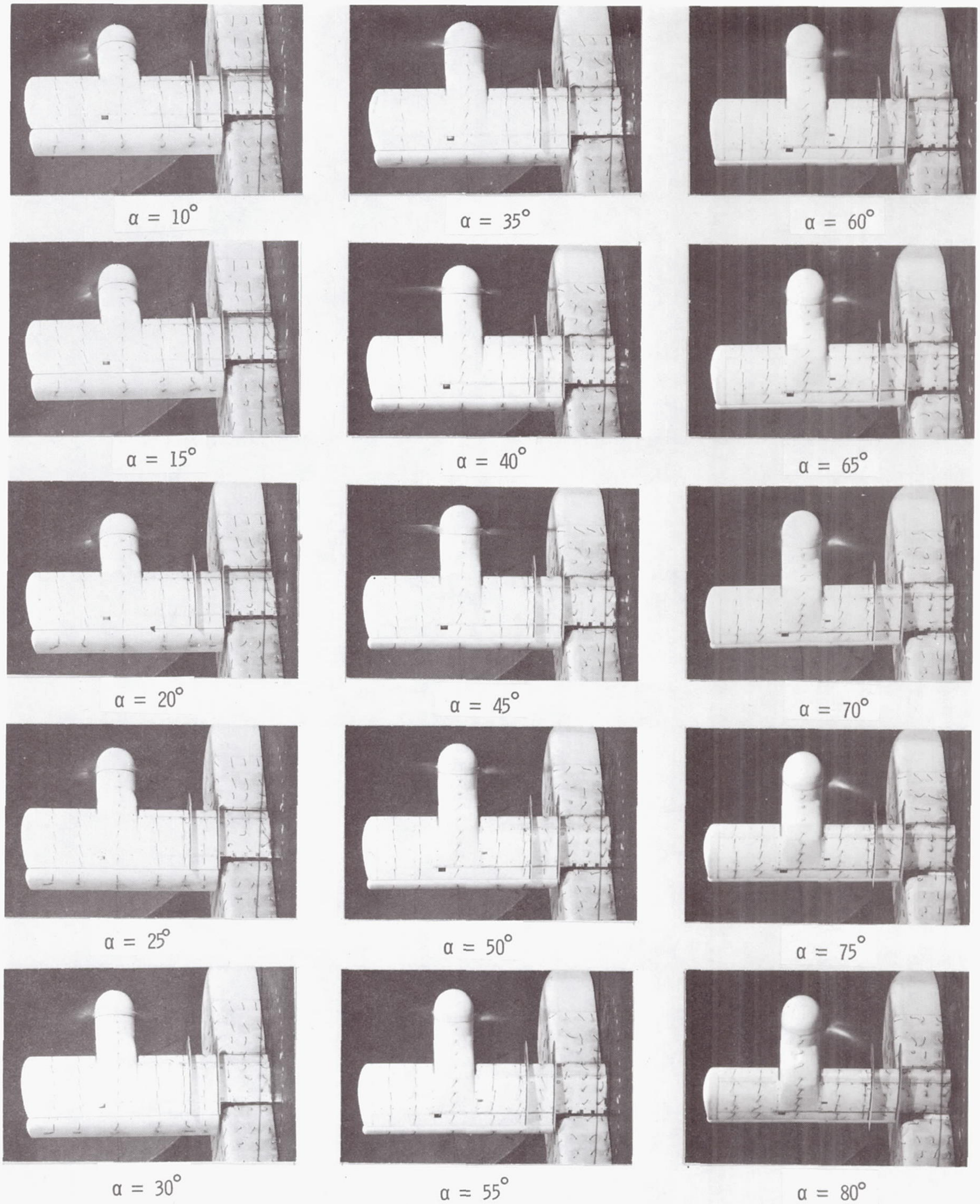

(b) Flow characteristics; $C_{T,s} = 0.90$.

Figure 27.- Continued.

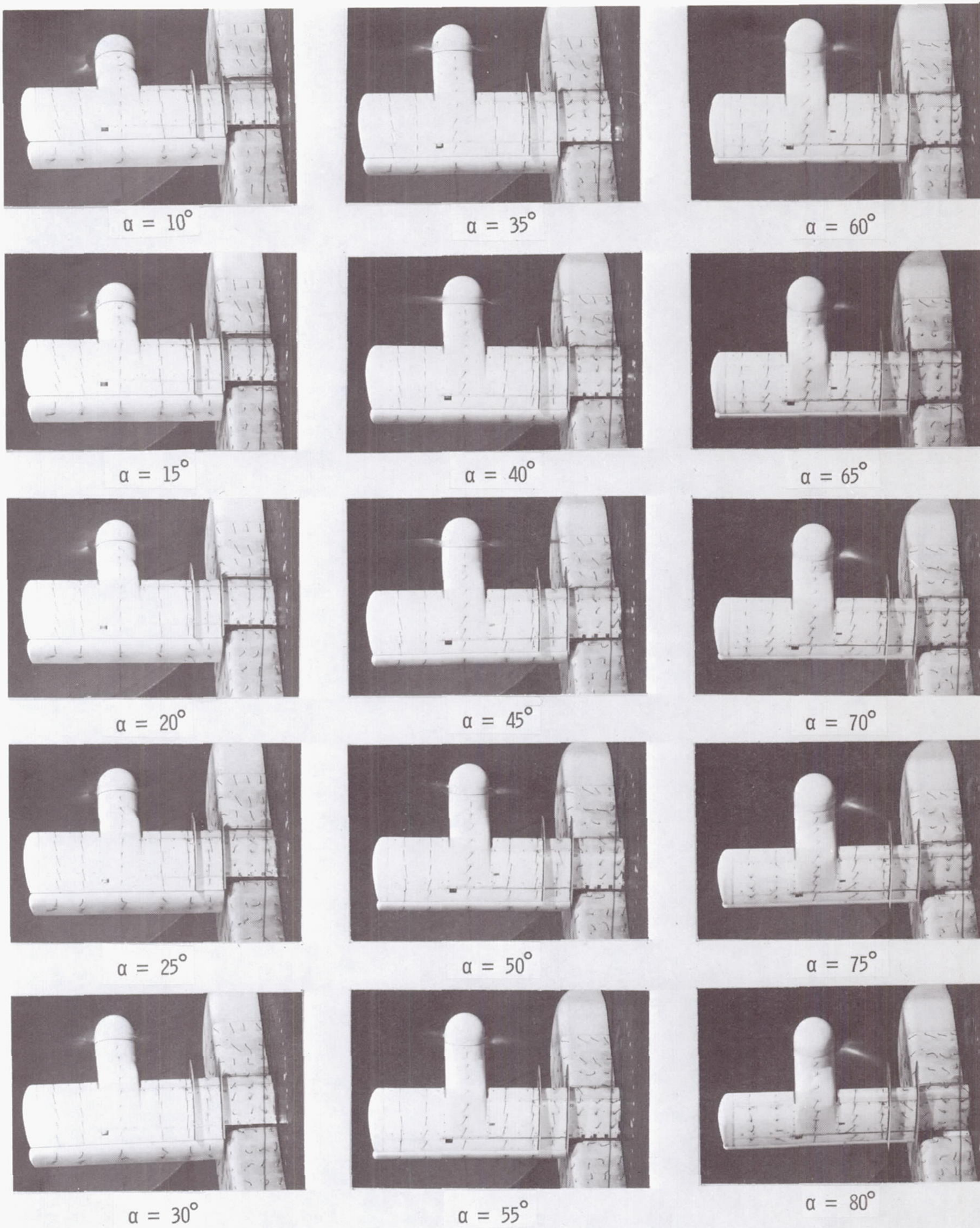

(c) Flow characteristics; $C_{T,s} = 0.80$.

Figure 27.- Continued.

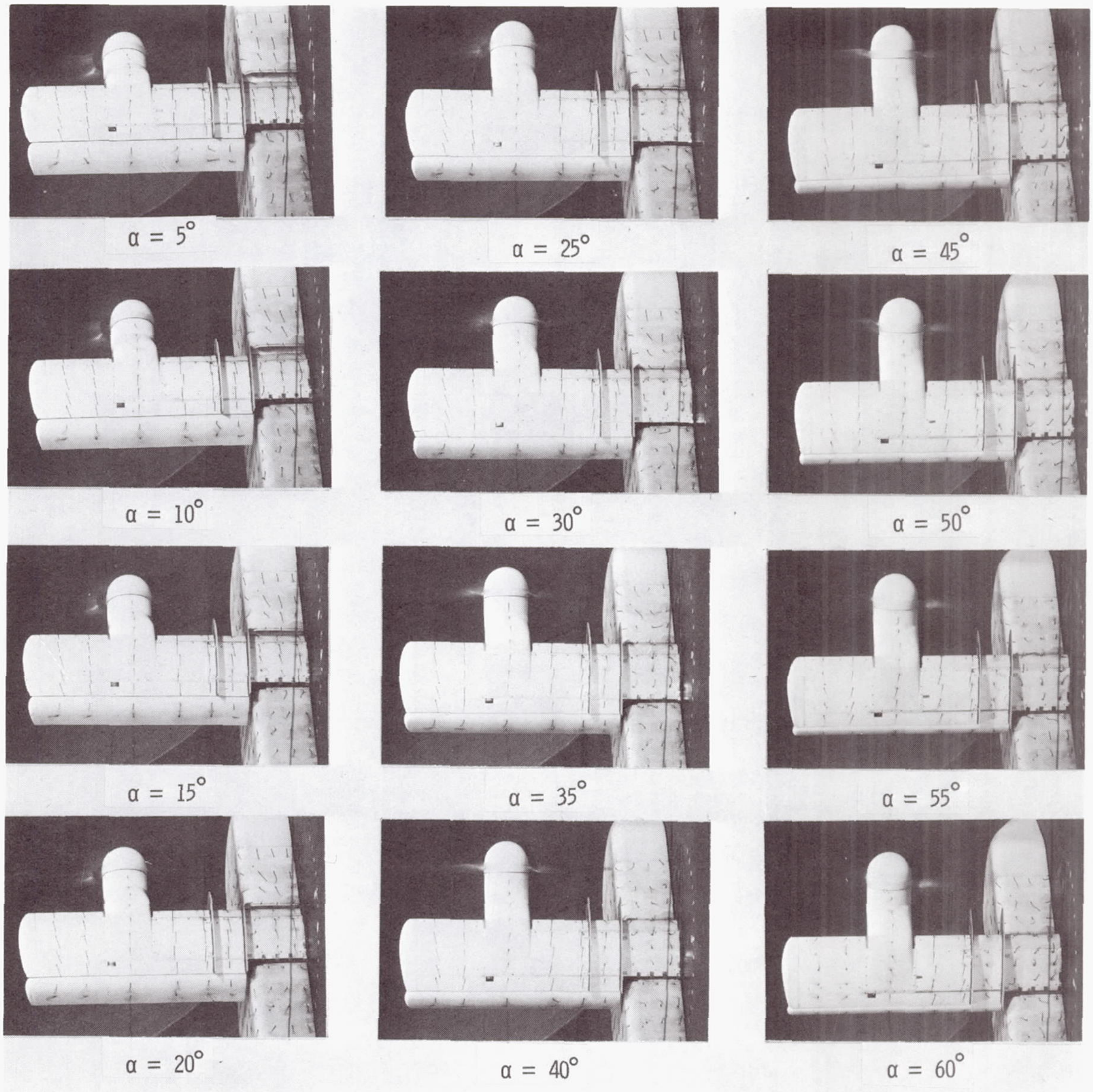

(d) Flow characteristics; $C_{T,s} = 0.60$.

Figure 27.- Continued.

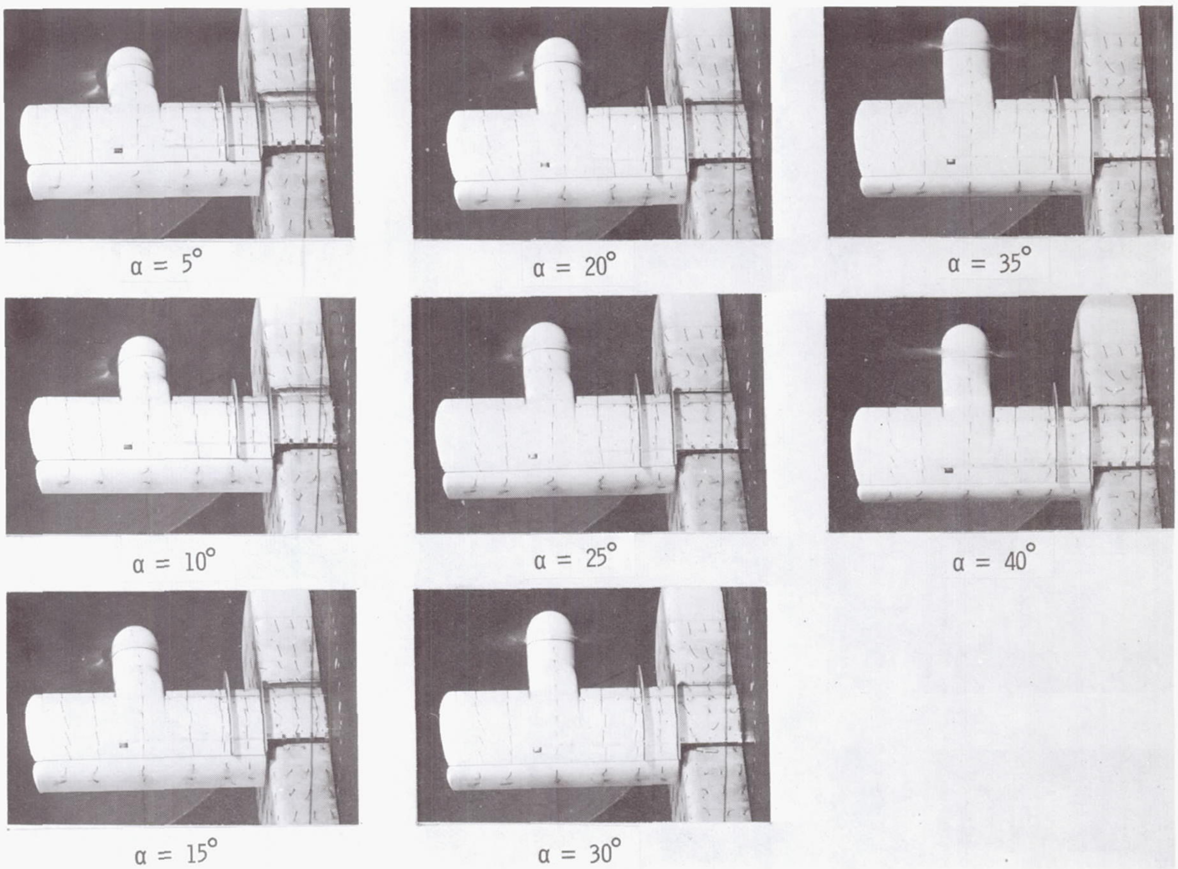

(e) Flow characteristics; $C_{T,s} = 0.30$.

Figure 27.- Concluded.

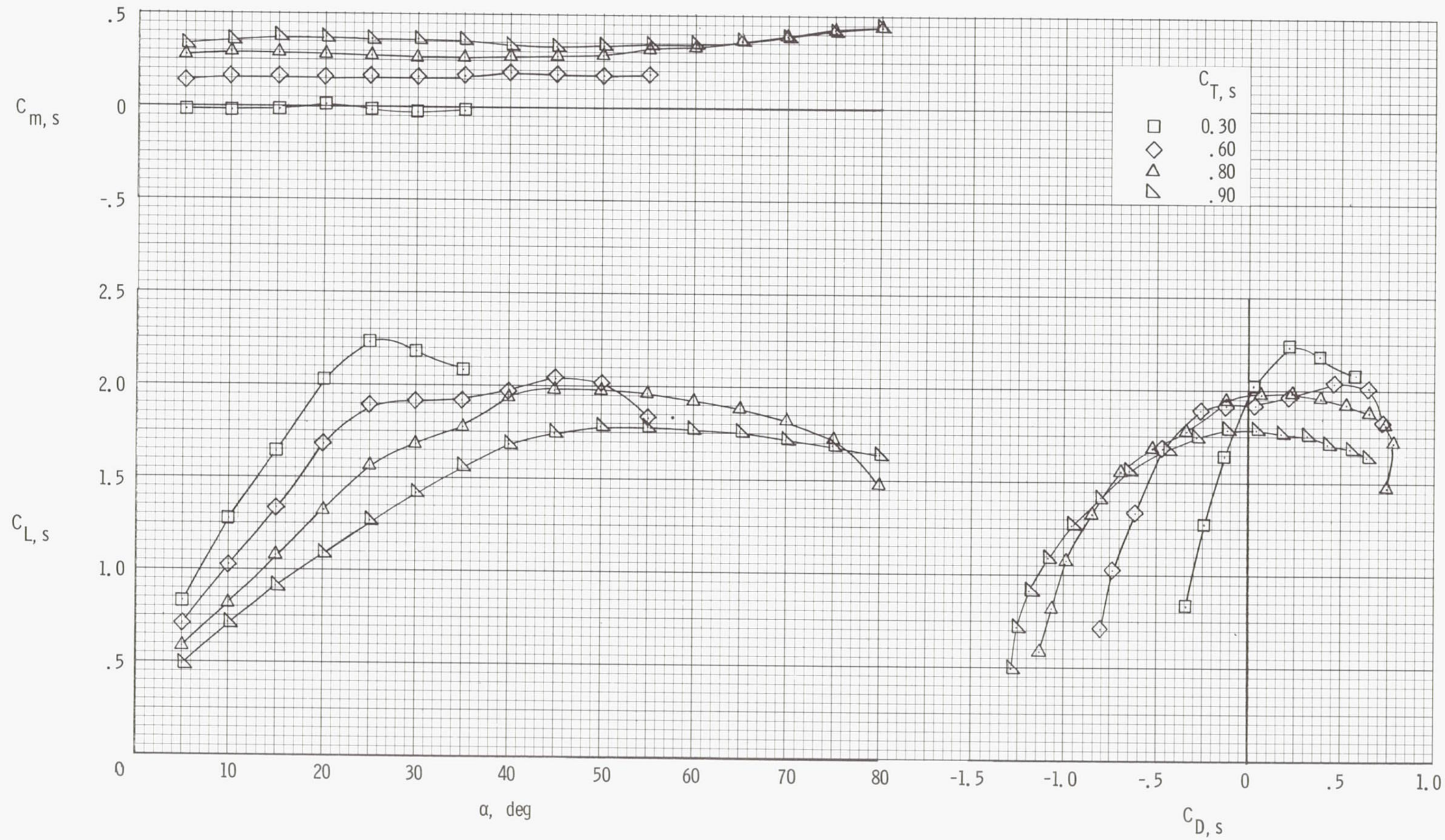

(a) Aerodynamic characteristics.

Figure 28.- Aerodynamic and flow characteristics of the wing with the propeller rotating up at the tip, inboard slat on, and $\delta_f = 20^{\circ}$.

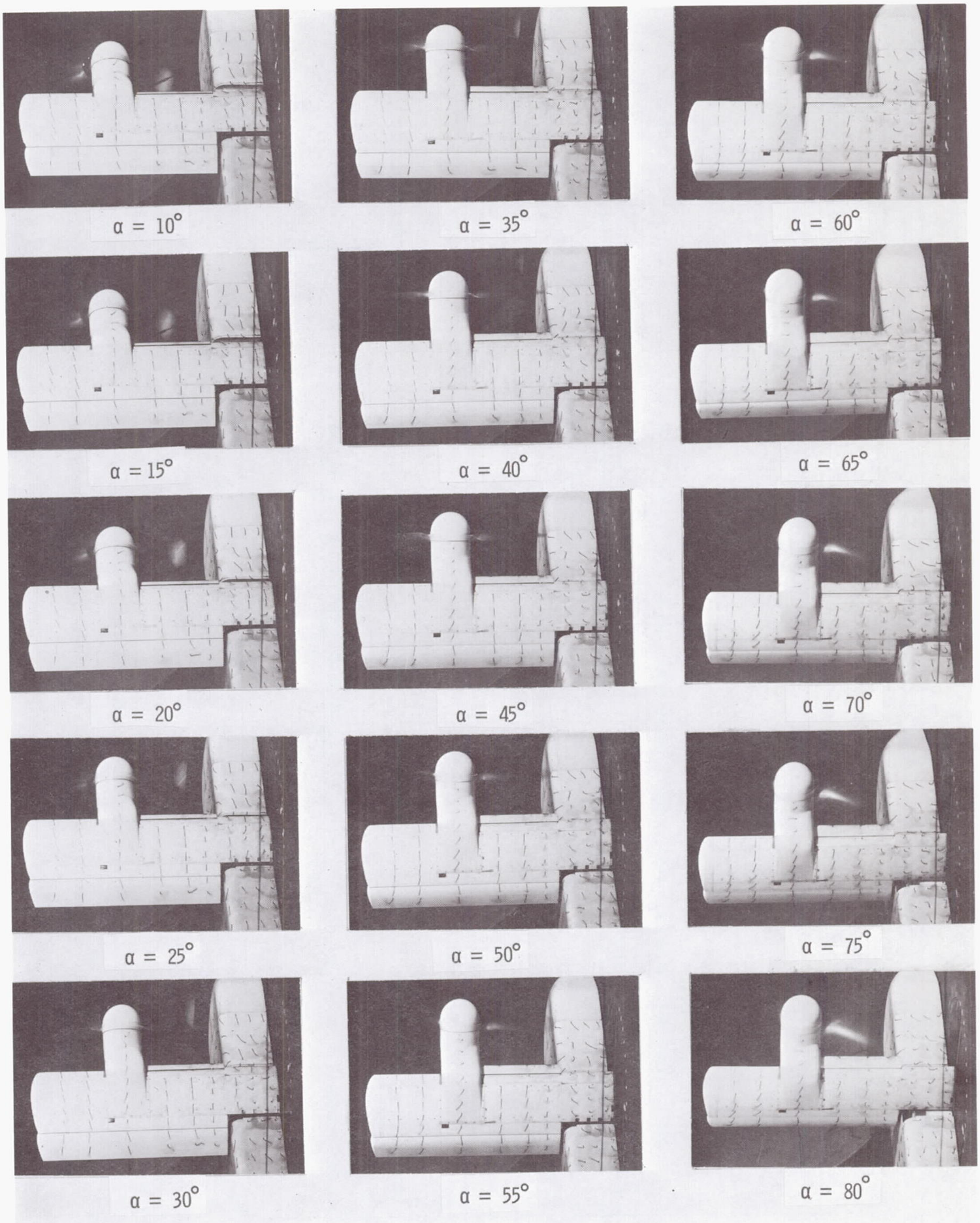

(b) Flow characteristics; $C_{T,s} = 0.90$.

Figure 28.- Continued.

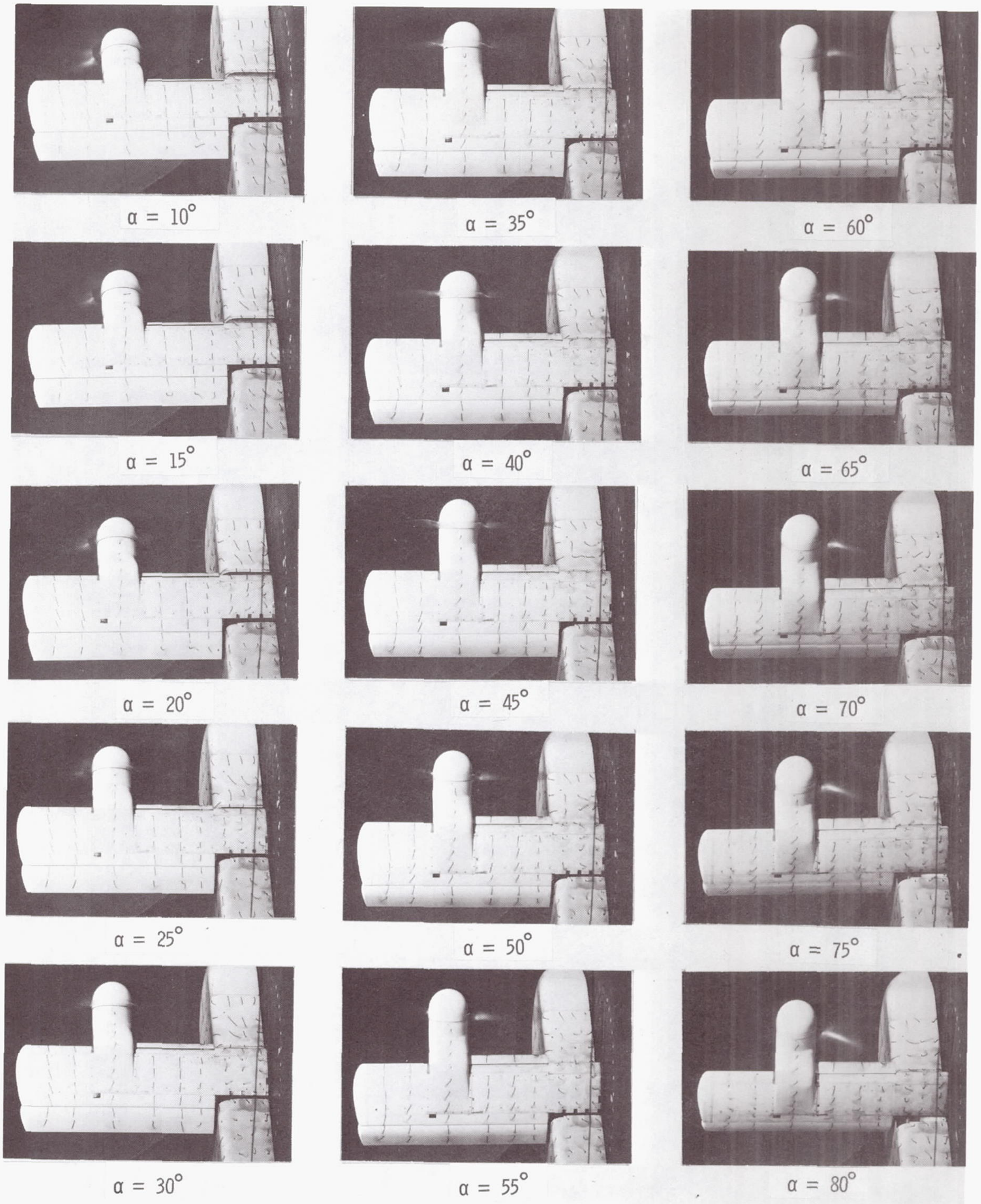

(c) Flow characteristics; $C_{T,s} = 0.80$.

Figure 28.- Continued.

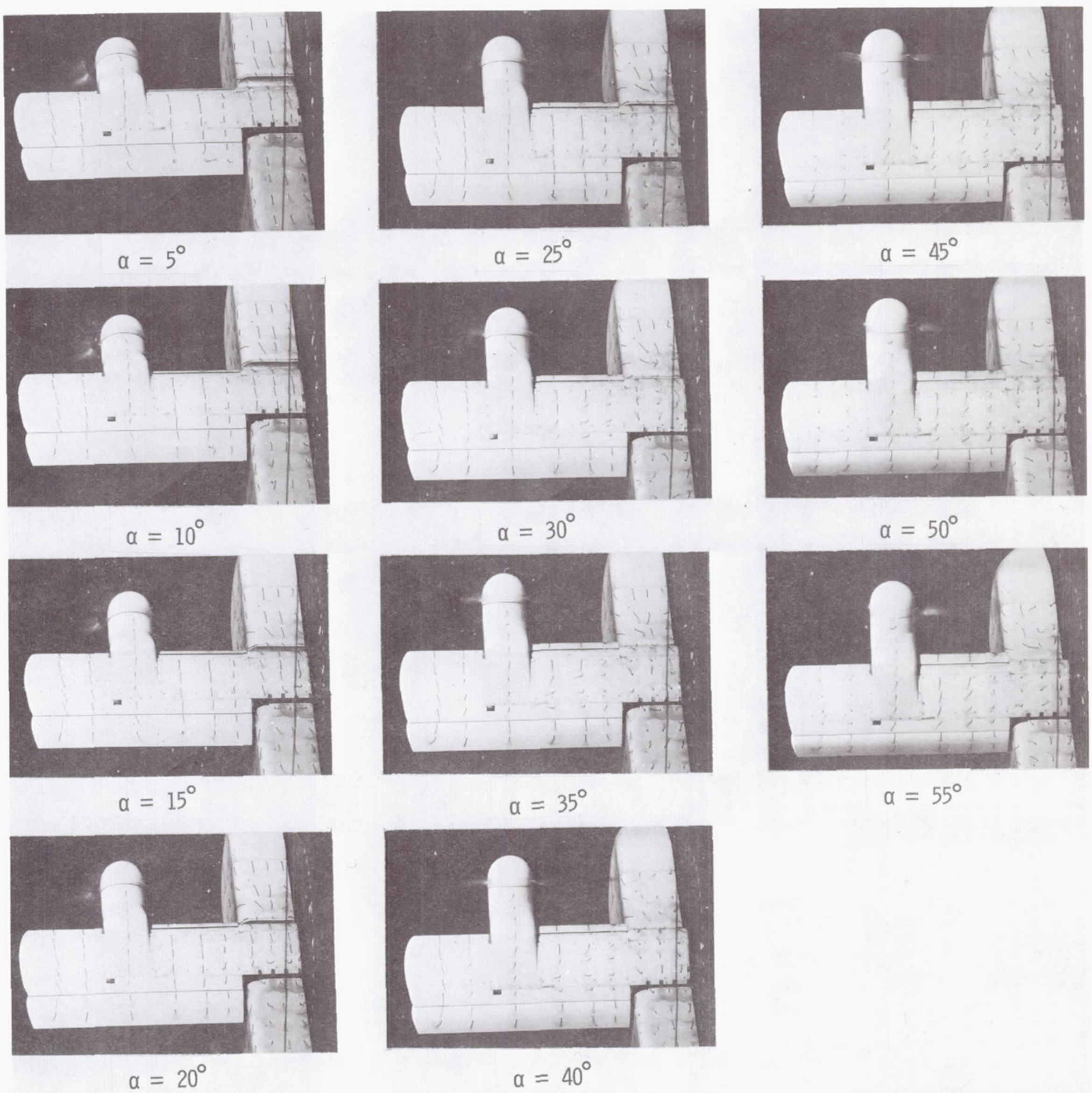

(d) Flow characteristics; $C_{T,s} = 0.60$.

Figure 28.- Continued.

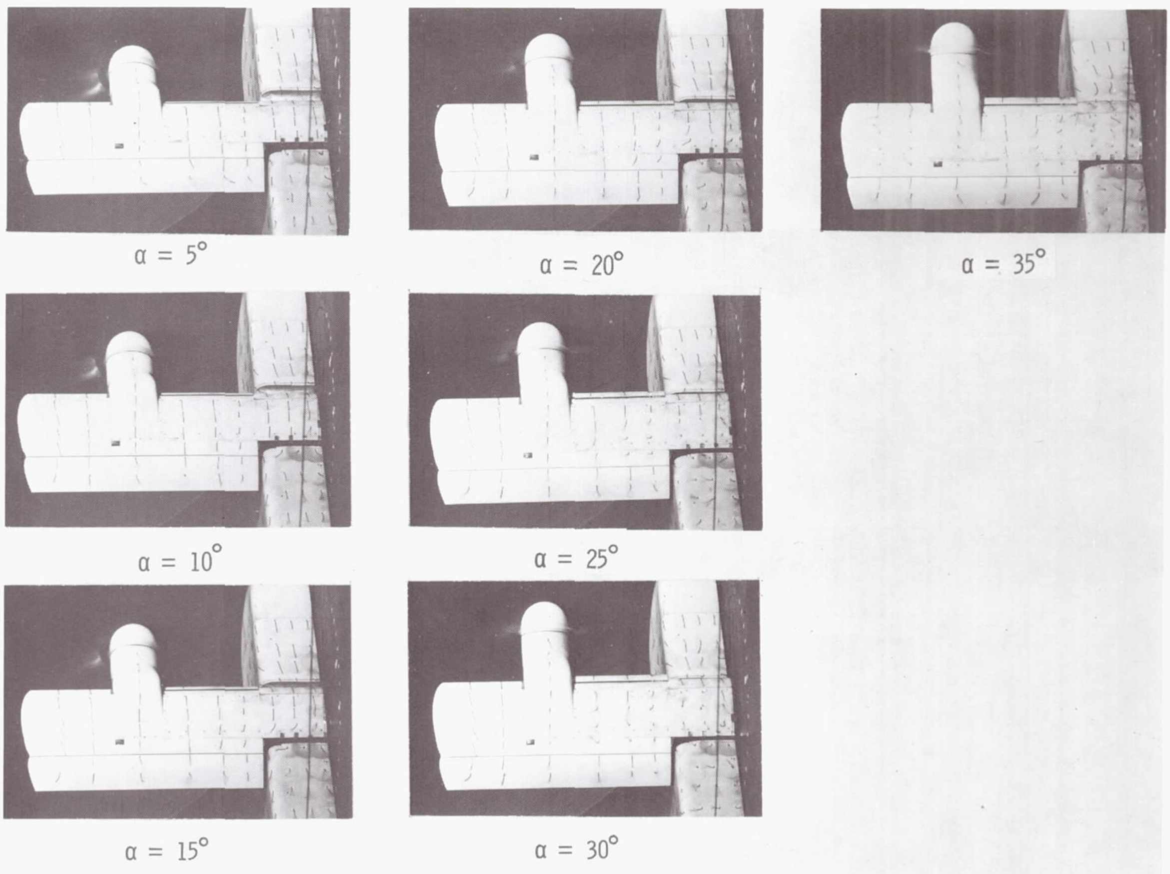

(e) Flow characteristics; $C_{T,s} = 0.30$.

Figure 28.- Concluded.

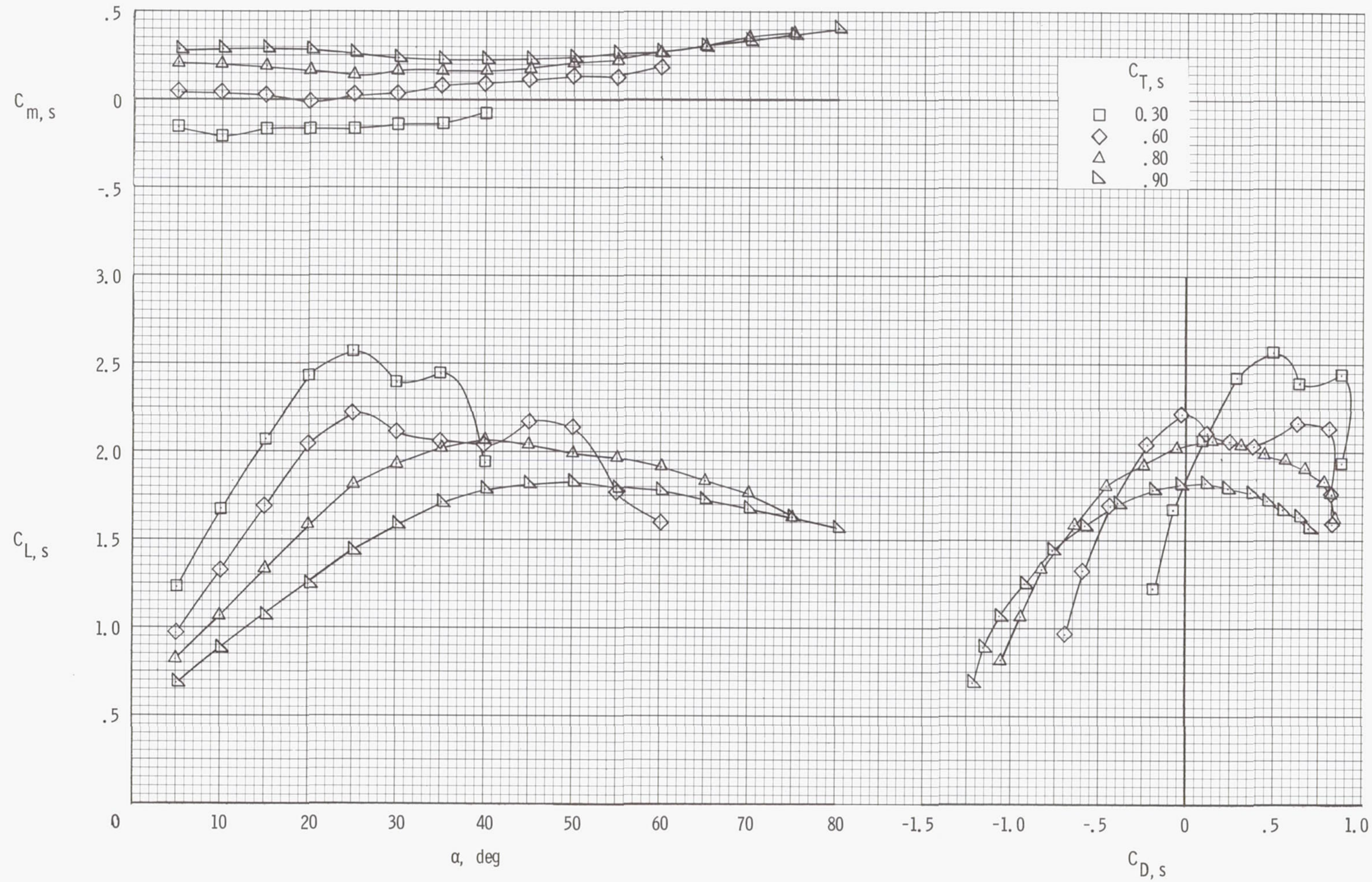

(a) Aerodynamic characteristics.

Figure 29.- Aerodynamic and flow characteristics of the wing with the propeller rotating up at the tip, inboard slat on, and $\delta_f = 40^o$.

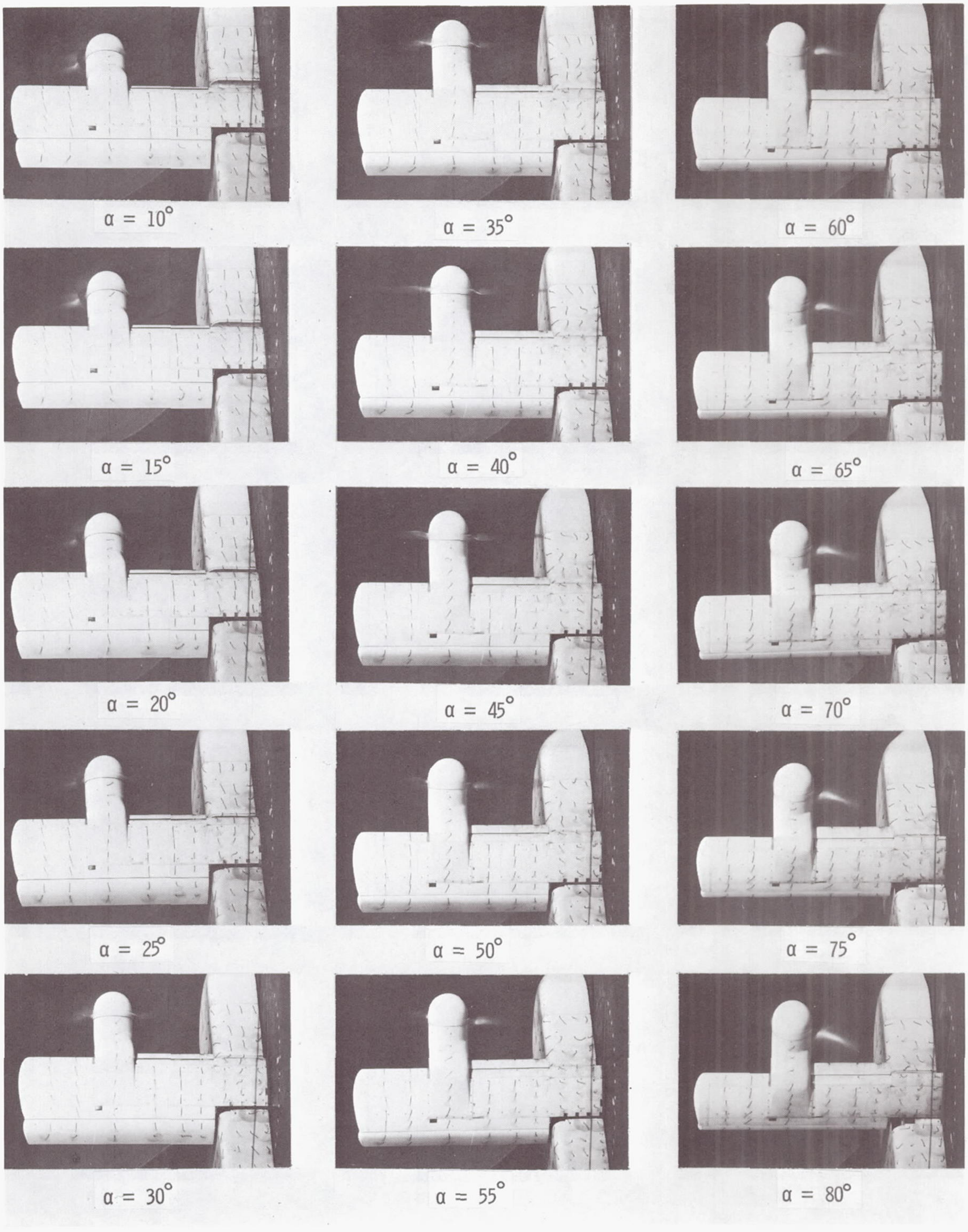

(b) Flow characteristics; $C_{T,s} = 0.90$.

Figure 29.- Continued.

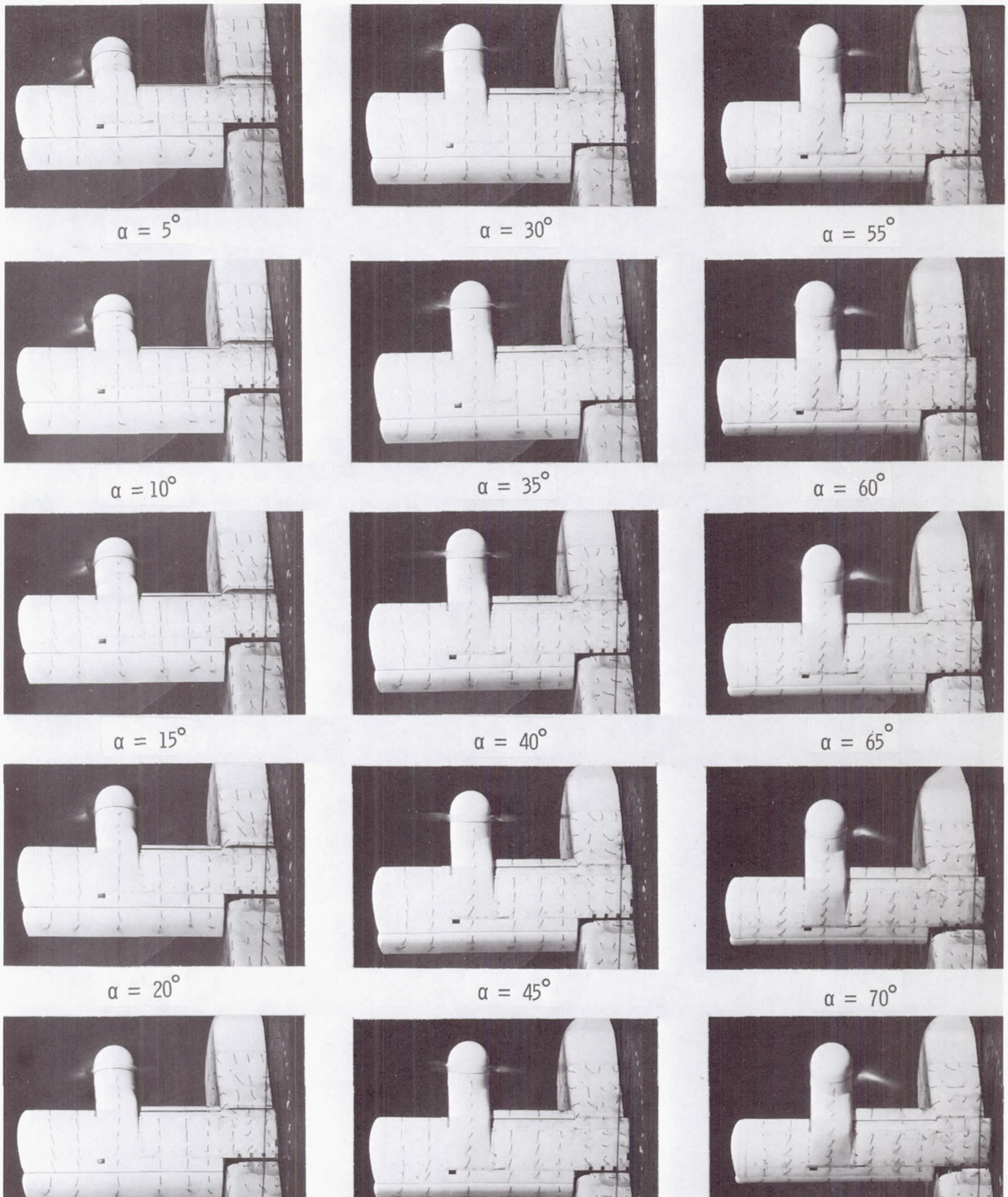

(c) Flow characteristics; $C_{T,s} = 0.80$.

Figure 29.- Continued.

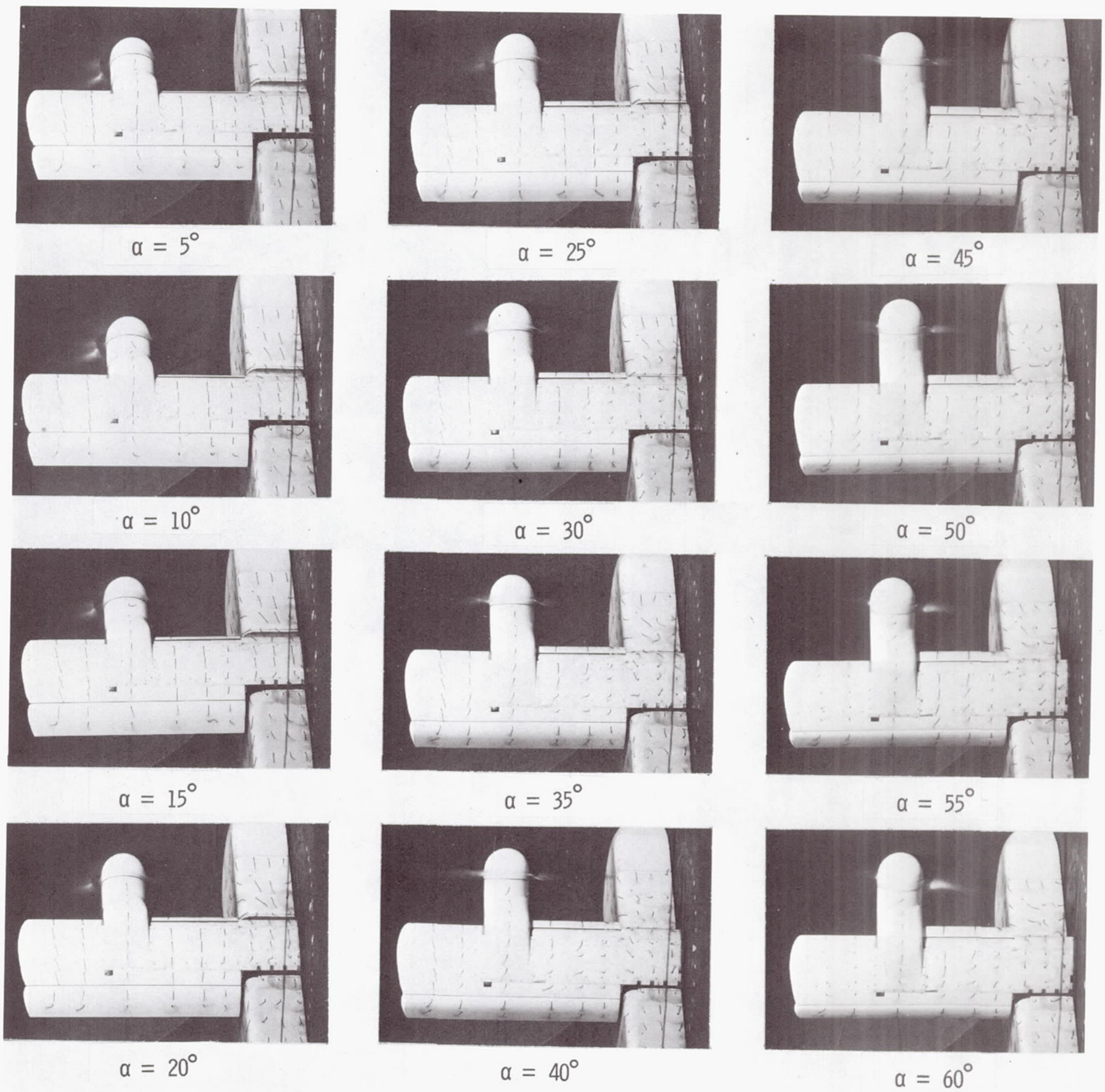

(d) Flow characteristics; $C_{T,s} = 0.60$.

Figure 29.- Continued.

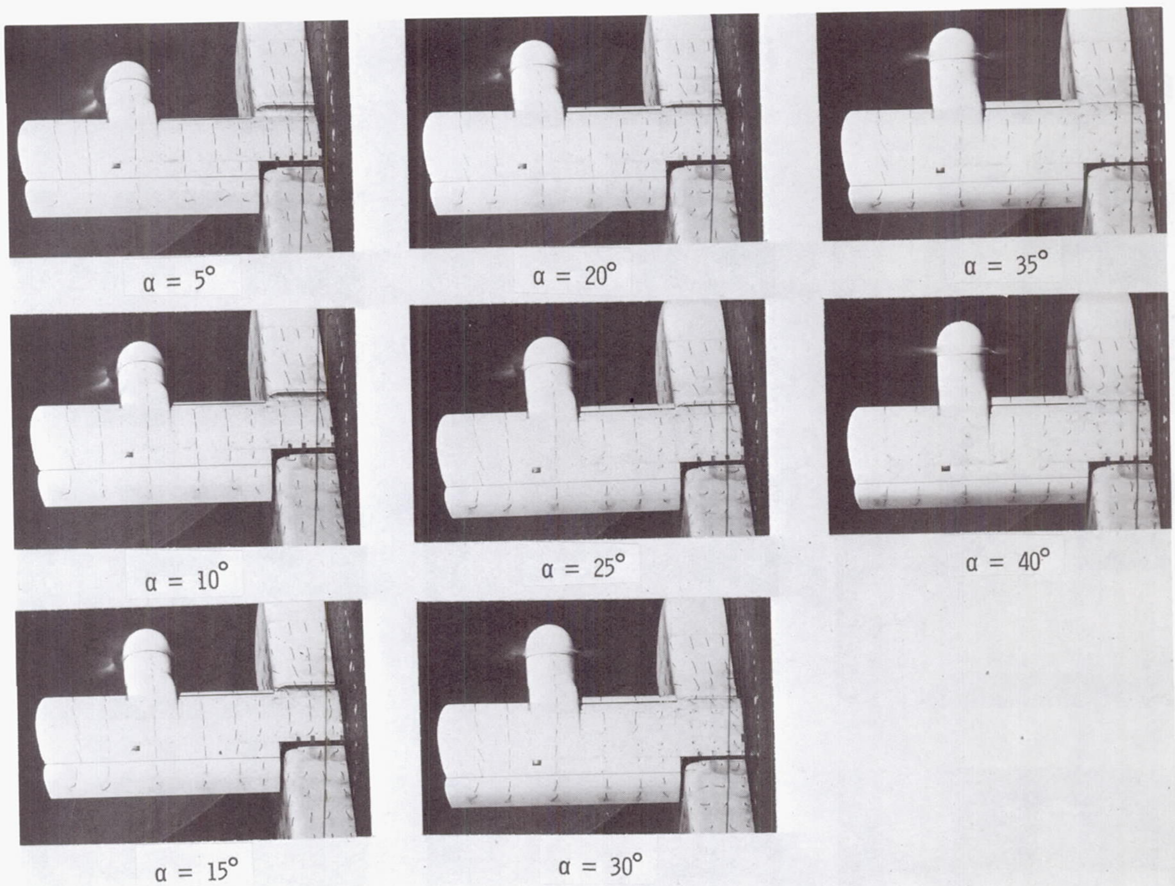

(e) Flow characteristics; $C_{T,s} = 0.30$.

Figure 29.- Concluded.

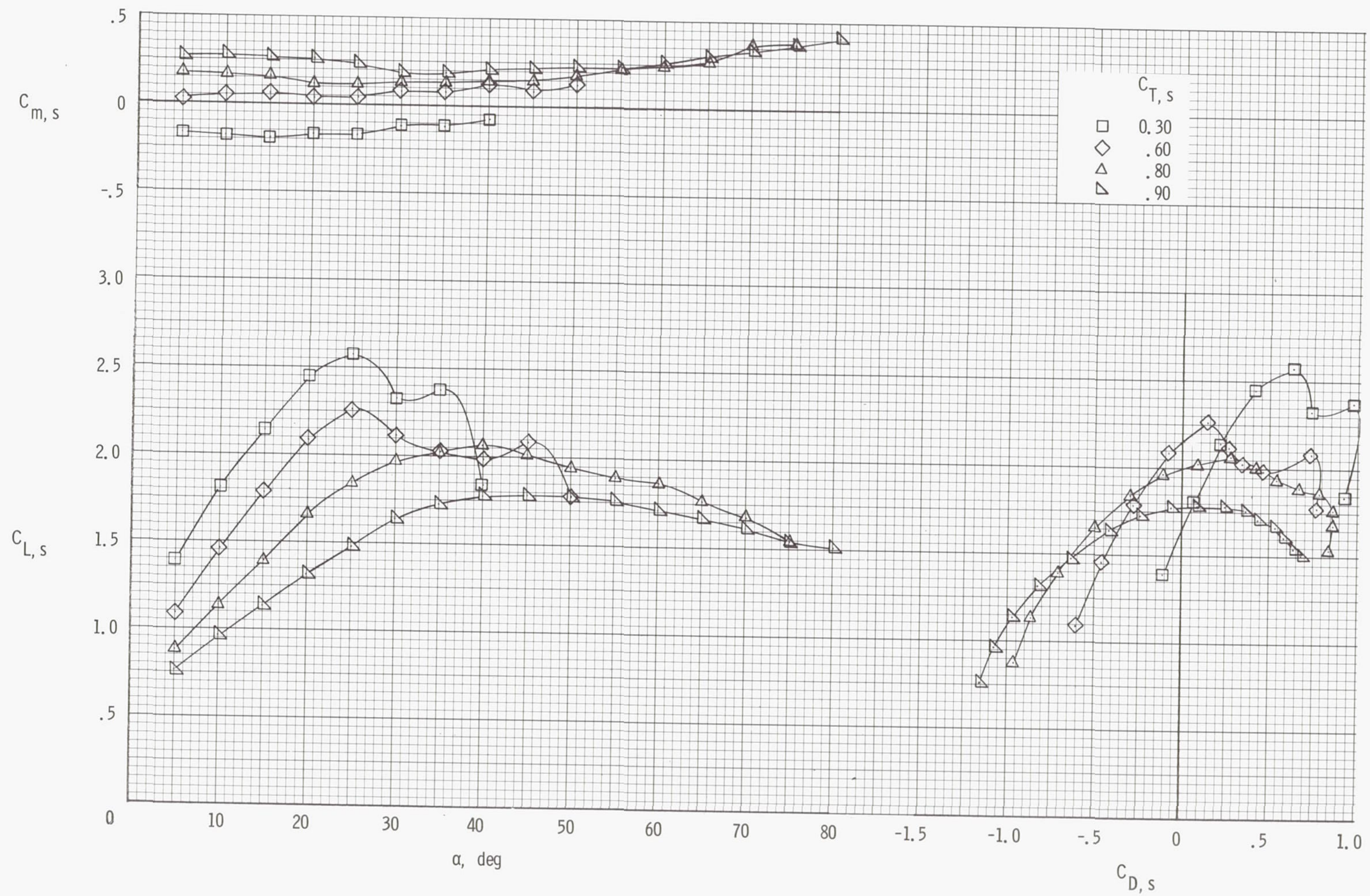

(a) Aerodynamic characteristics.

Figure 30.- Aerodynamic and flow characteristics of the wing with the propeller rotating up at the tip, inboard slat on, and $\delta_f = 60^0$.

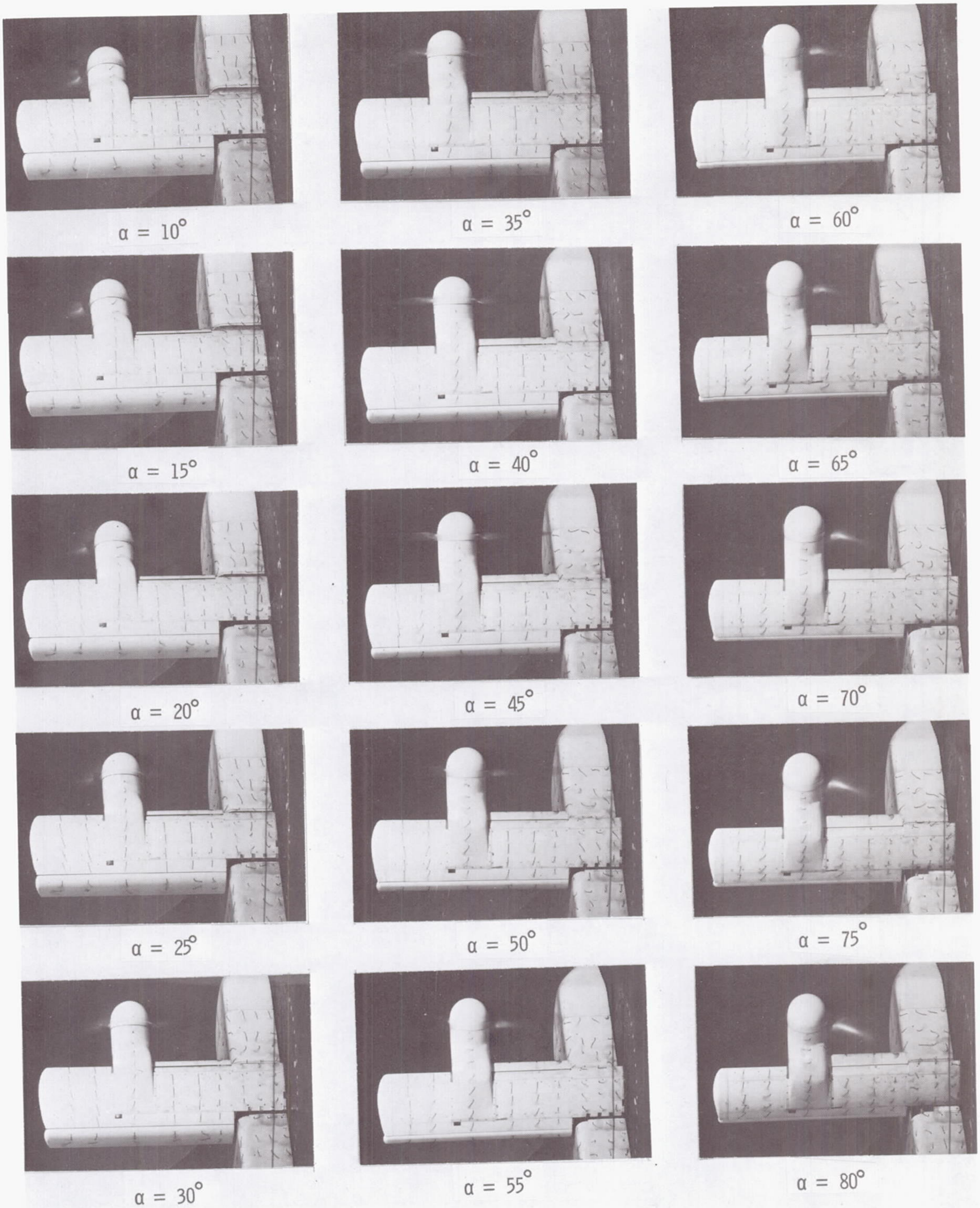

(b) Flow characteristics; $C_{T,s} = 0.90$.

Figure 30.- Continued.

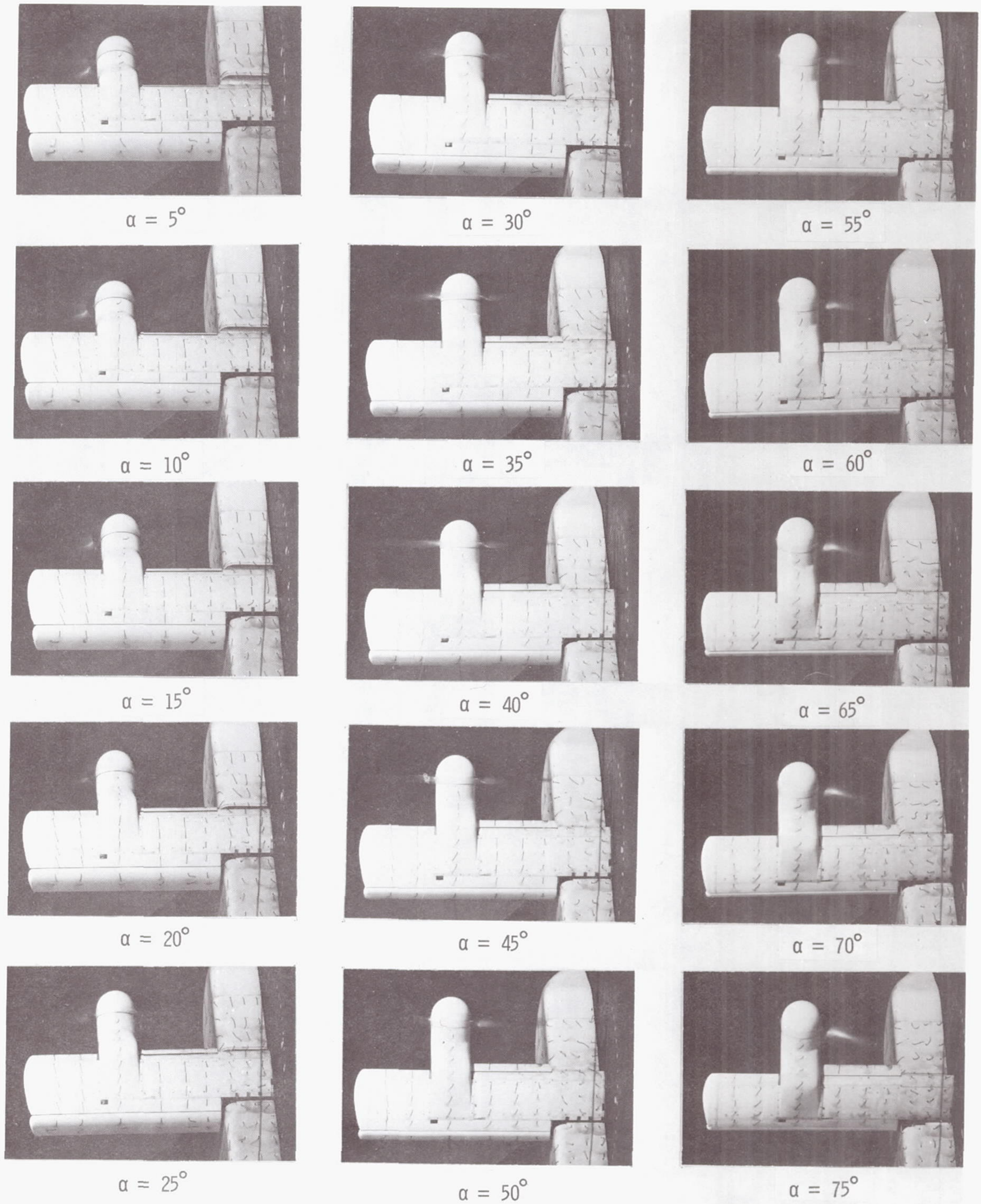

(c) Flow characteristics; $C_{T,s} = 0.80$.

Figure 30.- Continued.

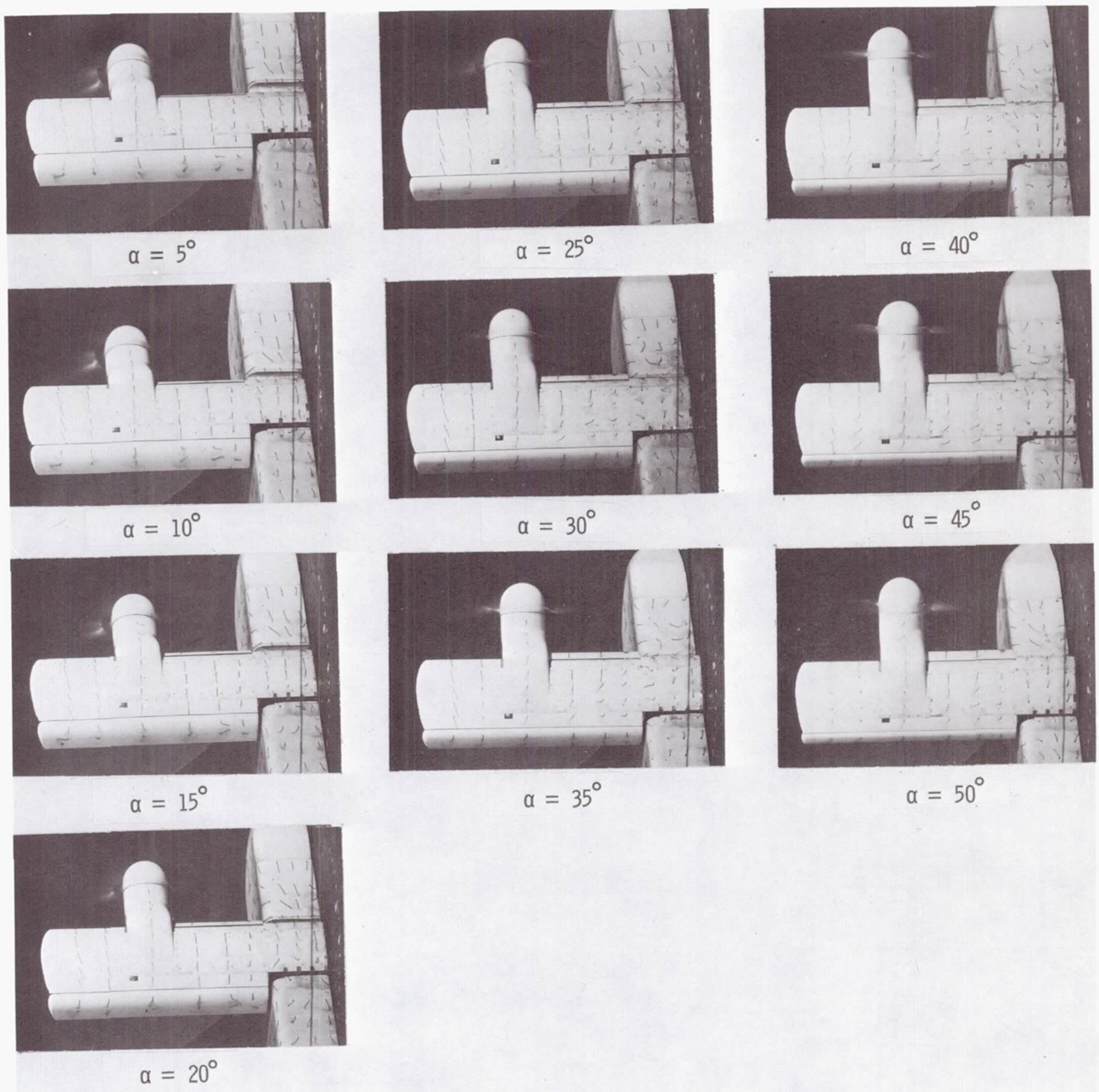

(d) Flow characteristics; $C_{T,s} = 0.60$.

Figure 30.- Continued.

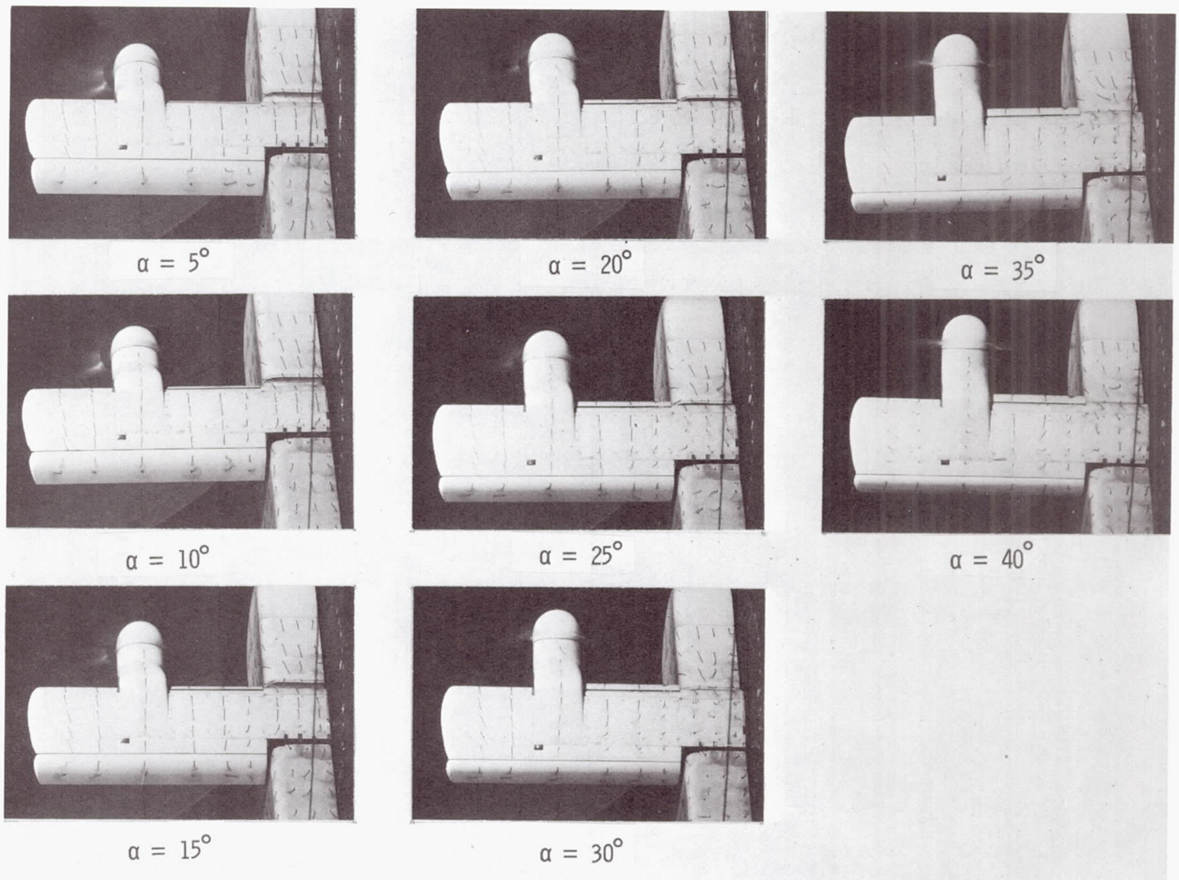

(e) Flow characteristics; $C_{T,s} = 0.30$.

Figure 30.- Concluded.

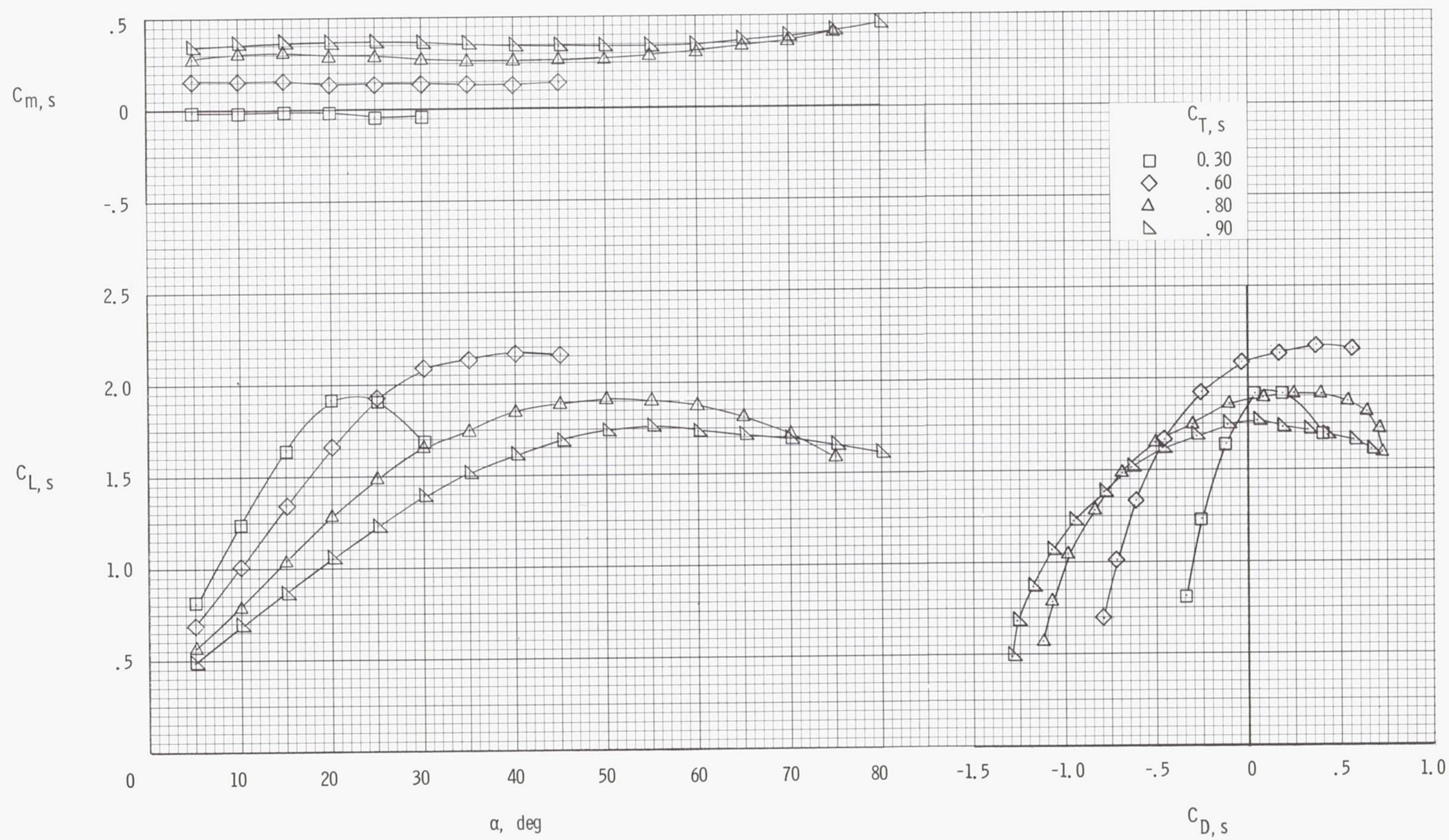

(a) Aerodynamic characteristics.

Figure 31.- Aerodynamic and flow characteristics of the wing with the propeller rotating up at the tip, inboard slat on, fences on, and $\delta_f = 20^0$.

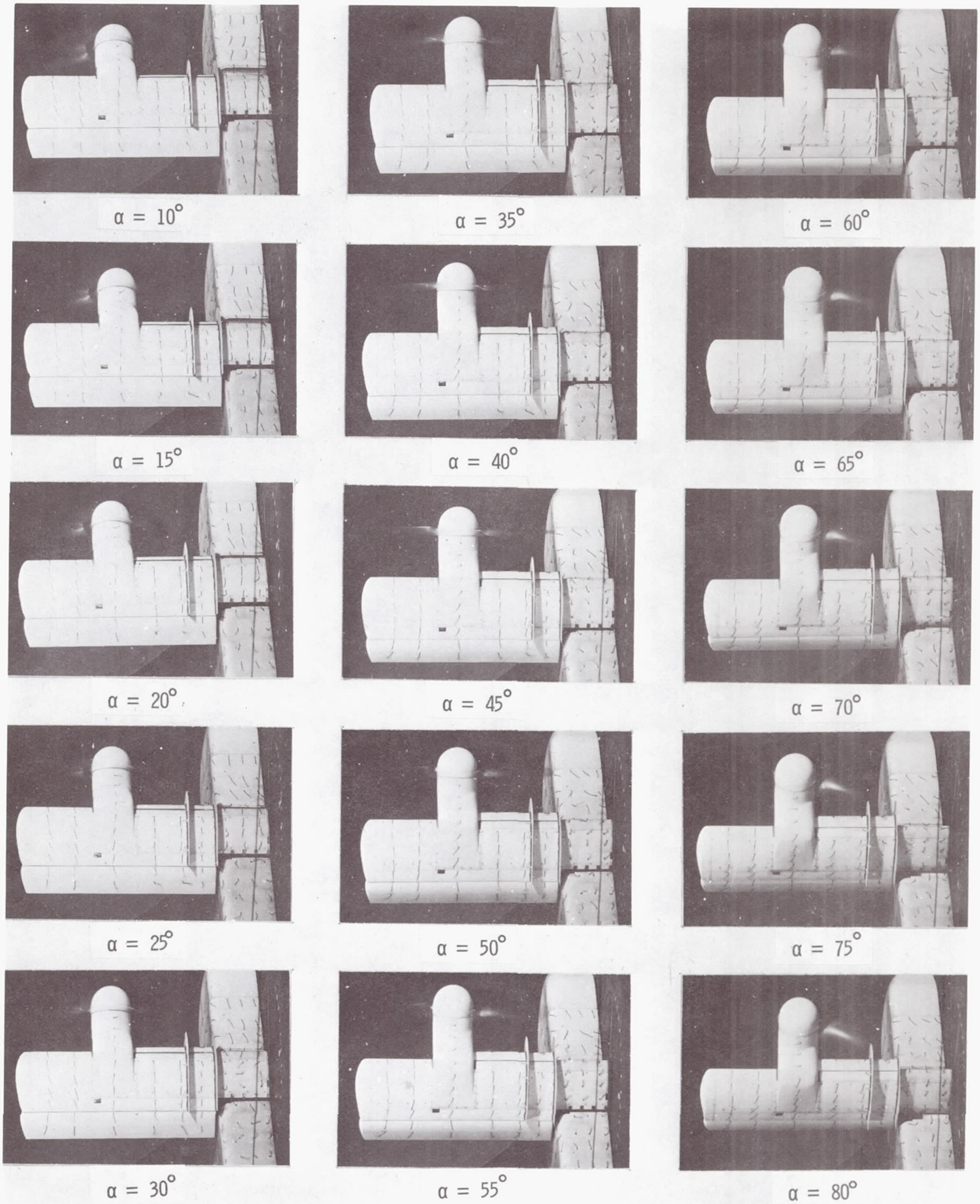

(b) Flow characteristics; $C_{T,s} = 0.90$.

Figure 31.- Continued.

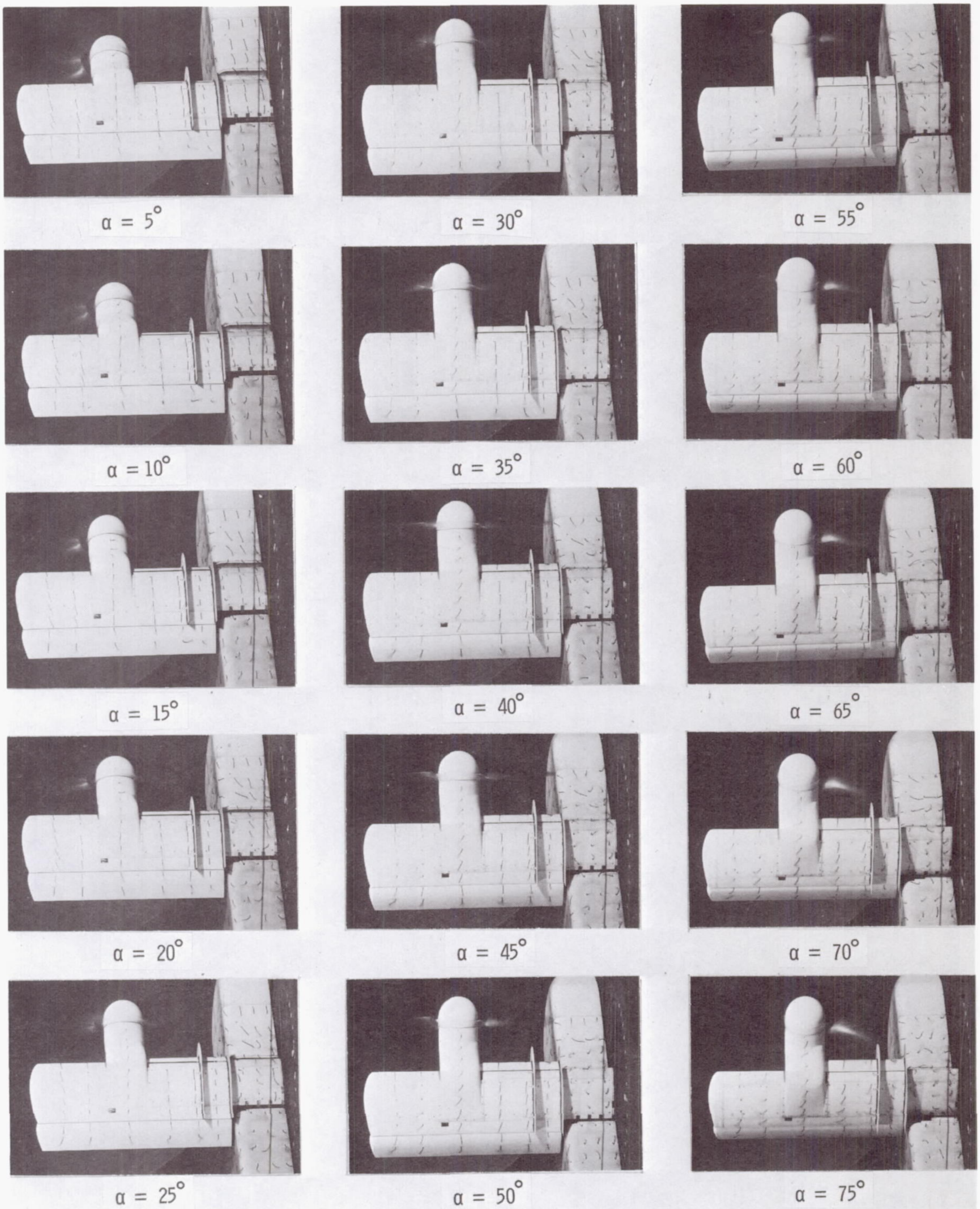

(c) Flow characteristics; $C_{T,s} = 0.80$.

Figure 31.- Continued.

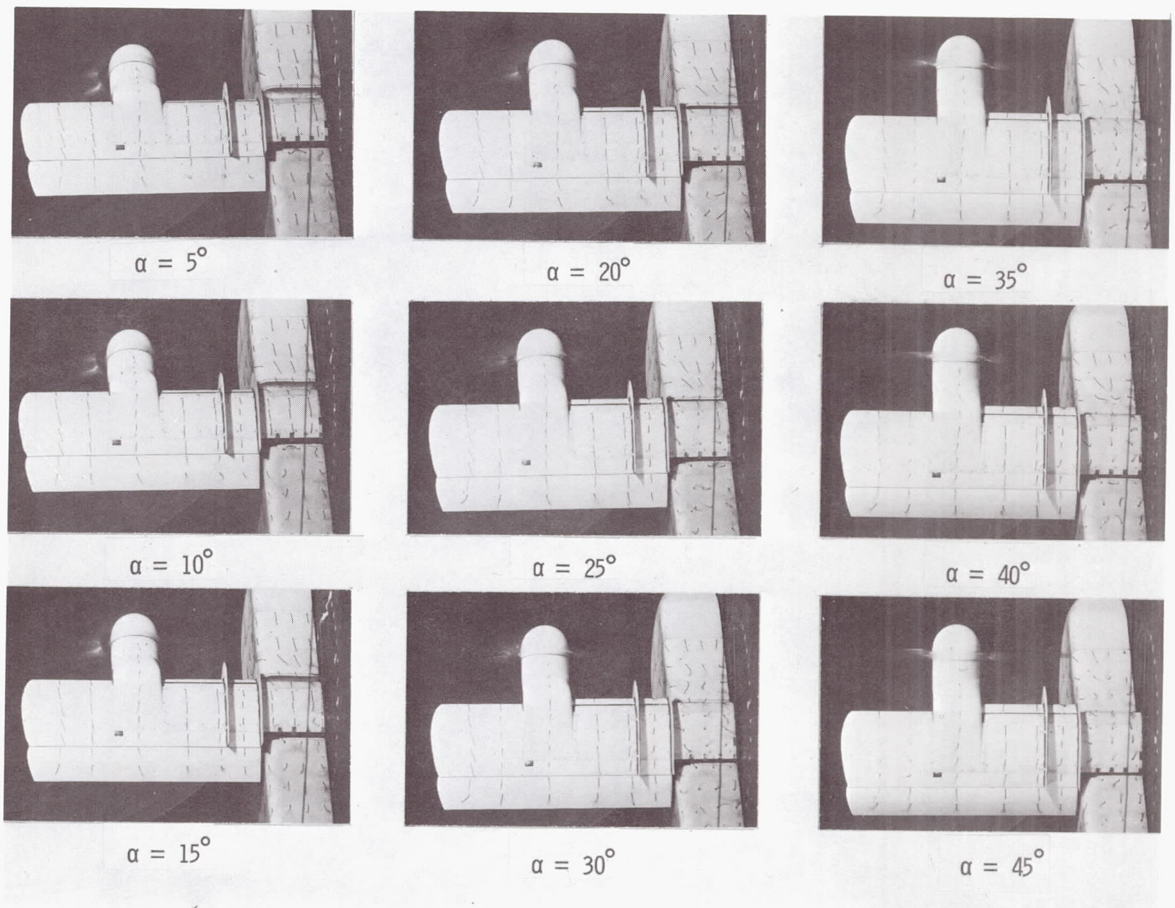

(d) Flow characteristics; $C_{T,s} = 0.60$.

Figure 31.- Continued.

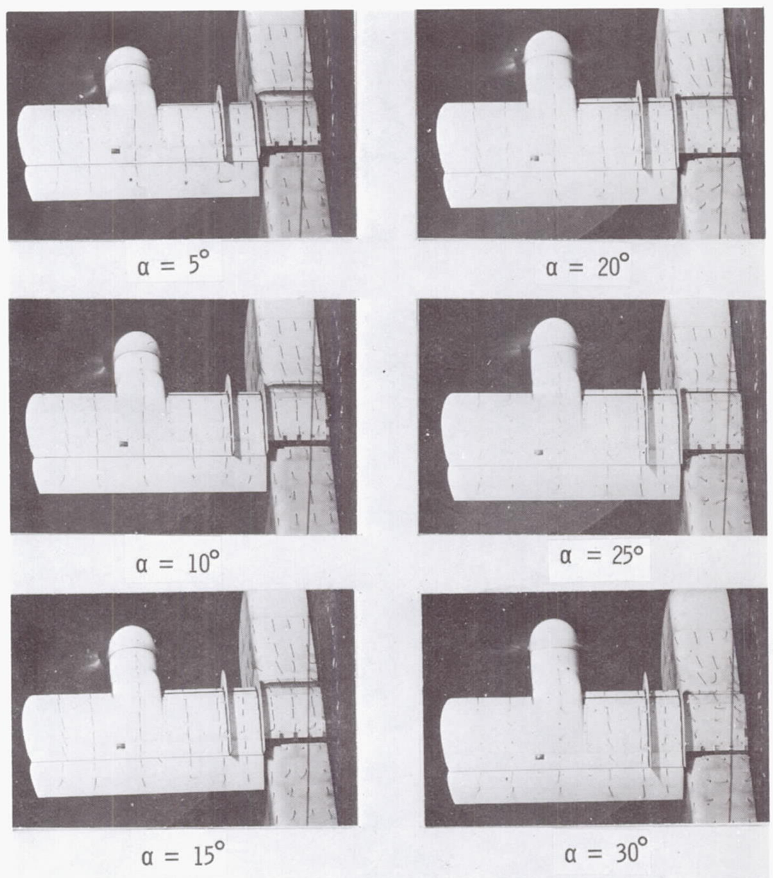

(e) Flow characteristics; $C_{T,s} = 0.30$.

Figure 31.- Concluded.

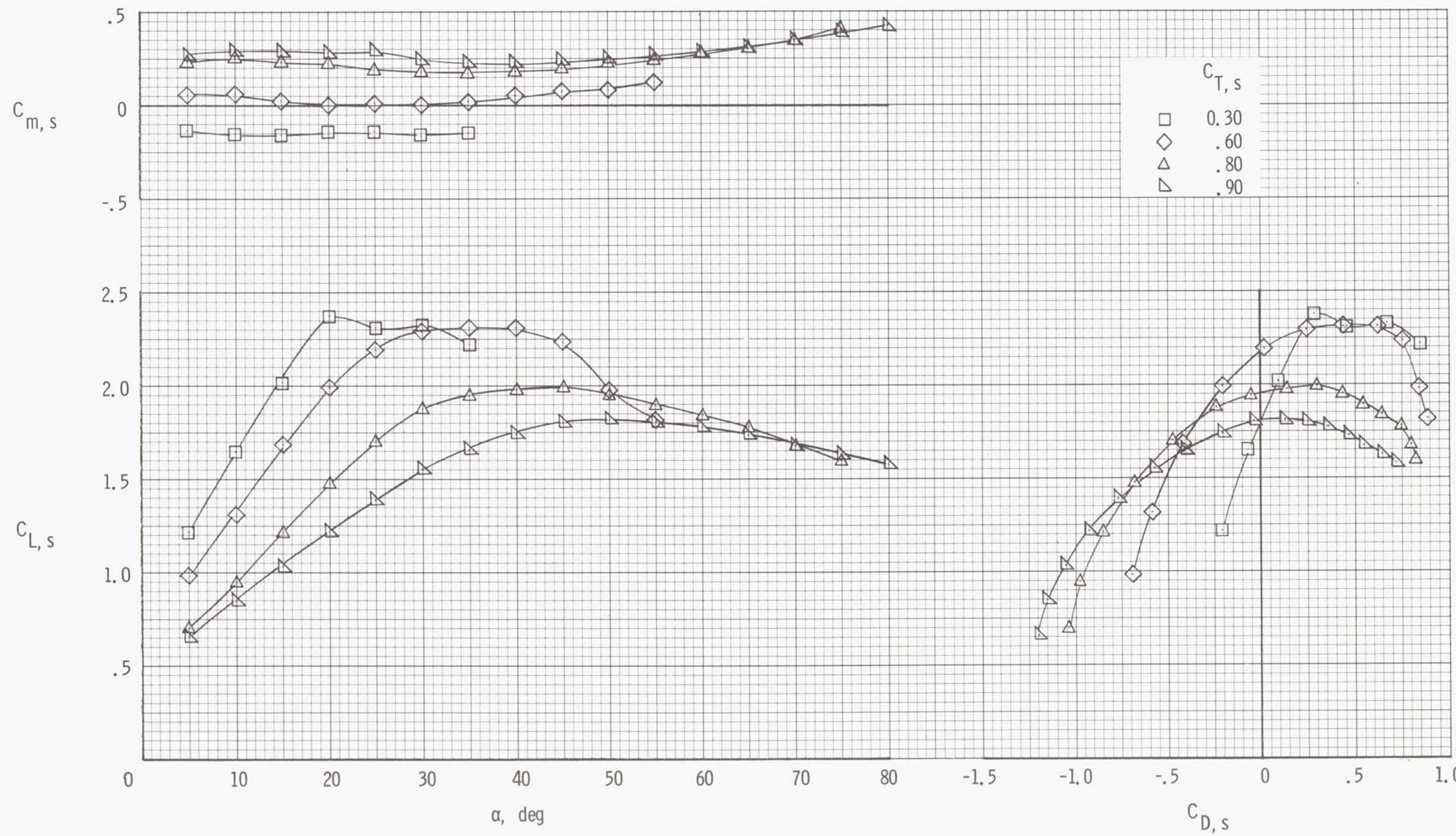

(a) Aerodynamic characteristics.

Figure 32.- Aerodynamic and flow characteristics of the wing with the propeller rotating up at the tip, inboard slat on, fences on, **and** $\delta_f = 40^0$.

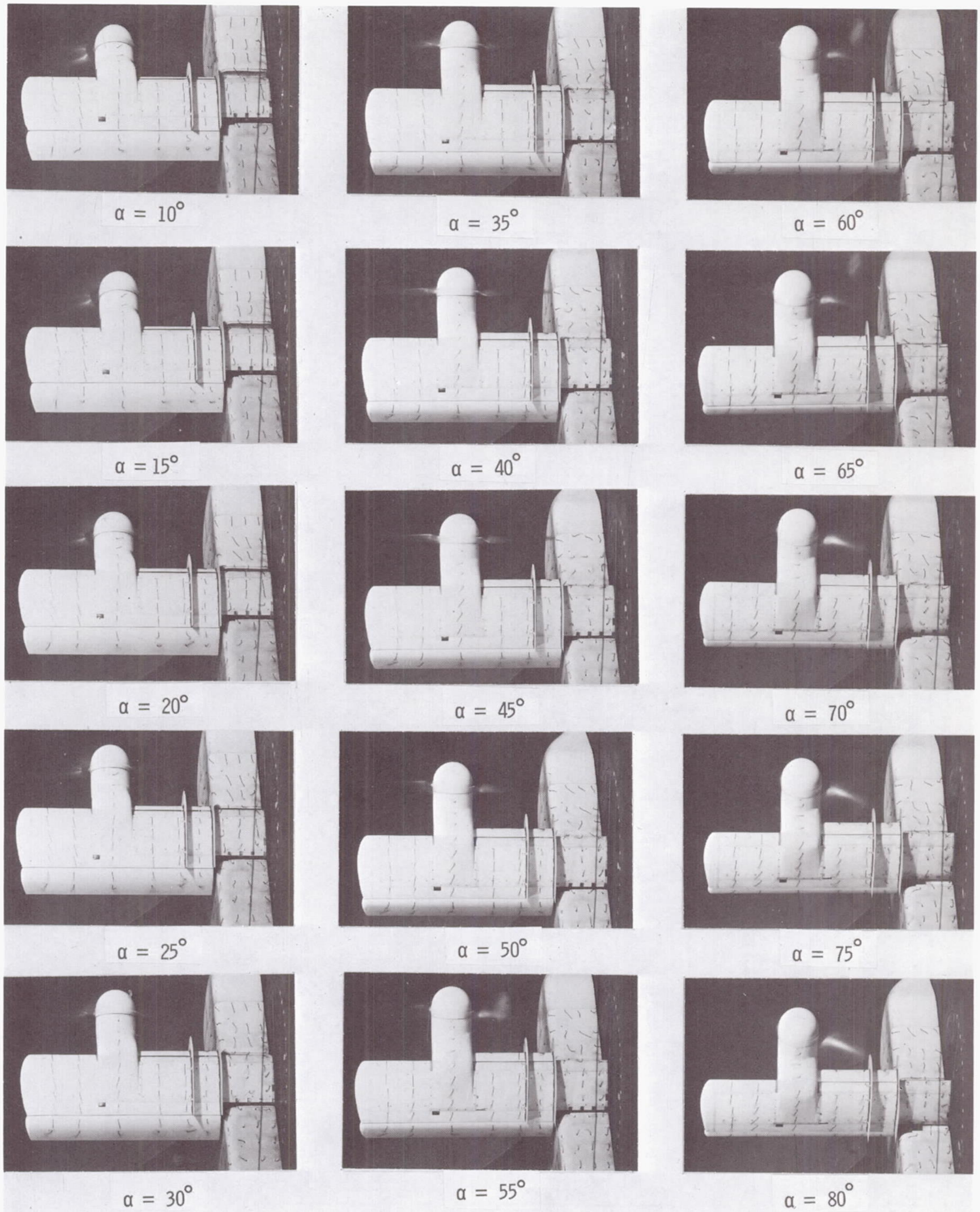

(b) Flow characteristics; $C_{T,s} = 0.90$.

Figure 32.- Continued.

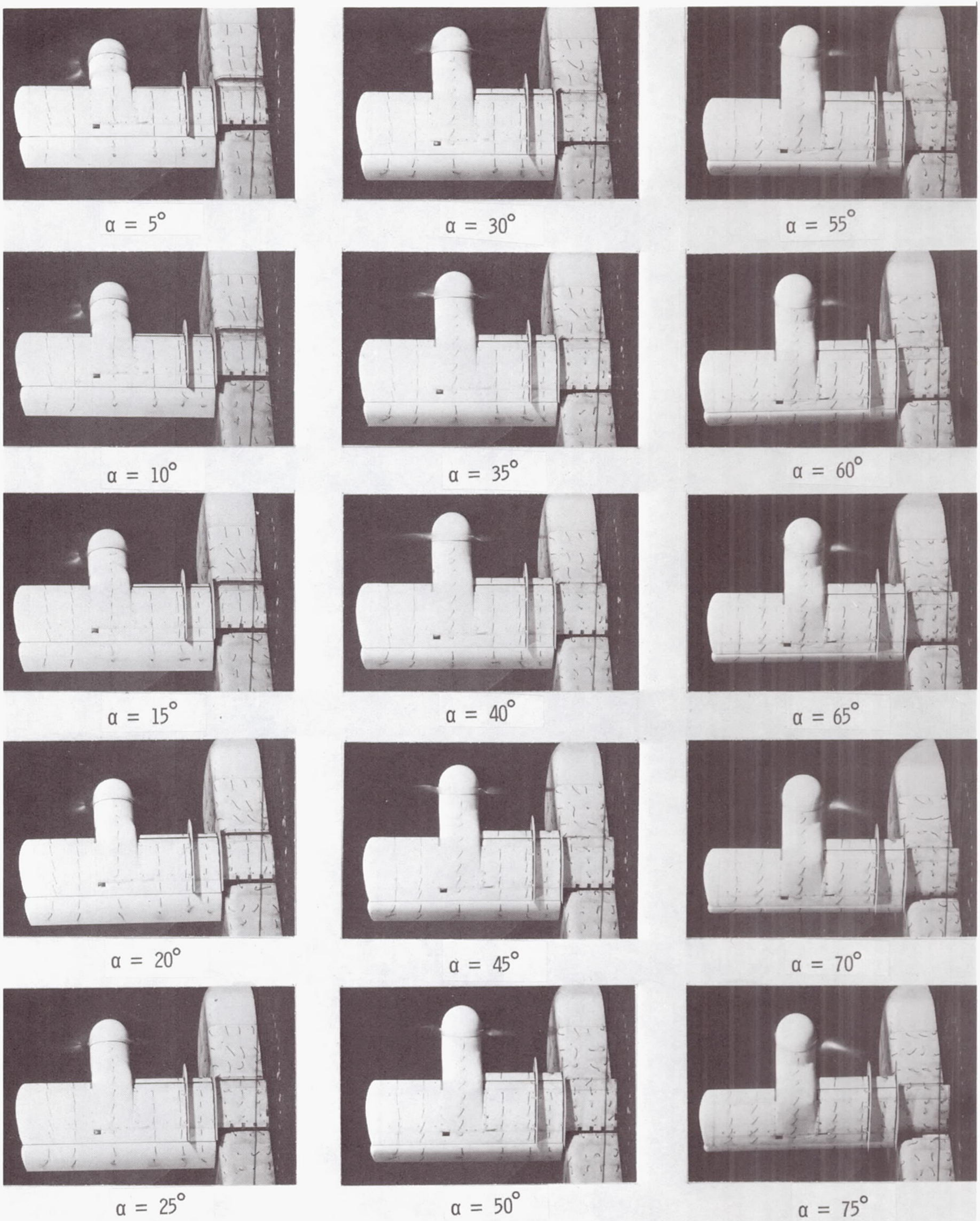

(c) Flow characteristics; $C_{T,s} = 0.80$.

Figure 32.- Continued.

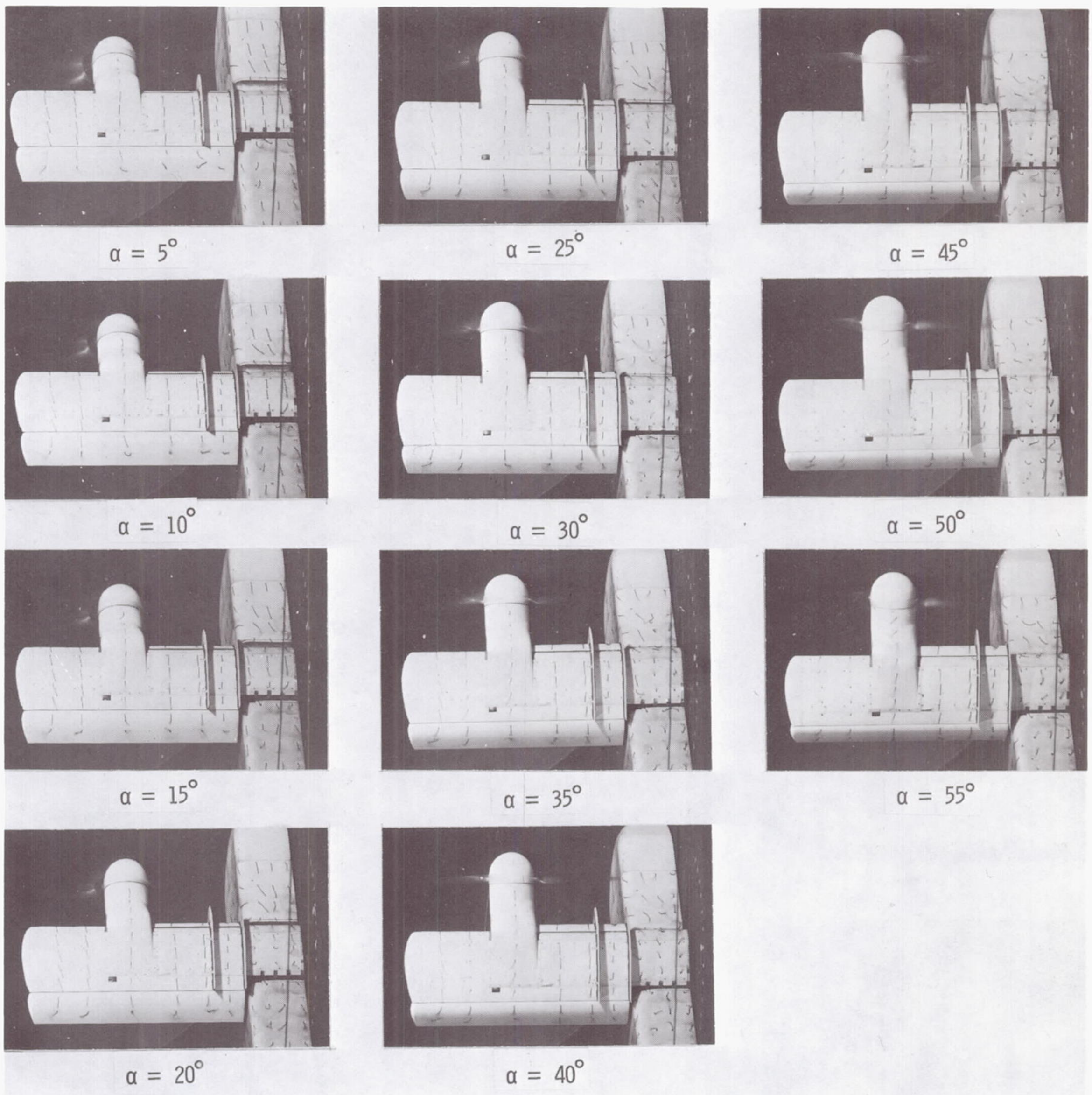

(d) Flow characteristics; $C_{T,s} = 0.60$.

Figure 32.- Continued.

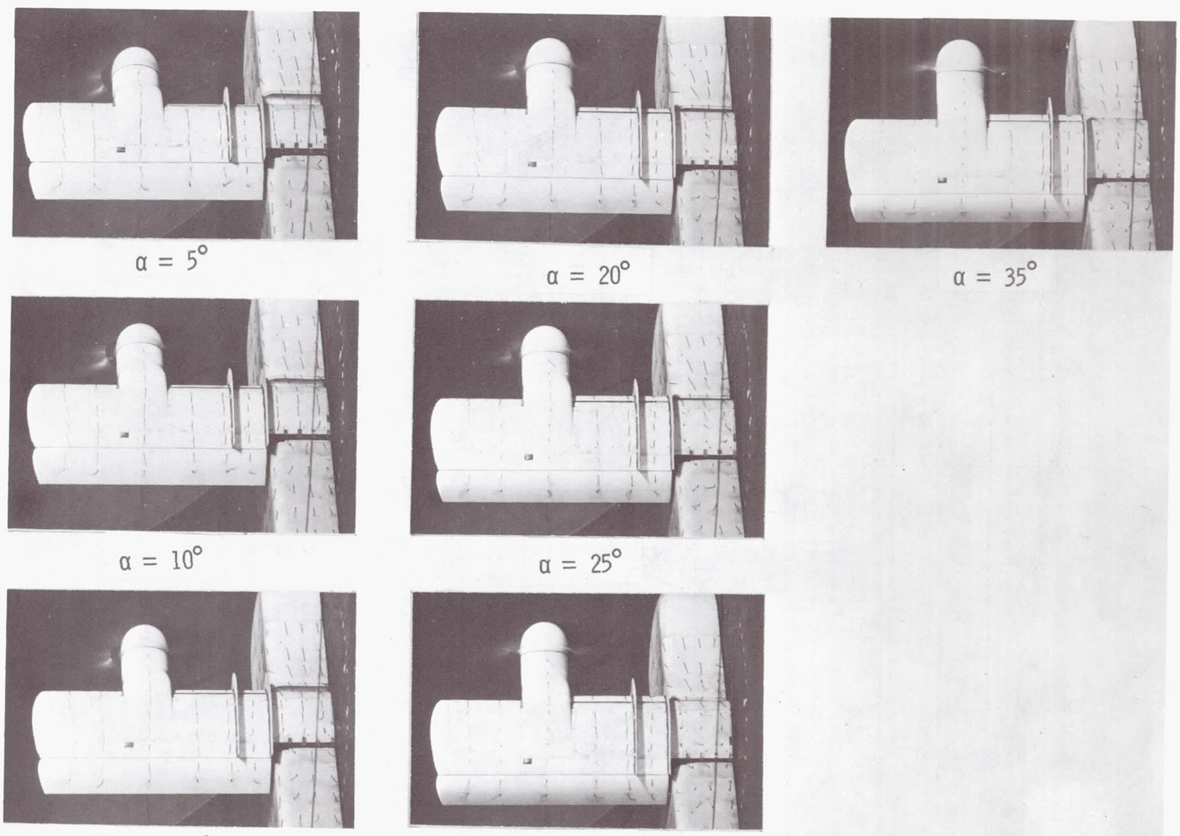

$\alpha = 5^\circ$ $\alpha = 20^\circ$ $\alpha = 35^\circ$

$\alpha = 10^\circ$ $\alpha = 25^\circ$

$\alpha = 15^\circ$ $\alpha = 30^\circ$

(e) Flow characteristics; $C_{T,s} = 0.30$.

Figure 32.- Concluded.

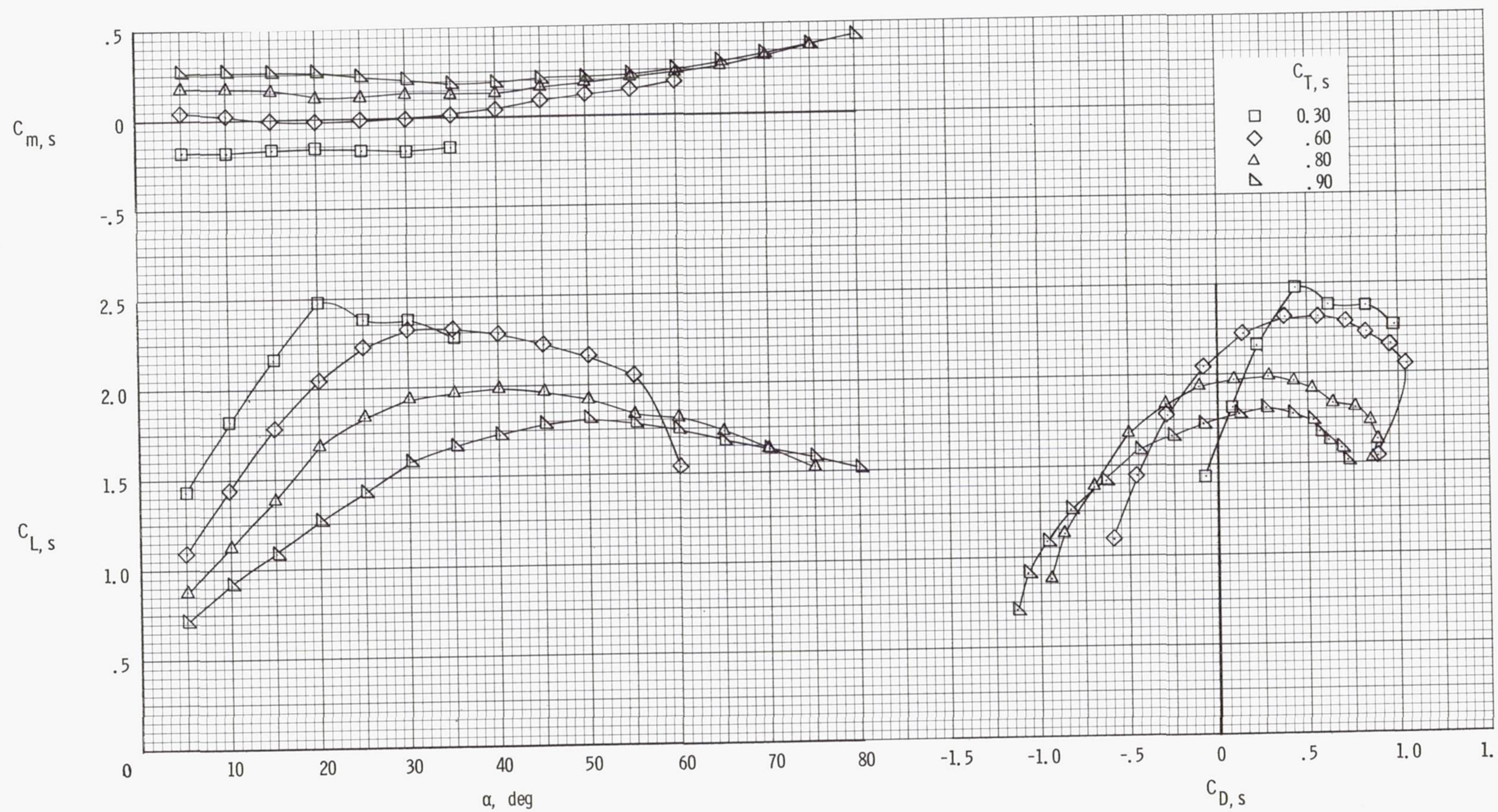

(a) Aerodynamic characteristics.

Figure 33.- Aerodynamic and flow characteristics of the wing with the propeller rotating up at the tip, inboard slat on, fences on, and $\delta_f = 60^{\circ}$.

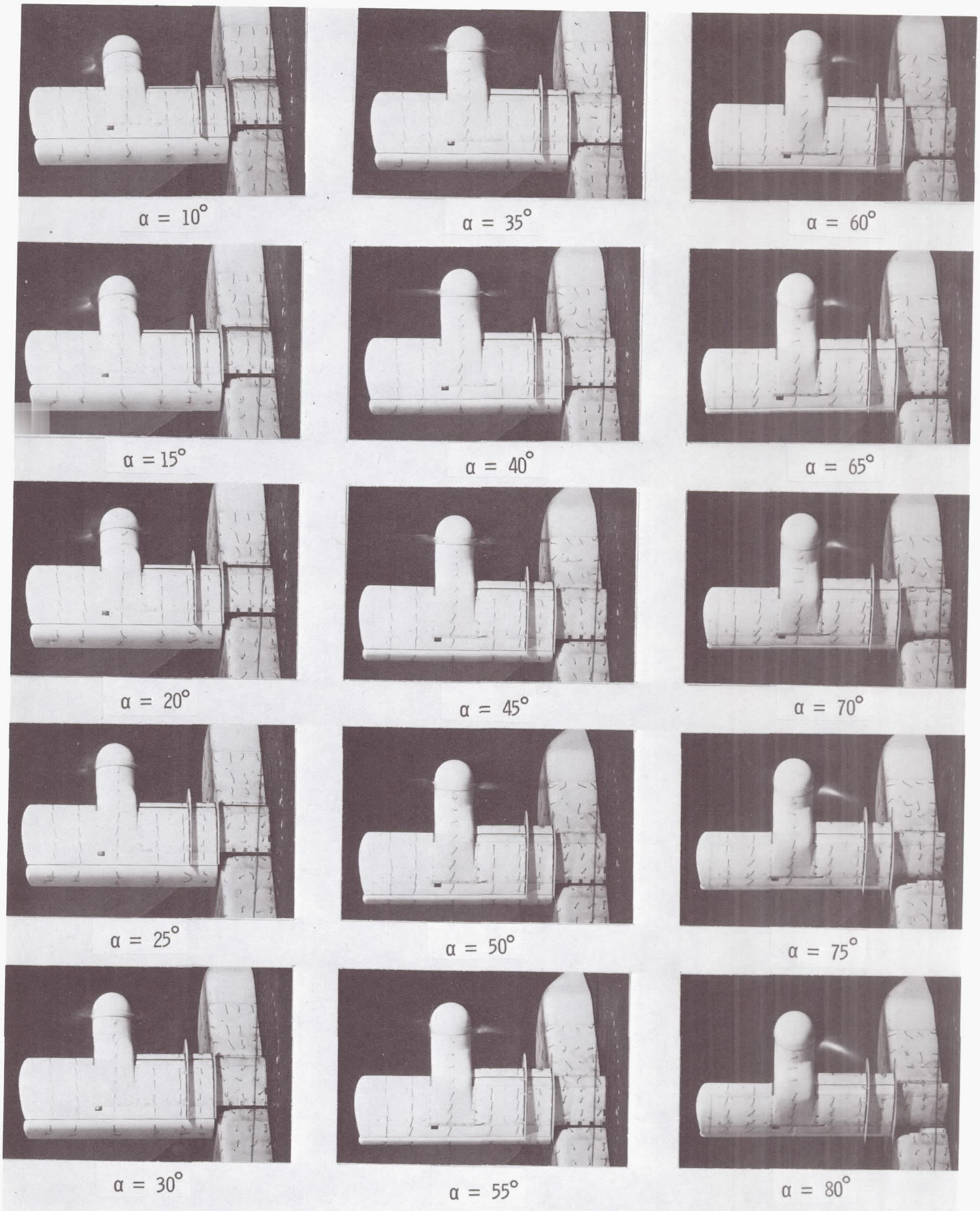

(b) Flow characteristics; $C_{T,s} = 0.90$.

Figure 33.- Continued.

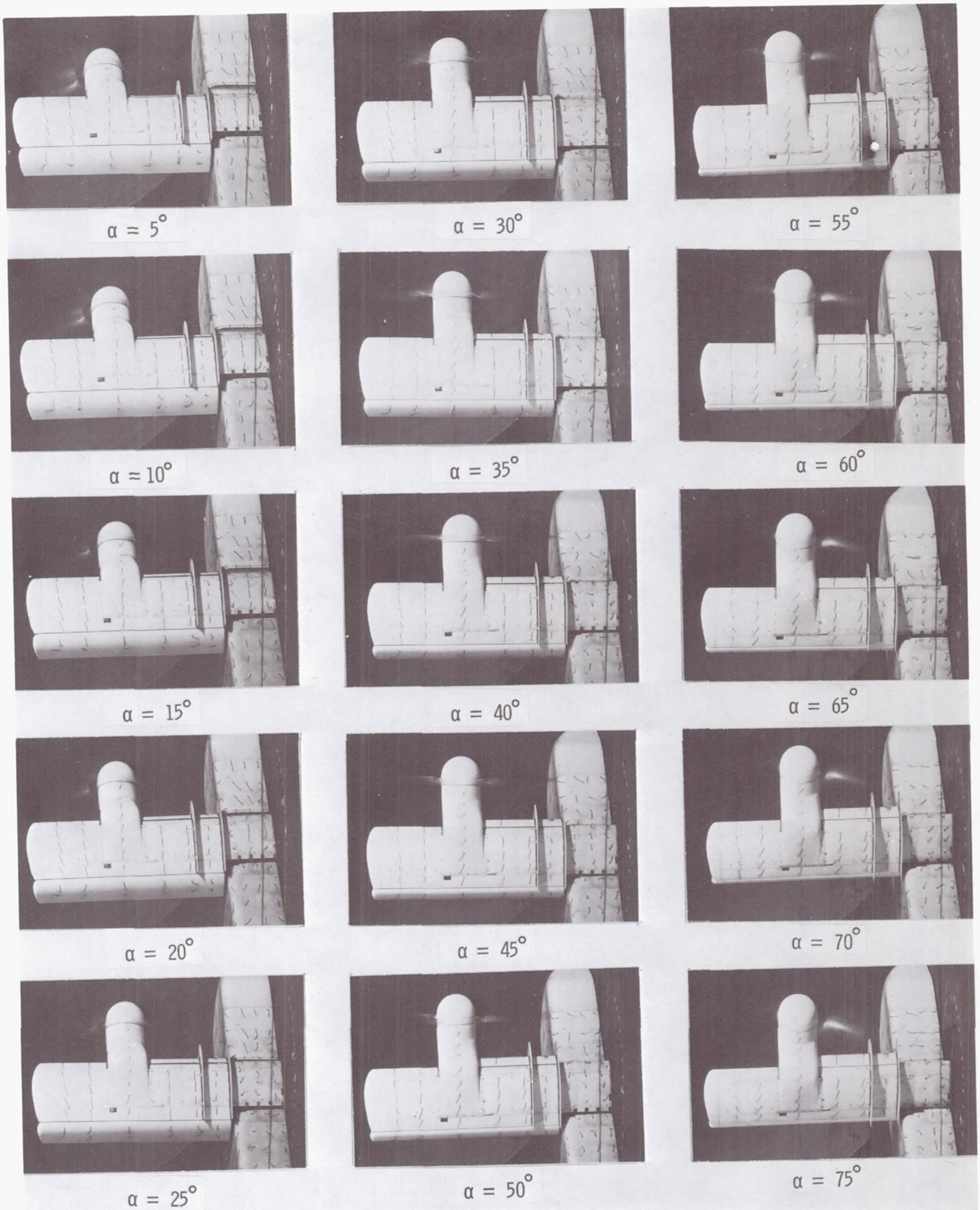

(c) Flow characteristics; $C_{T,s} = 0.80$.

Figure 33.- Continued.

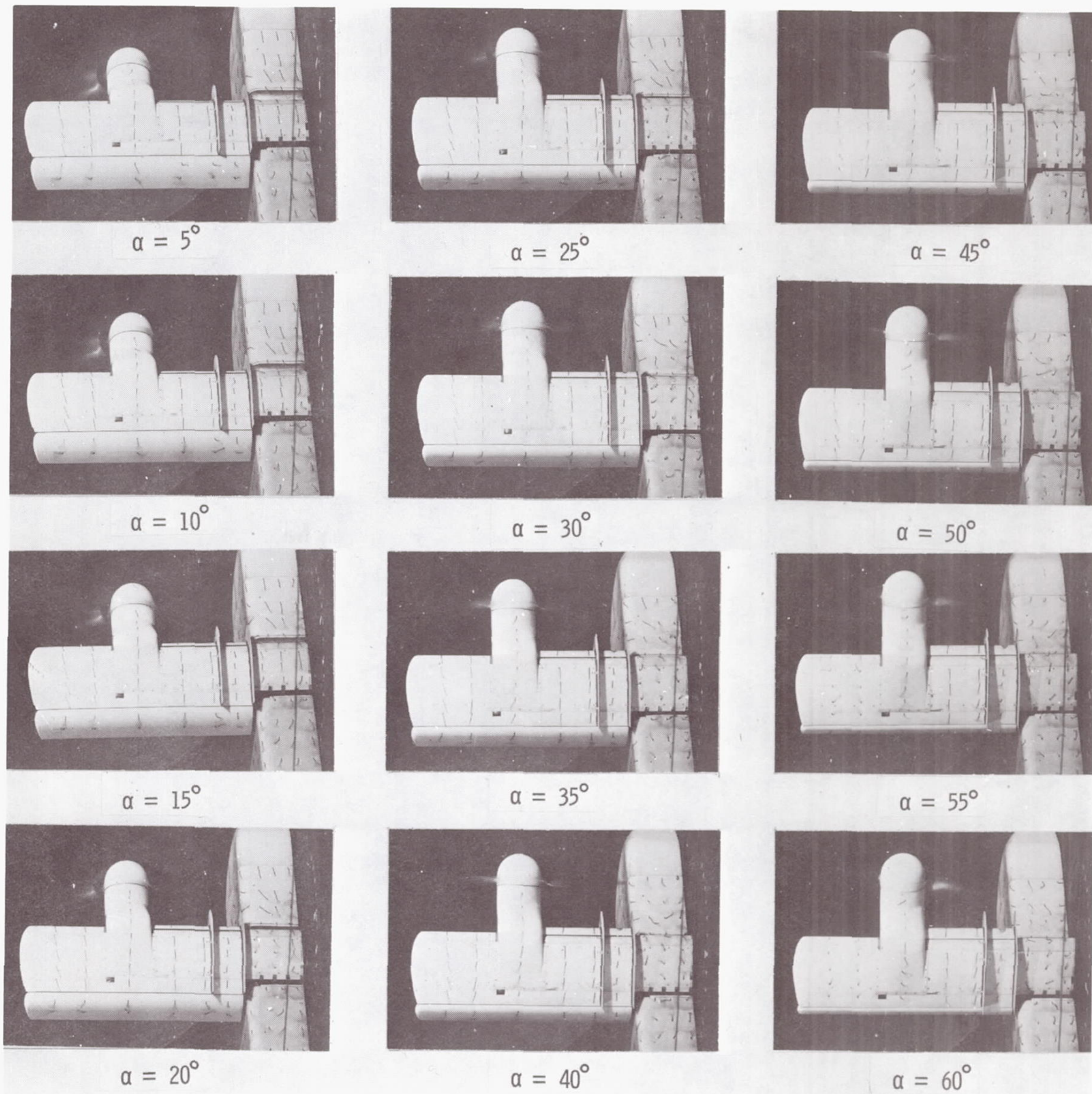

(d) Flow characteristics; $C_{T,s} = 0.60$.

Figure 33.- Continued.

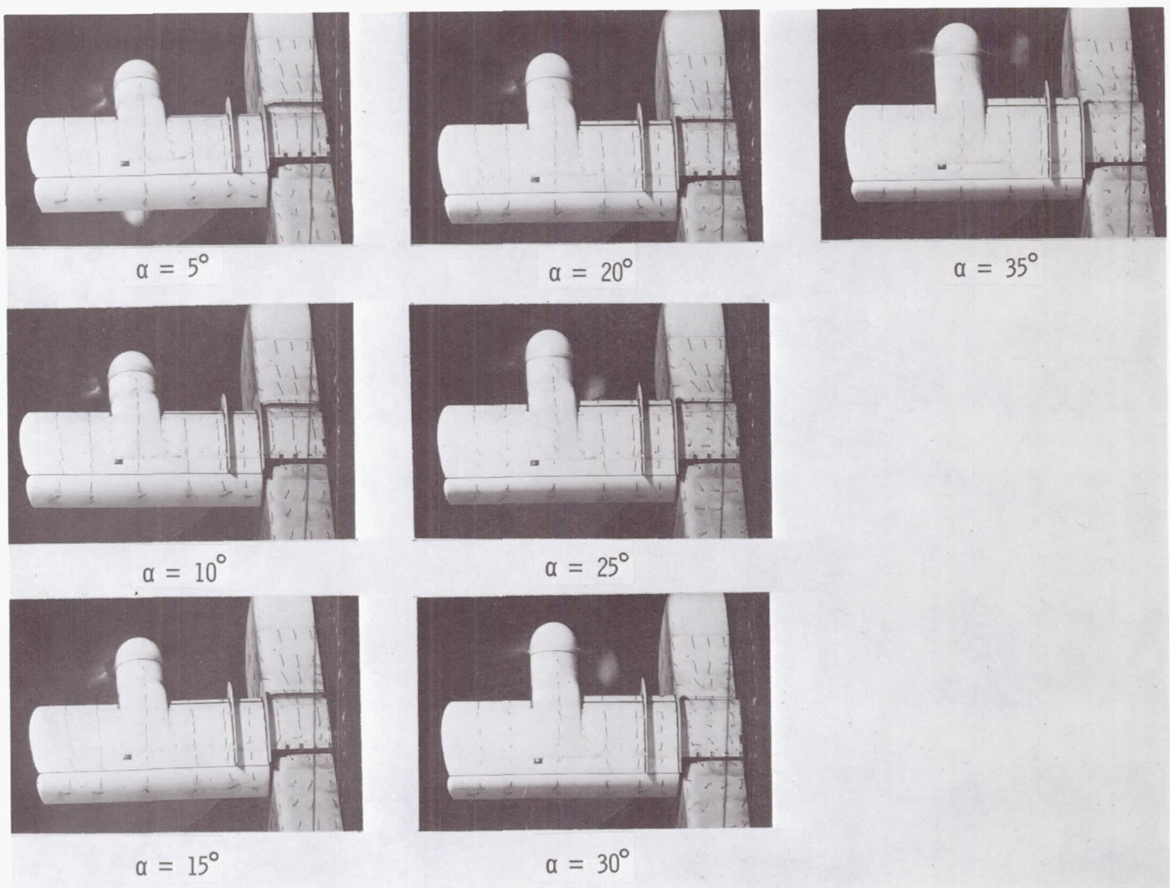

(e) Flow characteristics; $C_{T,s} = 0.30$.

Figure 33.- Concluded.

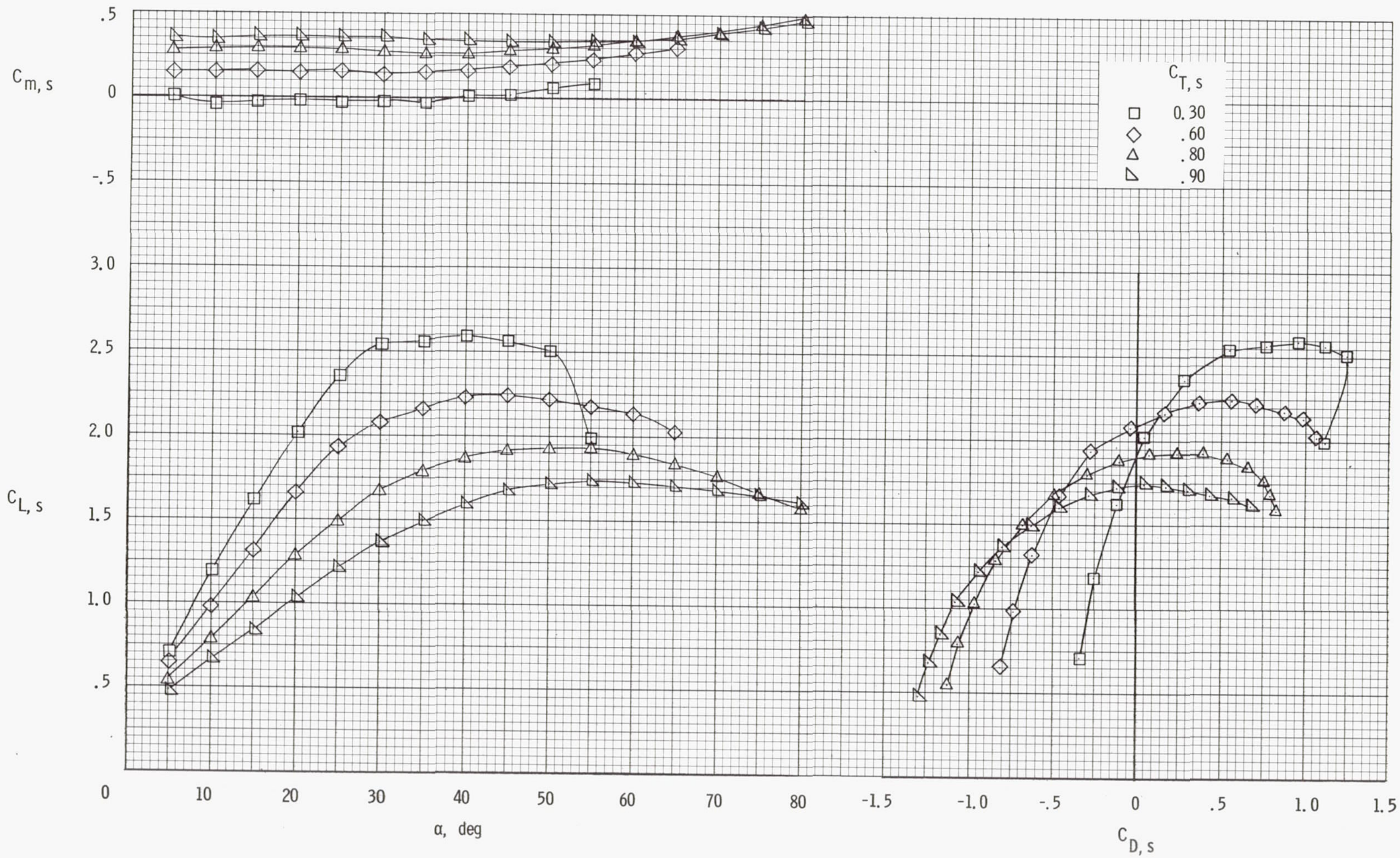

(a) Aerodynamic characteristics.

Figure 34.- Aerodynamic and flow characteristics of the wing with the propeller rotating up at the tip, full-span slat on, fences on, and $\delta_f = 20^0$.

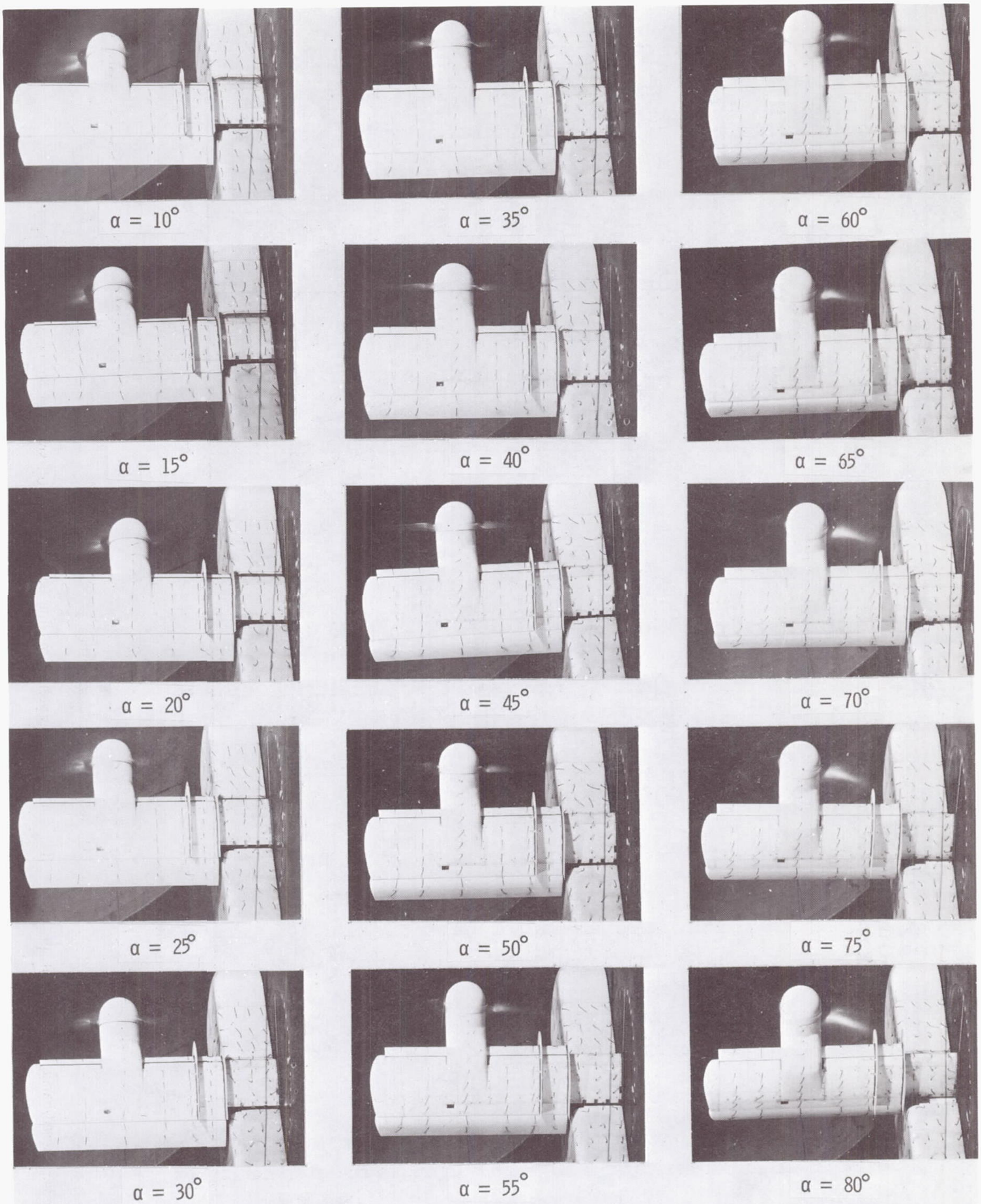

(b) Flow characteristics; $C_{T,s} = 0.90$.

Figure 34.- Continued.

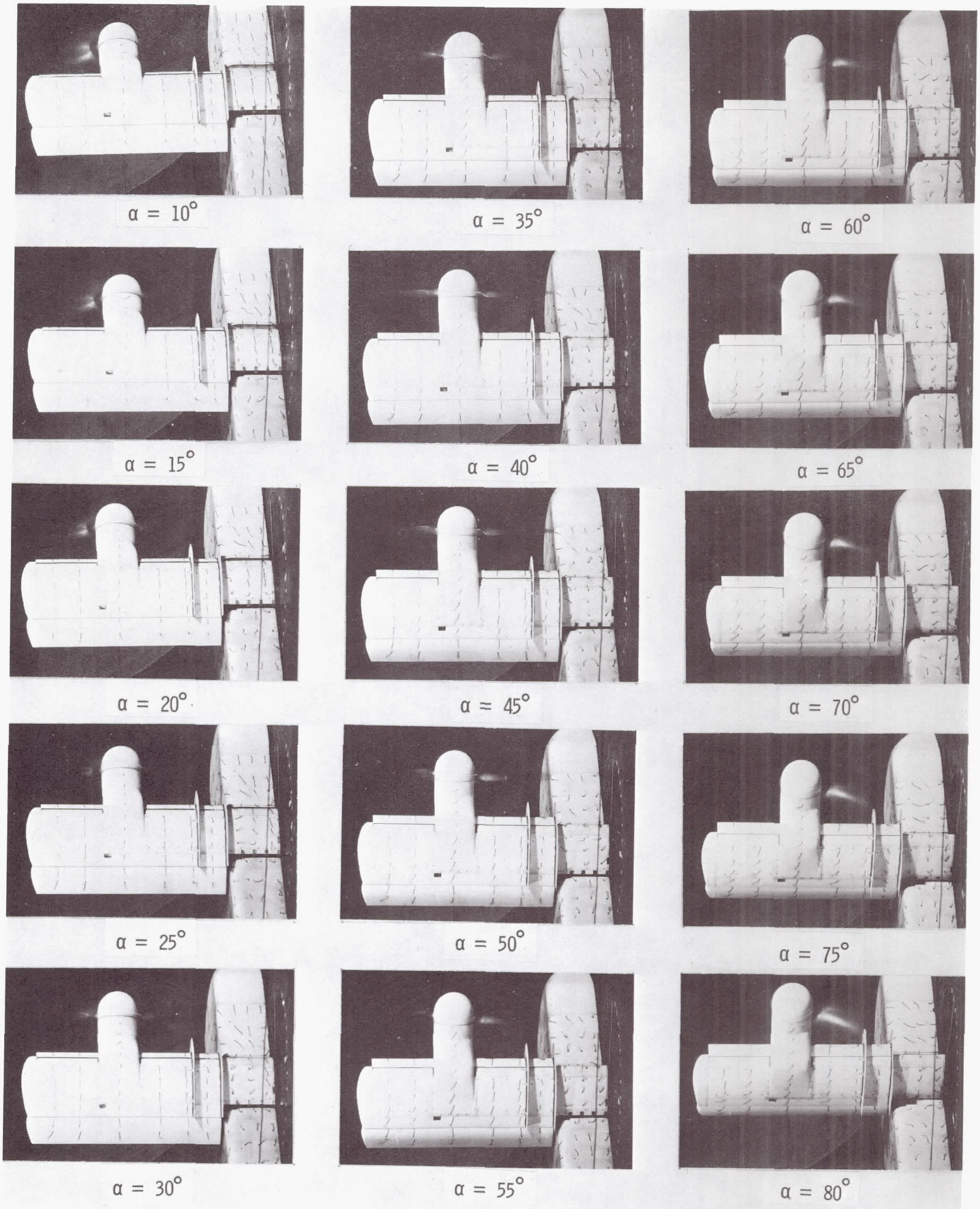

(c) Flow characteristics; $C_{T,s} = 0.80$.

Figure 34.- Continued.

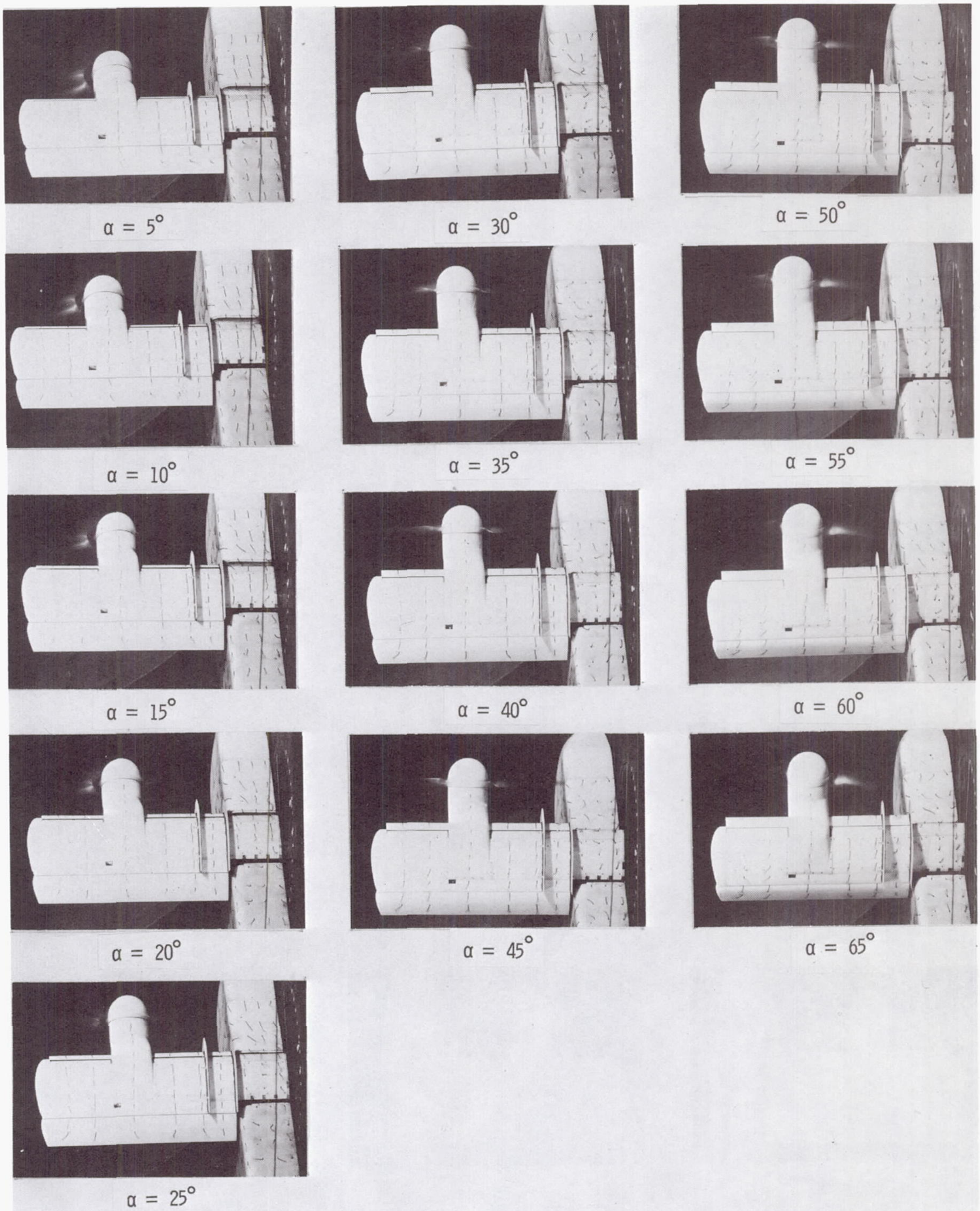

(d) Flow characteristics; $C_{T,s} = 0.60$.

Figure 34.- Continued.

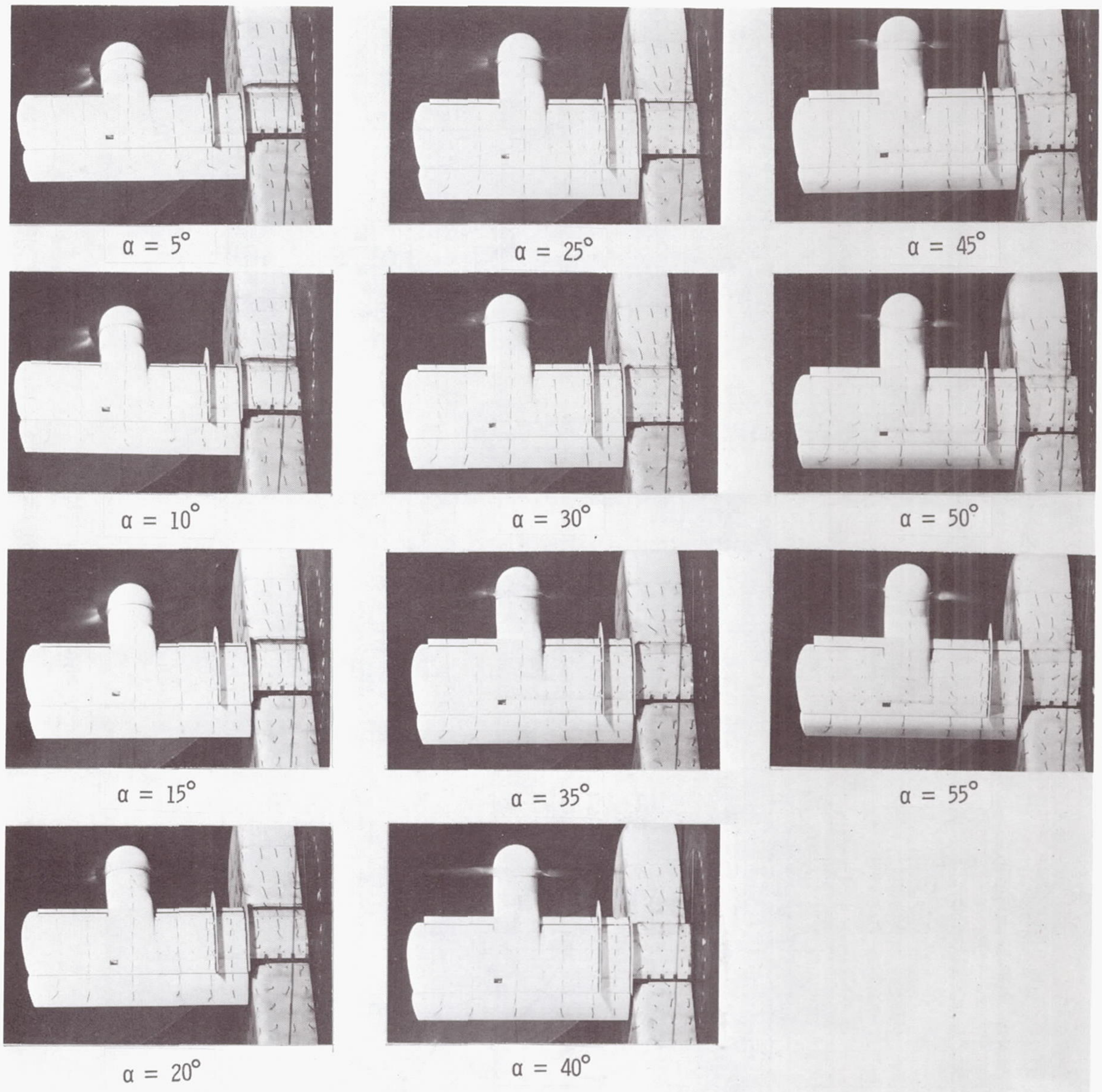

(e) Flow characteristics; $C_{T,s} = 0.30$.

Figure 34.- Concluded.

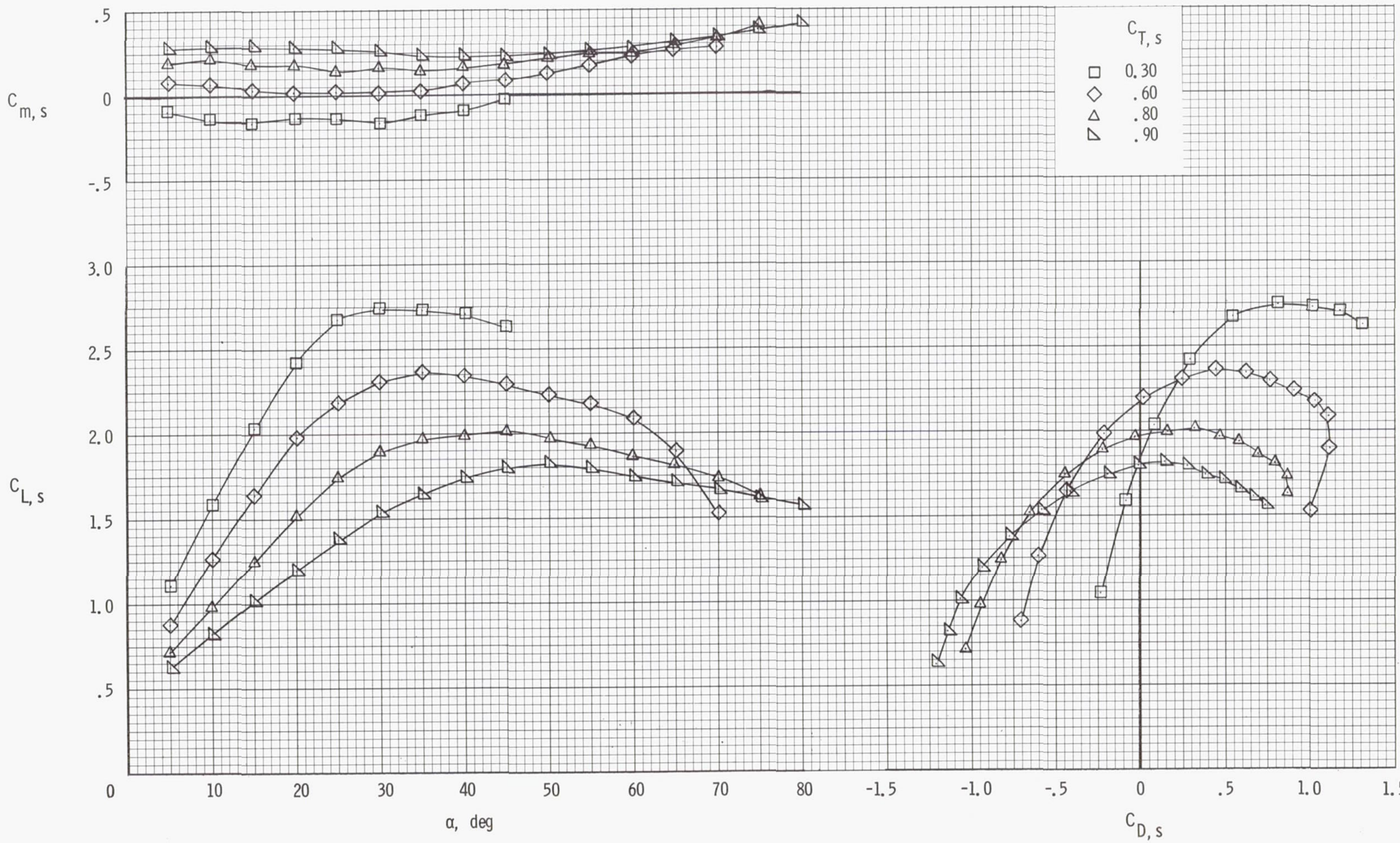

(a) Aerodynamic characteristics.

Figure 35.- Aerodynamic and flow characteristics of the wing with the propeller rotating up at the tip, full-span slat on, fences on, and $\delta_f = 40^o$.

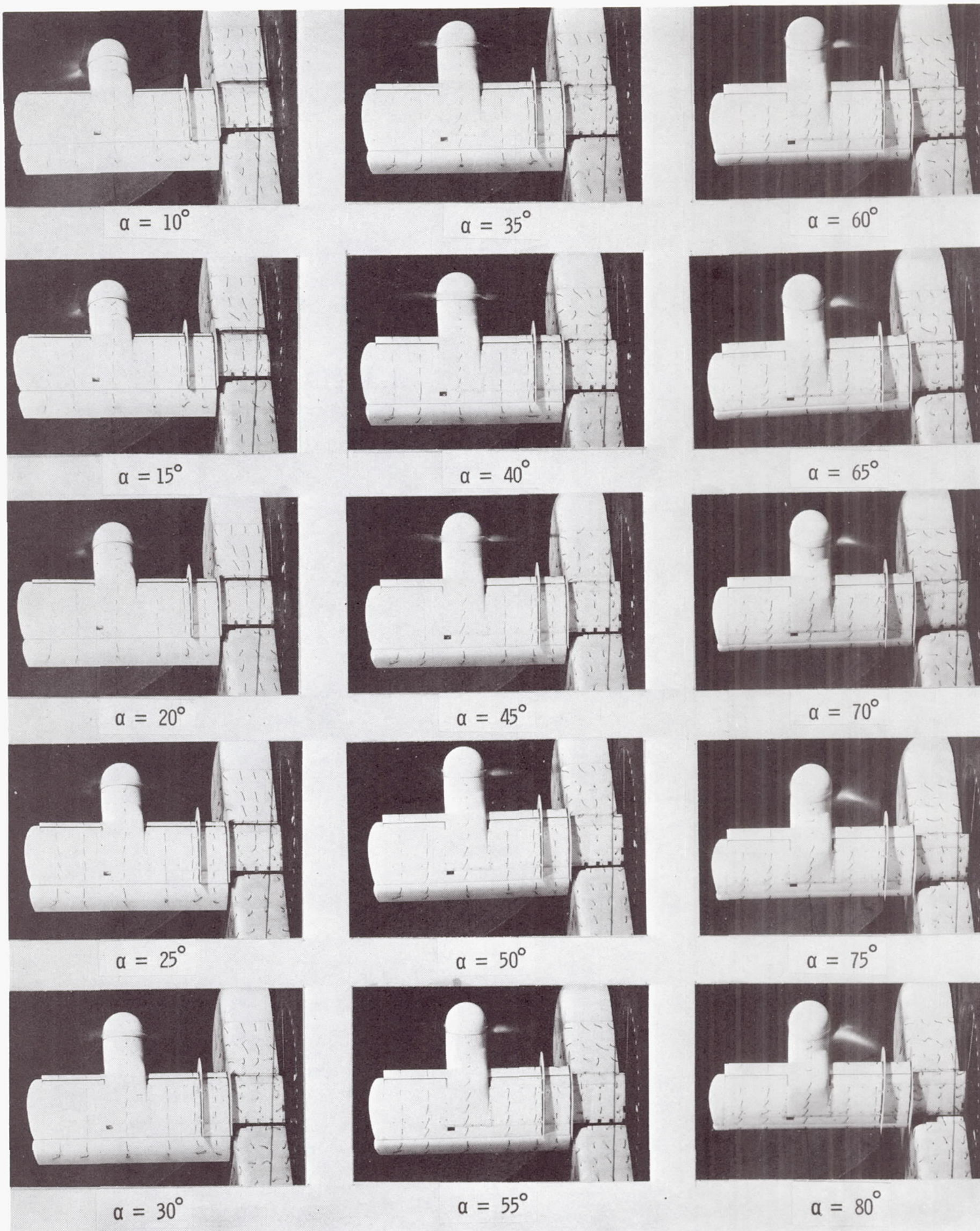

(b) Flow characteristics; $C_{T,s} = 0.90$.

Figure 35.- Continued.

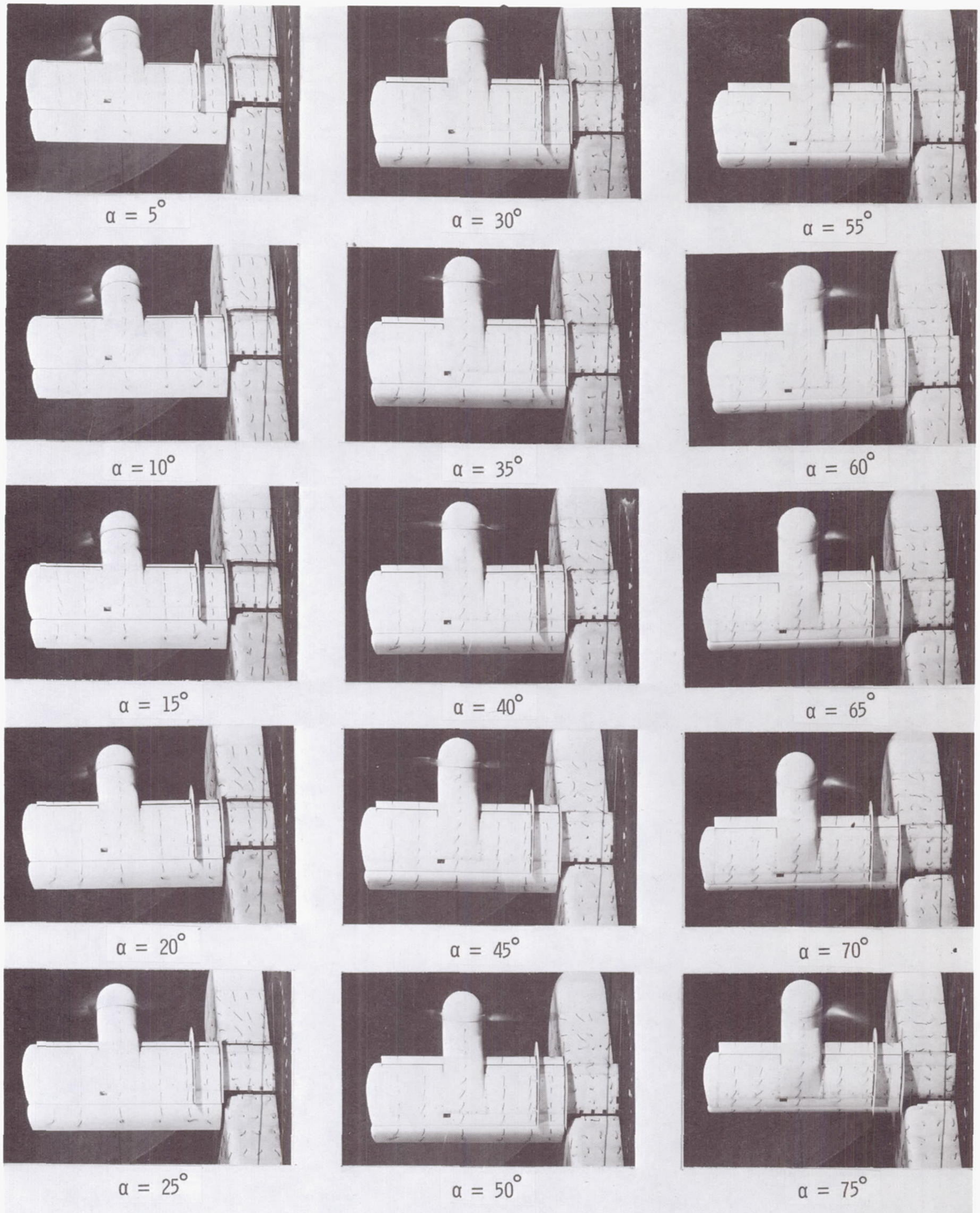

(c) Flow characteristics; $C_{T,s} = 0.80$.

Figure 35.- Continued.

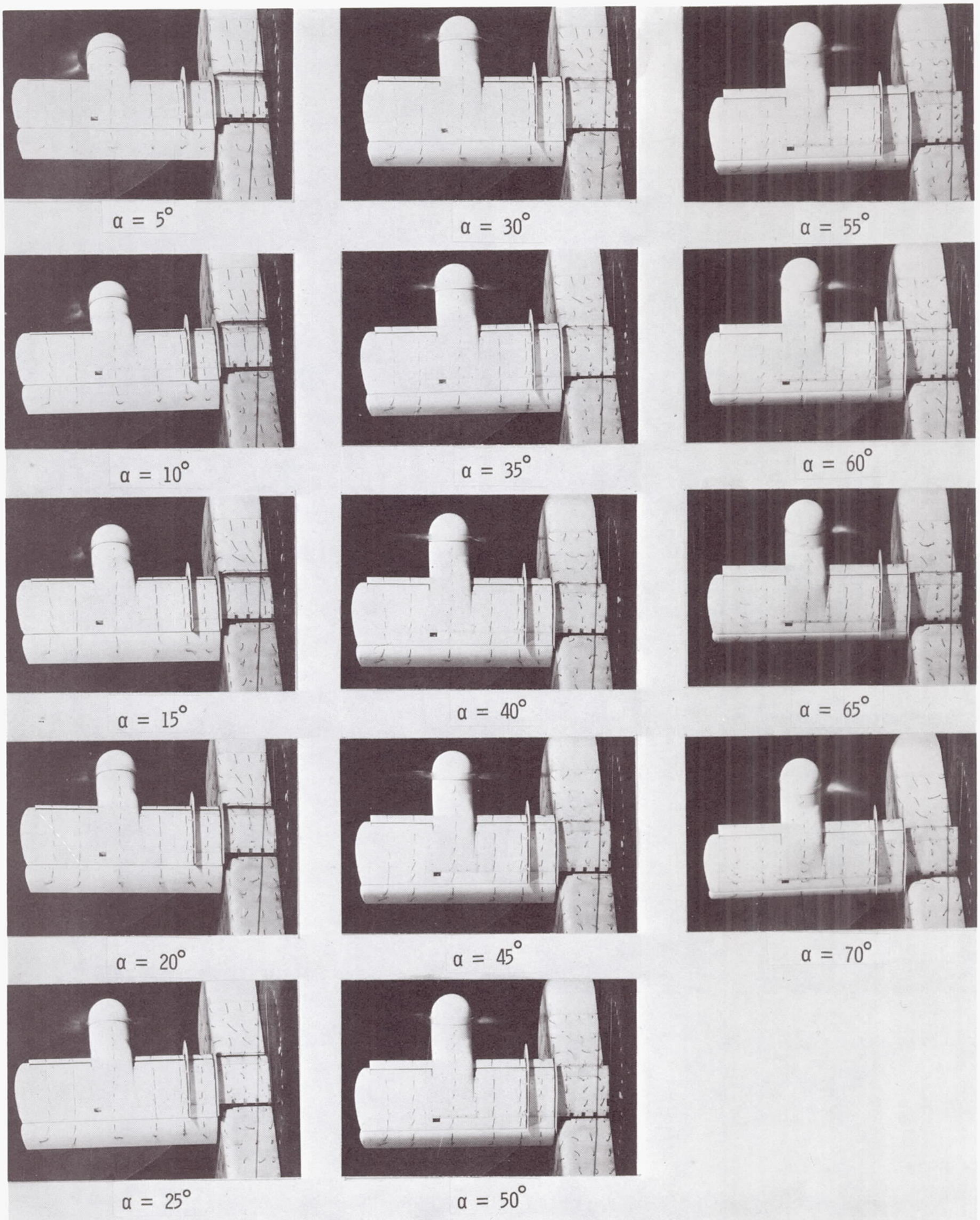

(d) Flow characteristics; $C_{T,s} = 0.60$.

Figure 35.- Continued.

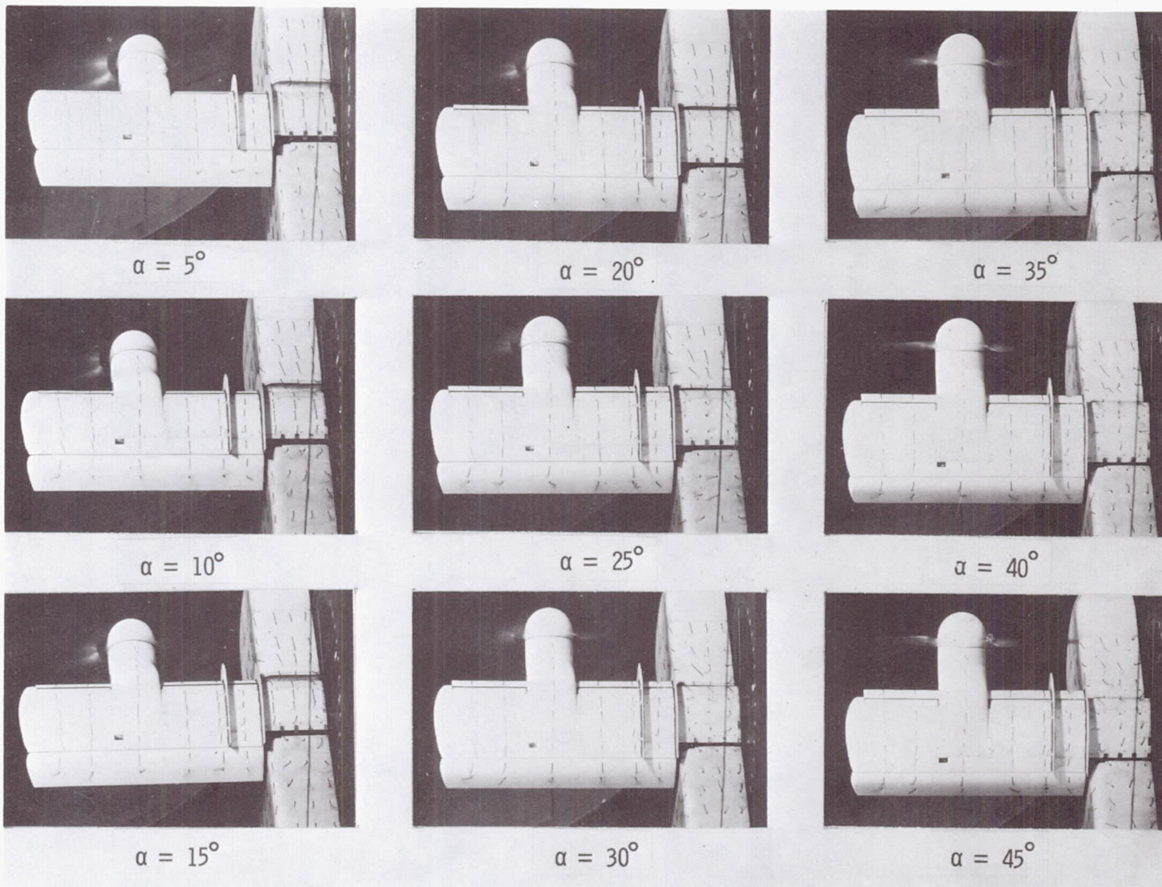

(e) Flow characteristics; $C_{T,s} = 0.30$.

Figure 35.- Concluded.

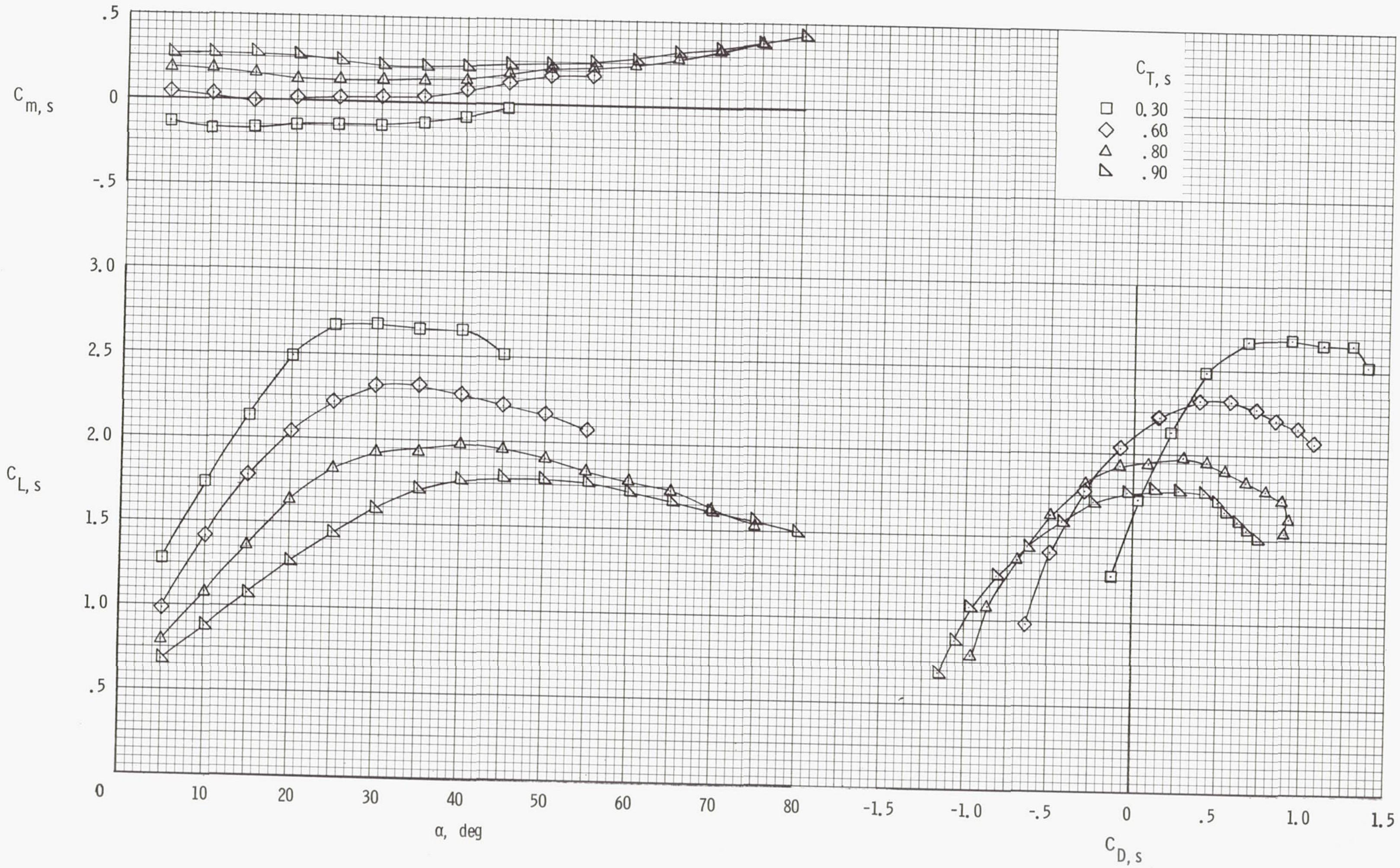

(a) Aerodynamic characteristics.

Figure 36.- Aerodynamic and flow characteristics of the wing with the propeller rotating up at the tip, full-span slat on, fences on, and $\delta_f = 60^o$.

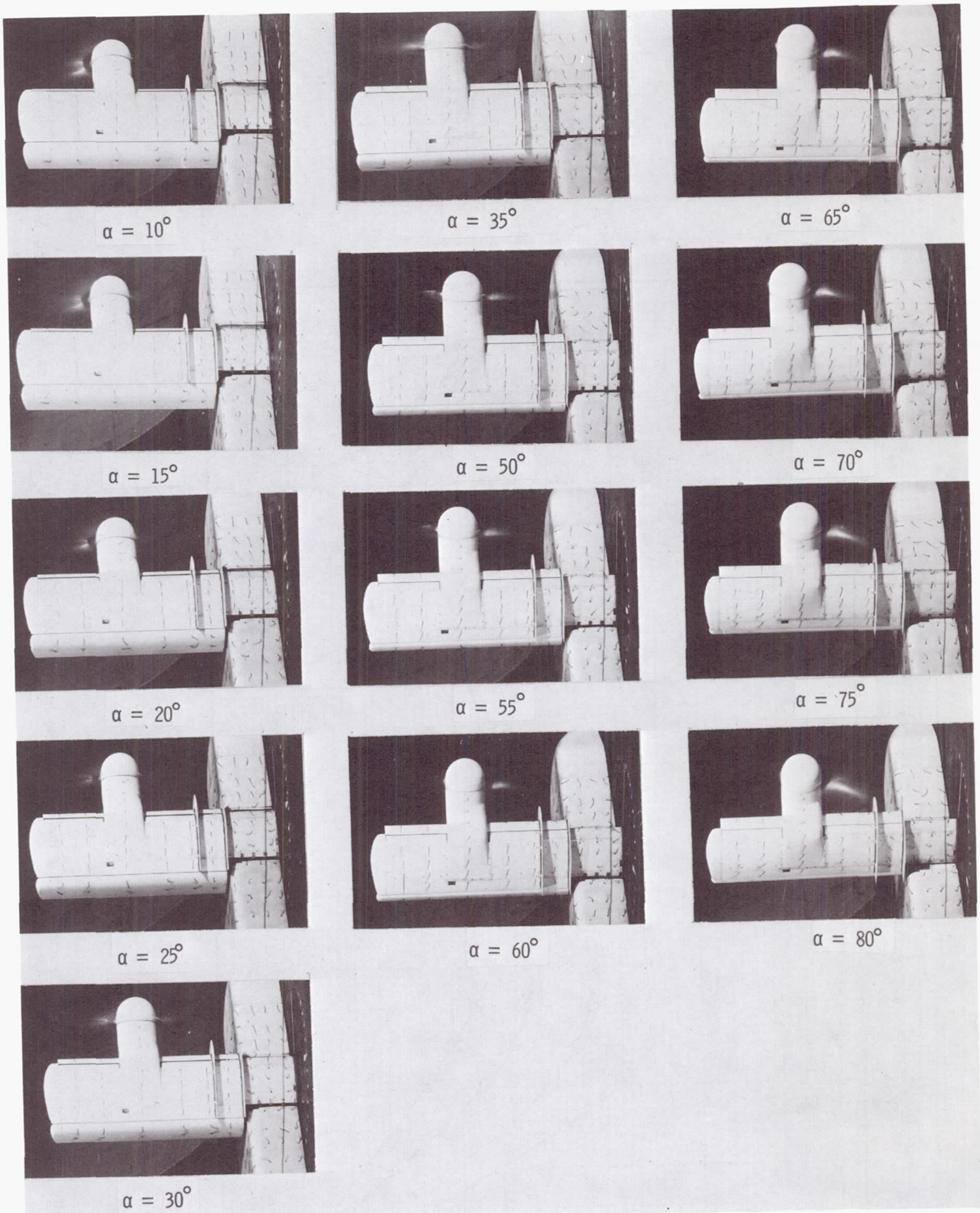

(b) Flow characteristics; $C_{T,s} = 0.90$.

Figure 36.- Continued.

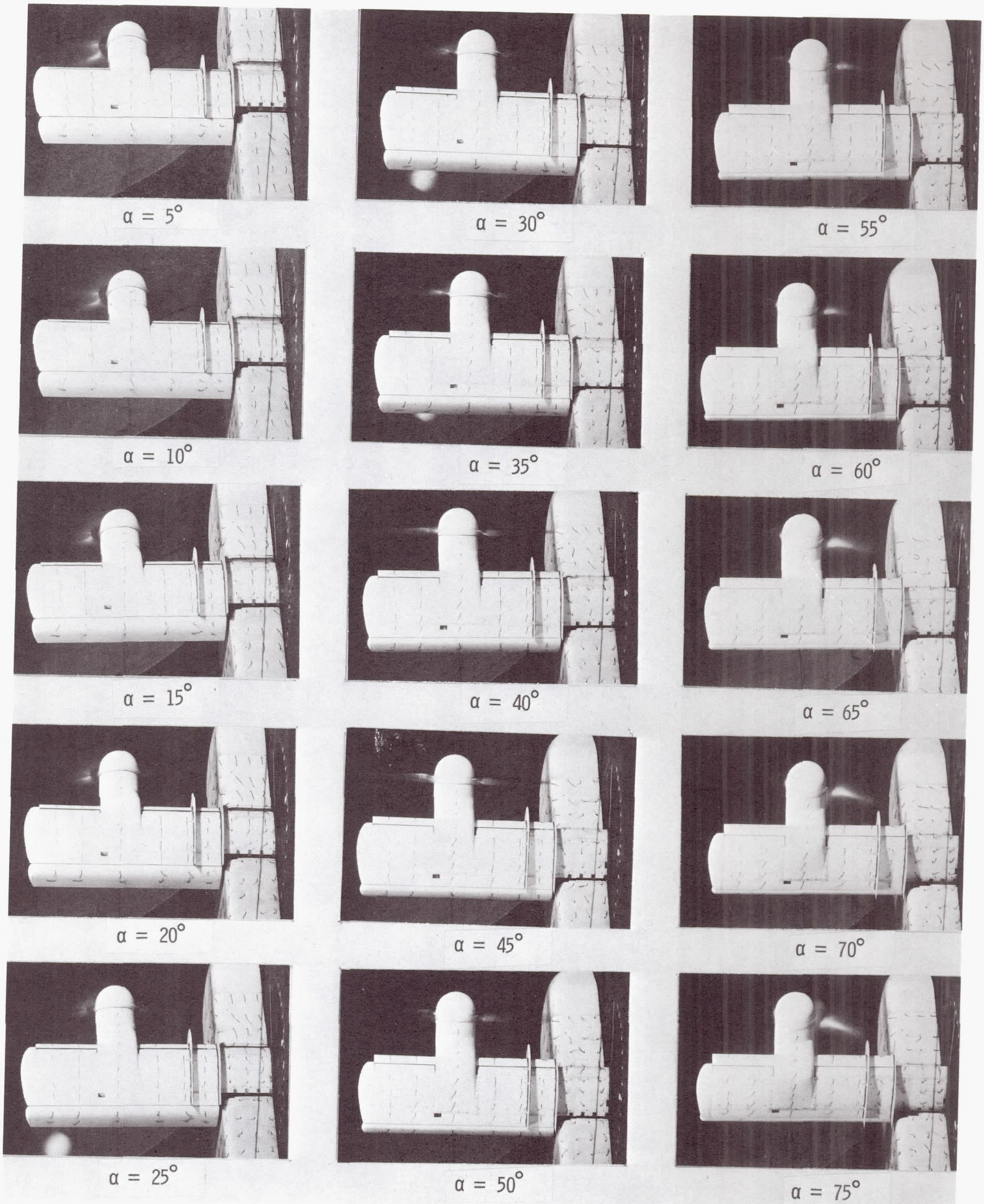

(c) Flow characteristics; $C_{T,s} = 0.80$.

Figure 36.- Continued.

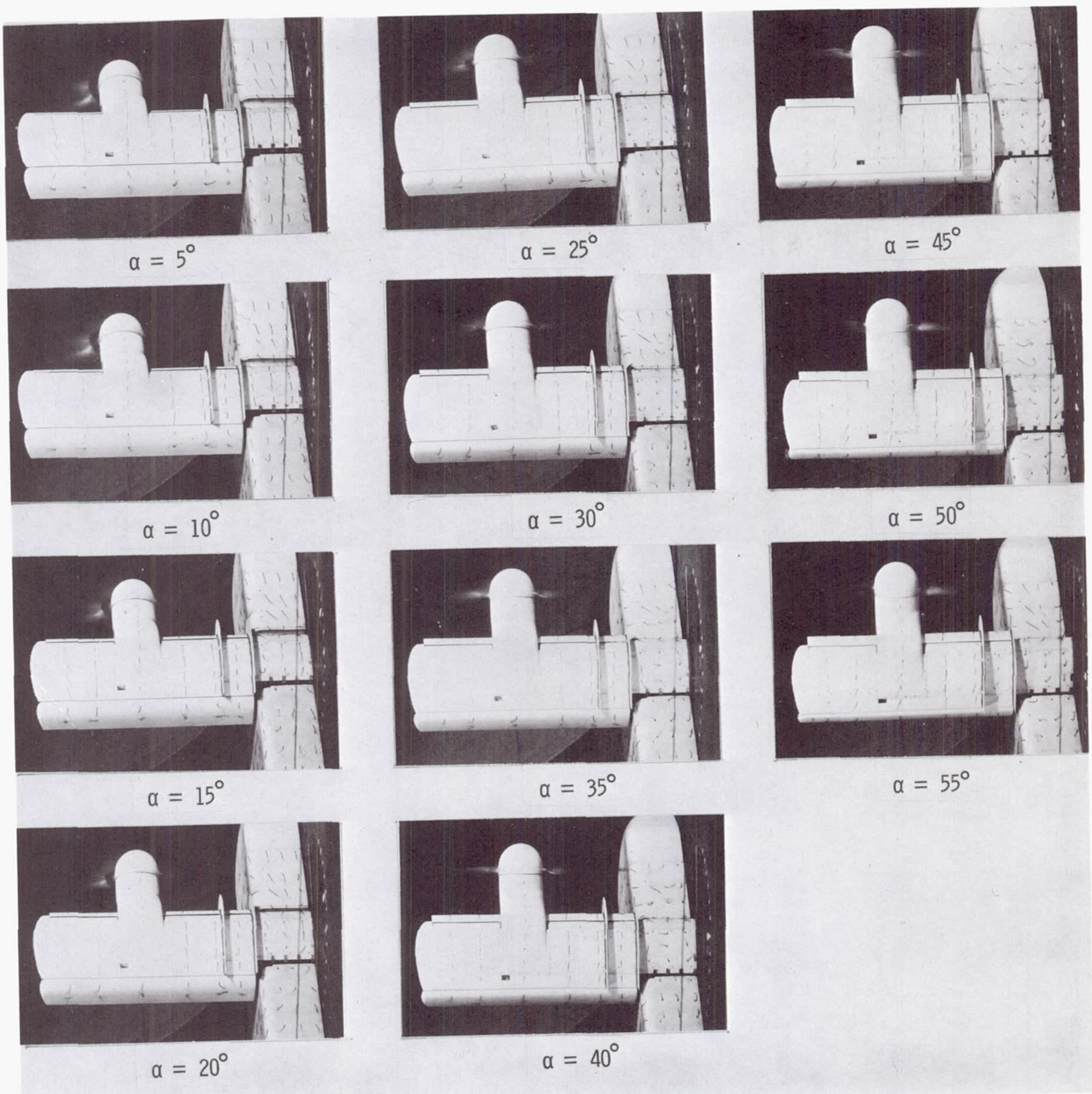

(d) Flow characteristics; $C_{T,s} = 0.60$.

Figure 36.- Continued.

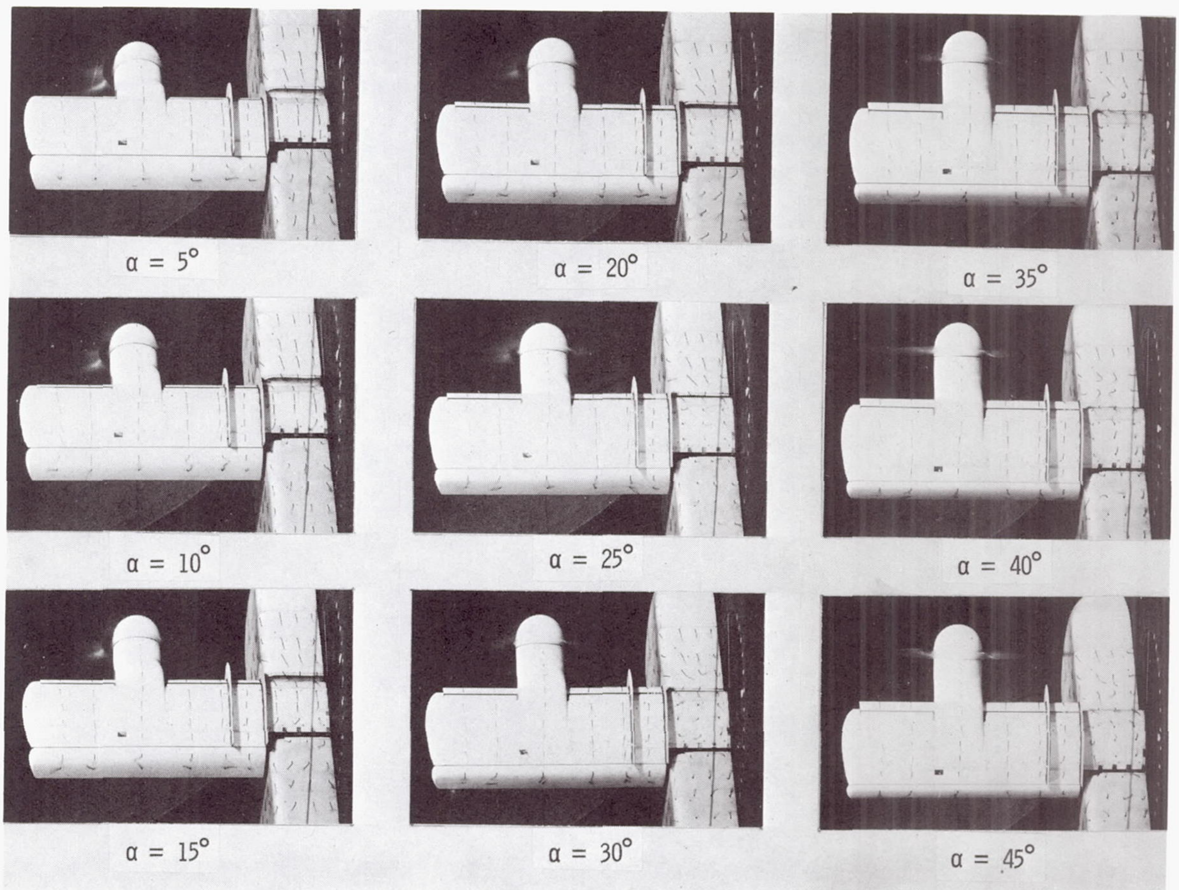

(e) Flow characteristics; $C_{T,s} = 0.30$.

Figure 36.- Concluded.